



INTERNATIONAL ATOMIC ENERGY AGENCY
UNITED NATIONS EDUCATIONAL, SCIENTIFIC AND CULTURAL ORGANIZATION
INTERNATIONAL CENTRE FOR THEORETICAL PHYSICS
I.C.T.P., P.O. BOX 586, 34100 TRIESTE, ITALY, CABLE: CENTRATOM TRIESTE



SMR/475-3

WORKSHOP ON ATMOSPHERIC LIMITED AREA MODELLING
15 October - 3 November 1990

"Boundary Layer Meteorology
Introductory Lectures"

D.J. CARSON
Hadley Centre for Climate Prediction and Research
Meteorological Office
Bracknell, United Kingdom

*Please note: These are preliminary notes intended for internal
distribution only.*

UNIVERSITY OF READING
DEPARTMENT OF METEOROLOGY
MSc Course in Meteorology
1990

BOUNDARY LAYER METEOROLOGY

Introductory Lectures

by

D J CARSON

Hadley Centre for Climate Prediction and Research

Hadley Centre
Meteorological Office
London Road
Bracknell
Berkshire RG12 2SY
UK

January 1990

BOUNDARY LAYER METEOROLOGY

INTRODUCTORY LECTURES

PREFACE

These notes form the basis of a set of introductory lectures on the atmospheric boundary layer given to the 1990 MSc Course in Meteorology at the Department of Meteorology, University of Reading. For fuller, more detailed discussions of the concepts and topics introduced, the student is referred to established text books on turbulence and the atmospheric boundary layer. The lecturer made full use of such texts and earlier lecture notes prepared by himself and colleagues (in particular Dr F B Smith) when compiling these lecture notes. A fairly comprehensive Book List is provided with the notes.

D J Carson
January 1990

THE ATMOSPHERIC BOUNDARY LAYER

BOOK LIST

- | | | |
|---------------------------------------|------|---|
| Batchelor, G.K. | 1960 | The Theory of Homogeneous Turbulence. Cambridge Univ. Press. |
| Eradslaw, P. | 1971 | An Introduction to Turbulence and its Measurement. Pergamon Press. |
| Brown, R.A. | 1974 | Analytical Methods in Planetary Boundary Layer Modelling. Adam Hilger. |
| Brunt, D. | 1941 | Physical and Dynamical Meteorology (2nd Ed.). Cambridge Univ. Press. |
| Csanady, G.T. | 1973 | Turbulent Diffusion in the Environment. D. Reidel Publishing Co. |
| Friedlander, S.K. and Topper, Leonard | 1961 | Turbulence, Classic Papers on Statistical Theory. Interscience Publishers, Inc. |
| Geiger, R. | 1965 | The Climate Near the Ground (Revised Ed.) Harvard Univ. Press. |
| Haugen, Duane A. | 1973 | Workshop on Micrometeorology. Editor Duane A. Haugen. American Meteorological Society. |
| Hinze, J.O. | 1959 | Turbulence, An Introduction to its Mechanism and Theory. McGraw-Hill Book Co. |
| Kraus, E.B. | 1972 | Atmosphere-Ocean Interaction. Clarendon Press. |
| Leslie, D.C. | 1973 | Developments in the theory of turbulence. Clarendon Press. |
| Lumley, J.L. and Panofsky, H.A. | 1964 | The Structure of Atmospheric Turbulence. Interscience Publishers (John Wiley & Sons). |
| Lonin, A.S. | 1970 | The Atmospheric Boundary Layer. Annual Review of Fluid Mechanics, Vol 2, pp 225-250. |
| Monin, A.S. and Yaglom, A.M. | 1975 | Statistical Fluid Mechanics: Mechanics of Turbulence Vol 2, Ed. John L. Lumley. The M.I.T. Press. |
| Monteith, J.L. | 1975 | Vegetation and the Atmosphere, Vol 1 Principles, Vol 2 Case Studies. Academic Press. |
| Kunn, R.E. | 1966 | Descriptive Micrometeorology. Academic Press. |

Panchev, S. 1971 Random Functions and Turbulence. Pergamon Press.

Panofsky, Hans A. 1974 The Atmospheric Boundary Layer Below 150 Metres. Annual Review of Fluid Mechanics, Vol 6, pp 147-177.

Pasquill, F. 1974 Atmospheric Diffusion, 2nd (Revised) Edition, Ellis Horwood Ltd., Chichester, distributed by John Wiley and Sons Ltd. 1st Edition, 1962 D. Van Nostrand Co. Ltd.

Plate, E.J. 1971 Aerodynamic Characteristics of Atmospheric Boundary Layers. U.S. Atomic Energy Commission Division of Technical Information Extension, Oak Ridge, Tennessee.

Priestley, C.H.B. 1959 Turbulent Transfer in the Lower Atmosphere. Univ. of Chicago Press.

Rosenberg, Norman J. 1974 Microclimate: The Biological Environment. John Wiley & Sons, A Wiley-Interscience Publication.

Sutton, O.G. 1949 Atmospheric Turbulence. Methuen & Co. Ltd.
1953 Micrometeorology. McGraw-Hill Book Co.

Taylor, G.I. 1960 The Scientific Papers of Sir Geoffrey Ingram Taylor. Vol II. Meteorology, Oceanography and Turbulent Flow. Ed. G.K. Batchelor. Cambridge Univ. Press.

Tennekes, H. and Lumley, J.L. 1972 A First Course in Turbulence. The M.I.T. Press.

Townsend, A.A. 1976 The Structure of Turbulent Shear Flow, Second Edition, Cambridge Monographs on Mechanics and Applied Mathematics. Cambridge Univ. Press.

Turner, J.S. 1973 Buoyancy Effects in Fluids. Cambridge Univ. Press.

Van Mieghem, J. 1973 Atmospheric Energetics. Clarendon Press.

Wippermann, F. 1973 The Planetary Boundary-Layer of the Atmosphere. Deutscher Wetterdienst.

THE ATMOSPHERIC BOUNDARY LAYER

UPDATED BOOKLIST (JANUARY 1990)

Stull, R B 1988 An Introduction to Boundary Layer Meteorology. Kluwer Academic Publishers

Arya, S Pal 1988 Introduction to Micrometeorology. Academic Press

Panofsky, H A and Dutton, J A 1984 Atmospheric Turbulence. Models and methods for engineering applications. John Wiley and Sons

Pasquill, F and Smith, F B 1983 Atmospheric Diffusion (Third Edition). Ellis Horwood Ltd, Chichester

Rosenberg, N J, Blad, B L and Verma, S B 1983 Microclimate. The Biological Environment. John Wiley & Sons

Nieuwstadt, F T M 1982 Atmospheric Turbulence and Air Pollution and van Dop, H (Eds) Modelling. A Course held in The Hague, Sept 1981. D. Reidel Publishing Co.

Brutsaert, Wilfried 1982 Evaporation into the Atmosphere. Theory, History, and Applications. D. Reidel Pub. Co.

Eagleson, P S (Ed) 1982 Land Surface Processes in Atmospheric General Circulation Models. Cambridge Univ. Press

McBean, G A et al 1979 The Planetary Boundary Layer. WMO Tech Note No 165, Editor G A McBean, WMO-No 530, Geneva

Stewart, R W 1979 The Atmospheric Boundary Layer. Third IMO Lecture, WMO-No 523, Geneva

Oke, T R 1978 Boundary Layer Climates. Methuen & Co Ltd Note : there is a more recent edition available in paperback.

BOUNDARY LAYER METEOROLOGY

INTRODUCTORY LECTURES

COURSE STRUCTURE 1990

1. INTRODUCTION

- 1.1 The Nature of Turbulent Flows
- 1.2 A Qualitative Definition of the Atmospheric Boundary Layer

2. THE STATISTICAL DESCRIPTION OF TURBULENCE

- 2.1 Mean Values, Fluctuations and Variances
- 2.2 Concept of an Eddy and Prandtl Mixing-length Theory
- 2.3 Correlations, Scale of Turbulence and Taylor's Hypothesis
- 2.4 The One-dimensional Spectrum of Turbulence
- 2.5 The Inertial Subrange

3. WIND AND SHEARING STRESS PROFILES IN THE ATMOSPHERIC BOUNDARY LAYER

- 3.1 The Equations of Motion and Continuity
- 3.2 The Eddy Shearing Stress
- 3.3 The Geostrophic Departure Method for Deriving $\bar{u}(z)$
- 3.4 Flux-gradient Relationships
- 3.5 The Ekman Spiral
- 3.6 The Leipzig Wind Profile
- 3.7 Balance of Forces within the Stationary Atmospheric Boundary Layer
- 3.8 Relation between Eddy Viscosity K_m and Mixing Length l_m

4. THE STRATIFIED ATMOSPHERIC BOUNDARY LAYER

- 4.1 The General Equations of Motion and Continuity
- 4.2 The Energy Equation of the Mean Motion
- 4.3 The Turbulent Energy Balance Equation
- 4.4 The Buoyancy Term in the Turbulent Energy Balance Equation
- 4.5 Special Cases of the Turbulent Energy Balance Equation
- 4.6 The Richardson Numbers
- 4.7 Kinematic Fluxes

5. THE SURFACE STRESS LAYER

6. THE STRATIFIED ATMOSPHERIC BOUNDARY LAYER NEAR THE GROUND :
THE SURFACE FLUX LAYER

- 6.1 The Monin-Obukhov Similarity Theory
- 6.2 The Neutral Surface-flux layer
- 6.3 The Unstable Surface-flux layer
- 6.4 The Stable Surface-flux Layer
- 6.5 Some Profile Comparisons
- 6.6 Variances of Turbulent Characteristics

7. PARAMETRIZATION OF THE LAND-SURFACE PROCESSES IN LARGE-SCALE NUMERICAL MODELS

8. SURFACE ROUGHNESS OVER THE SEA

9. THE ATMOSPHERIC BOUNDARY LAYER AS A WHOLE

- 9.1 Rossby Number Similarity Theory for the Whole Atmospheric Boundary Layer
- 9.2 Development of a Convectively Unstable Boundary Layer

THE ATMOSPHERIC BOUNDARY LAYER

INTRODUCTORY LECTURES

1. INTRODUCTION

1.1 The Nature of Turbulent Flows

Most flows occurring in nature and in engineering applications are turbulent.

Some turbulent flows can be readily observed e.g. the flow of water in rivers or around bridge piers; the growth of cumulus clouds; the development of plumes from power station or industrial stacks. Turbulence also occurs in the jet stream and along frontal surfaces.

We all have some idea what is meant by turbulent flow as opposed to laminar flow. In laminar flow each particle follows the precise path of its predecessors and the essential feature is that there is no mixing of adjacent layers of the fluid.

It is very difficult however to give a precise definition of turbulence. All we can do is list some of the characteristics of turbulent flows (see e.g. Lumley and Panofsky (1964), Tennekes and Lumley (1972)).

(1) Irregularity or randomness. This makes a deterministic approach to turbulence problems impossible; instead one relies on statistical methods.

(2) Diffusivity. This is a very important feature of turbulent flows and causes rapid mixing and increased rates of momentum, heat and mass transfer. If a flow pattern looks random but does not exhibit spreading of velocity fluctuations through the surrounding fluid, it is not turbulent.
e.g. contrails of a jet aircraft.

(3) Large Reynolds Numbers. Recall that the Reynolds number, Re , is essentially the ratio of the inertial to the frictional (or viscous) forces in the fluid flow.

$$\begin{array}{l} \text{Inertia terms: } \rho \frac{\partial u}{\partial t}, \rho u \frac{\partial u}{\partial x} \text{ etc.} \\ \text{Friction terms: } \mu \frac{\partial^2 u}{\partial x^2} \text{ etc.} \\ \text{Pressure gradient terms: } \frac{\partial p}{\partial x} \end{array} \quad \left| \quad \begin{array}{l} \rho \frac{U^2}{l} \\ \mu \frac{U}{l^2} \end{array} \quad \mu = \text{dynamic viscosity}$$
$$Re = \frac{\rho U l}{\mu} = \frac{U l}{\nu}$$

U is a 'characteristic' fluid velocity,

l is a 'characteristic' length

$\nu = \mu/\rho$ is the kinematic viscosity,

$F = \mu \frac{du}{dz}$ is the viscous shearing stress.

The Reynolds number indicates whether inertial or viscous effects predominate; Re small, < 1 , the pattern of flow is shaped chiefly by the viscosity, Re large, $> 10^4 - 10^5$, inertial effects far more important than viscous effects.

Reynolds (1883) showed experimentally that turbulent flow is not sustained for $Re \lesssim 2000$.

For air at sea-level temperature and pressure: $\nu = 15 \times 10^{-6} \text{ m}^2 \text{ sec}^{-1}$; for turbulent eddies in atmospheric boundary layer (with $U = 0.5 \text{ msec}^{-1}$ and $l = 300 \text{ m}$ as representative values) $Re \sim 10^7$.

Turbulent flows, then, always occur at high Reynolds numbers. The turbulence often originates as an instability of laminar flows if Re becomes too large. The instabilities are related to the interaction of viscous terms and non-linear inertial terms in the equations of motion and this interaction is very complex.

The absence of sufficiently powerful mathematical methods means that the equations are virtually intractable. This leads to numerical and trial and error methods where the non-linear concepts and mathematical tools have to be developed along the way.

(4) Turbulence is rotational and three-dimensional. The flow is characterised by high levels of fluctuating vorticity. An important vorticity-maintenance mechanism known as vortex stretching is absent in 2-dim flow. The vorticity vector is a measure of the angular velocity of small fluid elements; the equations governing its evolution relate to those expressing the conservation of angular momentum - vorticity increases when angular momentum is compressed into smaller cross-section.

Vortex stretching is the mechanism that gives hurricanes and tornadoes their destructive force.

(5) Dissipation. Turbulent flows are always dissipative i.e. mechanical energy is being transformed into internal energy. Viscous shear stresses perform deformation work which increases the internal energy of the fluid at the expense of the kinetic energy of the turbulence. Turbulence, then, needs a continuous supply of energy to make up for the viscous losses. If no energy is supplied the turbulence decays rapidly.

(6) Continuum. Turbulence is a continuum phenomenon, governed by the equations of fluid dynamics. Even the smallest scales occurring in a turbulent flow are usually far larger than any molecular length scale. The smallest wavelength in turbulence is called the "Kolmogorov microscale"; in atmospheric turbulence, its value is typically about 1 mm.

(7) Turbulence is a feature of the fluid flow, not the fluid.

1.2 A Qualitative Definition of the Atmospheric Boundary Layer

Appealing to our intuitive ideas about turbulent boundary layers, we know that, for example, there exists a region close to the banks of a river where there is marked shear in the fluid flow and a much reduced flow as the bank is

approached. In this 'boundary layer' the flow is determined by the nature of the bank itself and the bank's presence partly determines the flow pattern across the river. If the rough bank were replaced by a much smoother one then we should expect the boundary layer to change in character and the flow to become faster than before.

Although we have not yet reached the stage where we can rigorously define what we mean by the atmospheric boundary layer we can relate it to our intuitive ideas of laboratory and other natural boundary layers.

Definition. The atmospheric boundary layer is the layer containing typically some 10% of the overlying mass of air in which the flow, driven by the pressure gradient, is controlled and modified partly by the aerodynamic friction of the underlying surface but also to an important extent by the density stratification of the air which results from differences in temperature of the surface and the air.

These differences in temperature arise over the land primarily in the course of the daily cycle of radiative heating and cooling of the ground, but they may also arise from the overflowing of air from warmer or cooler regions of the earth.

In the aerodynamic sense the boundary layer is simply the layer from which momentum is extracted and transferred downward to overcome surface friction.

The important role played by the buoyancy forces generated by surface heating and cooling and the presence of moisture helps distinguish the atmospheric boundary layer from classical laboratory boundary layers.

It is found that the flow in the atmospheric boundary layer is turbulent except possibly in very stable conditions e.g. in strong inversion situations at night.

The density stratification is of no importance only in strong wind conditions when the sky is heavily overcast. Then the depth and structure of the boundary layer are governed by mechanical mixing generated by instabilities in the shear flow due to the effects of the surface friction. This type of boundary layer is called a neutral boundary layer. We shall discuss such classifications later.

Another difficulty with the atmospheric boundary layer is that the upper bound of the layer is not uniquely specified. There is no obvious means of fixing the depth of this layer. Each of the factors already mentioned viz. the extraction of momentum from the layer due to surface friction and the transfer of heat and moisture through the layer, provides an estimate of the extent of the turbulent atmospheric boundary layer. In certain conditions the values obtained are reasonably compatible but in other situations there is still argument about the compatibility of the separate values.

The daytime value of the depth is typically in the range 0.5-2 km (50-200 mb thick). The night-time depth is generally much shallower and in extremely stable conditions may be only a few tens of metres.

Fig. A gives a schematic representation of a typical diurnal variation in the depth of the atmospheric boundary layer.

Consider the diurnal cycle of events close to a uniform surface covered with short grass, on a clear summer's day when the synoptic FMSL chart indicates small horizontal gradients of pressure, i.e. the situation is optically stable or anticyclonic.

During the day the surface temperature rises considerably above that of the air immediately adjacent to it and the flow becomes unstable and highly turbulent. As the sun sets, radiation from the surface causes the ground temperature to fall rapidly below that of the air with the result that the layers immediately in contact with the surface are cooled and become denser than those above. The flow is stable.

The maintenance of the turbulent state implies that masses of air are being moved continually in the vertical. If the fall in density with height is very marked then considerable work has to be done in lifting the denser masses against the gravitational field, at the expense of the energy of the mean motion. In such circumstances turbulent motion is less pronounced and may even be completely suppressed. This means that the supply of momentum from the free stream to replace that absorbed by friction at the surface is reduced because of the reduction in mixing and the flow, as a whole, tends to settle down to low motion in parallel layers.

e.g. Smoke from a fire of rubbish or weeds, vigorously scattered by the wind during the day, drifts in thin, dense sheets or plumes for considerable distances, without mixing, in the evening.

If the sky remains clear and the synoptic situation remains the same the stable period will last until shortly after dawn when the incoming short-wave radiation heats the ground and the lowest layers. Less dense air is now nearest the surface and the buoyancy effects now enhance any mechanically generated turbulent motions. About an hour after sunrise the near-laminar light-time flow gives way to turbulent flow which continues throughout the day.

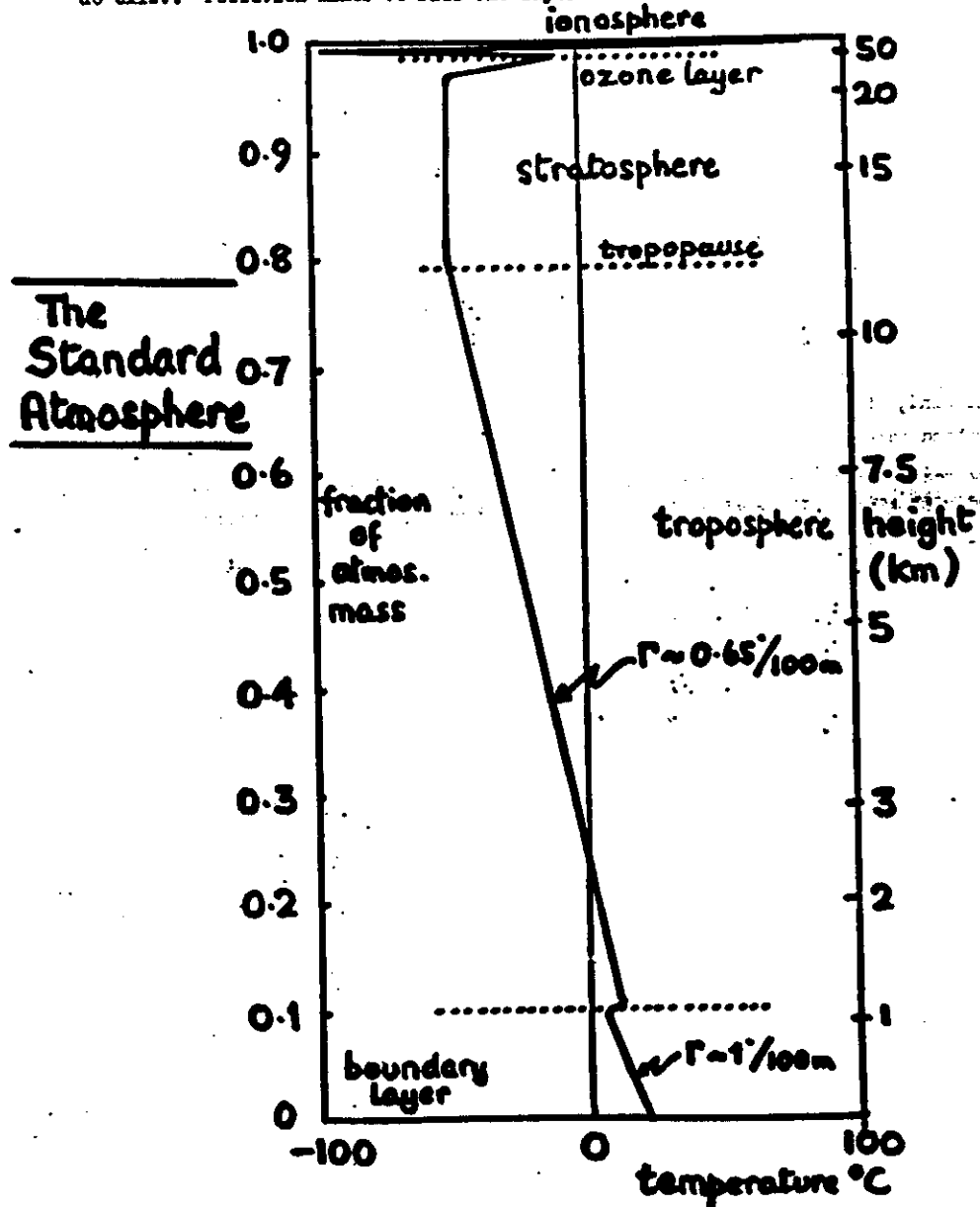
In general, then, the turbulent flow in the atmospheric boundary layer, especially over the land, exhibits a marked diurnal variation, the turbulence being marked during the daytime and small at night. If the sky is completely overcast and there is a moderate-high wind, buoyancy effects can be neglected and the degree of turbulence shows little variation by day and night. Otherwise the density stratification of the lowest layers cannot be ignored.

Finally, it is very difficult to reproduce the atmospheric boundary layer flows in wind tunnels. We must rely then almost entirely on observations made in the open where control is impossible and conditions are rarely, if ever, exactly the same on different occasions.

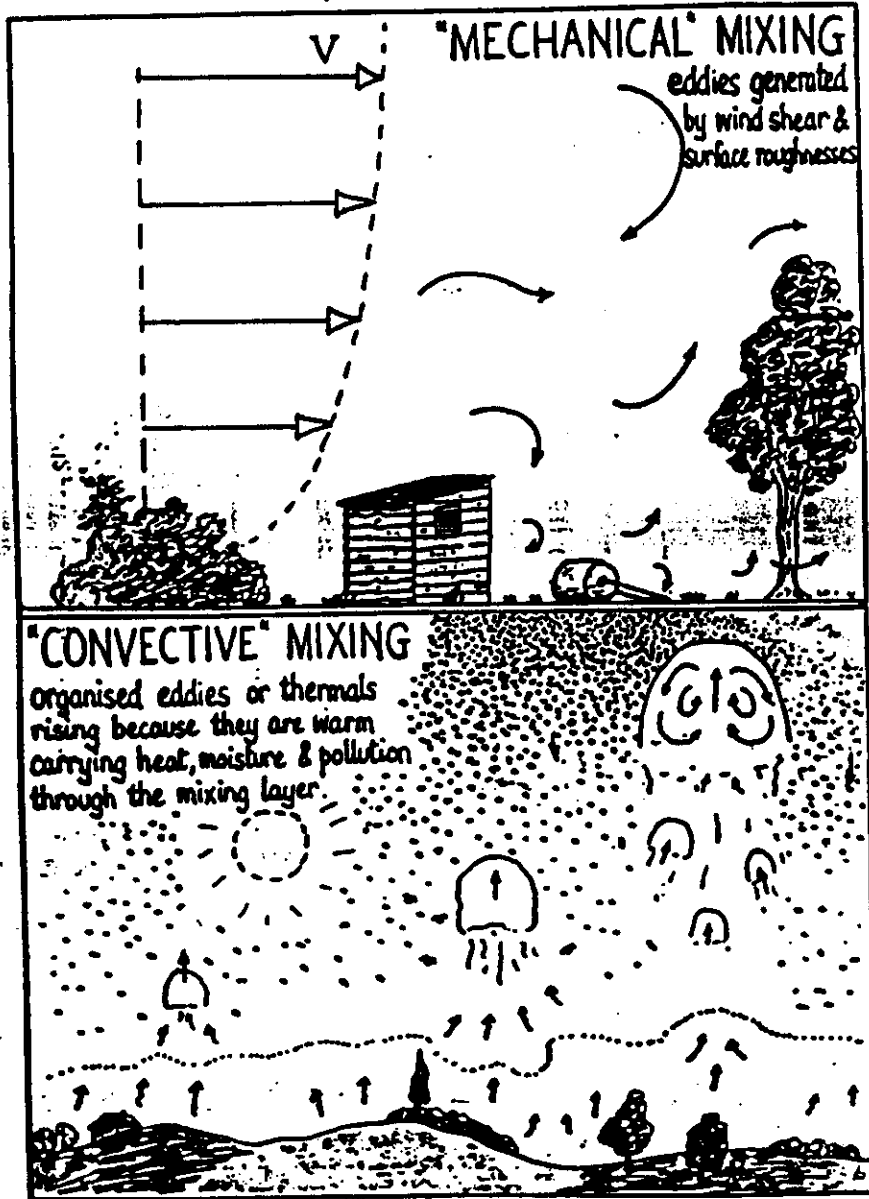
Because of the nature of the basic parameters required to determine the stability of the flow in a fluid of variable density gradient, it is necessary to obtain very accurate measurements of the gradients of velocity, temperature and moisture content.

A schematic representation of the structure of the atmosphere. Normally pollutants are emitted at relatively low level and are hence within the lowest layer described as the boundary layer. This layer is however of very variable depth. It is that part of the atmosphere that is under the direct influence of the underlying surface and the fluxes of heat, momentum and moisture that exist between the ground and the air. Since these fluxes depend on the nature of the surface, the time of day, and the past history of the air, the depth of the layer can vary from a few tens of metres at night to one or two kilometres during a warm sunny day.

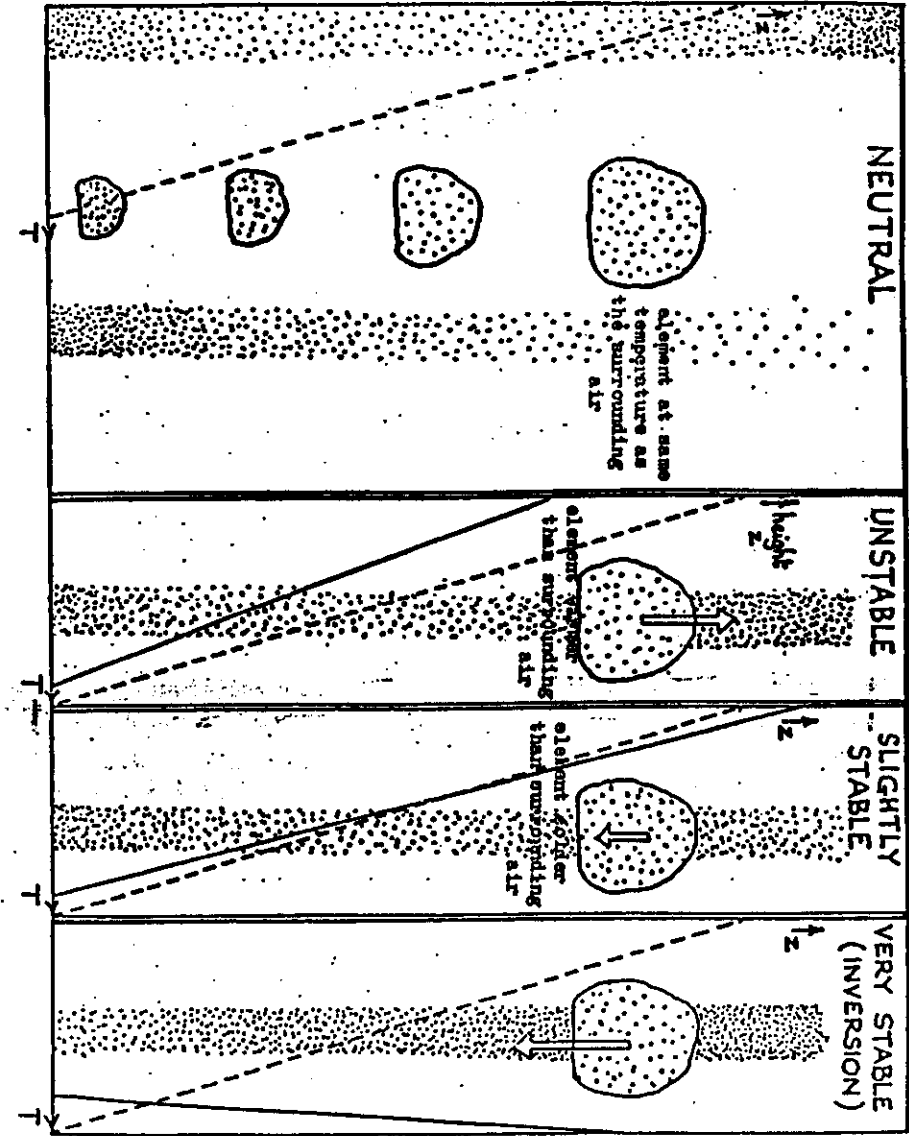
The boundary layer is by definition a rather well mixed layer although gradients do exist. Pollution mixes to fill the layer after an hour or so.



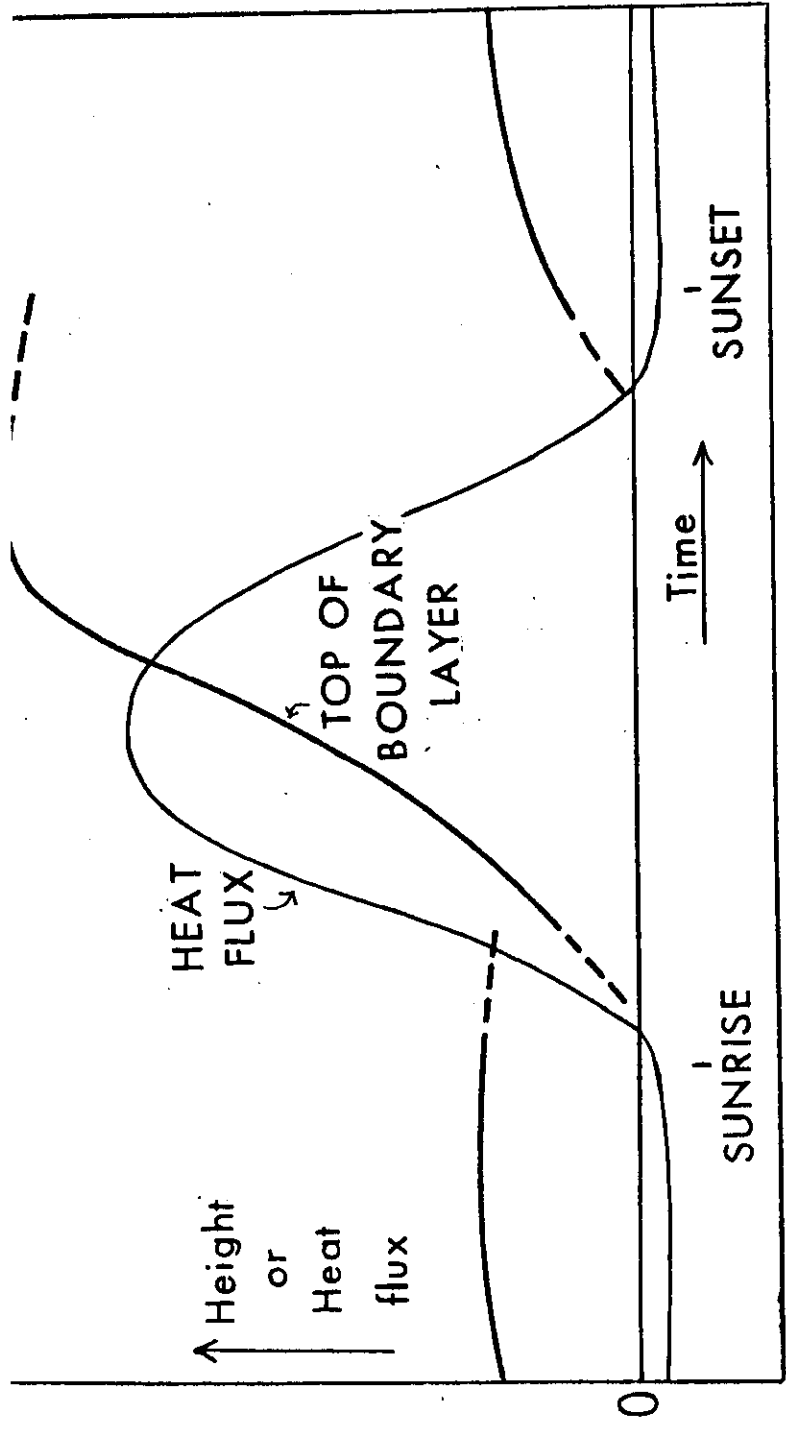
The influence of the underlying surface is spread through the boundary layer by random motions on a variety of scales, called eddies or turbulence. Although random, the characteristics of these eddies do depend in a definable way on height, on the depth of the boundary layer, and in particular on the way they are generated. The two pictures below indicate the two main sources of turbulent energy: the top picture indicates that the roughness of the ground slows the airstream down and thereby generates a wind speed gradient with height which only has to be perturbed to generate a tumbling action and turbulence. The lower picture indicates that a warmed ground gives off heat to the overlying



airstream, and this heat causes vertical motion, as in any fluid, which may be small-scale at first but tends to become more organised and larger with increasing height.



— actual temperature profile in the air
 - - - adiabatic temperature profile followed by the displaced element of air
 ↑ the force on the element resulting from the difference in temperature



SCHEMATIC REPRESENTATION OF THE DIURNAL EVOLUTION OF THE DEPTH OF THE ATMOSPHERIC BOUNDARY LAYER

FIGURE A

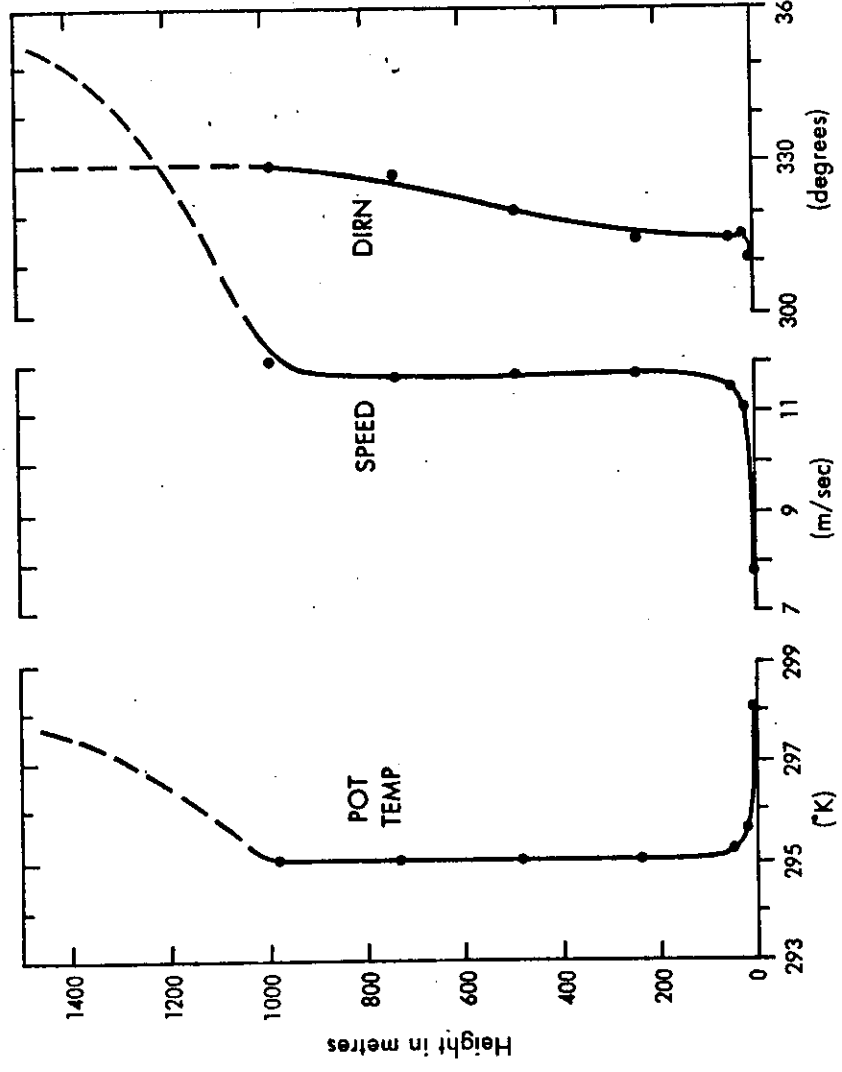


Figure 1. Mean profiles associated with a convective boundary layer

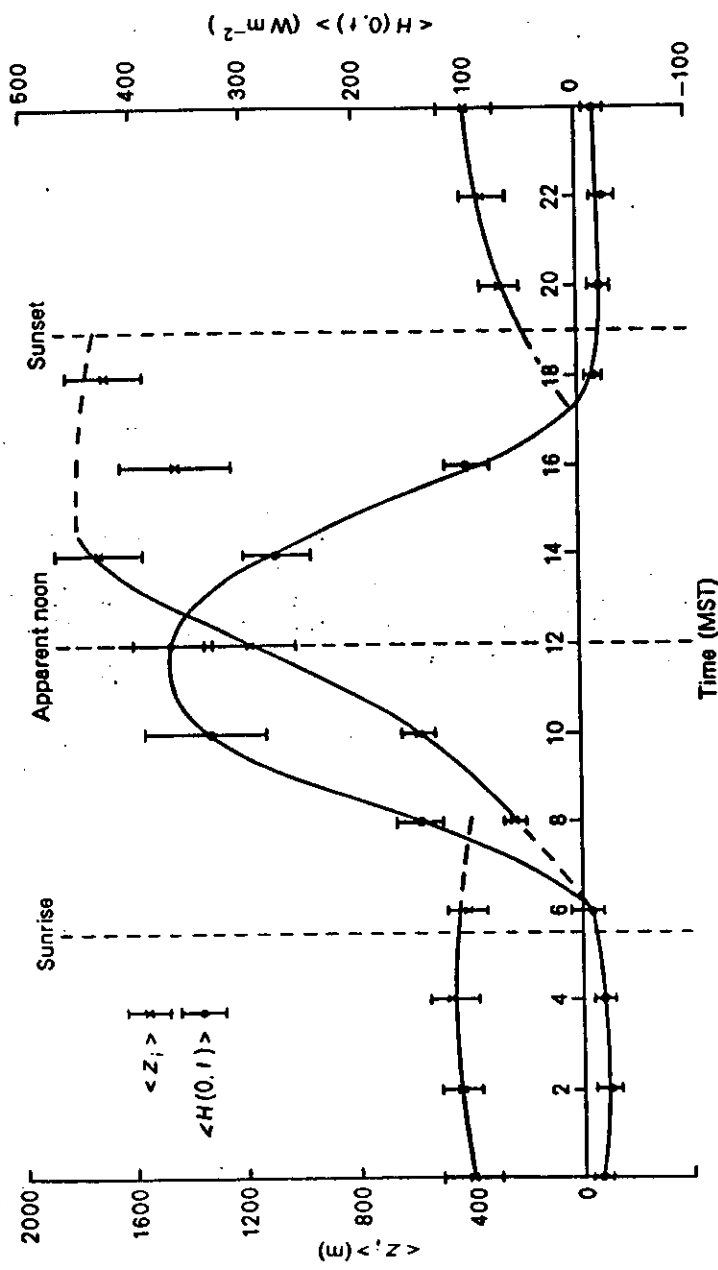


Figure 3. The mean boundary layer thickness, $\langle z_i \rangle$, and sensible heat flux at the surface, $\langle H(0, t) \rangle$, deduced for the O'Neill data, plotted with standard errors as functions of time of day (Mean Solar Time). Carson (1973)

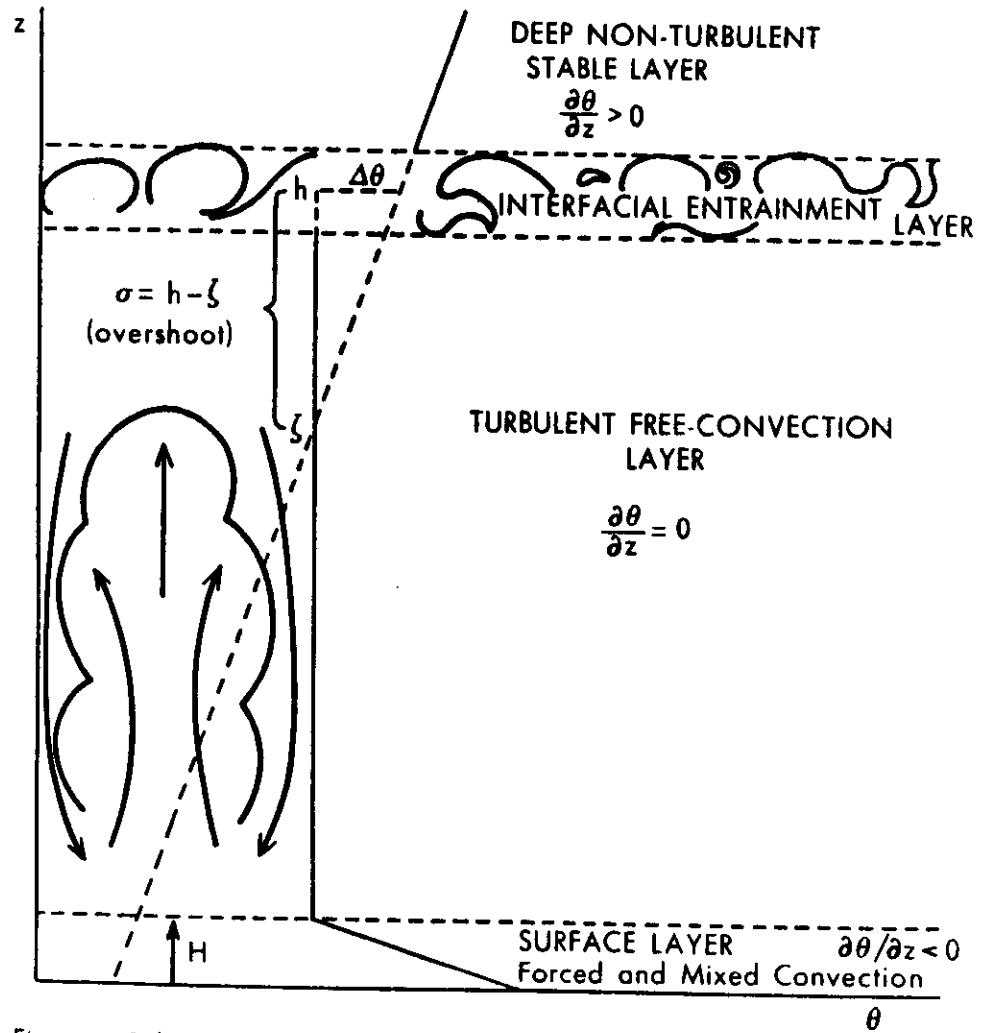


Figure 4. Schematic representation of the developing convectively unstable boundary layer and the adopted potential temperature profile, $\theta(z)$. Carson (1973)

Unstable conditions usually occur during the day, especially when the sun is warming the ground. Neutral conditions are associated with windy and cloudy conditions when mechanically generated turbulence dominates turbulence generated from thermal sources. Stable conditions are normally associated with night-time conditions, especially when there is little cloud and the winds are rather light. The ground is then cooled by radiation...heat is radiated away into outer space....and the ground is then colder than the overlying air. Heat then flows downward from the air to the ground. The increase of temperature with height is called an inversion and as we

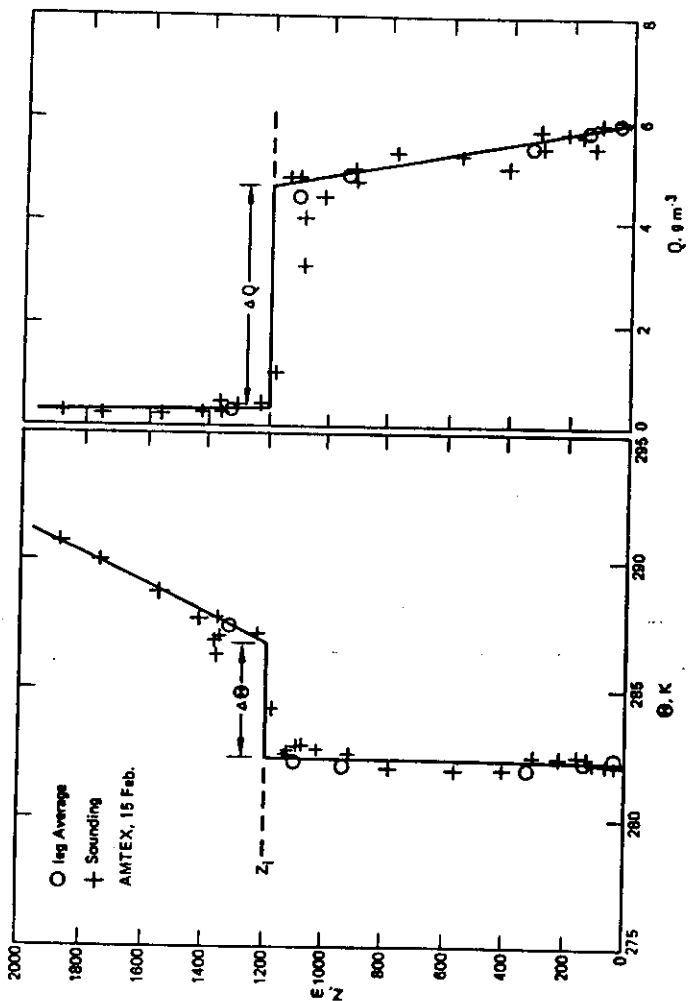
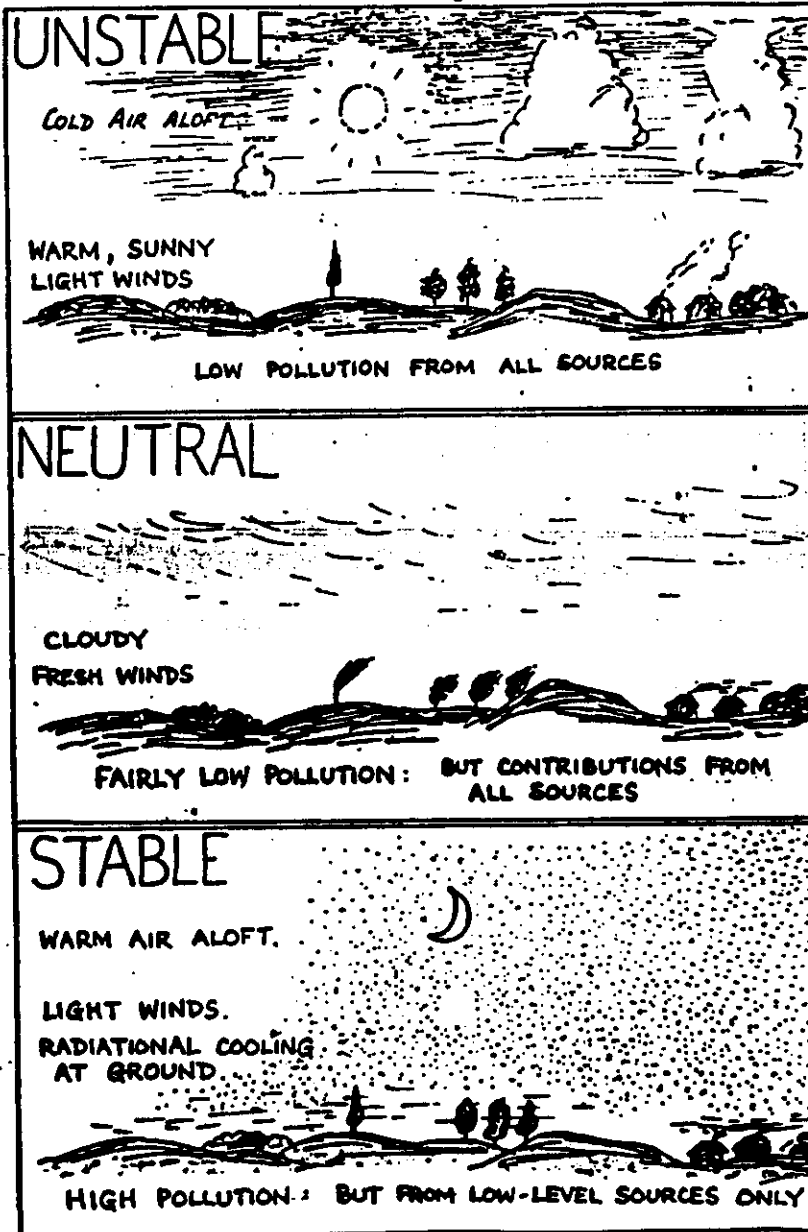


Figure 2 Vertical profiles of mean potential temperature and mean absolute humidity as measured over the sea in the AMTEX experiments. Note the strong jumps in both properties at z_1 . (Figure reproduced from McBean et al (1979))



shall see turbulence is drained of energy in an inversion, and tends to die out. Little mixing then takes place and, for example, bonfire smoke moves away with almost no vertical spreading. 48

The stability of the air has a marked effect on the behaviour of plumes. In unstable conditions the vertical motions are large and well organised. They tend to break up the plume into discrete puffs, some of which reach the ground rather quickly. In neutral conditions there is still plenty of turbulence but the scale of the motions is smaller. These smaller eddies help the plume to expand but are not large enough to tear the plume apart so well. In stable conditions, the eddies are weak and small. The plume only grows slowly.

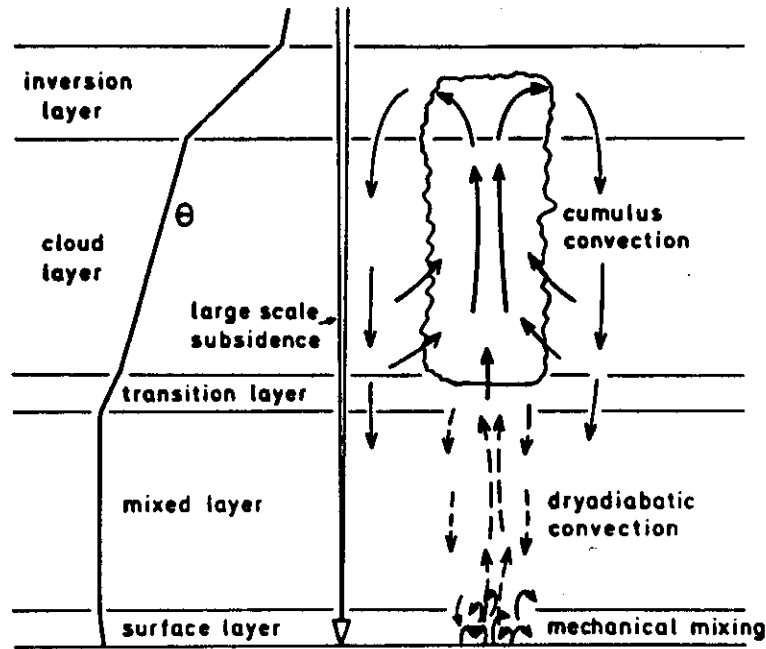
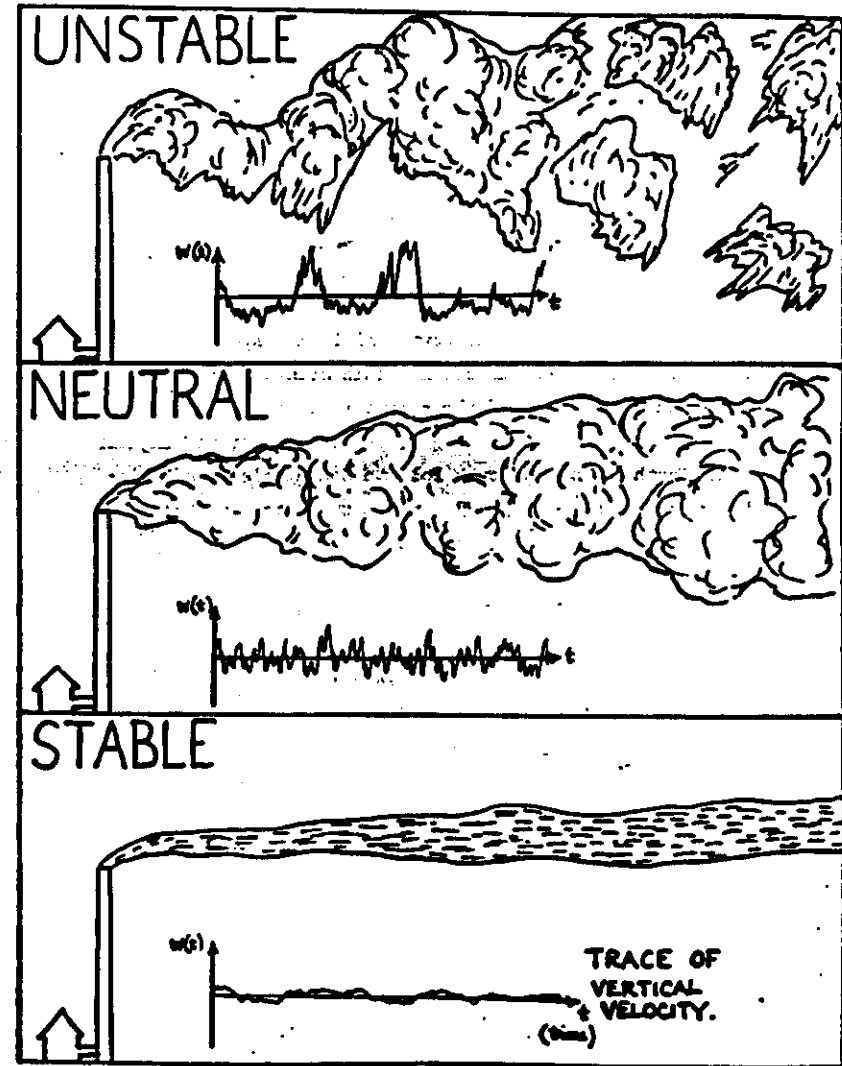
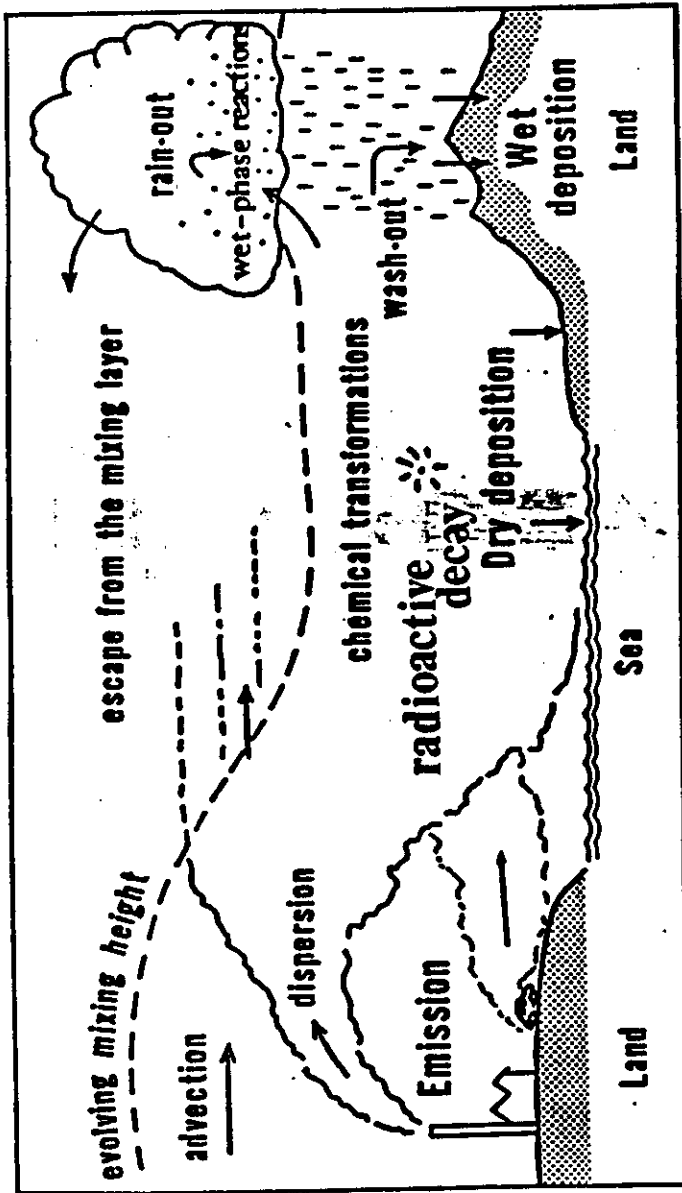


Figure 8. Scheme of dominant processes in a multilayered atmospheric boundary layer. θ = potential temperature.





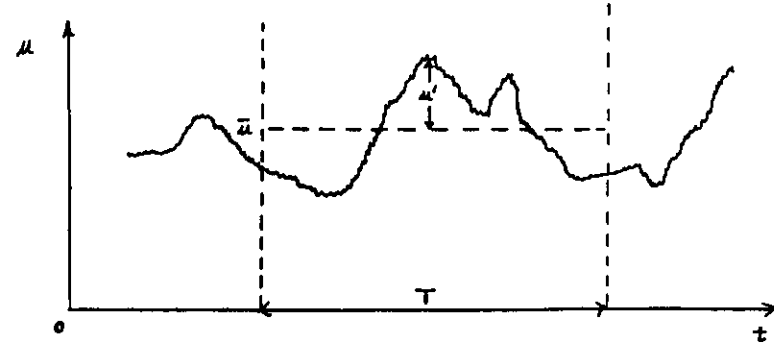
Processes involved in the deposition of atmospheric pollutants

Hazardous pollutants can be released from sources either continuously in very small amounts or accidentally in much larger amounts. The wind carries the pollutant away to affect other areas. Both wind speed and wind direction are important in this. Turbulence within the boundary layer will diffuse the pollutant both laterally and vertically. This spreads the "plume". This spreading is important; it mixes the material with other trace materials in the ambient airstream and may result in chemical transformations. The spreading will also result in the pollutant reaching the ground and the top of the boundary layer. In the former case, the pollutant may be taken up by the surface (dry deposition) whereas in the latter case some of the pollutant may leak out of the b.l. into the troposphere above. Radioactive decay may also take place. Sometimes the pollutant is affected by precipitation when it may be partly, if not wholly, washed out (wet deposition).

2. THE STATISTICAL DESCRIPTION OF TURBULENCE

2.1 Mean Values, Fluctuations and Variances

The quantitative specification of turbulent fluctuations relies on the principle that the whole motion can be resolved into a fluctuating component superimposed on a general mean flow.



Consider any quantity which will fluctuate because of the turbulent motion.

In particular, consider the wind vector \underline{v} .

Let $V(x,y,z,t) = \sqrt{u(x,y,z,t), v(x,y,z,t), w(x,y,z,t)}$ be the wind velocity at the point (x,y,z) (relative to the conventionally defined rectangular axes for atmospheric flow) at time t .

The mean velocity \bar{V} , with components $\bar{u}, \bar{v}, \bar{w}$, is defined at a fixed point at time t by,

$$\bar{u} = \frac{1}{T} \int_{t-\frac{1}{2}T}^{t+\frac{1}{2}T} u dt' ; \quad \bar{v} = \frac{1}{T} \int_{t-\frac{1}{2}T}^{t+\frac{1}{2}T} v dt' ; \quad \bar{w} = \frac{1}{T} \int_{t-\frac{1}{2}T}^{t+\frac{1}{2}T} w dt' , \tag{2.1.1}$$

where T is an arbitrary interval called the period of sampling or, simply the sampling time.

In general $\bar{V} = (\bar{u}, \bar{v}, \bar{w}) = f_n(x,y,z,t,T)$ and in practice there are complications in the interpretation of the term 'mean'.

If the mean velocity so constructed is to be characteristic of the motion as a whole then T must be sufficiently long to include an adequate number of fluctuations.

On the other hand a very long sample period might mask important changes that are taking place in the flow.



e.g. the general level of the velocity might be steadily rising or falling during the period chosen, so that the motion could not properly be represented by a single constant mean velocity. Strictly $\bar{V} \equiv \bar{V}(t)$.

A time-varying mean motion introduces many complications into the analysis and we shall suppose that either the mean flow is steady or that the changes in u, v, w are sufficiently rapid to allow an interval T to be defined in which $(\bar{u}, \bar{v}, \bar{w})$ vary only slowly. This greatly simplifies the analysis.

Having defined a mean flow \bar{V} , the instantaneous departure of the actual flow \underline{V} from the mean is defined by

$$\underline{V}' = \underline{V} - \bar{V} \quad (2.1.2)$$

i.e. $(u', v', w') = (u - \bar{u}, v - \bar{v}, w - \bar{w})$

The fluctuation \underline{V}' is often called the turbulent or eddy velocity.

Note that in steady mean flow $\bar{V}' \equiv 0$ since e.g.

$$\bar{u}' = \frac{1}{T} \int_{t-\frac{1}{2}T}^{t+\frac{1}{2}T} (u - \bar{u}) dt' = \bar{u} - \bar{u} = 0.$$

The relations $\overline{u'} = \overline{v'} = \overline{w'} = 0$ must be satisfied, either exactly or to a high degree of approximation, before progress can be made, and this is equivalent to assuming that some measure of regularity exists even in turbulent motion.

Because the fluctuations in the natural wind have periods varying from a fraction of a second to many minutes the choice of a period for the construction of a representative mean value is usually a matter of importance.

The above procedure is used to construct mean values of any other entities which fluctuate because of the turbulence, e.g. temperature, specific humidity, concentrations of pollutants such as SO₂, CO etc.

Most standard meteorological instruments are designed to give good approximations to the mean value over intervals of the order of a minute or so. The study of atmospheric turbulence means that the instruments must be specially designed to record the fluctuations themselves.

Other quantities are fundamental in any general statistical description of turbulent flow.

Let s be some fluctuating parameter such that

$$s = \bar{s} + s'$$

Variance of s

$$\sigma_s^2 = \frac{1}{T} \int_{t-\frac{1}{2}T}^{t+\frac{1}{2}T} (s - \bar{s})^2 dt' = \frac{1}{T} \int_{t-\frac{1}{2}T}^{t+\frac{1}{2}T} s'^2 dt' = \overline{s'^2} \quad (2.1.3)$$

Standard Deviation of s

$$\sigma_s = \sqrt{\overline{s'^2}} \quad (2.1.4)$$

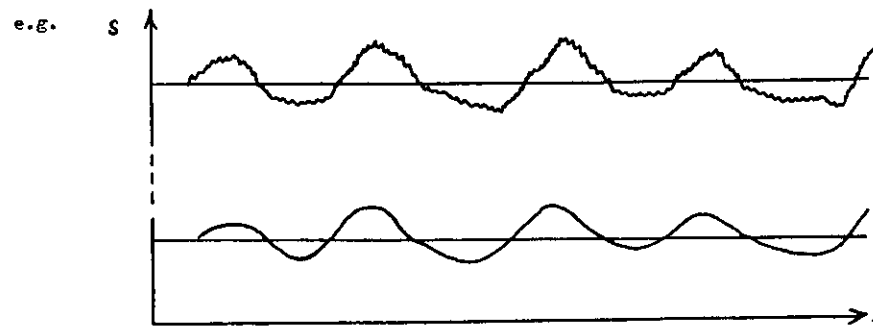
Intensity of turbulent fluctuations

$$i_s = \frac{\sigma_s}{\bar{s}} \quad (2.1.5)$$

ex. $\sigma_u^2 = \overline{u'^2}$ represents kinetic energy in the component of turbulent motion in the x-direction.

$i_u = \frac{[\overline{u'^2}]^{1/2}}{\bar{u}}$ specifies the intensity of the turbulent fluctuations.

The quantities σ_s , i_s provide a specification of the spread about the mean flow and the mixing quality of the flow. However, on their own they are insufficient to define the flow and its actions,



Both the above time series for s have roughly the same σ_s but the variations in s are quite different. We do not as yet have any measure of the rapidity of the fluctuations.

2.2 Concept of an Eddy and Prandtl Mixing-length Theory

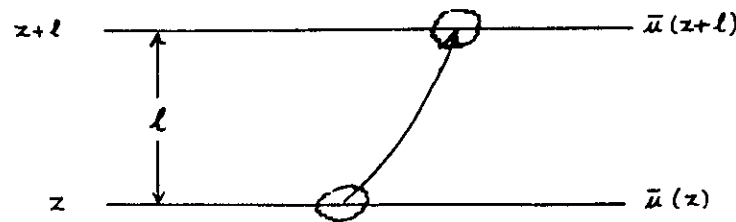
In early attempts to provide a general theoretical framework it was assumed that the turbulent fluctuations were a consequence of the random motions of discrete independent masses of fluid, called eddies. This led to the Prandtl mixing-length theory - see e.g. Sutton (1953) p.72.

As a result of the general disorder within the fluid motion, eddies were supposed to spring into existence in some undefined way and then after moving unaltered over a certain path, were supposed to become once more indistinguishable from the surrounding fluid. In this the life of an eddy was supposed to be something like that of a molecule of gas between successive collisions.

The idea of mixing action was implicit in the model and the length of the path of an eddy, analogous to the mean free path of a molecule, was termed the mixing-length.

Mixing-length theories are now mainly of historical interest. They provided a mechanistic picture of transport of fluid properties such as momentum, heat and water vapour at a rate proportional to the gradient of the particular quantity.

Consider the transfer of the u -component of the wind velocity:



The absorption of the eddy into the motion at the new level gives rise to a fluctuation u' where

$$\begin{aligned} u' &= \bar{u}(z+l) - \bar{u}(z) \\ &= l \frac{d\bar{u}}{dz} + \dots \end{aligned} \quad (2.2.1)$$

The mixing-length hypothesis is that l is a unique length which characterizes the local intensity of the turbulent mixing at any level but which, unlike the mean free path, may be a function of position and the flow properties.

The discontinuous action implied by such theories is quite artificial and the modern treatment of turbulent motion emphasizes the continuous nature of the motion.

Modern treatments stem from the work of G I Taylor (1921, 1935) - see Papers 14, 27, 28 in Taylor (1960) - who regarded the velocity as varying continuously in space and time.

2.3 Correlations, Scale of Turbulence and Taylor's Hypothesis

It is still useful to speak in terms of 'eddies' and a first step is to say something about their 'size'. This is done in terms of the differences in velocity existing instantaneously between one point and another in the fluid.

ex. Small eddies, as previously conceived, would impose differences in velocity between two relatively close points whereas large eddies would more often than not give velocities which would be similar at the two points.

The statistical representation is provided by the space-correlation coefficient between the velocities at two points a specified distance apart. If eddy sizes are large compared to this distance the correlation coefficient will tend to be high and vice versa.

Consider fluctuations in s at two points \underline{x} and $\underline{x} + \underline{r}$ in a turbulent fluid, the correlation between $s'(\underline{x})$ and $s'(\underline{x} + \underline{r})$ will, in general, vary with \underline{x} and \underline{r} .

The correlation coefficient between fluctuations separated by \underline{r} is

$$R_s(\underline{x}, \underline{r}) = \frac{\overline{s'(\underline{x}) s'(\underline{x} + \underline{r})}}{[\overline{s'^2(\underline{x})} \cdot \overline{s'^2(\underline{x} + \underline{r})}]^{1/2}} \quad (2.3.1)$$

and should generally decrease with increase of separation \underline{r} .

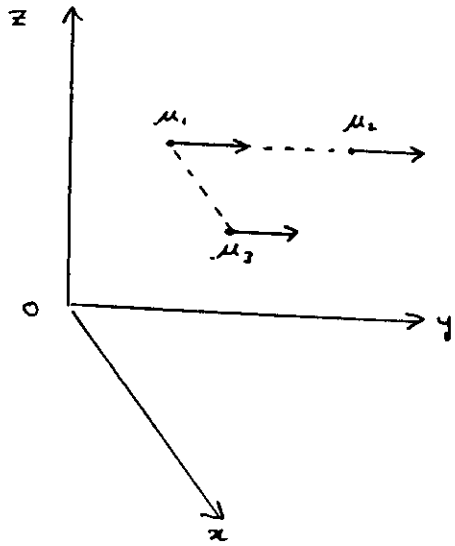


If the turbulence is homogeneous then the statistical properties $R_s(\underline{x}, \underline{r})$ and $\overline{s'^2(\underline{x})}$ are independent of position and we can write

$$R_s(\underline{r}) = \frac{\overline{s'(\underline{x}) s'(\underline{x} + \underline{r})}}{\overline{s'^2}} \quad (2.3.2)$$

HOMOGENEOUS AND ISOTROPIC TURBULENCE

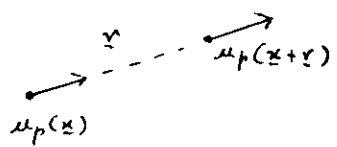
It is convenient to introduce the concepts of LONGITUDINAL and TRANSVERSE (or LATERAL) correlation coefficients.



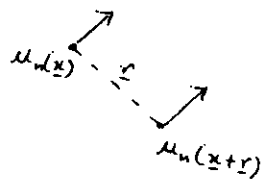
LONGITUDINAL CORRELATION BETWEEN u_1 and u_2

TRANSVERSE CORRELATION BETWEEN u_1 and u_3 .

More generally:



LONGITUDINAL where u_p is \parallel to r



TRANSVERSE where u_n is \perp to r
(i.e. u_n is normal to r)

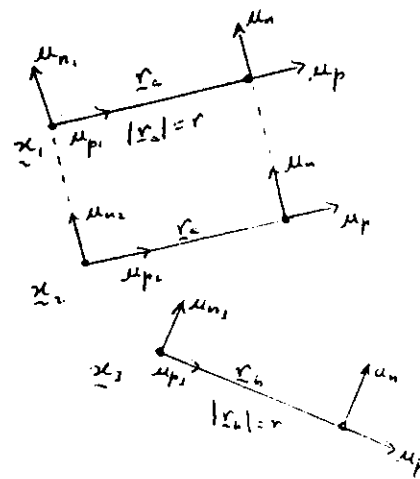
The distinction between the longitudinal and transverse forms is a consequence of the vector nature of the property being considered, and does not arise in the case of a scalar property such as temperature.

NB // For vector properties take care to correlate like components relative to the separation vector r .

HOMOGENEOUS TURBULENCE. The turbulence is homogeneous (spatially) if the statistical properties $R_p(x, r)$ and $\overline{v_i^2}(x)$ are independent of position, x .

i.e. The turbulence statistics depend only on the spatial separation of the two points ($r = x_2 - x_1$), not on x_1 and x_2 separately.

Example: R_{u_p} is the longitudinal correlation coefficient
 R_{u_n} is the transverse correlation coefficient.



$$R_{u_p} \neq R_{u_n}$$

$$\begin{cases} R_{u_{p1}} = R_{u_{p2}} \neq R_{u_{p3}} \\ R_{u_{n1}} = R_{u_{n2}} \neq R_{u_{n3}} \end{cases}$$

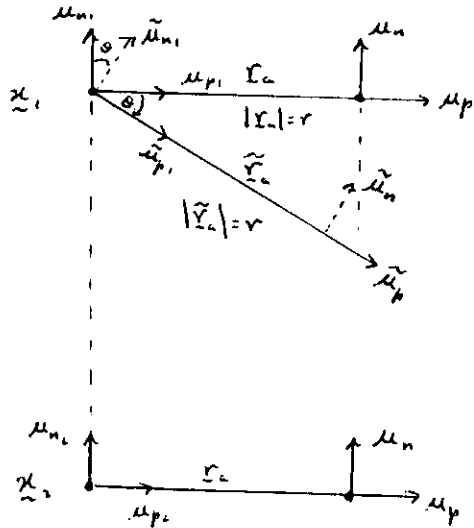
$$\begin{cases} R_{u_p} \equiv R_{u_p}(r) \\ R_{u_n} \equiv R_{u_n}(r) \end{cases}$$

ISOTROPIC TURBULENCE

The turbulence is isotropic if the statistical properties at a point are independent of orientation. The statistical properties depend only on position (\underline{x}) and scalar separation.

Example: R_{ij} , R_{uu} as defined above.

$$R_{ij} \neq R_{ji}$$



$$\begin{cases} R_{u_1 u_1} = R_{\tilde{u}_1 \tilde{u}_1} \neq R_{u_2 u_2} \\ R_{u_1 u_2} = R_{\tilde{u}_1 \tilde{u}_2} \neq R_{u_2 u_1} \end{cases}$$

$$\begin{cases} R_{ij} \equiv R_{ij}(\underline{x}, r) \\ R_{uu} \equiv R_{uu}(\underline{x}, r) \end{cases}$$

For practical work, the definition of (local) isotropy is most useful when combined with the property of homogeneity.

In that case, with reference to the above diagram:

$$R_{ij} \neq R_{ji}$$

$$\begin{cases} R_{u_1 u_1} = R_{\tilde{u}_1 \tilde{u}_1} = R_{u_2 u_2} \\ R_{u_1 u_2} = R_{\tilde{u}_1 \tilde{u}_2} = R_{u_2 u_1} \end{cases} \begin{cases} R_{ij} \equiv R_{ij}(r) \\ R_{uu} \equiv R_{uu}(r) \end{cases}$$

The sharpness of the decrease of $R_S(r)$ with r is a reflection of the eddy sizes and can be represented by a length l_s along some axis, defined by

$$l_s = \int_0^{\infty} R_S(r) dr \quad (2.3.3)$$

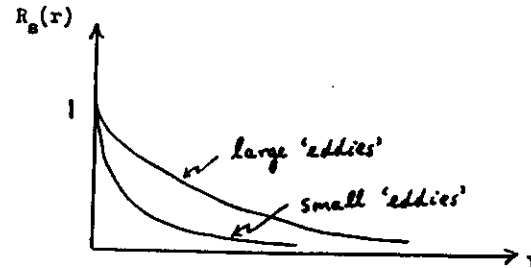
provided that the integral converges.

The length l_s called the integral scale of turbulence represents the 'average size of the eddies' or length scale of the fluctuations, without implying any definite model of an eddy.

Recap

Remember that we are trying to change our concept of an eddy from that of the classical theories where eddies are thought of as discrete independent masses of fluid which spring into existence due to the general disorder within the fluid motion and then transport properties of the flow over some length, l , before again being mixed into the surrounding fluid. The mixing-length, l , in such theories gives a measure of the size of the transporting eddies.

We are now trying to reformulate the eddy concept in terms of the statistical properties of the continuously varying turbulent motions and the first step is to say something about the 'eddy' size. For this purpose we correlate the instantaneous fluctuations in the flow at two points in the fluid and an indication of eddy size is provided by the sharpness of the decrease of $R_S(r)$, or, equivalently, by the area under the $R_S(r)$ curve.



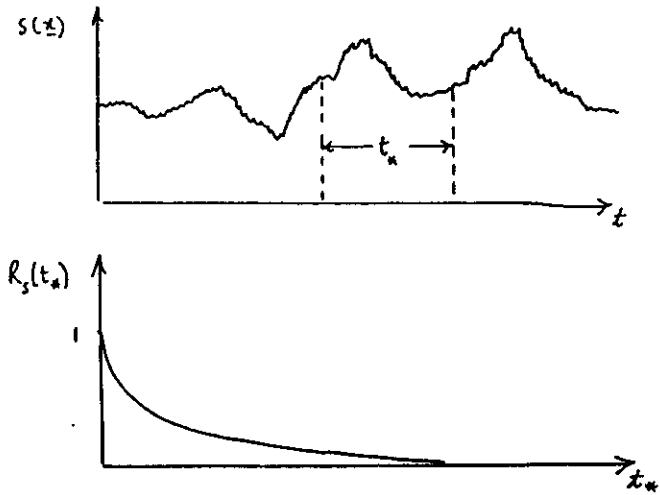
It is not easy to simply redefine an eddy in the new framework. The 'eddy' must either be thought of in classical terms as a discrete mass of fluid or this physical picture must be abandoned and the eddy concept accepted in terms of scales of turbulence defined in a statistical sense.

A time-correlation coefficient, $R_S(t_*)$, an auto-correlation coefficient, is also defined in terms of the eddy fluctuations at a fixed point at instants separated by t_* .

$$R_S(t_*) = \frac{\overline{s'(\underline{x}, t) s'(\underline{x}, t+t_*)}}{\overline{s'^2(\underline{x})}}$$

for homogeneous, stationary turbulent flow.

In an analogous fashion to the fall of $R_s(r)$ with increasing r , $R_s(t_*)$ decreases with increasing t_* .



If $R_s(t_*)$ falls away rapidly from $t_* = 0$ then the eddies are very small, if slowly then the eddies are large.

Just as we defined an integral length scale l_s in terms of $R_s(r)$, so we can define an integral time-scale τ_s such that

$$\tau_s = \int_0^{\infty} R_s(t_*) dt_* \quad (2.3.5)$$

Taylor's Hypothesis for Homogeneous, Steady Turbulence

If the sequence of variations of s at a fixed point is assumed to be determined by the passage over the fixed point of an unchanging pattern of turbulence, it follows that, along the direction of the mean flow

$$R_s(t_*) = R_s(r) \quad \text{where } r = \bar{u}t_* \quad (2.3.6)$$

This is also called the frozen-turbulence approximation and it can be shown from considerations based on the equations of motion that it is valid only if u is very large compared to the rate at which the fluctuations are changing. e.g. $u'/\bar{u} \ll 1$.

$$\left. \begin{aligned} R_s(t_*) &= \frac{s'(x,t) s'(x,t+t_*)}{\overline{s'^2}} \\ R_s(-r) &= \frac{s'(x,t) s'(x-r,t)}{\overline{s'^2}} \end{aligned} \right\}$$

If the turbulence is 'frozen-in' then

$$s'(x, t+t_*) = s'(x-r, t)$$

where

$$t_* = r/\bar{u}$$

$$\therefore R_s(t_*) = R_s(-r).$$

Since flow is homogeneous, $R_s(r)$ is an even function.

$$R_s(r) = \frac{s'(x,t) s'(x+r,t)}{\overline{s'^2}}$$

$$\text{Put } X = x+r \quad = \frac{s'(x-r,t) s'(x,t)}{\overline{s'^2}} = R_s(-r)$$

$$\therefore \underline{R_s(t_*) = R_s(r)}$$

It follows that

$$l_s = \int_0^{\infty} R_s(r) dr = \bar{u} \int_0^{\infty} R_s(t_*) dt_* = \bar{u} \tau_s$$

i.e.

$$\underline{l_s = \bar{u} \tau_s} \quad (2.3.7)$$

2.4. The One-dimensional Spectrum of Turbulence

The introduction of $R_s(t_*)$ and τ_s helps to characterize the rapidity with which the variations in s are occurring.

If the fluctuations are occurring slowly then even for fairly big values of t_* the instrument will be affected by much the same value of s , $R_s(t_*)$ will remain high, and τ_s will be fairly large. On the other hand, with predominantly rapid fluctuations, $R_s(t_*)$ will show a substantial fall even for small values of t_* and τ_s will tend to be small.

We can go further with this last idea, for if the variations are composed of some rather rapid fluctuations superimposed on some rather slow ones, then the former will tend to make $R_s(t_*)$ fall off rapidly at first, while the latter will tend to maintain it at a moderately high level for appreciable values of t_* .

To generalise; the precise shape of the correlogram will reflect the manner in which the whole variation is subscribed to by various frequencies of oscillation.

The variance $\overline{s'^2}$ measures the average level of the turbulent energy and is thus built up by contributions from fluctuations of different frequencies.

The energy spectrum or power spectrum function $F_s(n)$, where n is frequency, is defined such that the fractional contribution to the variance $\overline{s'^2}$ from frequencies between n and $n + dn$ is $F_s(n) dn$.

$$\text{Thus } \overline{s'^2} = \int_0^{\infty} \overline{s'^2} F_s(n) dn$$

$$\text{or } \int_0^{\infty} F_s(n) dn = 1 \quad (2.4.1)$$

$F_s(n)$ is also called the spectral density.

Using Fourier analysis techniques Taylor showed that $R_s(t_*)$ and $F_s(n)$ are related by

$$R_s(t_*) = \int_0^{\infty} F_s(n) \cos 2\pi n t_* dn \quad (2.4.2)$$

and therefore from the Fourier integral theorem

$$F_s(n) = 4 \int_0^{\infty} R_s(t_*) \cos 2\pi n t_* dt_* \quad (2.4.3)$$

Therefore, knowing $R_s(t_*)$, $F_s(n)$ can be calculated and vice versa.

The immediate practical importance of this approach is that it brings out the idea of a continuous range of eddy sizes (size being identified with inverse frequency) and provides a way of identifying those sizes which are of most significance as regards kinetic energy.

On physical grounds a relation must exist between $R_s(t_*)$ and $F_s(n)$.

For large eddies $R_s(t_*)$ falls to zero with increasing t_* more slowly than when the eddies are small. Hence if $R_s(t_*)$ has a large spread on the t_* -axis, the spectrum will be restricted to relatively low frequencies, and vice versa.

Turbulent fluctuations are usually measured as variations in time rather than space and hence it is appropriate to introduce the spectrum of turbulence in terms of frequency. However, there is also a need to discuss variations in space and as then we can replace $R_s(t_*)$ by $R_s(r)$ so we can replace $F_s(n)$ by

Because it refers to the fractional contribution rather than the absolute contribution to the variance, $F_s(n)$ is often described as the normalised, 1-dimensional energy spectrum, power spectrum function or spectral density. A corresponding absolute spectrum function $S_s(n) = \overline{s'^2} F_s(n)$ is defined by

$$\int_0^{\infty} S_s(n) dn = \overline{s'^2}$$

34

normalised

$F_s(k)$ a/wave number power spectrum function where $F_s(n)$ and $F_s(k)$ along the mean flow direction are usually assumed to be related by the Taylor hypothesis in the sense that

Also, we can define an absolute wave number power spectrum function, $S_s(k) = \overline{s'^2} F_s(k)$ (2.4.4)

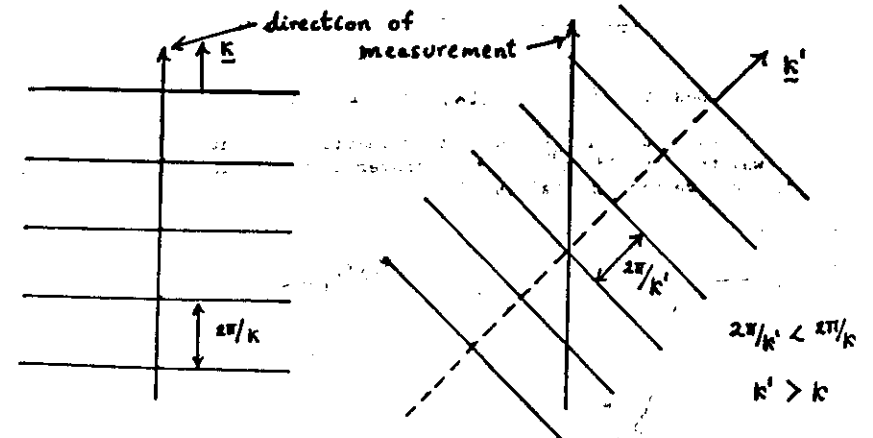
We note that $\overline{s'^2} F_s(n) = S_s(k)$ where $n = \overline{u} k$

$$[F_s(n)]_{n=0} = 4 \int_0^{\infty} R_s(t_*) dt_* = 4 \tau_s \quad (2.4.5)$$

and $[F_s(k)]_{k=0} = 4 \int_0^{\infty} R_s(r) dr = 4 l_s \quad (2.4.6)$

The integral scale is determined by the very slow or very large-scale fluctuations. Consequently the evaluation of the true scale is often very difficult or even impossible in practice.

Note that $F_s(n)$, $F_s(k)$ are one-dimensional spectra describing fluctuations along a line. These are to be distinguished from 3-dimensional spectral functions. The finite limit of $F_s(k)$ as $k \rightarrow 0$ represents a projected effect of 'waves' with finite wave number and with the normals to their crests inclined to the reference line.



When plotting $F_s(n)$ a wide range of frequencies is normally involved, though the majority of the change in $F_s(n)$ occurs at low frequencies. The result of the $F_s(n)$ vs n plot is a very awkward spectrum shape.

It is more common to plot $n F_s(n) vs. \ln n$ which gives a much more convenient graph while preserving the condition that the area under the curve, between specified limits of n , still represents the fraction of the total variance contributed by frequencies between these limits

$$\text{i.e.} \quad \int_{n_1}^{n_2} n F_s(n) d(\ln n) = \int_{n_1}^{n_2} F_s(n) dn \quad (2.4.7)$$

Furthermore the frequency n_m at which the logarithmic spectral density is maximum can be related to τ_s (or alternatively, k_m can be related to l_s).

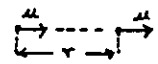
This is a useful device for estimating the time-scale (length-scale) when the complete spectrum is not observed on the low frequency side - though one can only apply it by making some assumption about the shape of the complete spectrum.

Example Two common one-dimensional spectra

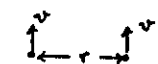
Some correlation curves have negative tails; many do not.

Consider a steady 2-dim flow such that $\bar{v} = (\bar{u}, \bar{v}, \bar{w}) = (\bar{u}, 0, 0)$

i.e. $\bar{w} = \bar{v} = 0$.

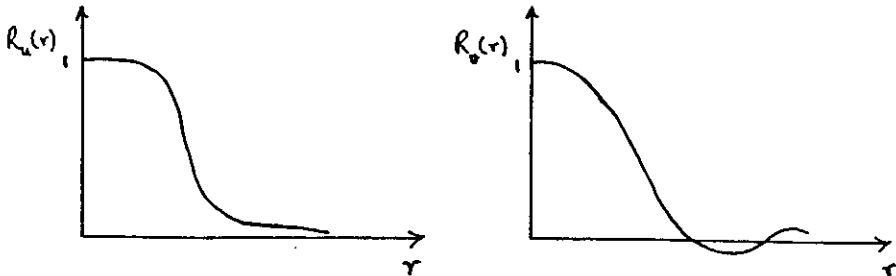
Longitudinal correlation $R_u(r) = \int_0^\infty F_u(k) \cos 2\pi k r dk$ 

Longitudinal spectrum

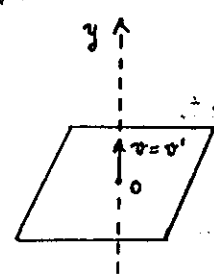
Transverse correlation $R_v(r) = \int_0^\infty F_v(k) \cos 2\pi k r dk$ 

The shapes of $F_u(k)$ and $F_v(k)$ are somewhat different.

Measured values of $R_u(r)$ do not ordinarily go negative (though there is no reason why they should not). The transverse correlation $R_v(r)$, however, does become negative for some values of r .



Consider a plane perpendicular to the y-direction.



Across this plane there should be no net mass flux since $\bar{v} \equiv 0$.

$$\therefore \int_{-\infty}^{\infty} \int_{-\infty}^{\infty} v(x, 0, z) dx dz = 0$$

Multiply by v at a particular point $(x_m, 0, z_m)$,

$$v(x_m, 0, z_m) \int_{-\infty}^{\infty} \int_{-\infty}^{\infty} v(x, 0, z) dx dz = 0$$

$$\therefore \int_{-\infty}^{\infty} \int_{-\infty}^{\infty} v'(x_m, 0, z_m) v'(x, 0, z) dx dz = 0$$

Put $x = x_m - r_x$ and $z = z_m - r_z$,

then

$$\int_{-\infty}^{\infty} \int_{-\infty}^{\infty} v'(x+r_x, 0, z+r_z) v'(x, 0, z) dr_x dr_z = 0$$

$$\text{i.e.} \quad \int_{-\infty}^{\infty} \int_{-\infty}^{\infty} R_v(r_x, 0, r_z) dr_x dr_z = 0$$

Therefore R_v must go negative somewhere in the x, z -plane. In other words, back flow is necessary somewhere in the plane in order to keep the net mass flux zero.

Example The Exponential Correlogram: See Fig. B

Consider a correlogram assumed to decay exponentially.

Atmospheric correlograms can sometimes be approximately represented in this way.

$$R_s(t_*) = \exp(-t_*/\tau_s) \quad (2.4.8)$$

$$\begin{aligned} F_s(n) &= 4 \int_0^{\infty} R_s(t_*) \cos 2\pi n t_* dt_* \\ &= 4 \tau_s \int_0^{\infty} e^{-t} \cos(2\pi n \tau_s t) dt \\ &= \frac{4 \tau_s}{(2\pi n \tau_s)^2 + 1} \end{aligned} \quad (2.4.9)$$

$$\begin{aligned} \left[I = \int_0^{\infty} e^{-t} \cos(2\pi n \tau_s t) dt \right. &= \left. \frac{e^{-t} \sin(2\pi n \tau_s t)}{2\pi n \tau_s} \right]_0^{\infty} + \int_0^{\infty} \frac{e^{-t} \sin(2\pi n \tau_s t)}{2\pi n \tau_s} dt \\ &= \left. -\frac{e^{-t} \cos(2\pi n \tau_s t)}{(2\pi n \tau_s)^2} \right]_0^{\infty} - \frac{I}{(2\pi n \tau_s)^2} = \frac{(1-I)}{(2\pi n \tau_s)^2} \\ \therefore I &= \frac{1}{(2\pi n \tau_s)^2 + 1} \end{aligned}$$

From (2.4.9) we have $\frac{F_s(n)}{\tau_s} = \frac{4}{a^2 + 1}$ (2.4.10)

where $a = 2\pi n \tau_s$ (2.4.11)

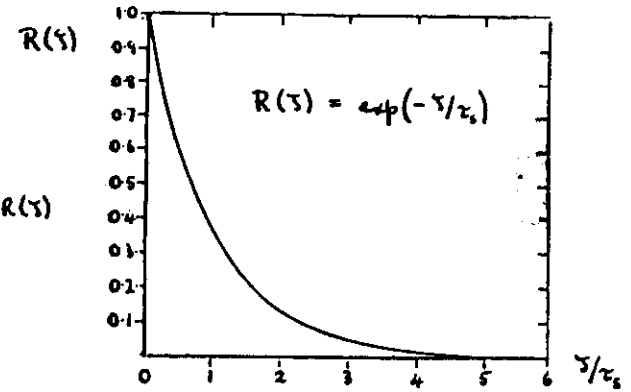
Note that $F_s(0) = 4 \tau_s$.

$$\begin{aligned} n F_s(n) &= \frac{4 n \tau_s}{(2\pi n \tau_s)^2 + 1} \\ &= \frac{2a}{\pi(a^2 + 1)} \end{aligned} \quad (2.4.12)$$

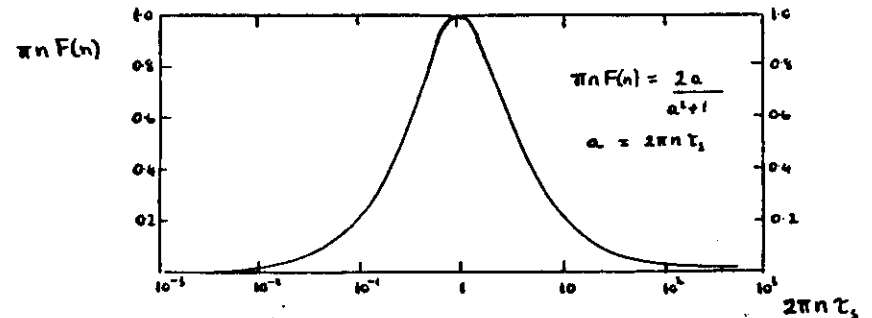
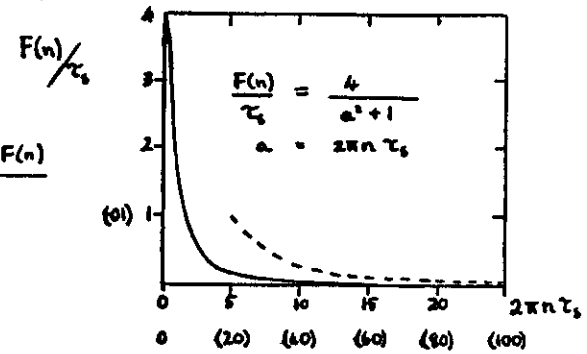
18

8

THE EXPONENTIAL
AUTO-CORRELOGRAM, $R(\tau)$



THE CORRESPONDING
SPECTRAL DENSITY, $F(n)$



THE CORRESPONDING LOGARITHMIC SPECTRAL DENSITY CURVE, $\pi n F(n)$

$$\left[n F_s(n) \right]_{\max} = 1/\pi \quad \text{at } n_*$$

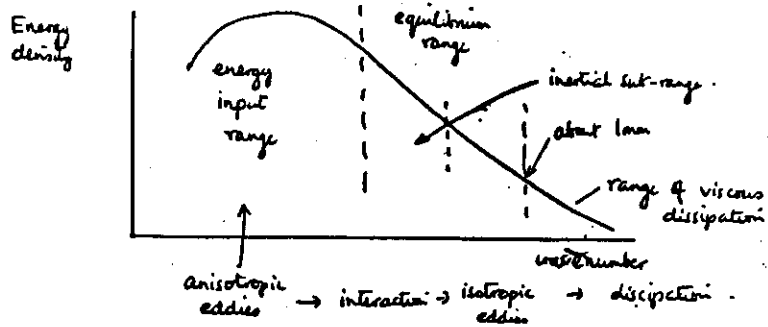
where $2\pi n_* \tau_s = 1$ (2.4.13)

i.e. $\tau_s = l_s / \bar{\mu} = 1 / 2\pi n_*$

and $l_s = \frac{\bar{\mu}}{2\pi n_*} = \frac{1}{2\pi k_*}$, since $n_* = \bar{\mu} k_*$ (2.4.14)

In this case there exist very simple relationships between τ_s and n_* and l_s and k_* .

It has been postulated that a universal equilibrium will exist when the Reynolds number is large enough (as it invariably is in atmospheric turbulence) for the energy-containing eddies and the dissipation ranges of lower number (the very small eddies when viscosity extracts kinetic energy) are to be widely separated. There may exist a considerable subrange within and at the lower end of the equilibrium range in which negligible dissipation occurs. Within this inertial subrange, the transfer of energy by inertial forces is the dominant processes (i.e. the transfer of energy to higher & higher wavenumbers - smaller & smaller "eddies" - by the stretching and pulling out of vortex lines by the interaction between eddies)



rate of energy transfer = ϵ = rate of energy dissipation / viscosity ν .

In the equilibrium range $E(x)$ must be a function of x, ϵ & ν .
On dimensional grounds:

$$E(x) = (\nu^5 \epsilon)^{1/4} F(x \nu^{-3/4} \epsilon^{-1/4})$$

The length $(\nu^2/\epsilon)^{1/4}$ is known as the Kolmogorov microscale and is regarded as defining the order of wavelength below which viscous action begins effectively to annihilate the turbulence. For measurement in the inertial sub-range, ν must drop out in the atmospheric boundary layer.

$$\therefore F(x \nu^{-3/4} \epsilon^{-1/4}) \approx (x \nu^{-3/4} \epsilon^{-1/4})^{-5/3} \text{ this microscale has a magnitude of order } l_{mm}$$

in order to cancel the $\nu^{3/4}$ in the coefficient

Then
$$E(x) = \alpha \epsilon^{2/3} x^{-5/3} \text{ for 3-dimensional turbulence}$$

$E(k)$ is the 3-dimensional energy spectrum function, defined by

$$\int_0^{\infty} E(k) dk = \overline{u'^2} + \overline{v'^2} + \overline{w'^2}$$

which is a measure of the mean turbulent kinetic energy.

$$\begin{cases} T = 2.26 \text{ km}^4 \\ -z = 7.27 \times 10^{-5} \text{ s}^{-1} \end{cases}$$

3. WIND AND SHEARING STRESS PROFILES IN THE ATMOSPHERIC BOUNDARY LAYER

3.1 The Equations of Motion and Continuity

The basic equations of motion for atmospheric flow are the Navier-Stokes equations for a viscous fluid:

$$\frac{D\underline{V}}{Dt} = \frac{\partial \underline{V}}{\partial t} + (\underline{V} \cdot \nabla) \underline{V} = -\frac{1}{\rho} \nabla p + f \underline{V} \times \underline{k} - g \underline{k} + \nu \nabla^2 \underline{V} + \frac{1}{3} \nabla (\nabla \cdot \underline{V}) \quad (3.1.1)$$

where ν is the kinematic viscosity ($= \mu/\rho$ where μ is dynamic viscosity), and the continuity equation is

$$\frac{D\rho}{Dt} + \rho \nabla \cdot \underline{V} = 0. \quad (3.1.2)$$

Further, let us assume at this stage that the atmospheric flow is incompressible and so

$$\frac{D\rho}{Dt} = 0. \quad (3.1.3)$$

The momentum equations become

$$\frac{\partial \underline{V}}{\partial t} + (\underline{V} \cdot \nabla) \underline{V} = -\frac{1}{\rho} \nabla p + f \underline{V} \times \underline{k} - g \underline{k} + \nu \nabla^2 \underline{V} \quad (3.1.4)$$

and the continuity equation is

$$\nabla \cdot \underline{V} = 0. \quad (3.1.5)$$

For turbulent flow we can write

$$\underline{V} = \overline{\underline{V}} + \underline{V}' \quad (3.1.6)$$

$$p = \overline{p} + p' \quad (3.1.7)$$

and we shall assume that the fluctuations in ρ from the mean value $\overline{\rho}$ are small.

By introducing the fluctuating and mean quantities into the equations of motion and continuity and averaging we obtain the equations for the mean motion

$$\frac{D\overline{\underline{V}}}{Dt} = -\frac{1}{\rho} \nabla \overline{p} + f \overline{\underline{V}} \times \underline{k} - g \underline{k} + \nu \nabla^2 \overline{\underline{V}} - \overline{(\underline{V}' \cdot \nabla) \underline{V}'} \quad (3.1.8)$$

where

$$\frac{D}{Dt} \equiv \frac{\partial}{\partial t} + (\overline{\underline{V}} \cdot \nabla), \quad \text{and} \quad \nabla \cdot \overline{\underline{V}} = 0. \quad (3.1.9)$$

Comparing (3.1.8) with (3.1.4) we see that we have additional terms which are independent of viscosity but depend on the fluctuations;

$$\begin{aligned} \overline{(\underline{V}' \cdot \nabla) \underline{V}'} &= \left(\frac{\partial}{\partial x} \overline{u'v'} + \frac{\partial}{\partial y} \overline{u'w'} + \frac{\partial}{\partial z} \overline{u'u'} \right) \begin{pmatrix} u' \\ v' \\ w' \end{pmatrix} \\ &= \left(\frac{\partial}{\partial x} \overline{u'^2} + \frac{\partial}{\partial y} \overline{u'v'} + \frac{\partial}{\partial z} \overline{u'w'} \right) \begin{pmatrix} u' \\ v' \\ w' \end{pmatrix} + \left(\frac{\partial}{\partial x} \overline{v'u'} + \frac{\partial}{\partial y} \overline{v'^2} + \frac{\partial}{\partial z} \overline{v'w'} \right) \begin{pmatrix} u' \\ v' \\ w' \end{pmatrix} + \left(\frac{\partial}{\partial x} \overline{w'u'} + \frac{\partial}{\partial y} \overline{w'v'} + \frac{\partial}{\partial z} \overline{w'^2} \right) \begin{pmatrix} u' \\ v' \\ w' \end{pmatrix} \end{aligned} \quad (3.1.10)$$

where we have made use of $\nabla \cdot \underline{V}' = 0$ from the continuity equation.

Now the term $\nu \nabla^2 \bar{V}$ can be written in terms of the viscous stresses defined by

$$F_{ij} = \mu \left(\frac{\partial \bar{u}_j}{\partial x_i} + \frac{\partial \bar{u}_i}{\partial x_j} \right) \quad \text{where } \mu = \nu \rho. \quad (3.1.11)$$

eg The normal viscous stresses are

$$F_{11} = 2\mu \frac{\partial \bar{u}}{\partial x} \quad \text{etc}$$

and the tangential stresses are

$$F_{12} = \mu \left(\frac{\partial \bar{v}}{\partial x} + \frac{\partial \bar{u}}{\partial y} \right) \quad \text{etc}$$

Using these definitions of F_{ij} and the continuity equation we can write

$$\nu \nabla^2 \bar{V} = \frac{1}{\rho} \left[\frac{\partial F_{11}}{\partial x} + \frac{\partial F_{12}}{\partial y} + \frac{\partial F_{13}}{\partial z}, \frac{\partial F_{21}}{\partial x} + \frac{\partial F_{22}}{\partial y} + \frac{\partial F_{23}}{\partial z}, \frac{\partial F_{31}}{\partial x} + \frac{\partial F_{32}}{\partial y} + \frac{\partial F_{33}}{\partial z} \right]$$

In an analogous fashion we see that we can now define stresses additional to the viscous stresses by

$$\tau_{ij} = -\rho \overline{u'_i u'_j} \quad (3.1.12)$$

such that

$$-\rho (\bar{V}' \cdot \nabla) \bar{V}' = \left[\frac{\partial \tau_{11}}{\partial x} + \frac{\partial \tau_{12}}{\partial y} + \frac{\partial \tau_{13}}{\partial z}, \frac{\partial \tau_{21}}{\partial x} + \frac{\partial \tau_{22}}{\partial y} + \frac{\partial \tau_{23}}{\partial z}, \frac{\partial \tau_{31}}{\partial x} + \frac{\partial \tau_{32}}{\partial y} + \frac{\partial \tau_{33}}{\partial z} \right] \quad (3.1.13)$$

These additional stresses are called the Reynolds stresses and as we shall see they indicate that the turbulent fluctuations cause transport of momentum across a surface in the fluid.

before proceeding further we make two observations:

- (i) In general the Reynolds stresses are much larger than the purely viscous stresses in the atmospheric boundary layer and we shall henceforth neglect the term $\nu \nabla^2 \bar{V}$.
- (ii) In boundary layer flow, changes in the horizontal plane are generally very small when compared to changes in the vertical.

Thus we may simplify (3.1.13) to

$$-\rho (\bar{V}' \cdot \nabla) \bar{V}' = \left(\frac{\partial \tau_{13}}{\partial z}, \frac{\partial \tau_{23}}{\partial z}, \frac{\partial \tau_{33}}{\partial z} \right) \quad (3.1.14)$$

and define the vector \bar{T} such that

$$\begin{aligned} \bar{T} &= (\tau_x, \tau_y, \tau_z) \equiv (\tau_{13}, \tau_{23}, \tau_{33}) \\ &= (-\rho \overline{u'w'}, -\rho \overline{v'w'}, -\rho \overline{w'^2}) \end{aligned} \quad (3.1.15)$$

The basic equations of motion for the mean flow in the atmospheric boundary layer are therefore

$$\frac{\partial \bar{V}}{\partial t} = \frac{\partial \bar{V}}{\partial t} + (\bar{V} \cdot \nabla) \bar{V} = -\frac{1}{\rho} \nabla \bar{p} + f \bar{V} \times \mathbf{k} - g \mathbf{k} + \frac{1}{\rho} \frac{\partial \bar{T}}{\partial z} \quad (3.1.16)$$

If we restrict these equations to the case of horizontal mean flow, $\bar{w} = 0$, we have

$$\frac{\partial \bar{V}}{\partial t} = \frac{\partial \bar{V}}{\partial t} + (\bar{V} \cdot \nabla) \bar{V} = -\frac{1}{\rho} \nabla \bar{p} + f \bar{V} \times \mathbf{k} + \frac{1}{\rho} \frac{\partial \bar{T}}{\partial z} \quad (3.1.17)$$

where $\bar{V} = (\bar{u}, \bar{v})$, $\nabla = \mathbf{i} \frac{\partial}{\partial x} + \mathbf{j} \frac{\partial}{\partial y}$,

and $\bar{T} = (\tau_x, \tau_y) = (\tau_{13}, \tau_{23}) = (-\rho \overline{u'w'}, -\rho \overline{v'w'})$. (3.1.18)

\bar{T} defines a tangential stress and is called the eddy shearing stress.

3.2 The Eddy Shearing Stress

\bar{T} may be thought of in 3 ways:

- (i) It represents the tangential shearing force exerted by one horizontal layer of air upon a second layer immediately in the proximity of the first. It is usually assumed that the force arises from the difference in mean velocity of the two layers resulting in the simplest situations from the motion of the atmosphere as a whole relative to the surface.
- (ii) It represents the vertical transport of momentum by the turbulent fluctuations. Since the ground exerts a drag on the moving air above, the momentum of the air near the ground would be rapidly lost unless it were replaced by this vertical flux of momentum downwards from above. The balance of the sink of momentum at the ground and the vertical flux of momentum largely determines the nature of the wind profile.

Definition: We can define the atmospheric boundary layer as that from which momentum is directly extracted and transferred downwards to overcome surface friction.

The mass of air crossing unit horizontal area in unit time is $\rho \bar{w}$. The vertical flux of any physical property s per unit mass of air is given by $\rho \bar{w}s$.

The mean flux is therefore $\rho \bar{w}s = \rho \bar{w} \bar{s} + \rho \overline{w's'}$

where it has been assumed that $\rho \propto \bar{e}$.

$\rho \bar{w} \bar{s}$ is the vertical flux of s by the mean motion (it is often assumed that $\bar{w} = 0$).

$\rho \overline{w's'}$ is the vertical flux of s by the turbulent fluctuations.

Thus the upward flux of momentum = $(\rho \overline{u'w'}, \rho \overline{v'w'})$.

Therefore $\bar{T} = (-\rho \overline{u'w'}, -\rho \overline{v'w'})$, the horizontal shearing stress is a measure of the downward flux of horizontal momentum.

- (iii) It represents the correlation between the vertical fluctuations of the wind vector and the horizontal fluctuations at any given point.

One method of measuring \bar{T} is to use very sensitive anemometers to form the eddy covariances $\overline{u'w'}$, $\overline{v'w'}$.

Although direct, this method suffers from the sampling errors arising from low-frequency eddies as previously discussed.

Most theoretical discussions treat \bar{T} as a function of z only, although in reality it will also be a function of x, y, t .

It is useful, as we shall see later, to define a velocity $V_a(z) = (\tilde{u}_a(z), \tilde{v}_a(z))$ such that

$$\tilde{u}_a(z) = \left| \frac{\tau_x(z)}{\rho} \right|^{1/2} = (|\overline{u'w'}|)^{1/2}, \quad (3.2.1)$$

$$\tilde{v}_a(z) = \left| \frac{\tau_y(z)}{\rho} \right|^{1/2} = (|\overline{v'w'}|)^{1/2}.$$

$V_a(z)$ is called the friction velocity and its components are essentially a measure of the correlation between u' and w' , and v' and w' .

Conventionally, the term friction velocity is also used for the speed

$$u_* (z) = \left[\frac{\tau(z)}{\rho} \right]^{1/2} \quad (3.2.2)$$

A particularly important value of $u_* (z)$ is the surface friction velocity defined by

$$u_* \equiv u_* (0) = \left[\frac{\tau(0)}{\rho} \right]^{1/2} \quad (3.2.3)$$

where $\tau(0)$ is the magnitude of the surface shearing stress.

The stress profile $\tau(z)$ depends on many factors but generally $\tau(z) = |\tau(z)|$ has its highest value at the ground and falls off to zero or some relatively small residual value at the 'top' of the boundary layer.

Definition This gives us a more formal definition of the atmospheric boundary layer or friction layer as the layer adjacent to the ground where turbulent stresses are significant.

Let h , the top of the boundary layer be defined such that

$$\tau(z) \leq \epsilon \quad \text{for } z > h \quad \text{where } \epsilon \text{ is a small parameter, ideally zero; i.e. we shall assume } \tau(z) = 0 \quad \text{for } z > h.$$

Although many single values of the shearing stress have been measured, directly measured profiles are only about to become readily available. There is such a lack of suitable atmospheric boundary layer data that even estimates of the nature of the full shearing stress profile are very scarce and these require restrictive assumptions about the general conditions or some statement about the relationship between the stress profile and the velocity profile.

3.3 The Geostrophic Departure Method for Deriving $\tau(z)$

Assuming stationarity and horizontal homogeneity for all the relevant variables, including the pressure gradient, the basic boundary layer equations of motion reduce to

$$\frac{\partial \tau}{\partial z} = -f \rho (\bar{V} - \underline{V}_g) \times \underline{k} \quad (3.3.1)$$

$$\text{where } \underline{V}_g = \frac{1}{f} (\underline{k} \times \nabla \bar{p}) \quad (3.3.2)$$

defines the geostrophic wind vector at any height z .

The mean wind near the surface \bar{V} can be regarded as the geostrophic wind modified by friction.

Integrate (3.3.1):

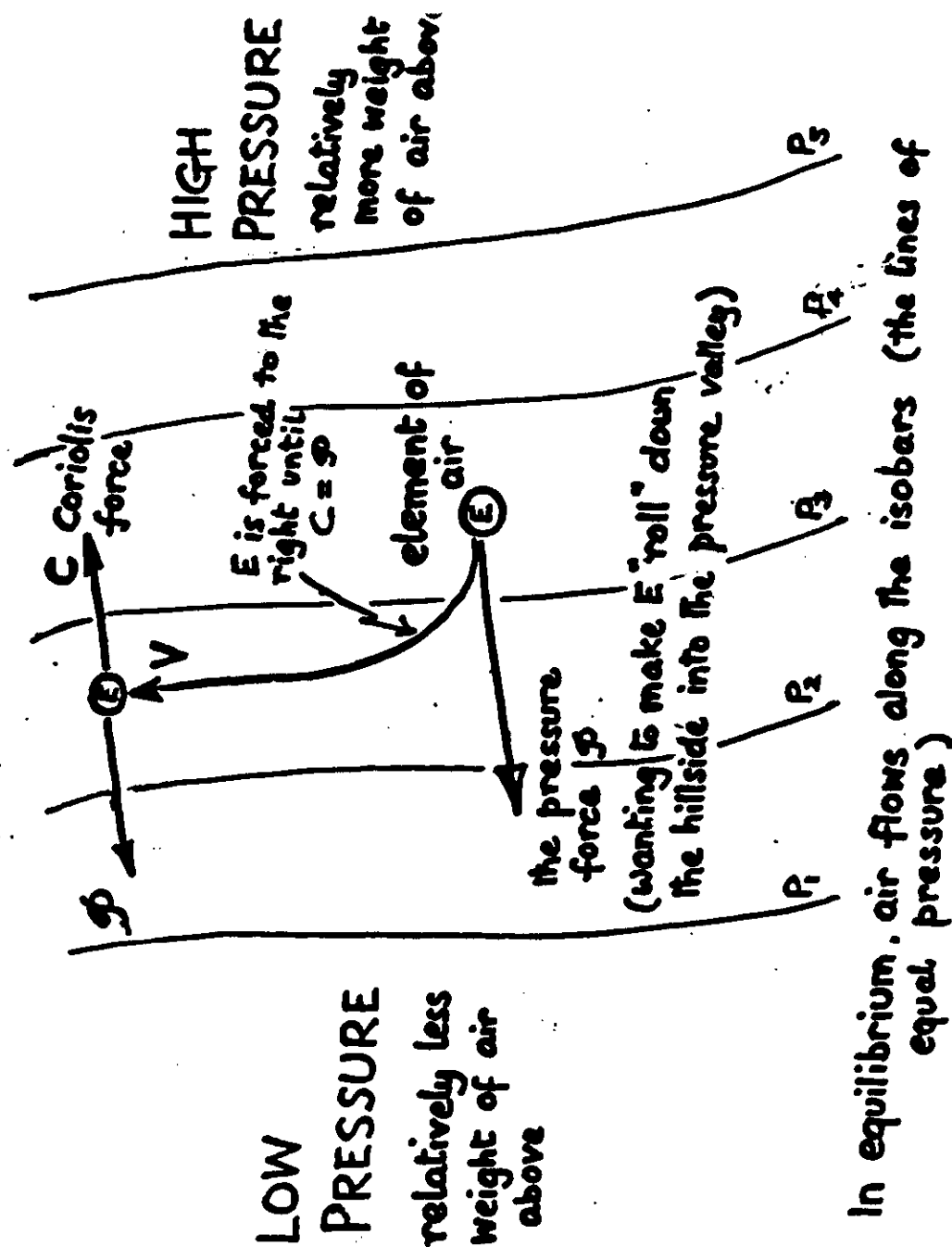
$$(a) \quad \tau(z) - \tau(0) = -f \int_0^z \rho (\bar{V} - \underline{V}_g) \times \underline{k} \, dz', \quad (3.3.3)$$

$$\text{or } (b) \quad \tau(z) = f \int_z^h \rho (\bar{V} - \underline{V}_g) \times \underline{k} \, dz'. \quad (3.3.4)$$

Therefore knowing the profiles of $\bar{V}(z)$ and $\underline{V}_g(z)$ we can either:

(a) express $\tau(z)$ in terms of the integral of the geostrophic departure, $\bar{V} - \underline{V}_g$, from the surface to z if the surface value $\tau(0)$ is known.

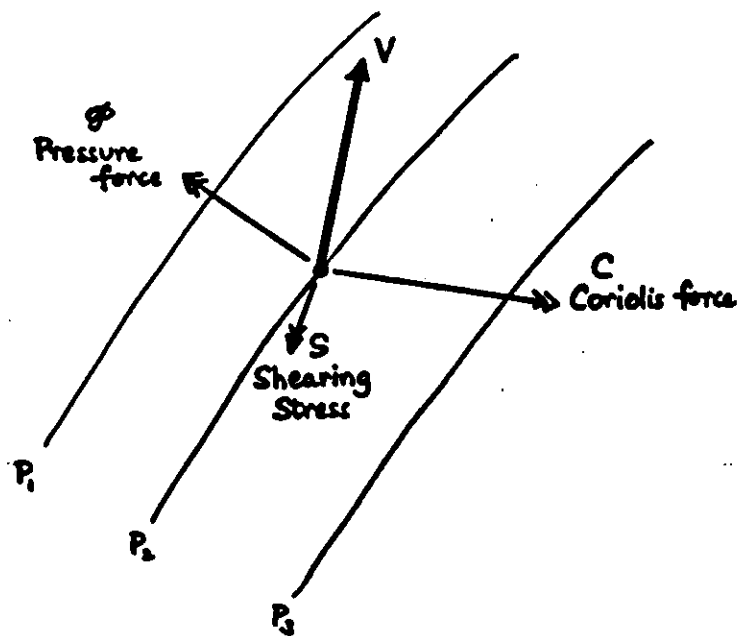
or (b) express $\tau(z)$ as the integral of the geostrophic departure from the height z to the top of the boundary layer, h , if this is known.



in the boundary layer a third force, called the shearing stress has to be taken into account.

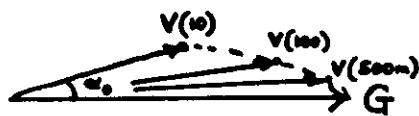
The shearing stress originates from the drag of the ground.

It normally falls in magnitude with height, to zero at the top of the boundary layer.



The 3 forces P , C and S must balance.

The velocity V is different to the geostrophic wind G in both magnitude and direction:



Typically $V(10) \approx \frac{1}{2} G$ and $\alpha_0 \approx 20^\circ$ during the day.

$$\text{NB } \underline{\tau}(0) = f \int_0^h \rho (\bar{V} - V_g) \times \underline{k} dz \quad (3.3.5)$$

Example

Suppose V_g is virtually constant in direction with height,

ie the thermal wind is parallel to the geostrophic wind.

Choose right-handed axes such that the x -direction coincides with the geostrophic wind direction.

In component form the equations of motion become,

$$\frac{\partial \tau_x}{\partial z} = -f \rho \bar{v} \quad (3.3.6)$$

$$\frac{\partial \tau_y}{\partial z} = f \rho (\bar{u} - V_g) \quad (3.3.7)$$

$$V_g = -\frac{1}{\rho f} \frac{\partial \bar{p}}{\partial y} = \frac{1}{\rho f} \left| \frac{\partial \bar{p}}{\partial y} \right| \quad (3.3.8)$$

with surface boundary conditions that

(i) $\underline{\tau}(z)$ is parallel to the limiting wind direction as the surface is approached (3.3.9)

(ii) $\bar{V}(0) = 0$ and $0 < \alpha(0) < \pi/2$ (3.3.10)
 where $\alpha(z) = \tan^{-1}(\bar{v}/\bar{u})$
 and $\alpha(0) = \lim_{z \rightarrow 0} \alpha(z)$ is the surface turning of the wind from the geostrophic wind direction.

$$\text{Approach (a): } \left. \begin{aligned} \tau_x(z) &= \tau(0) \cos \alpha(0) - f \int_0^z \rho \bar{v} dz' \\ \tau_y(z) &= \tau(0) \sin \alpha(0) + f \int_0^z \rho (\bar{u} - V_g) dz' \end{aligned} \right\} \quad (3.3.11)$$

$$\text{Approach (b): } \left. \begin{aligned} \tau_x(z) &= f \int_0^z \rho \bar{v} dz' \\ \tau_y(z) &= -f \int_0^z \rho (\bar{u} - V_g) dz' \end{aligned} \right\} \quad (3.3.12)$$

These methods are suitable only in fairly ideal stationary conditions when V_g is well-defined.

3.4 Flux-gradient Relationships

Recall that from molecular theory the fully viscous stresses in laminar flow can be defined by

$$F_{ij} = \mu \left(\frac{\partial \bar{u}_i}{\partial x_j} + \frac{\partial \bar{u}_j}{\partial x_i} \right) \quad (3.4.1)$$

so that in conditions of horizontal homogeneity the tangential stresses become

$$F_{13} = \mu \frac{\partial \bar{u}}{\partial z} \quad (3.4.2)$$

$$F_{23} = \mu \frac{\partial \bar{v}}{\partial z}$$

ie We can write $\underline{F} = (F_x, F_y) = (F_{13}, F_{23})$

$$= \mu \frac{\partial \bar{V}}{\partial z} = \rho \nu \frac{\partial \bar{V}}{\partial z}, \quad (3.4.3)$$

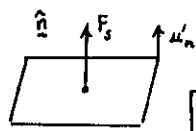
where, from molecular theory

$$\nu = \frac{1}{3} c \ell \quad (3.4.4)$$

where C is the mean molecular velocity and l is the mean free path of the molecules.

In contrast no adequate physical theory is known which expresses the Reynolds stresses in terms of the mean velocity components and their derivatives. It becomes necessary then to introduce empirical or semi-empirical relations between the turbulent stresses and the mean flow.

A natural first step is to carry over the results from the kinetic theory of gases and to relate the local rate of transport across a fixed surface, F_s , of some quantity S per unit mass of air, to the local gradient of mean S measured normal to the surface such that



$$F_s = \rho \overline{u_n s'} = -A_s \frac{\partial \bar{S}}{\partial n} = -\rho K_s \frac{\partial \bar{S}}{\partial n}$$

$$\left[\text{Kinematic flux} = F_s / \rho = \overline{u_n s'} \right] \quad (3.4.5)$$

where A_s is called the exchange coefficient or austausch coefficient and K_s is called the eddy diffusivity or eddy diffusion coefficient.

The negative sign denotes that the gradient is being measured in the direction of the flux.

It should be stressed that such flux-gradient relationships for turbulent atmospheric flows are semi-empirical and have not been adequately verified in the atmosphere.

The analysis up to this point is purely formal and we may look upon (3.4.5) as giving the definition, in a strictly mathematical sense, of the function K_s ,

$$K_s = - \frac{\overline{u_n s'}}{\partial \bar{S} / \partial n} \quad (3.4.6)$$

which is independent of any physical modelling of the turbulent transport processes, and gives us no information about the behaviour of the function K_s . In general K_s for turbulent transports is different for transport in different directions and is a function of position and other parameters of the turbulent flow.

If we were to assume however, as in molecular theory, that K_s is constant then physically we would be implying a diffusion model which might not be applicable for turbulent transports in the atmospheric boundary layer.

Two properties characterise molecular motion:

- (i) The molecules move very quickly but have a very short mean free path (at normal temperatures and pressures)
- (ii) The velocities between collisions are very weakly correlated.

On the other hand in the atmosphere elements of fluid:

- (i) Move with speeds which are small compared to the velocity of sound but over distances which are of the order of the height above ground.
- (ii) The velocity changes continuously with a slowly decreasing correlation-time.

The analogy between molecular motion and the motion of elements of the air is therefore not a very good one and strictly the 'K-theory' approach should be used with caution.

In spite of the theoretical difficulties in fully accepting a diffusion model the K-theories and the accompanying mixing-length theories have their part to play in the development of the theory of atmospheric turbulence.

In particular we can deduce some simple properties of the wind and stress profiles in very restricted conditions if we adopt the flux-gradient relationship

$$\underline{\tau} = A_m(z) \frac{\partial \underline{V}}{\partial z} = \rho K_m(z) \frac{\partial \underline{V}}{\partial z} \quad (3.4.7)$$

where $A_m(z)$ and $K_m(z)$ are taken to be scalar coefficients. K_m is called the eddy viscosity in analogy to ν .

Note that this wind-stress relationship requires that $\underline{\tau}$ be parallel to $\frac{\partial \underline{V}}{\partial z}$ throughout the boundary layer.

3.5 The Ekman Spiral

The simplest analytical approach considers stationary flow, horizontal homogeneity, the geostrophic wind and the eddy viscosity constant with height.

Basic equations of motion are

$$\frac{\partial \underline{\tau}}{\partial z} = -f \rho (\underline{V} - \underline{V}_g) \times \underline{k} \quad (3.5.1)$$

where
$$\underline{\tau} = \rho K_m \frac{\partial \underline{V}}{\partial z} \quad (3.5.2)$$

with boundary conditions

$$\underline{V}(0) = 0 \quad (3.5.3)$$

and

$$\lim_{z \rightarrow \infty} \underline{V}(z) = \underline{V}_g$$

Write

$$\underline{V}_a = (\underline{u}_a, \underline{v}_a) = \underline{V} - \underline{V}_g \quad (3.5.4)$$

then the equations of motion become

$$\frac{\partial^2 \underline{V}_a}{\partial z^2} + \frac{f}{K_m} (\underline{V}_a \times \underline{k}) = 0, \quad (3.5.5)$$

since $\frac{\partial \underline{V}_g}{\partial z} = 0$,

with boundary conditions
$$\underline{V}_a(0) = -\underline{V}_g \quad (3.5.6)$$

$$\lim_{z \rightarrow \infty} \underline{V}_a(z) = 0$$

In component form (3.5.5) becomes

$$\left. \begin{aligned} \frac{\partial^2 \underline{u}_a}{\partial z^2} + \frac{f}{K_m} \underline{v}_a &= 0 \\ \frac{\partial^2 \underline{v}_a}{\partial z^2} - \frac{f}{K_m} \underline{u}_a &= 0 \end{aligned} \right\} \quad (3.5.7)$$

$$V_a = \bar{u}_a + i \bar{v}_a$$

then the above equations combine to

$$\begin{aligned} \frac{\partial^2 V_a}{\partial z^2} &= \frac{i f}{K_m} V_a \\ &= (i+1)^2 \frac{f}{2K_m} V_a \\ &= \lambda^2 V_a \quad \text{where } \lambda = (i+1) \sqrt{\frac{f}{2K_m}} \end{aligned} \quad (3.5.8)$$

choose axes such that the x-axis coincides with the geostrophic wind direction, the boundary conditions are

$$V_a(0) = -V_g \quad (3.5.9)$$

$$\lim_{z \rightarrow \infty} V_a(z) = 0$$

general solution of (3.5.8) is

$$V_a = A e^{\lambda z} + B e^{-\lambda z} \quad (3.5.10)$$

boundary condition at the top of the layer gives $A=0$

that at the surface gives $B = -V_g$

so the solution is

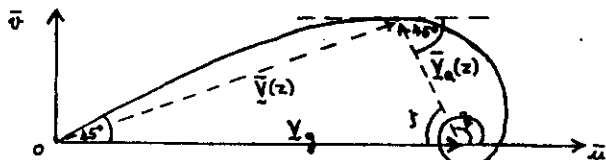
$$V_a = -V_g \exp[-\gamma(1+i)z] \quad (3.5.11)$$

$$\gamma = \sqrt{\frac{f}{2K_m}} \cdot z \quad (3.5.12)$$

$$\left. \begin{aligned} \bar{u}_a &= \bar{u} - V_g = -V_g e^{-\gamma} \cos \gamma \\ \bar{v}_a &= \bar{v} = V_g e^{-\gamma} \sin \gamma \end{aligned} \right\} \quad (3.5.13)$$

wind hodograph (graph of \bar{u} against \bar{v}) for positive γ , is an equiangular spiral with $\bar{u} = V_g$, $\bar{v} = 0$ as the limit point as $\gamma \rightarrow \infty$ called the Ekman Spiral.

A type of solution was derived by Ekman for wind-driven ocean currents.



It is easy to show that the solution is an equiangular spiral with the constant angle that the curve makes with the radius vector from the 'origin' at $(V_g, 0)$ equal to 45° .

$$\bar{v}_a = |\bar{v}_a| = V_g e^{-\gamma}$$

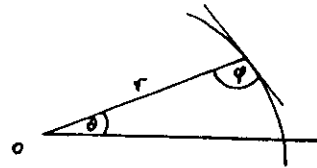
$$\tan \psi = \frac{\bar{v}_a}{\bar{u}_a} = -\tan \gamma = \tan(\pi - \gamma)$$

$$\psi = \pi - \gamma$$

$$\therefore \bar{v}_a = V_g e^{-\pi} e^{\gamma} = V_g e^{-\pi} e^{\gamma \cot \pi/4} \quad (3.5.14)$$

27 51

c.f. Equation for an equiangular spiral is $r = a e^{\theta \cot \phi}$, $\phi = \text{constant}$.



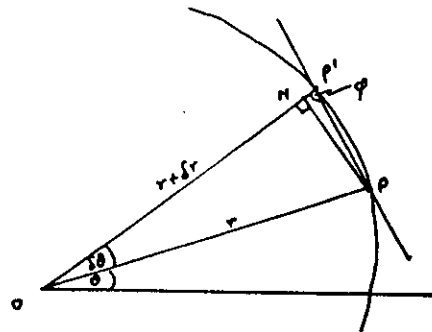
$$\begin{aligned} \tan \phi &= \frac{PN}{P'H} \\ &= \frac{r \sin \delta \theta}{r + \delta r - r \cos \delta \theta} \end{aligned}$$

$$= \frac{r \sin \delta \theta}{\delta r + 2r \sin^2(\frac{1}{2} \delta \theta)}$$

$$\lim_{\delta r, \delta \theta \rightarrow 0} \tan \phi = \lim_{\delta r, \delta \theta \rightarrow 0} \left[\frac{r \delta \theta}{\delta r} + \dots \right] = r \frac{d\theta}{dr}$$

$$\frac{1}{r} \frac{dr}{d\theta} = \cot \phi \quad \text{and if } \phi = \text{constant}$$

$$\underline{r = a e^{\theta \cot \phi}}$$

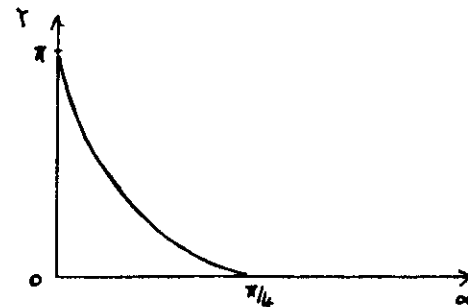


This classical analysis has no practical value; however, despite the adoption of a quite unrealistic profile for K_m it does predict some broad features of the observed atmospheric boundary layer wind profile.

(i) The angle α which the wind makes with the geostrophic wind direction is given by

$$\tan \alpha = \frac{\bar{v}}{\bar{u}} = \frac{\sin \gamma}{e^{-\gamma} - \cos \gamma} \quad (3.5.15)$$

α decreases continuously from $\pi/4$ at the surface to zero for the first time at $\gamma = \pi$.

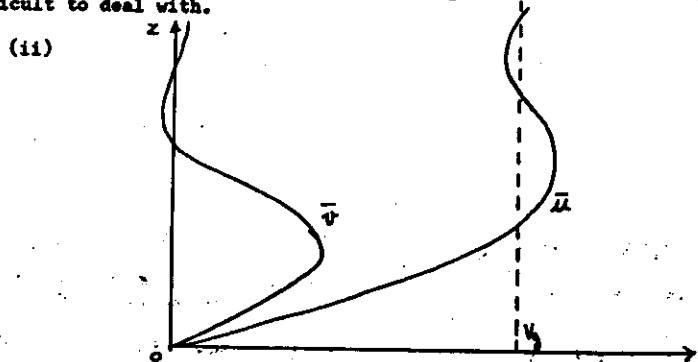


28 52

The effect of surface friction results in the wind being deflected towards low pressure from the free-stream direction so that the near surface wind is inclined to the isobars at an angle $\alpha(0)$.

The term Ekman layer is often used to denote the layer in which the wind turns steadily from its near surface direction to that of the free-stream wind at the top of the boundary layer.

In reality $\alpha(0)$ depends on the stability of the boundary layer, the value of the free-stream wind at the top of the boundary layer (taken to be the geostrophic wind throughout these lectures) and the roughness of the underlying surface. Typical observed values in mid-latitudes range from about 5° over relatively smooth ground in very unstable conditions to about 30° over rough ground in near neutral conditions. Stable conditions give very large cross-isobar flows which are very difficult to deal with.



Profiles of \bar{u} , $\bar{\psi}$ allow supergeostrophic wind speeds in the boundary layer.

Wind speed approaches geostrophic value fairly quickly but wind direction becomes parallel to the geostrophic wind direction more slowly.

The wind first attains geostrophic direction when $\bar{\psi} = \pi$

$$\text{is at } z_* = \frac{\bar{\psi}}{\sqrt{f/2K_m}} = \frac{\pi}{\sqrt{f/2K_m}}$$

Typically $z_* = 1 \text{ km}$, $f = 10^{-4} \text{ sec}^{-1}$ (mid-latitudes)

$$\therefore K_m = \frac{f z_*^2}{2\pi^2} \sim \frac{10^{-4} \cdot 10^{10}}{2 \cdot 10} = 5 \times 10^4 \text{ cm}^2 \text{ sec}^{-1} = 5 \text{ m}^2 \text{ sec}^{-1}$$

$$\text{c.f. } \nu \sim 0.15 \text{ cm}^2 \text{ sec}^{-1} = 15 \times 10^{-6} \text{ m}^2 \text{ sec}^{-1}$$

Therefore, atmospheric mixing is on a scale much greater than molecular diffusion.

3.6 The Leipzig Wind Profile

There are many complicating factors in the atmospheric boundary layer which prevent the classical Ekman spiral approach being of any practical value.

The general lack of suitable atmospheric boundary layer data has meant that, until fairly recently, undue attention and importance have been given to some careful and detailed wind measurements made by Mildner on 20 October 1931 at Leipzig, which gave rise to the so-called Leipzig Wind Profile.

The Leipzig data were obtained from a series of 29 double theodolite pilot balloon ascents made during a seven-hour period (0915 - 1615 GMT), the wind field was stated to be steady and uniform and the measured mean lapse rate throughout the layer of $6.5 \times 10^{-3} \text{ K.m}^{-1}$ indicated that the air was slightly stable.

Figures C - E illustrate profiles of \bar{V} , $\bar{\psi}$, \bar{u} , \bar{v} , V_g , α , τ , A through the atmospheric boundary layer based on a recent analysis by Carson and Smith (1973) of the Leipzig data.

See also: Clarke, R H 1970 'Observational Studies in the Atmospheric Boundary Layer', Quart. J. R. Met. Soc., 96, 91 - 114.

3.7 Balance of Forces within the Stationary Atmospheric Boundary Layer

Figure F illustrates the balance of forces in a stationary atmospheric boundary layer with no thermal wind effect.

Note: (i) Geostrophic balance at the top of the boundary layer.

(ii) Balance between $\partial \bar{\psi} / \partial z$ and $\bar{V} \rho$ at the surface.

(iii) $\frac{\partial \bar{\psi}}{\partial z}$ is greatest at the surface.

TABLE 5. Vertical profiles from the analysis by Carson and Smith (1973) of the Leipzig Wind Profile data.

These profiles provided the best fit to the hypothesis that the shearing stress vector and the velocity shear vector are parallel. Right-handed cartesian axes are used such that the x-direction coincides with the geostrophic wind direction.

Useful quantities associated with these profiles:

$$\alpha(o) = 25.0^\circ$$

$$f = 1.14 \times 10^{-4} \text{ s}^{-1}, \quad g = 9.80665 \text{ m s}^{-2}, \quad R = 287 \text{ joule kg}^{-1} \text{ K}^{-1}$$

$$\rho(o) = 1.25 \text{ kg m}^{-3}, \quad T(o) \doteq 291.5 \text{ K (estimated)}$$

$$L = -6.5 \times 10^{-3} \text{ K m}^{-1} \text{ (constant temperature lapse rate)}$$

$$|\partial \tau / \partial y| = 2.33 \times 10^{-3} \text{ N m}^{-3} \text{ (c.f. Mildner's synoptic estimate of } 2.5 \times 10^{-3} \text{ N m}^{-3}\text{)}$$

$$V_g(o) = 16.33 \text{ m s}^{-1}, \quad \zeta(o) = 0.469 \text{ N m}^{-2}, \quad \dot{u}_s = 0.61 \text{ m s}^{-1}$$

$$\text{Formulae: } \rho(z) = \rho(o) [1 + Lz/T(o)]^{-(1+g/RL)}$$

$$= \rho(o) (1 - 2.23 \times 10^{-5} z)^{4.256}, \quad z \text{ in metres.}$$

$$V_g(z) = V_g(o) \rho(o) / \rho(z).$$

ρ kg m ⁻³	V_g m s ⁻¹	u m s ⁻¹	v m s ⁻¹	V m s ⁻¹	α deg	ζ_x N m ⁻²	ζ_y N m ⁻²	ζ N m ⁻²	θ deg	A kg m ⁻¹ s ⁻¹	K m ² s ⁻¹	z m
1.250	16.33	0	0	0	25.0	0.425	0.198	0.469	25.0	0	0	0
1.244	16.41	9.24	4.17	10.13	24.3	0.400	0.126	0.420	17.4	9.6	7.7	13.3
1.238	16.49	10.54	4.43	11.43	22.8	0.370	0.079	0.378	12.1	15.4	12.5	22.5
1.232	16.57	11.67	4.57	12.54	21.4	0.338	0.041	0.341	7.0	15.7	12.7	24.2
1.226	16.65	12.70	4.70	13.54	20.3	0.306	0.010	0.306	1.9	16.0	13.1	26.2
1.221	16.73	13.58	4.69	14.36	19.1	0.273	-0.015	0.273	-3.2	16.1	13.2	27.8
1.215	16.81	14.40	4.61	15.12	17.8	0.241	-0.035	0.243	-8.3	16.2	13.3	29.8
1.209	16.89	15.06	4.48	15.72	16.6	0.209	-0.050	0.215	-13.4	15.9	13.1	31.1
1.203	16.97	15.71	4.29	16.28	15.3	0.179	-0.061	0.189	-18.7	13.6	11.3	28.5
1.197	17.05	16.36	3.96	16.84	13.6	0.151	-0.067	0.165	-24.0	12.2	10.2	27.5
1.192	17.13	16.91	3.66	17.30	12.2	0.125	-0.070	0.143	-29.4	12.1	10.2	29.4
1.186	17.22	17.37	3.36	17.69	11.0	0.101	-0.071	0.123	-35.1	11.5	9.7	30.0
1.180	17.30	17.76	3.02	18.02	9.6	0.079	-0.069	0.105	-41.1	11.1	9.4	31.7
1.175	17.38	18.05	2.71	18.25	8.5	0.060	-0.066	0.089	-47.6	10.7	9.1	33.1
1.169	17.47	18.28	2.37	18.43	7.4	0.043	-0.061	0.074	-54.8	9.6	8.2	32.7
1.163	17.55	18.46	2.06	18.58	6.4	0.028	-0.055	0.062	-62.8	8.1	6.9	30.1
1.158	17.64	18.64	1.69	18.71	5.2	0.016	-0.049	0.052	-71.9	6.6	5.7	27.1
1.152	17.72	18.69	1.33	18.74	4.1	0.0047	-0.047	0.047	-84.3	6.2	5.4	26.5
1.147	17.81	18.70	0.94	18.73	2.9	-0.0011	-0.038	0.038	-91.7	5.0	4.4	24.0
1.141	17.89	18.63	0.54	18.64	1.7	-0.0074	-0.034	0.034	-102.3	4.0	3.5	20.4
1.134	18.00	18.50	0	18.50	0	-0.006	-0.018	0.019	-108.4	-	-	-

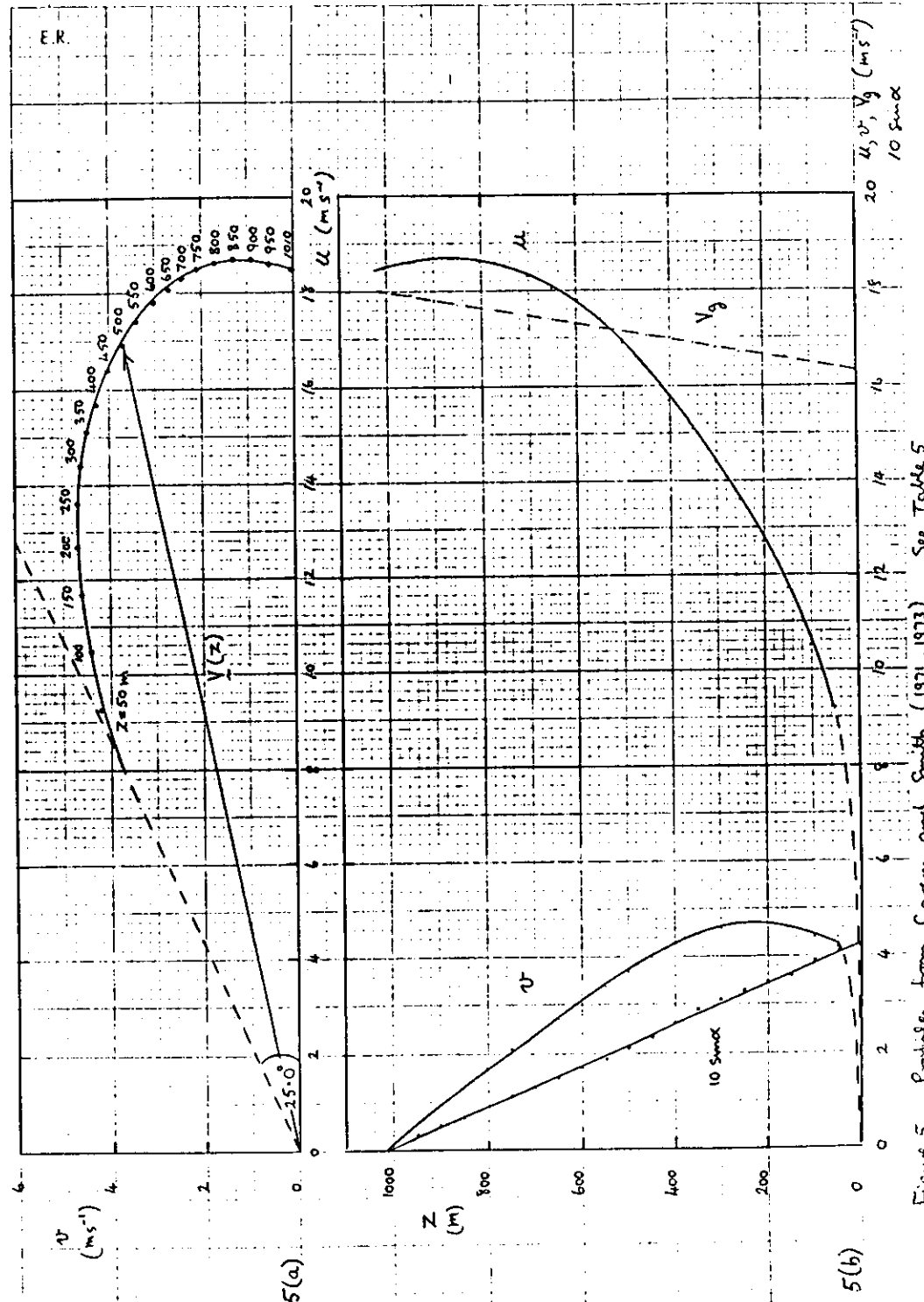


Figure 5. Profiles from Carson and Smith (1971, 1973). See Table 5.

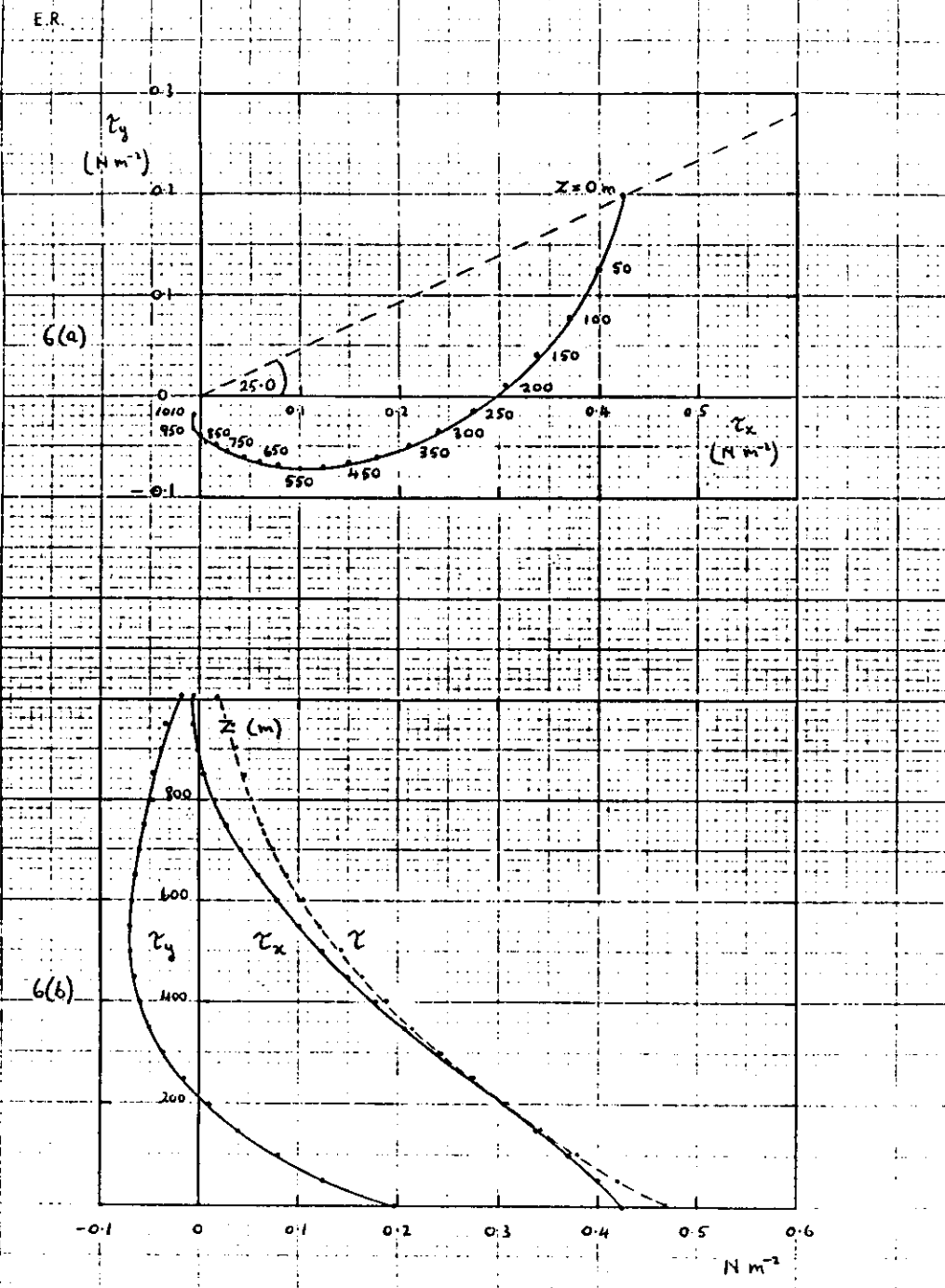


Figure 6. Eddy shearing stress profiles from Carson and Smith (1971, 1973).
See Table 5.

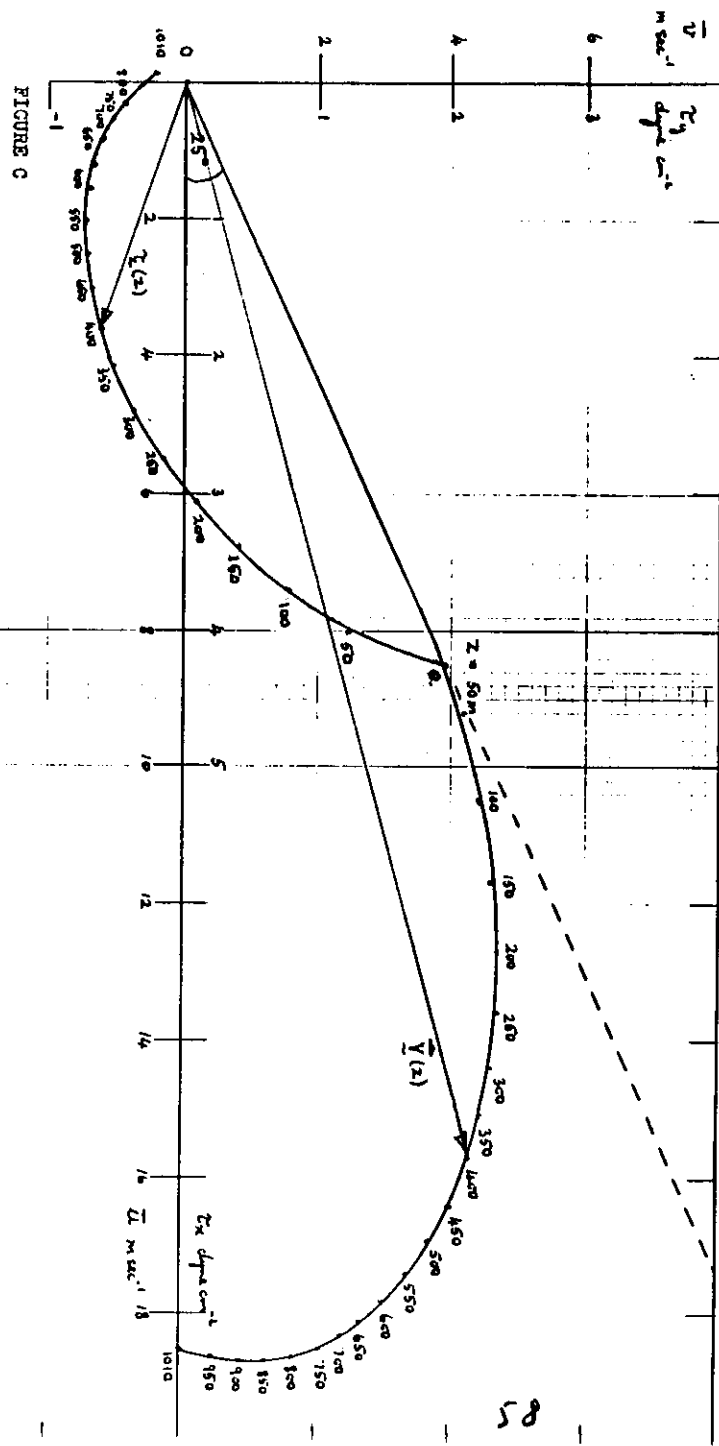


FIGURE 7

MEAN WIND AND SHEARING STRESS HODOGRAPHS BASED ON 1931-LEIPZIG DATA ANALYSED BY CARSON & SMITH, QUART. J. R. MET. SOC. (1973), 99, 11-17

FIGURE D

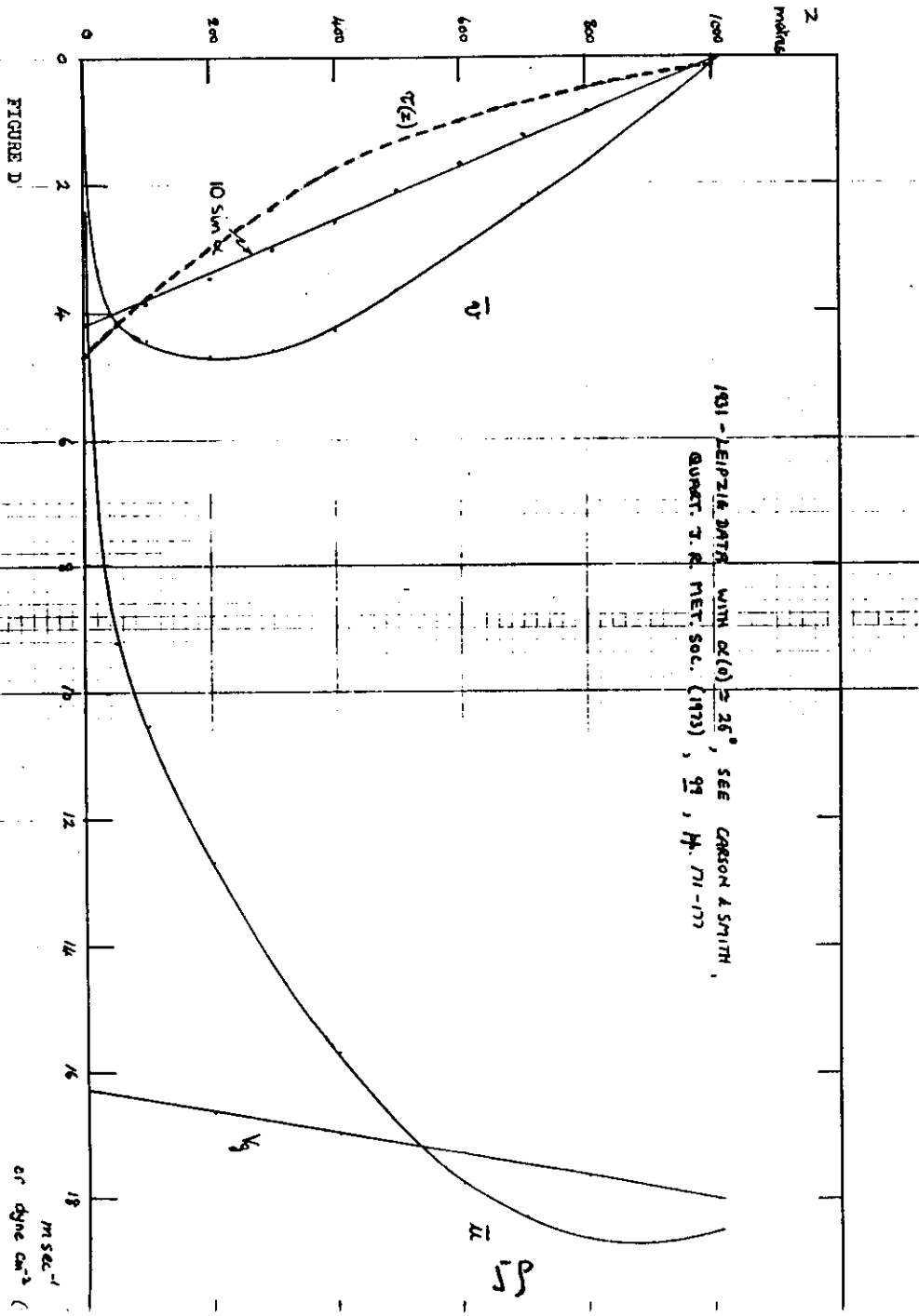
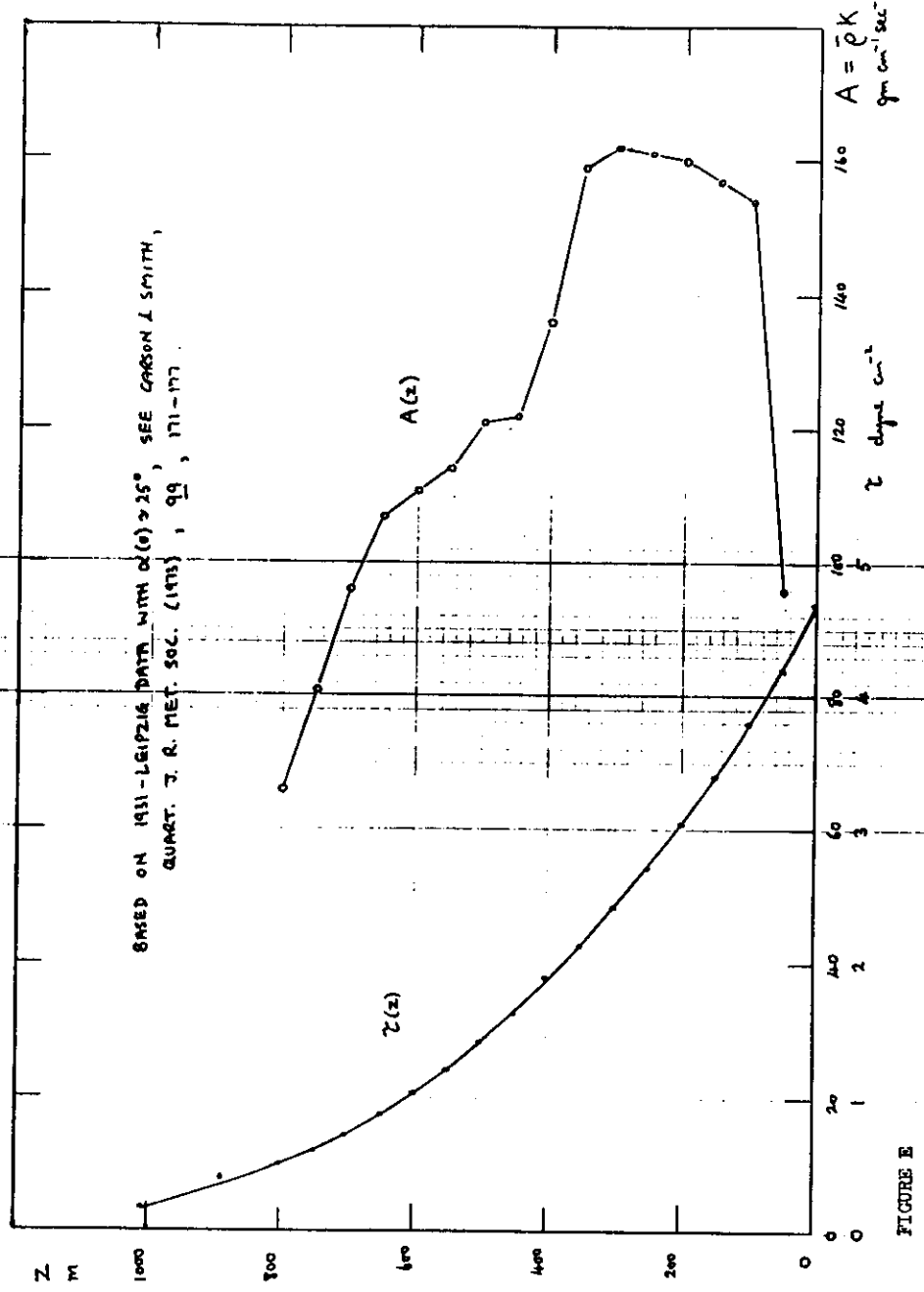


FIGURE E

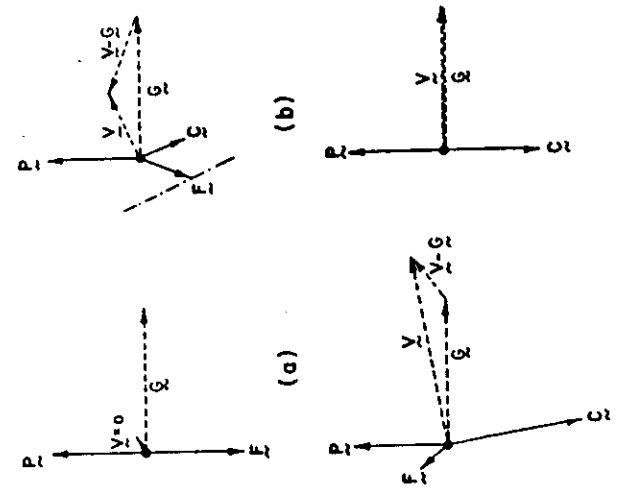
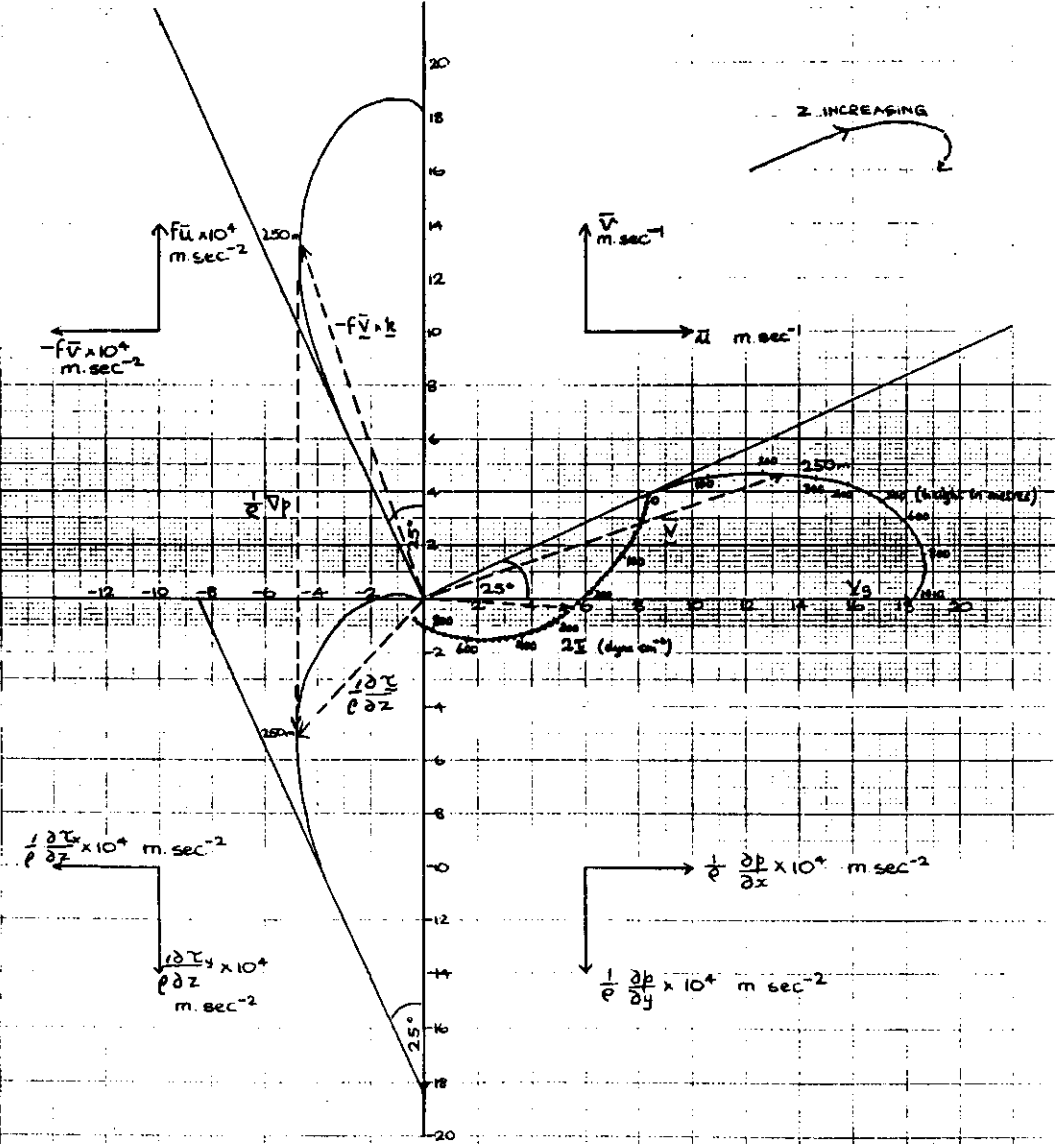


BALANCE OF FORCES IN A STATIONARY ATMOSPHERIC BOUNDARY LAYER

WITH NO THERMAL WIND

$$\frac{1}{\rho} \frac{\partial \bar{u}}{\partial z} = \frac{1}{\rho} \nabla p - \bar{v} \times \bar{k}$$

$$\frac{1}{\rho} \nabla p = \text{constant} = (0, -fv_g)$$



$$\vec{F} = \frac{1}{\rho} \frac{\partial \bar{p}}{\partial z}$$

$$\vec{C} = -\frac{1}{\rho} \nabla p$$

$$\vec{C} = f \bar{V} \times \bar{k}$$

$$0 = -\frac{1}{\rho} \nabla p + f \bar{V} \times \bar{k} + \frac{1}{\rho} \frac{\partial \bar{u}}{\partial z}$$

$$0 = \vec{P} + \vec{C} + \vec{F}$$

Fig. 6.4 Schematic of the balance of forces on a fluid parcel at different heights in a barotropic PBL: (a) at the surface, (b) in the surface layer, (c) in the middle of the PBL, (d) at the top of the PBL. Actual and geostrophic velocities are also indicated. [After Arya (1986).]

(VALUES BASED ON 1931-LEIPZIG DATA, SEE CARSON & SMITH, Quart. J. R. Met. Soc. (1973), 99, pp 171-177)

FIGURE 6

61

62

3.8 RELATION BETWEEN EDDY VISCOSITY K_H AND MIXING LENGTH l_m

cf Section 2.2 Concept of an Eddy and Prandtl Mixing-length Theory.

Consider the case of a horizontally homogeneous, horizontal mean flow

$$\bar{\underline{v}}(z) = (\bar{u}(z), \bar{v}(z), 0)$$

The Prandtl mixing-length hypothesis implies that velocity fluctuations at a level z occur as a result of mixing with the environment, at this level, of fluid parcels arriving from different levels above and below.

We shall adopt the convention that:

- the "mixing-length" $l < 0$ if the fluid parcel has arrived from a level below z , i.e. $w' > 0$
- the "mixing-length" $l > 0$ if the fluid parcel has arrived from a level above z , i.e. $w' < 0$

Consider a parcel from $z_1 = z_2 + l$ mixing with the mean flow at z_2 .

By the mixing-length hypothesis, this gives rise to a fluctuation

$$\begin{aligned} \underline{v}' &= \bar{\underline{v}}(z_1) - \bar{\underline{v}}(z_2) \\ &= \bar{\underline{v}}(z_2 + l) - \bar{\underline{v}}(z_2) \\ &\approx l \frac{\partial \bar{\underline{v}}}{\partial z} \end{aligned}$$

The kinematic eddy momentum flux $\equiv \overline{v'w'}$
 (τ/ρ)

$$\equiv \overline{lw'} \cdot \frac{\partial \bar{v}}{\partial z}$$

Assume (following Prandtl) that in a turbulent flow the velocity fluctuations are of the same order of magnitude in all directions, such that

$$|w'| \sim |v'|$$

where $\text{sgn}(w') = -\text{sgn}(l)$ (This follows from the earlier definition of l)

Therefore,

$$\begin{aligned} w' &\sim -\text{sgn}(l)|v'| \\ &\sim -\text{sgn}(l) \left| l \frac{\partial \bar{v}}{\partial z} \right| = -l \left| \frac{\partial \bar{v}}{\partial z} \right| \end{aligned}$$

and $\tau/\rho = -\overline{v'w'} = -\overline{lw'} \cdot \frac{\partial \bar{v}}{\partial z} \sim +l^2 \cdot \frac{\partial \bar{v}}{\partial z} \left| \frac{\partial \bar{v}}{\partial z} \right|$

Define a mean mixing length l_m , which is proportional to the r.m.s. value of l

$$l_m^2 \sim \overline{l^2}$$

then $\tau/\rho = -\overline{v'w'} = +l_m^2 \frac{\partial \bar{v}}{\partial z} \left| \frac{\partial \bar{v}}{\partial z} \right|$

The eddy diffusivity K_m is defined such that

$$\tau/\rho = K_m \frac{\partial \bar{v}}{\partial z}$$

Therefore $K_m = \overline{l_m^2 \left| \frac{\partial \bar{v}}{\partial z} \right|} = \overline{l_m^2 \left[\left(\frac{\partial \bar{u}}{\partial z} \right)^2 + \left(\frac{\partial \bar{v}}{\partial z} \right)^2 \right]^{1/2}}$

Example

Observations in the ABL close to the surface in neutral conditions suggest that

$$l_m = kz$$

$$K_m = k u_* z$$

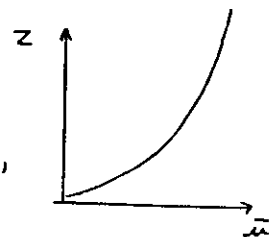
where u_* is the surface friction velocity and k is a constant (≈ 0.4).

From above relationship between K_m and l_m we have

$$K_m = l_m^2 \left| \frac{\partial \bar{v}}{\partial z} \right|$$

Consider $\bar{v} = (\bar{u}, 0, 0)$

and observe that $\frac{\partial \bar{u}}{\partial z} > 0$ close to the surface,



then

$$K_m = l_m^2 \frac{\partial \bar{u}}{\partial z}$$

i.e. $k u_* z = k^2 z^2 \frac{\partial \bar{u}}{\partial z}$

$$\frac{\partial \bar{u}}{\partial z} = \frac{u_*}{kz}$$

i.e. $\bar{u}(z) = \frac{u_*}{k} \ln(z/z_0)$

where z_0 is a constant of integration, defined such that

$$\bar{u}(z_0) = 0.$$

4. THE STRATIFIED ATMOSPHERIC BOUNDARY LAYER

4.1 The General Equations of Motion and Continuity

We now consider the dynamical equations which govern the stratified atmospheric boundary layer and work towards the definitions and meanings of stability parameters such as the flux and gradient Richardson numbers.

Notation

(i) In the following all vector and tensor components refer to the usual right-handed Cartesian coordinate system, fixed in the rotating earth, x_i ($i = 1, 2, 3$).

$$x_1 = x, x_2 = y, x_3 = z$$

(ii) Kronecker delta

$$\delta_{ij} = \begin{cases} 1 & i = j \\ 0 & i \neq j \end{cases}$$

(iii) $\epsilon_{ijk} = \begin{cases} 1 & i, j, k \text{ all unequal and in cyclic order} \\ -1 & i, j, k \text{ all unequal but not in cyclic order} \\ 0 & \text{any two of } i, j, k \text{ are equal} \end{cases}$

$$\left[\begin{array}{l} \text{Alternatively: } \begin{cases} 1 & \text{if } i, j, k \text{ is an even permutation of } 1, 2, 3 \\ -1 & \text{if } i, j, k \text{ is an odd permutation of } 1, 2, 3 \\ 0 & \text{if } i, j, k \text{ is not a permutation of } 1, 2, 3 \end{cases} \end{array} \right]$$

(iv) General Coriolis parameter: $\underline{f} = 2 \underline{\Omega} = (0, 2 \Omega \cos \varphi, 2 \Omega \sin \varphi)$

(v) Summation convention: whenever the same letter occurs twice in a product it is to be summed over all values (1, 2, 3).

$$\text{ex. } \frac{1}{2} \mu_i^2 = \frac{1}{2} (\mu^2 + v^2 + w^2), \quad \frac{\partial \mu_i}{\partial x_i} = \frac{\partial \mu}{\partial x} + \frac{\partial v}{\partial y} + \frac{\partial w}{\partial z}$$

(vi) If $\underline{e}_1, \underline{e}_2, \underline{e}_3$ form a right-handed Cartesian basis

i.e. they are mutually orthogonal unit vectors, then

$$\underline{e}_i \cdot \underline{e}_j \times \underline{e}_k = \epsilon_{ijk}$$

and from this and the summation convention it follows that if

$$\underline{a} = a_i \underline{e}_i, \quad \underline{b} = b_i \underline{e}_i \quad \text{and} \quad \underline{c} = c_i \underline{e}_i = \underline{a} \times \underline{b}$$

$$c_i = \underline{e}_i \cdot \underline{c} = \underline{e}_i \cdot \underline{a}_j \underline{e}_j \times b_k \underline{e}_k = \epsilon_{ijk} a_j b_k$$

Therefore, the coriolis acceleration components

$$(\underline{f} \times \underline{V})_i = \epsilon_{ijk} f_j \mu_k = f_j \mu_k - f_k \mu_j \quad (i, j, k \text{ in cyclic order}) \quad (4.1.1)$$

ex. y -component: $i = 2$

$$\begin{aligned} (\underline{f} \times \underline{V})_x &= 2 \Omega \cos \varphi \cdot w - 2 \Omega \sin \varphi v \\ &\approx -f v = (\underline{f}_k \times \underline{V})_x \end{aligned}$$

The continuity equation:

Consider the mass flux vector $\rho u_i = \bar{\rho} \bar{u}_i + \rho' u'_i$

On taking mean values we have

It is observed that the relative fluctuations of density are much smaller than the fluctuations u'_i and we take

$$\bar{\rho} u_i \approx \bar{\rho} \bar{u}_i \quad \text{to a high degree of approximation.} \quad (4.1.2)$$

It must be emphasized that while small compared to $\bar{\rho} \bar{u}_i$, the term $\rho' u'_i$ is not zero. In fact it will be seen that a term involving $\rho' u'_i$ plays an important part in the turbulent kinetic energy equation.

The full equation of continuity is

$$\frac{D\rho}{Dt} + \rho \frac{\partial u_k}{\partial x_k} = 0 \quad (4.1.3)$$

or

$$\frac{\partial \rho}{\partial t} + \frac{\partial (\rho u_k)}{\partial x_k} = 0 \quad (4.1.4)$$

Taking mean values and using (4.1.2) we obtain

$$\bar{\rho} \frac{\partial \bar{u}_k}{\partial t} + \bar{\rho} \frac{\partial \bar{u}_k}{\partial x_k} = 0 \quad (4.1.5)$$

or

$$\frac{\partial \bar{\rho}}{\partial t} + \frac{\partial (\bar{\rho} \bar{u}_k)}{\partial x_k} = 0 \quad (4.1.6)$$

as the continuity equation of the mean motion.

Although previously we took $\frac{D\rho}{Dt} = 0$

i.e. $\frac{\partial u_k}{\partial x_k} = 0$

it has been argued (Calder, K. L. (1949) Quart. J.R. Met. Soc. 75, 71-88) that although for small-scale turbulence

$$\frac{\partial u'_k}{\partial x_k} = 0 \quad (4.1.7)$$

to a high degree of approximation, the corresponding result for the mean motion viz. $\frac{\partial \bar{u}_k}{\partial x_k} = 0$, is not true in general save as a rough approximation.

We shall adopt then (4.1.5) and (4.1.6) as the continuity equation for the mean flow and (4.1.4) as the continuity equation for the eddy motion.

The physical significance of (4.1.7) is that the small-scale motion does not move the fluid elements far enough for them to be in a region of different density.

The equations of motion:

The general equations of motion can be written,

$$\rho \frac{D u_i}{D t} + \rho \epsilon_{ijk} f_j u_k = -\rho \frac{\partial \Phi}{\partial x_i} + \frac{\partial p_{ik}}{\partial x_k} \quad (4.1.8)$$

where Φ is the gravitational potential function and the stress tensor p_{ik} is given by

$$p_{ik} = p_{ki} = -p \delta_{ik} + \mu \left\{ \left(\frac{\partial u_i}{\partial x_k} + \frac{\partial u_k}{\partial x_i} \right) - \frac{2}{3} \delta_{ik} \left(\frac{\partial u_j}{\partial x_j} \right) \right\} \\ = -p \delta_{ik} + M_{ik}, \text{ say.} \quad (4.1.9)$$

Introducing mean and fluctuating components (as in Section 3.1) and taking the mean, the equations for the mean motion are

$$\bar{\rho} \frac{D \bar{u}_i}{D t} + \bar{\rho} \epsilon_{ijk} f_j \bar{u}_k = -\bar{\rho} \frac{\partial \Phi}{\partial x_i} + \frac{\partial (\bar{p}_{ik} + \tau_{ik})}{\partial x_k} \quad (4.1.10)$$

where $\tau_{ik} = -\bar{\rho} \overline{u'_i u'_k}$ are the Reynolds stresses. (4.1.11)

4.2 The Energy Equation of the Mean Motion

Let $\bar{c}_i = (\underline{f} \times \bar{V})_i$ be the coriolis acceleration for the mean flow then

$$\bar{u}_i \bar{c}_i = \bar{u}_1 \bar{c}_1 + \bar{u}_2 \bar{c}_2 + \bar{u}_3 \bar{c}_3 \\ = \bar{u}_1 (f_2 \bar{u}_3 - f_3 \bar{u}_2) + \bar{u}_2 (f_3 \bar{u}_1 - f_1 \bar{u}_3) + \bar{u}_3 (f_1 \bar{u}_2 - f_2 \bar{u}_1) \\ = 0. \quad (4.2.1)$$

The physical significance of this is that the coriolis force being perpendicular to the flow does no mechanical work.

Also since the gravitational field is constant we can write

$$\bar{u}_i \frac{\partial \Phi}{\partial x_i} = \frac{D \Phi}{D t} \quad \text{since} \quad \frac{\partial \Phi}{\partial t} = 0. \quad (4.2.2)$$

Multiply (4.1.10) by \bar{u}_i :

$$\bar{\rho} \frac{D}{D t} \left(\frac{1}{2} \bar{u}_i^2 + \Phi \right) = \bar{u}_i \frac{\partial}{\partial x_k} (\bar{p}_{ik} + \tau_{ik}) \\ = \frac{\partial}{\partial x_k} (\bar{p}_{ik} \bar{u}_i + \tau_{ik} \bar{u}_i) - (\bar{p}_{ik} + \tau_{ik}) \frac{\partial \bar{u}_i}{\partial x_k} \quad (4.2.3)$$

The L.H.S. represents the rate of increase following the mean motion of the total mechanical energy (kinetic + potential) of the mean motion of unit volume of the fluid.

$\frac{\partial}{\partial x_k} (\bar{p}_{ik} \bar{u}_i + \tau_{ik} \bar{u}_i)$ represents the rate per unit volume at which the mean total apparent stresses do work on the mean motion.

$(\bar{p}_{ik} + \tau_{ik}) \frac{\partial \bar{u}_i}{\partial x_k}$ represents the total rate of transformation per unit volume of mechanical energy of the mean motion into other forms of energy.

4.3 The Turbulent Energy Balance Equation

Equations of Motion:

$$\rho \frac{D u_i}{D t} + \rho \epsilon_{ijk} f_j u_k = -\rho \frac{\partial \bar{\Phi}}{\partial x_i} + \frac{\partial p_{ik}}{\partial x_k} \quad (4.3.1)$$

Equation of continuity:

$$\frac{\partial \rho}{\partial t} + \frac{\partial (\rho u_k)}{\partial x_k} = 0 \quad (4.3.2)$$

Multiply continuity equation by u_i and add to equations of motion

$$\frac{\partial (\rho u_i)}{\partial t} + \frac{\partial (\rho u_i u_k)}{\partial x_k} + \rho \epsilon_{ijk} f_j u_k = -\rho \frac{\partial \bar{\Phi}}{\partial x_i} + \frac{\partial p_{ik}}{\partial x_k} \quad (4.3.3)$$

Multiply by u_i and recall that $\epsilon_{ijk} f_j u_k u_i \equiv 0$ (See (4.2.1))¹ and

$$\begin{aligned} u_i \frac{\partial (\rho u_i)}{\partial t} + u_i \frac{\partial (\rho u_i u_k)}{\partial x_k} &= \rho u_i \frac{\partial u_i}{\partial t} + \cancel{u_i^2 \frac{\partial \rho}{\partial t}} + \rho u_i u_k \frac{\partial u_i}{\partial x_k} \\ &\quad + \cancel{u_i^2 \frac{\partial (\rho u_k)}{\partial x_k}} \\ &= \frac{1}{2} \rho \frac{\partial u_i^2}{\partial t} + \frac{1}{2} \rho u_k \frac{\partial u_i^2}{\partial x_k} \\ &= \frac{\partial}{\partial t} \left[\frac{1}{2} \rho u_i^2 \right] + \frac{\partial}{\partial x_k} \left[\frac{1}{2} \rho u_i^2 u_k \right] \\ &\quad - \cancel{\frac{1}{2} u_i^2 \frac{\partial \rho}{\partial t}} - \cancel{\frac{1}{2} u_i^2 \frac{\partial (\rho u_k)}{\partial x_k}} \end{aligned}$$

Therefore

$$\frac{\partial}{\partial t} \left[\frac{1}{2} \rho u_i^2 \right] + \frac{\partial}{\partial x_k} \left[\frac{1}{2} \rho u_i^2 u_k \right] = -\rho u_i \frac{\partial \bar{\Phi}}{\partial x_i} + u_i \frac{\partial p_{ik}}{\partial x_k} \quad (4.3.4)$$

The mean values and neglect terms involving ρ' in comparison with those containing $\bar{\rho}$

$$\text{e.g. } \overline{\rho u_i^2} = (\bar{\rho} + \rho') (\bar{u}_i^2 + 2 \bar{u}_i u_i' + u_i'^2) = \bar{\rho} \bar{u}_i^2 + \bar{\rho} u_i'^2 \quad (4.3.5)$$

$$\begin{aligned} \overline{\rho u_i^2 u_k} &= \overline{(\bar{\rho} + \rho') (\bar{u}_i^2 + 2 \bar{u}_i u_i' + u_i'^2) (\bar{u}_k + u_k')} \\ &= \bar{\rho} (\bar{u}_i^2 \bar{u}_k + \bar{u}_i^2 \bar{u}_k + 2 \bar{u}_i \overline{u_i' u_k'} + \overline{u_i'^2 u_k'}) \end{aligned} \quad (4.3.6)$$

However we must write

$$\overline{\rho u_i \frac{\partial \bar{\Phi}}{\partial x_i}} = (\bar{\rho} \bar{u}_i + \rho' u_i') \frac{\partial \bar{\Phi}}{\partial x_i} \quad (4.3.7)$$

Although $\overline{\rho' u_i} \ll \bar{\rho} \bar{u}_i$ it is not zero, and since the final energy equation for the turbulent fluctuations is one relating small quantities and will be derived by subtracting two equations containing much larger terms, and in particular both containing $\overline{\rho' u_i \frac{\partial \bar{\Phi}}{\partial x_i}}$, it cannot be neglected.

$$p_{ik} = \bar{p}_{ik} + p'_{ik}$$

$$\begin{aligned} \overline{u_i \frac{\partial p_{ik}}{\partial x_k}} &= \overline{u_i \frac{\partial \bar{p}_{ik}}{\partial x_k}} + \overline{u_i \frac{\partial p'_{ik}}{\partial x_k}} \\ &= \frac{\partial (\bar{u}_i \bar{p}_{ik})}{\partial x_k} - \bar{p}_{ik} \frac{\partial \bar{u}_i}{\partial x_k} + \frac{\partial (\overline{u_i' p'_{ik}})}{\partial x_k} - \overline{p'_{ik} \frac{\partial u_i'}{\partial x_k}} \end{aligned} \quad (4.3.8)$$

Substituting (4.3.5) - (4.3.8) in meaned (4.3.4) we obtain

$$\begin{aligned} &\frac{\partial}{\partial t} \left[\frac{1}{2} \bar{\rho} (\bar{u}_i^2 + u_i'^2) \right] + \frac{\partial}{\partial x_k} \left[\frac{1}{2} \bar{\rho} \bar{u}_k (\bar{u}_i^2 + u_i'^2) \right] \\ &+ \frac{\partial}{\partial x_k} \left[\bar{\rho} \bar{u}_i \overline{u_i' u_k'} + \frac{1}{2} \bar{\rho} \overline{u_i'^2 u_k'} \right] \\ &= -\bar{\rho} \bar{u}_i \frac{\partial \bar{\Phi}}{\partial x_i} - \overline{\rho' u_i'} \frac{\partial \bar{\Phi}}{\partial x_i} + \frac{\partial (\bar{u}_i \bar{p}_{ik})}{\partial x_k} - \bar{p}_{ik} \frac{\partial \bar{u}_i}{\partial x_k} \\ &+ \frac{\partial (\overline{u_i' p'_{ik}})}{\partial x_k} - \overline{p'_{ik} \frac{\partial u_i'}{\partial x_k}} \end{aligned} \quad (4.3.9)$$

Put $\Psi = \frac{1}{2} (\overline{u_i^2} + \overline{u_i'^2})$

$$\begin{aligned} \frac{\partial}{\partial t} [\overline{\rho \Psi}] + \frac{\partial}{\partial x_k} [\overline{\rho \Psi u_k}] &= \overline{\frac{\partial}{\partial t} (\rho \Psi)} + \overline{\rho \Psi \frac{\partial u_k}{\partial x_k}} \\ &= \overline{\Psi \left[\frac{\partial \rho}{\partial t} + \rho \frac{\partial u_k}{\partial x_k} \right]} + \overline{\rho \frac{\partial \Psi}{\partial t}} \\ &= \overline{\rho \frac{\partial \Psi}{\partial t}} \quad \text{using (4.1.5)}. \end{aligned}$$

∴ Equation (4.3.9) becomes

$$\begin{aligned} \overline{\rho \frac{\partial}{\partial t} \left\{ \frac{1}{2} (\overline{u_i^2} + \overline{u_i'^2}) + \Phi \right\}} &= - \overline{\rho' u_i' \frac{\partial \Phi}{\partial x_i}} + \frac{\partial}{\partial x_k} (\overline{\rho' u_i' u_k} + \overline{u_i' \tau_{ik}}) \\ &\quad - \overline{\rho' u_k \frac{\partial u_i}{\partial x_k}} + \frac{\partial}{\partial x_k} (\overline{u_i' \rho' u_k}) - \overline{\rho' u_k \frac{\partial u_i}{\partial x_k}} \\ &\quad - \frac{\partial}{\partial x_k} \left[\frac{1}{2} \overline{\rho u_i'^2 u_k} \right]. \end{aligned} \quad (4.3.10)$$

This is the equation of the mean rate of change of the total mechanical energy of the motion.

Subtract (4.2.3), the energy equation for the mean motion:

$$\begin{aligned} \overline{\rho \frac{\partial}{\partial t} \left\{ \frac{1}{2} \overline{u_i'^2} \right\}} &= - \overline{\rho' u_i' \frac{\partial \Phi}{\partial x_i}} + \overline{\tau_{ik} \frac{\partial u_i}{\partial x_k}} + \frac{\partial}{\partial x_k} (\overline{u_i' \rho' u_k}) \\ &\quad - \overline{\rho' u_k \frac{\partial u_i}{\partial x_k}} - \frac{\partial}{\partial x_k} \left[\frac{1}{2} \overline{\rho u_i'^2 u_k} \right] \end{aligned} \quad (4.3.11)$$

This is the equation for the mean rate of change in the mechanical energy of the eddy motion per unit volume.

Let us now consider the form of certain of the terms in (4.3.11):

(i) $-\overline{\rho' u_i' \frac{\partial \Phi}{\partial x_i}} = -g \overline{\rho' u_i'}$

This is the rate of working of the gravitational field on the eddy flux of mass arising from the correlation between the density and the velocity fluctuations.

(ii) Recall from (4.1.2) that

$$p_{,k} = -p \delta_{ik} + M_{ik}$$

Now

$$\overline{\rho' u_k \frac{\partial u_i}{\partial x_k}} = - \overline{\rho' \left(\frac{\partial u_i}{\partial x_j} \right)} + \overline{M'_{ik} \frac{\partial u_i}{\partial x_k}}$$

The first term on the R.H.S. is zero since $\frac{\partial u_j}{\partial x_j} = 0$ from (4.1.7)

$$\begin{aligned} \overline{M'_{ik} \frac{\partial u_i}{\partial x_k}} &= \overline{\mu \left\{ \left(\frac{\partial u_i}{\partial x_k} + \frac{\partial u_k}{\partial x_i} \right) - \frac{2}{3} \delta_{ik} \left(\frac{\partial u_j}{\partial x_j} \right) \right\} \frac{\partial u_i}{\partial x_k}} \\ &\equiv \overline{\rho' \epsilon}, \text{ say.} \end{aligned}$$

This term which is essentially positive, represents the mean rate of molecular dissipation per unit volume of turbulent kinetic energy.

$$S_{ij} = \left\{ \frac{\partial u_i}{\partial x_j} + \frac{\partial u_j}{\partial x_i} \right\}$$

$$S_{ij} S_{ij} = \left(\frac{\partial u_i}{\partial x_j} \right)^2 + \left(\frac{\partial u_j}{\partial x_i} \right)^2 + 2 \frac{\partial u_i}{\partial x_j} \frac{\partial u_j}{\partial x_i}$$

$$= 2 \left\{ \left(\frac{\partial u_i}{\partial x_j} \right)^2 + \frac{\partial u_i}{\partial x_j} \frac{\partial u_j}{\partial x_i} \right\}$$

$$\therefore \overline{\rho' \epsilon} = \mu \overline{\left\{ \left(\frac{\partial u_i}{\partial x_j} \right)^2 + \frac{\partial u_i}{\partial x_j} \frac{\partial u_j}{\partial x_i} \right\}} = \frac{\mu}{2} \overline{S_{ij} S_{ij}}$$

In horizontally homogeneous conditions,

$$\frac{1}{2} \overline{S_{ij} S_{ij}} = \overline{\left(\frac{\partial u}{\partial z} \right)^2 + \left(\frac{\partial v}{\partial z} \right)^2 + 2 \frac{\partial u}{\partial z} \frac{\partial v}{\partial z}}$$

$$\text{since } \frac{\partial u}{\partial x} + \frac{\partial v}{\partial y} + \frac{\partial w}{\partial z} = 0 \text{ (incompressible)}$$

(iii)

$$\frac{\partial}{\partial x_k} (\overline{u_i' \rho' u_k}) = - \frac{\partial}{\partial x_i} (\overline{u_i' \rho'}) + \frac{\partial}{\partial x_k} (\overline{u_i' M'_{ik}})$$

$$= - \overline{u_i' \frac{\partial \rho'}{\partial x_i}} - \overline{\rho' \frac{\partial u_i'}{\partial x_i}} + \frac{\partial}{\partial x_k} (\overline{u_i' M'_{ik}})$$

$$\text{Now } \frac{\partial}{\partial x_k} (\overline{u'_i u'_k}) = \mu \left\{ \frac{\partial^2}{\partial x_k^2} (\frac{1}{2} \overline{u_i'^2}) + \frac{\partial^2}{\partial x_i \partial x_k} (\overline{u'_i u'_k}) \right\}$$

These terms have the character of a molecular diffusion effect and depend upon inhomogeneity of the distribution of mean values. They are assumed to be small and are neglected in comparison with the other terms in (4.3.11).

(iv) The remaining term from (iii) $\overline{u'_k \frac{\partial p'}{\partial x_k}}$ can be coupled with the last term in (4.3.11) to give,

$$\overline{u'_k \frac{\partial p'}{\partial x_k}} + \frac{\partial}{\partial x_k} \left[\frac{1}{2} \bar{\rho} \overline{u'_i u'_k} \right] = \frac{\partial}{\partial x_k} \left[\overline{u'_k (p' + \frac{1}{2} \bar{\rho} u_i'^2)} \right]$$

Collecting the results from (i) - (iv) we can rewrite (4.3.11),

$$\bar{\rho} \frac{\partial \bar{\mathcal{E}}}{\partial t} = -g \overline{\rho' w'} + \tau_{ik} \frac{\partial \bar{u}_i}{\partial x_k} - \frac{\partial}{\partial x_k} \left[\overline{u'_k (p' + \frac{1}{2} \bar{\rho} u_i'^2)} \right] - \bar{\rho} \epsilon \quad (4.3.12)$$

$$\text{where } \bar{\mathcal{E}} = \frac{1}{2} \overline{u_i'^2} = \frac{1}{2} (\overline{u'^2 + v'^2 + w'^2}) \quad (4.3.13)$$

is the mean turbulent kinetic energy.

If we further assume that the mean flow is horizontal, i.e. $\bar{w} = 0$ and that horizontal gradients can be neglected compared to vertical gradients then (4.3.12) reduces to,

$$\begin{aligned} \frac{\partial \bar{\mathcal{E}}}{\partial t} &= -\frac{g}{\bar{\rho}} \overline{\rho' w'} + \frac{\tau_x}{\bar{\rho}} \frac{\partial \bar{u}}{\partial z} + \frac{\tau_y}{\bar{\rho}} \frac{\partial \bar{v}}{\partial z} - \frac{1}{\bar{\rho}} \frac{\partial}{\partial z} \left[\overline{w' (p' + \bar{\rho} \mathcal{E})} \right] - \epsilon \\ &= -\frac{g}{\bar{\rho}} \overline{\rho' w'} - \frac{\overline{u' w'}}{\bar{\rho}} \frac{\partial \bar{u}}{\partial z} - \frac{\overline{v' w'}}{\bar{\rho}} \frac{\partial \bar{v}}{\partial z} - \frac{1}{\bar{\rho}} \frac{\partial}{\partial z} \left[\overline{w' (p' + \bar{\rho} \mathcal{E})} \right] - \epsilon \end{aligned} \quad (4.3.14)$$

$$\text{where } \epsilon = \nu \left\{ \left(\frac{\partial u'}{\partial z} \right)^2 + \left(\frac{\partial v'}{\partial z} \right)^2 + 2 \left(\frac{\partial w'}{\partial z} \right)^2 \right\} \quad (4.3.15)$$

$$\nu = \mu / \bar{\rho}$$

4.3.1 The Turbulent Kinetic Energy Balance Equation - Résumé

For a fuller discussion of the Turbulent Kinetic Energy Balance Equation see Chapter 5, An Introduction to Boundary Layer Meteorology, R B Stull, 1988.

Turbulent kinetic energy (TKE) is one of the most important variables in micrometeorology, because it is a measure of the intensity of turbulence. It is directly related to the momentum, heat, and moisture transports through the boundary layer. TKE is also sometimes used as a starting point for approximations of turbulent diffusion.

The individual terms in the TKE balance equation describe physical processes that generate turbulence. The relative balance of these processes determines the ability of the flow to maintain turbulence or become turbulent, and thus indicates flow stability. Some important dimensionless groups and scaling parameters are also based on terms in the TKE balance equation.

We shall adopt (4.3.12) as our most general form of the TKE balance equation:

$$\bar{\rho} \frac{\partial \bar{\mathcal{E}}}{\partial t} = \bar{\rho} \frac{\partial \bar{\mathcal{E}}}{\partial t} + \bar{\rho} \bar{u}_j \frac{\partial \bar{\mathcal{E}}}{\partial x_j} = -g \overline{\rho' w'} + \tau_{ik} \frac{\partial \bar{u}_i}{\partial x_k} - \frac{\partial}{\partial x_k} \left[\overline{u'_k (p' + \bar{\rho} \mathcal{E})} \right] - \bar{\rho} \epsilon$$

$$\text{i.e. } \frac{\partial \bar{\mathcal{E}}}{\partial t} + \bar{u}_j \frac{\partial \bar{\mathcal{E}}}{\partial x_j} = \underbrace{-\frac{g}{\bar{\rho}} \overline{\rho' w'}}_{\text{I}} - \underbrace{\frac{\tau_{ik} \bar{u}_i}{\bar{\rho}} \frac{\partial \bar{u}_i}{\partial x_k}}_{\text{II}} - \underbrace{\frac{1}{\bar{\rho}} \frac{\partial}{\partial x_k} \left[\overline{u'_k (p' + \bar{\rho} \mathcal{E})} \right]}_{\text{III}} - \underbrace{\frac{1}{\bar{\rho}} \frac{\partial}{\partial x_k} \left[\overline{u'_k p'} \right]}_{\text{VI}} - \underbrace{\epsilon}_{\text{VII}}$$

where $\bar{\mathcal{E}} = \frac{1}{2} \overline{u_i'^2} = \frac{1}{2} (\overline{u'^2 + v'^2 + w'^2})$ is the mean turbulent kinetic energy (often represented by $\bar{\mathcal{E}}$)

and $\tau_{ik} = -\bar{\rho} \overline{u'_i u'_k}$ are the Reynolds stresses.

- Term I represents local storage or tendency of TKE.
- Term II describes the advection of TKE by the mean wind.
- Term III is the buoyant production or consumption term. It is a production or loss term, typically positive during daytime over land (i.e. in convectively unstable conditions) and negative at night over land (i.e. in nocturnal stable conditions).
- Term IV is a mechanical, or shear production/loss term. The momentum flux $\overline{u'_i u'_k}$ is usually of opposite sign from the mean wind shear, because the momentum of the wind is usually lost downward to the ground. Thus, Term IV results in a positive contribution to TKE when multiplied by a negative sign, i.e. this normally a production term.

Term V represents the turbulent transport of TKE. It describes how TKE is moved around by the turbulent eddies.

Term VI is a pressure correlation term that describes how TKE is redistributed by the pressure perturbations. It is often associated with oscillations in the air, e.g. due to buoyancy or gravity-wave effects.

Term VII represents the viscous dissipation of TKE i.e. the conversion of TKE into heat. Recall that turbulence is dissipative. This term is a loss term that always exists whenever TKE is non-zero. Physically, this means that turbulence will tend to decrease and disappear with time, unless it can be generated locally or transported in by mean, turbulent, or pressure processes. Thus, TKE is not a conserved quantity. The ABL can be turbulent only if there are specific physical processes generating the turbulence.

NB ϵ , the viscous dissipation of TKE was introduced (in a physical sense) in Section 2.5, The Inertial Subrange.

If we assume horizontal mean flow, i.e. $\bar{u} = 0$, and horizontal homogeneity, then the above general form of the TKE balance equation reduces to the simplified form of (4.3.14).

$$\frac{\partial \bar{\epsilon}}{\partial t} = \underbrace{-\frac{g}{\bar{\rho}} \overline{\rho'w'}}_{\text{I}} - \underbrace{\overline{w'w'} \frac{\partial \bar{u}}{\partial z}}_{\text{II}} - \underbrace{\overline{v'w'} \frac{\partial \bar{v}}{\partial z}}_{\text{III}} - \underbrace{\frac{1}{\bar{\rho}} \frac{\partial (\bar{\rho}w'\epsilon)}{\partial z}}_{\text{IV}} - \underbrace{\frac{1}{\bar{\rho}} \frac{\partial (w'p')}{\partial z}}_{\text{V}} - \underbrace{\epsilon}_{\text{VI}} \quad \text{VII}$$

Terms V and VI are often combined to give

$$D = \frac{1}{\bar{\rho}} \frac{\partial}{\partial z} [w'(p' + \bar{\rho} \epsilon)]$$

where D represents the divergence per unit mass of the vertical flux of eddy kinetic energy and potential energy due to the pressure fluctuations.

4.4 The Buoyancy Term in the Turbulent Energy Balance Equation

4.4.1 The Perfect Gas Law and Virtual Temperature

The equation of state for air is, to a very good approximation, the perfect gas law

$$p = \frac{R^*}{m} \rho T \quad (4.4.1.1)$$

where R^* is the universal gas constant ($8.31 \text{ joule mole}^{-1} \text{ K}^{-1}$), m is the mean molecular weight of all the gases.

The mean is usually taken as a harmonic mean, weighted according to the concentration by mass of the various component gases.

We consider the air as consisting of dry air and water vapour and so

$$\begin{aligned} \frac{1}{m} &= \frac{(1-q)}{m_d} + \frac{q}{m_w} \\ &= \frac{1}{m_d} \left[1 + q \left(\frac{m_d}{m_w} - 1 \right) \right] \\ &= \frac{1}{m_d} [1 + 0.61q], \quad \text{since } \frac{m_d}{m_w} = \frac{29}{18}, \end{aligned} \quad (4.4.1.2)$$

where q , the specific humidity, is the mass of water vapour present per gram of moist air.

$$\therefore p = \frac{R^*}{m_d} \rho T (1 + 0.61q). \quad (4.4.1.3)$$

It is customary to define the virtual temperature, T_v , such that

$$T_v = T (1 + 0.61q) \quad (4.4.1.4)$$

and then we can write

$$p = \frac{R^*}{m_d} \rho T_v = R_d \rho T_v \quad (4.4.1.5)$$

where R_d is the gas constant for dry air ($0.287 \text{ joule gm}^{-1} \text{ K}^{-1}$).

The virtual temperature of a sample of moist air is that temperature at which dry air of the same total pressure would have the same density as the given sample.

The relative fluctuations of p , ρ and T_v are very small compared to the turbulent velocity fluctuations, u' , and so since these properties are related by the equation of state (4.4.1.5) we have to a high degree of approximation

$$\frac{p'}{p} = \frac{\rho'}{\rho} + \frac{T_v'}{T_v} \quad (4.4.1.6)$$

Further, relative fluctuations of p are in general very small compared to those of T_v and ρ and so

$$\rho' = -\bar{\rho} \frac{T_v'}{T_v}, \quad (4.4.1.7)$$

again to a high degree of approximation.

4.4.2 Heat and Water Vapour Fluxes

The buoyancy term of the turbulent kinetic energy balance equation can be written, using (4.4.1.7), as

$$\begin{aligned} -\frac{g}{\bar{\rho}} \overline{\rho' w'} &= \frac{g}{T_v} \overline{w' T_v'} \\ &\approx \frac{g}{T_v} \overline{w' T'} + 0.61 g \overline{w' q'}, \end{aligned} \quad (4.4.2.1)$$

neglecting higher order terms.

We can therefore define

$$H = \bar{\rho} c_p \overline{w' T'} \quad (4.4.2.2)$$

which is the vertical flux of sensible heat due to the eddy motion, c_p being the specific heat at constant pressure, and

$$E = \bar{\rho} \overline{w' q'} \quad (4.4.2.3)$$

which is the vertical flux of water vapour due to the eddy motion, related to the latent heat flux Q by

$$Q = \mathcal{L} E = \bar{\rho} \mathcal{L} \overline{w' q'} \quad (4.4.2.4)$$

where \mathcal{L} is the latent heat of condensation of water.

$$\begin{aligned} \therefore -\frac{g}{\bar{\rho}} \overline{\rho' w'} &= \frac{g}{\bar{\rho} \bar{c}_p \bar{T}} (H + 0.61 \bar{c}_p \bar{T} E) = \frac{g}{\bar{\rho} \bar{c}_p \bar{T}} (H + 176 \bar{c}_p E) \\ &= \frac{g}{\bar{\rho} \bar{c}_p \bar{T}} (H + 0.61 \bar{c}_p \bar{T} Q) \approx \frac{g}{\bar{\rho} \bar{c}_p \bar{T}} (H + 0.07 Q) \end{aligned} \quad (4.4.2.5)$$

$$\text{where } \bar{T} \approx 15^\circ \text{C} \approx 288 \text{ K}, \quad 0.61 \bar{T} \approx 176 \text{ K}, \quad 0.61 \bar{c}_p \bar{T} \approx 0.07.$$

We note that Q must be about 15 times larger than H to be of equal importance in the buoyancy term. This term is therefore often neglected, particularly over relatively dry land surfaces. It can however be very important over vegetated land surfaces or over water surfaces.

As with the eddy momentum flux we can formulate the flux-gradient relationships

$$H = -\bar{\rho} c_p K_H \frac{\partial \bar{\theta}}{\partial z} = -\bar{\rho} c_p \mu_* T_* \quad (4.4.2.6)$$

$$\text{and } E = -\bar{\rho} K_w \frac{\partial \bar{q}}{\partial z} = -\bar{\rho} \mu_* q_* \quad (4.4.2.7)$$

thereby defining the turbulent exchange coefficients K_H and K_w and also the scaling parameters T_* , q_* .

$$\text{Recall that } -\tau = -\bar{\rho} K_m \frac{\partial \bar{u}}{\partial z} = -\bar{\rho} \mu_*^2,$$

where the x -axis is assumed aligned along the mean wind.

We could also write

$$\begin{aligned} \frac{H + 0.61 \bar{c}_p \bar{T} E}{\bar{\rho} \bar{c}_p} &\approx \frac{H}{\bar{\rho} \bar{c}_p} + 176 \frac{E}{\bar{\rho}} = -\mu_* (T_* + 176 q_*) \\ &= -\mu_* \phi_* \quad , \text{ say,} \end{aligned}$$

$$\text{i.e. } \mathcal{H} = H + 0.61 \bar{c}_p \bar{T} E \approx -\bar{\rho} \bar{c}_p \mu_* \phi_* \quad (4.4.2.8)$$

Note that the temperature used in the flux-gradient relationship for the sensible heat transfer is the potential temperature θ since this is the temperature which is conserved in the large scale mixing.

Recall

$$\theta = T \left(\frac{1000}{p} \right)^{\kappa}$$

where p is in mb

and $\kappa = R / c_p$.

θ is the temperature that a parcel of air would have if it was brought adiabatically to the 1000 mb pressure level.

If the atmosphere is a perfect gas in hydrostatic equilibrium,

i.e.

$$p = R \rho T$$

and

$$\frac{\partial p}{\partial z} = -g \rho$$

then

$$\begin{aligned} \frac{1}{\theta} \frac{\partial \theta}{\partial z} &= \frac{1}{T} \frac{\partial T}{\partial z} - \frac{\kappa}{p} \cdot \frac{\partial p}{\partial z} \\ &= \frac{1}{T} \frac{\partial T}{\partial z} + \frac{R}{g R \rho T} g \rho \\ &= \frac{1}{T} \left(\frac{\partial T}{\partial z} + \Gamma \right) \end{aligned}$$

where

$$\Gamma = g / c_p \approx 9.8 \text{ K km}^{-1}$$

is called the dry adiabatic lapse rate.

Alternative representations of (4.5.1) are,

$$\frac{\partial \bar{E}}{\partial t} = \frac{g}{\bar{\rho} c_p T} (H + 0.61 c_p \bar{T} E) + \frac{\tau_x}{\bar{\rho}} \frac{\partial \bar{u}}{\partial z} + \frac{\tau_y}{\bar{\rho}} \frac{\partial \bar{v}}{\partial z} - D - \epsilon \quad (4.5.3)$$

$$= -\frac{g}{T} \left[K_H \frac{\partial \bar{\theta}}{\partial z} + 0.61 \bar{T} K_w \frac{\partial \bar{q}}{\partial z} \right] + K_M \left(\frac{\partial \bar{u}}{\partial z} \right)^2 + K_M \left(\frac{\partial \bar{v}}{\partial z} \right)^2 - D - \epsilon \quad (4.5.4)$$

The divergence term and the buoyancy term may take either sign.

It is often assumed that conditions are stationary, hence $\partial \bar{E} / \partial t = 0$, and this is an acceptable simplification in many circumstances. Even with this simplification there remains a complex balance in which the relative importance of the terms undoubtedly varies substantially.

Let us consider a few special cases where the balance may be simplified.

(i) Neutral flow

The general impression is that mechanical production and dissipation are the dominant terms.

$$\epsilon \approx \frac{\tau}{\bar{\rho}} \cdot \frac{\partial \bar{V}}{\partial z} = K_M \left[\left(\frac{\partial \bar{u}}{\partial z} \right)^2 + \left(\frac{\partial \bar{v}}{\partial z} \right)^2 \right] \quad (4.5.5)$$

(ii) Stable flow

Near the ground the energy budget terms are not reliably estimated but the broad expectation is of a rough balance between mechanical production and loss by viscous dissipation and working against buoyancy forces.

$$\epsilon \approx \frac{\tau}{\bar{\rho}} \cdot \frac{\partial \bar{V}}{\partial z} + \frac{g}{\bar{\rho} c_p T} (H + 0.61 c_p \bar{T} E) \quad (4.5.6)$$

(iii) Unstable flow

The vertical divergence of the vertical flux of turbulent kinetic energy may be significant typically decreasing from a positive value near the ground to a negative value in the upper part of the layer.

4.5 Special Cases of the Turbulent Energy Balance Equation

With the results of Section 4.4 the turbulent energy balance equation (4.3.14) can be rewritten,

$$\frac{\partial \bar{E}}{\partial t} = \frac{g}{T} \overline{w'T'} + 0.61 g \overline{w'q'} - \overline{w'w'} \frac{\partial \bar{u}}{\partial z} - \overline{v'w'} \frac{\partial \bar{v}}{\partial z} - D - \epsilon \quad (4.5.1)$$

$$\text{where } D = \frac{1}{\bar{\rho}} \frac{\partial}{\partial z} \left[\overline{w'(p' + \bar{p} \epsilon)} \right] \quad (4.5.2)$$

which represents the divergence per unit mass of the vertical flux of eddy kinetic energy and potential energy due to the pressure fluctuations.

At some intermediate level there should be a negligible divergence term, leaving the balance essentially between the buoyancy production and dissipation,

$$E \approx \frac{g}{\rho \bar{q}} (H + 0.61 \bar{q} \bar{T} E), \quad (4.5.7)$$

the mechanical production also possibly having fallen to a negligible value.

However the details of the precise balances are not yet settled and much more work is required to clarify the position in general.

4.6 The Richardson Numbers

In his original analysis Richardson, L.F. (1925) Phil. Mag., London, 42, p.81, neglected the dissipation and divergence terms and used the simple balance equation for the case of initially very slight turbulence

$$\begin{aligned} \frac{\partial \bar{E}}{\partial t} &= K_M \left(\frac{\partial \bar{u}}{\partial z} \right)^2 - \frac{g}{\bar{T}} K_M \frac{\partial \bar{\theta}}{\partial z} \\ &= K_M \left(\frac{\partial \bar{u}}{\partial z} \right)^2 \left[\frac{K_M}{K_H} - \frac{g \partial \bar{\theta} / \partial z}{\bar{T} \left(\frac{\partial \bar{u}}{\partial z} \right)^2} \right] \\ &= K_M \left(\frac{\partial \bar{u}}{\partial z} \right)^2 \left[\frac{K_M}{K_H} - Ri \right] \end{aligned} \quad (4.6.1)$$

where the x-axis is directed along the mean wind and the buoyancy term due to the water vapour flux has been neglected.

Further, assuming $K_H = K_M$, Richardson concluded that slightly turbulent motion would remain turbulent if $Ri < 1$ and would be suppressed if $Ri > 1$.

The question of the suppression (or initiation) of turbulence is much more complex than this.

There are now theoretical support and experimental evidence for initiation of turbulence in a stably stratified fluid at $Ri < \frac{1}{4}$. There is still much discussion on the value of Ri needed for suppression of turbulence but the current tendency is to accept a value near 1 as originally and simply estimated.

Quite apart from consideration of its critical value for suppression of turbulence the Richardson number is used as a general stability parameter.

The ratio of the production due to buoyancy forces to that due to the Reynolds stresses is called the flux Richardson number, R_f .

$$\begin{aligned} R_f &= \frac{-\frac{g}{\rho} \overline{w' \theta'}}{\overline{u' w'} \frac{\partial \bar{u}}{\partial z} + \overline{v' w'} \frac{\partial \bar{v}}{\partial z}} \\ &\approx \frac{\frac{g}{\bar{T}} \overline{w' \theta'} + 0.61 g \overline{w' q'}}{\overline{u' w'} \frac{\partial \bar{u}}{\partial z} + \overline{v' w'} \frac{\partial \bar{v}}{\partial z}} \\ &= \frac{\frac{g}{\rho \bar{q}} (H + 0.61 \bar{q} \bar{T} E)}{-\frac{E}{\rho} \cdot \frac{\partial \bar{V}}{\partial z}} \\ &= \frac{g}{\bar{T}} \left\{ \frac{K_M \frac{\partial \bar{\theta}}{\partial z} + 0.61 \bar{T} K_M \frac{\partial \bar{q}}{\partial z}}{K_M \left[\left(\frac{\partial \bar{u}}{\partial z} \right)^2 + \left(\frac{\partial \bar{v}}{\partial z} \right)^2 \right]} \right\} \end{aligned} \quad (4.6.2)$$

We usually accept $K_H = K_M$ and so

$$R_f \approx \frac{g}{\bar{T}} \cdot \frac{K_H}{K_M} \left[\frac{\frac{\partial \bar{\theta}}{\partial z} + 0.61 \bar{T} \frac{\partial \bar{q}}{\partial z}}{\left(\frac{\partial \bar{u}}{\partial z} \right)^2 + \left(\frac{\partial \bar{v}}{\partial z} \right)^2} \right] \quad (4.6.3)$$

[It is usually seen as

$$R_f \approx \frac{g}{\bar{T}} \cdot \frac{K_H}{K_M} \frac{\partial \bar{\theta} / \partial z}{\left(\frac{\partial \bar{u}}{\partial z} \right)^2} \quad (4.6.4)$$

where the effects of water vapour are negligible and the x-axis is aligned along the mean wind.]

In (4.6.3) all the quantities except K_H/K_M are directly measurable and it is not obvious how K_H/K_M will vary with conditions.

For these reasons the gradient Richardson number, Ri , is commonly used, where

$$Ri = \frac{g}{T} \left[\frac{\frac{\partial \bar{\theta}}{\partial z} + 0.61 \bar{T} \frac{\partial \bar{q}}{\partial z}}{\left(\frac{\partial \bar{u}}{\partial z}\right)^2 + \left(\frac{\partial \bar{v}}{\partial z}\right)^2} \right] \quad (4.6.5)$$

$$= \frac{K_M}{K_H} R_f, \text{ if } K_M = K_H$$

Often seen as
$$Ri \approx \frac{g}{T} \cdot \frac{\partial \bar{\theta} / \partial z}{(\partial \bar{u} / \partial z)^2} \quad (4.6.6)$$

- | |
|--|
| $\left. \begin{aligned} Ri, R_f &> 0 \text{ for stably stratified flow} \\ &= 0 \text{ for neutrally stratified flow} \\ &< 0 \text{ for unstably stratified flow} \end{aligned} \right\}$ |
|--|

Large values of Ri, R_f indicate that buoyancy dominates whereas small values indicate that buoyancy has little effect on the flow.

At $Z = 1$ m over grassland in mid-latitudes Ri is typically in the range $[-0.1, 0.1]$

4.7 Kinematic Fluxes

Flux is the transfer of a quantity per unit area per unit time

For convenience the eddy fluxes of momentum, heat and water vapour are expressed in kinematic form.

Let F_s denote the mean vertical turbulent flux of some conservative quantity whose mean value is \bar{s} . From definitions already introduced, we can express the general form of the kinematic flux F_s as

$$F_s = \overline{w's'} = -K_s \frac{\partial \bar{s}}{\partial z} = -\mu_s s_x$$

where
$$\mu_s = \sqrt{\frac{\tau}{\rho}}$$

MOMENTUM
$$F_v \equiv -\frac{\tau}{\rho} = |(\overline{u'w'}, \overline{v'w'})| = -K_M \left| \frac{\partial \bar{v}}{\partial z} \right| = -\mu_s^2$$

SENSIBLE HEAT
$$F_\theta \equiv \frac{H}{\rho c_p} = \frac{\overline{w'T'}}{\rho c_p} = -K_H \frac{\partial \bar{\theta}}{\partial z} = -\mu_s T_x$$

WATER VAPOUR FLUX
$$F_q \equiv \frac{E}{\rho} = \frac{\overline{w'q'}}{\rho} = -K_w \frac{\partial \bar{q}}{\partial z} = -\mu_s q_x$$

5. THE SURFACE-STRESS LAYER

Adjacent to the surface we can define a layer in which the stress has changed by less than some small percentage from its surface value, i.e. formally we can define a layer such that

$$\frac{|\tau(0) - \tau(z)|}{\tau(0)} \leq \epsilon \quad \text{for all } z \text{ in the layer} \quad (5.1)$$

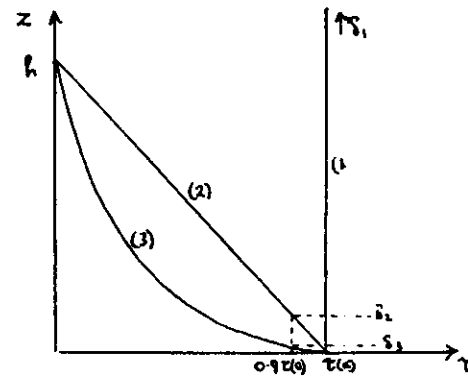
where ϵ is some small value, say about 0.1-0.2.

The layer so-defined is commonly called the constant-stress layer since, by definition, $\tau(0)$ is a good first order approximation to $\tau(z)$ at any level within the layer.

Unfortunately this terminology can be misleading and it is better to avoid it by using the more appropriate surface-stress layer.

It is most important to realise that we have said nothing here about the value $\frac{\partial \tau}{\partial z}$ which we have already seen has its maximum value close to the surface in the simple stationary atmospheric boundary layer (see Section 3.7 and Fig. F).

e.g. Consider the 3 profiles as shown.



Let δ_i be the depth of the surface-stress layer.

Curve (1): $\frac{\partial \tau}{\partial z} = 0$ for all z

$$\therefore \delta_1 \rightarrow \infty$$

Curve (2): $\frac{\partial \tau}{\partial z} = \text{const.}, z < h$

$\therefore \frac{\partial \tau}{\partial z} = \text{constant}$ within the surface-stress layer, $z \leq \delta_2$.

Curve (3): $\frac{\partial \tau}{\partial z}$ has its maximum value as $z \rightarrow 0$

$$\frac{\partial \tau}{\partial z} \rightarrow 0 \text{ as } z \rightarrow h$$

$\therefore \frac{\partial \tau}{\partial z}$ has its maximum value within the surface-stress layer, $z \leq \delta_1$.

It is the third situation which typically applies in the atmospheric boundary layer.

Therefore $\tau(z)$ can be treated as a constant in the surface-stress layer only if it appears undifferentiated. Recall that as $z \rightarrow 0$ the coriolis term in the equations of motion becomes increasingly less important in the balance of forces until $\frac{1}{\rho} \frac{\partial \tau}{\partial z}$ effectively balances the pressure gradient acceleration $\frac{1}{\rho} \nabla p$.

The depth of the surface-stress layer is generally some small fraction of the total depth of the boundary layer and is determined by the gradient of τ near the surface. The bigger the value of $\frac{\partial \tau}{\partial z}$ the shallower the layer where the criterion (5.1) will hold.

It can be shown that, typically, a good approximation for $\frac{\partial \tau}{\partial z}$ is given by

$$\frac{\partial \tau}{\partial z} \approx \frac{\partial p}{\partial y} \sin \alpha \quad (5.2)$$

and
$$\sin \alpha \approx \sin \alpha(0) \left(1 - \frac{z}{h}\right) \quad (5.3)$$

$$\therefore \tau(z) - \tau(0) \approx \frac{\partial p}{\partial y} \sin \alpha(0) \cdot z \left(1 - \frac{z}{2h}\right)$$

i.e.
$$\tau(0) \approx -\frac{\partial p}{\partial y} \sin \alpha(0) \cdot \frac{h}{2}$$

$$\therefore \frac{\tau(0) - \tau(z)}{\tau(0)} \approx \frac{2z}{h} \left(1 - \frac{z}{2h}\right) \approx \frac{2z}{h} \quad \text{for } \frac{z}{h} \ll 1. \quad (5.4)$$

Therefore

$$0.1 \leq \epsilon \leq 0.2$$

$$\Rightarrow 0.1 \frac{h}{2} \leq \delta \leq 0.2 \frac{h}{2}$$

Typically, $h \approx 1$ km and so $\delta \approx 50$ -100 m.

Therefore we are dealing with a layer perhaps some tens of metres thick.

We can extend the definition from surface-stress layer to surface-flux layer in which, by definition, the coriolis force (and hence the turning of the wind with height) may be ignored, and the vertical fluxes of momentum, heat and water vapour are closely approximated by their surface values (i.e. in this layer they are assumed to be virtually constant with height).

There will in general be three estimates of the depth of this layer, $\delta_m, \delta_n, \delta_w$ corresponding to the profiles of the different fluxes. On many occasions δ_m, δ_n and δ_w will imply approximately the same depth but on other occasions they could differ widely. e.g. Night time conditions with a radiation flux present are difficult to deal with.

6. THE STRATIFIED ATMOSPHERIC BOUNDARY LAYER NEAR THE GROUND:

THE SURFACE-FLUX LAYER

6.1 The Monin-Osukhlov Similarity Theory

The Monin-Osukhlov similarity hypothesis for the surface-flux layer is the most widely accepted approach for describing the properties of the surface layer.

Brought down to the very simplest terms, similarity methods depend on the possibility of being able to express the unknown variables in non-dimensional form, there being suitable argument for saying there exist a length-scale, a velocity-scale (or time-scale) and a temperature scale relevant in doing this. The non-dimensional forms are then postulated to be universal in character and this will hold as long as the scales remain the relevant ones.

The Monin-Osukhlov similarity hypothesis for the fully turbulent surface-flux layer (where the coriolis force is neglected) states that for any transferable property, the distribution of which is homogeneous in space and stationary in time, the vertical flux/profile relation is determined uniquely by the parameters

$$\frac{g}{T}, \frac{\tau(0)}{\bar{\rho}}, \frac{H(0)}{\bar{\rho} c_p}, \frac{E(0)}{\bar{\rho}} \quad (6.1.1)$$

which is equivalent to the set

$$\frac{g}{T}, \mu_* , T_* , q_* \quad (q_* = T_* + 176 q_{*s}) \quad (6.1.2)$$

where $\frac{g}{T}$ is the Archimedean buoyancy parameter.

N.B. In the atmosphere it is well-established that, except possibly within a very thin layer adjacent to the surface when the ground is quite smooth, the molecular fluxes of momentum and heat are negligibly small in comparison with the corresponding Reynolds fluxes due to turbulence. In this case the flow is said to be fully turbulent and no longer depends on molecular parameters such as ν and k where k is the thermal diffusivity ($= K_T / \rho c_p$, K_T = thermal conductivity). There is then close to the surface a very thin viscous sub-layer.

Instead of using the buoyancy parameter g/\bar{T} it is convenient to use the length-scale, L , uniquely defined by g/\bar{T} , u_* , q_* by the relation

$$\begin{aligned} L &= \frac{u_*^2 \bar{T}}{kg \varphi_*} \\ &= - \frac{u_*^3 \bar{\rho} \bar{q} \bar{T}}{kg H} \quad (\text{from (4.4.2.8)}) \\ &= - \frac{u_*^3 \bar{\rho} \bar{q} \bar{T}}{kg [H + 0.61 q_* \bar{T} E]} \quad (6.1.3) \end{aligned}$$

and called the Monin-Obukhov length. L is effectively constant in the surface-flux layer. k is the von Kármán constant (≈ 0.4) and is conventionally introduced solely as a matter of convenience. With upward heat flux taken as positive, L is negative.

Thus L , u_* , T_* , q_* (φ_*) (6.1.4) may be taken as the set of basic parameters which uniquely determine the vertical flux/profile relations.

Dimensional analysis leads to flux-gradient relationships which may be expressed in the general form

$$\frac{\partial \bar{s}}{\partial z} = \frac{s_*}{kz} \varphi_s(z/L) \quad (6.1.5)$$

where s_* is related to the vertical flux F_s such that

$$\begin{aligned} F_s &= -\bar{\rho} u_* s_* = -\bar{\rho} u_* kz \frac{\partial \bar{s}/\partial z}{\varphi_s(z/L)} \\ &= -\bar{\rho} K_s \frac{\partial \bar{s}}{\partial z} \quad (6.1.6) \end{aligned}$$

\bar{s} is the mean amount of the property in unit mass of air, s_* is a scaling parameter for \bar{s} in the surface-flux layer, K_s is the effective eddy diffusivity for the transfer of s .

The $\varphi_s(z/L)$ are universal functions of z/L only and may be different for different properties. They are not specified by the theory and must be determined by observations. The overall observational evidence is that the φ_s decrease in unstable stratification ($L < 0$) and increase in stable stratification ($L > 0$).

The profiles themselves are obtained by integrating (6.1.5)

$$\bar{s}(z) - \bar{s}(z_r) = \frac{s_*}{k} \left[\bar{\Phi}_s(z/L) - \bar{\Phi}_s(z_r/L) \right] \quad (6.1.7)$$

where z_r is some reference level at which \bar{s} is known.

In particular the nature of the similarity formulation implies a logarithmic singularity in the $\bar{\Phi}_s$'s as $z \rightarrow 0$.

This is avoided by defining the level z_0 as the virtual height at which \bar{s} attains its surface value. In general, z_0 which is characteristic of the underlying surface, is different for the wind, temperature and specific humidity profiles. However in the absence of further information it is usual to use z_0 derived from the wind profiles for all three.

This level, denoted z_0 , is defined as the virtual height at which $\bar{u} = 0$ and is called the surface roughness length. It is a characteristic of the surface and is usually independent of the flow.

Values of z_0 range from 1.2×10^{-2} cm for a relatively smooth sea surface to about 1m over a city or forest.

A typical value close to an extensive and uniform short grass surface would be 1-3 cm depending on the height of the grass.

Most of the standard text books on the subject will provide a table of values for different surfaces.

From (6.1.5) and (6.1.6) our complete set of profile relationships is:

$$\text{Momentum} \quad \frac{\partial \bar{u}}{\partial z} = \frac{u_*}{kz} \varphi_u(z/L) ; \tau = \bar{\rho} u_*^2 = \bar{\rho} K_m \frac{\partial \bar{u}}{\partial z} \quad (6.1.8)$$

$$\text{Heat} \quad \frac{\partial \bar{\theta}}{\partial z} = \frac{T_*}{kz} \varphi_\theta(z/L) ; H = -\bar{\rho} c_p u_* T_* = -\bar{\rho} c_p K_h \frac{\partial \bar{\theta}}{\partial z} \quad (6.1.9)$$

$$\text{Water Vapour} \quad \frac{\partial \bar{q}}{\partial z} = \frac{q_*}{kz} \varphi_q(z/L) ; E = -\bar{\rho} u_* q_* = -\bar{\rho} K_w \frac{\partial \bar{q}}{\partial z} \quad (6.1.10)$$

Other general relations are:

$$(i) \quad K_s = \frac{k u_* z}{\varphi_s(z/L)} \quad (6.1.11)$$

and therefore $K_s \varphi_s = k u_* z$ which is independent of s .

i.e. $K_m \varphi_m = K_u \varphi_u = K_w \varphi_w = k u_* z$ in the surface-flux layer.

$$\begin{aligned}
 (ii) \quad R_f &= \frac{g (H + 0.61 q_p \bar{T} E)}{-\rho q_p \bar{T} \frac{\tau}{\rho} \frac{\partial \bar{u}}{\partial z}} \\
 &= \frac{\mu_a^* k z}{k L \cdot \mu_a^* \cdot \mu_a \phi_m(z/L)} \\
 &= \frac{z}{L} \left[\frac{1}{\phi_m(z/L)} \right] \quad (6.1.12)
 \end{aligned}$$

and

$$\begin{aligned}
 Ri &= \frac{k_m}{k_u} \cdot R_f \quad (\text{taking } k_u = k_w) \\
 &= \frac{z}{L} \left(\frac{k_m}{k_u \phi_m} \right) \\
 &= \frac{z}{L} \left(\frac{\phi_H(z/L)}{\phi_m^2(z/L)} \right) \quad (6.1.13)
 \end{aligned}$$

6.2 The Neutral Surface-flux Layer

In neutral conditions the buoyancy effects vanish from the relations and we find that $\phi_m \approx 1$ when k is the von Kármán constant.

Therefore $L \rightarrow \pm \infty$, $R_f = Ri = 0$, $K = k u_* z$ (6.2.1)

$$\frac{\partial \bar{u}}{\partial z} = \frac{\mu_a}{k z} \quad (6.2.2.)$$

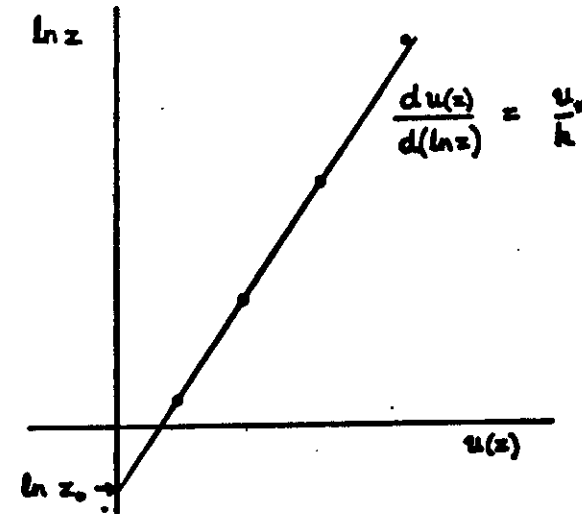
$$\therefore \bar{u}(z) = \frac{\mu_a}{k} \ln \frac{z}{z_0} \quad (6.2.3)$$

The neutral logarithmic wind-profile can be derived also by appealing to laboratory studies or from the classical mixing-length approach. The von Kármán constant, k , is the constant of integration established for equivalent formulae for laboratory flows in rough pipes and over rough plates.

k is normally taken to be about 0.4, although there are arguments which suggest that k can vary within the range $0.35 \leq k \leq 0.42$ in atmospheric flow.

NEUTRAL CONDITIONS (zero heat flux)

WIND PROFILE



z_0 is called the **SURFACE ROUGHNESS**

τ is the **SURFACE DRAG** or **SHEARING STRESS**

dimensions $[\tau] = \text{force/unit area}$

$$= \frac{\text{mass} \times \text{acceleration}}{\text{area}}$$

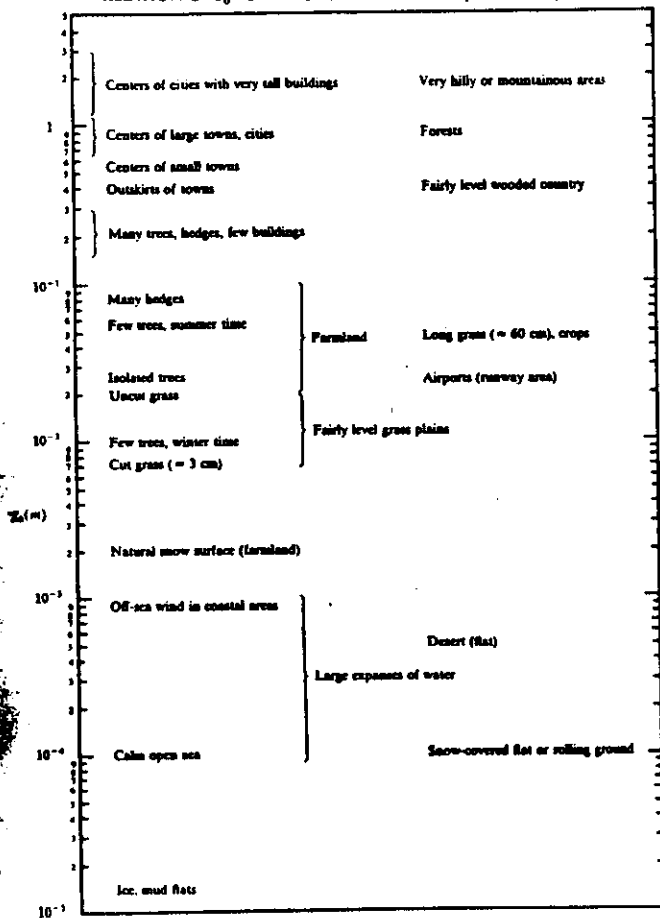
$$= \text{density} \times \frac{\text{volume} \times \text{acceleration}}{\text{area}}$$

$$= \text{density} \times \frac{L^3 \times LT^{-2}}{L^2}$$

$$= \text{density} \times [LT^{-1}]^2$$

$$\therefore \frac{\tau}{\rho} = (\text{velocity})^2 \equiv u_*^2, \text{ the FRICTION VELOCITY}$$

RELATION OF z_0 TO VARIOUS TERRAIN TYPES (ESDU, 1974)



Reprinted with permission.

Table 1. Reproduced from Panofsky and Dutton (1984).

In a plot of $u(z)$ vs. $\bar{u}(z)$, the gradient gives u_* and the intercept on the z -axis provides z_0 .

Over certain types of terrain e.g. cities, forests or other vegetative canopies the log-profile becomes valid for $z > 2h_c$ where h_c is the height of the roughness elements. Below this height the air flow is determined by the nature of the roughness elements and the flow within the roughness elements, the canopy flow, is governed by a different balance of forces than for the flow above.

It is found necessary to shift the height origin to a level d , the zero-plane displacement such that the profile becomes

$$\bar{u}(z) = \frac{u_*}{k} \ln \left[\frac{z-d}{z_0} \right] \quad (6.2.4)$$

In general d is a complex function of height and nature of the roughness elements, spacing of the roughness elements and stability.

e.g. For an extensive uniform pine forest at Thetford, $d \approx 0.75 h_c$, with some variation related to variations in tree-spacing, and $z_0 \approx 1m$.

(See e.g. Smith, F.B., Carson, D.J. and Oliver, H.R. (1972) 'Mean wind-direction shear through a forest canopy', Boundary-Layer Meteorology, 2, 178-190).

z_0 for a given surface can also be a function of the wind speed.

e.g. (i) a surface covered with long grass or certain crops becomes smoother in appearance in high winds because of deformation of the individual roughness elements by the wind giving rise to streamlining effects.

(ii) the sea-surface changes in nature according to wind speed.

The shearing stress is often represented in terms of a drag coefficient, C_D , by

$$\tau(z) = \bar{\rho} u_*^2 = \bar{\rho} C_D \bar{u}^2(z) \quad (6.2.5)$$

so that in neutral conditions

$$C_D \equiv C_D(z, z_0) = \left[\frac{u_*}{\bar{u}(z)} \right]^2 = \frac{k^2}{\left[\ln \left(\frac{z}{z_0} \right) \right]^2} \quad (6.2.6)$$

Note that C_D is a function of z and z_0 . Surface drag coefficients are often quoted for $z = 10 m$.

An alternative formulation is to define a geostrophic drag coefficient, C_g , by

$$\tau(0) = \bar{\rho} C_g V_g^2 \quad (6.2.7)$$

where V_g is the geostrophic wind speed at the top of the boundary layer.

Therefore,
$$C_g = \left(\frac{\mu_n}{V_g} \right)^2 \quad (6.2.8)$$

and is generally a function of a stability parameter such as

$$\mu = \frac{k \mu_n}{fL} \quad (6.2.9)$$

and a parameter called the surface Rossby number, defined by

$$R_o = \frac{V_g}{f z_o} \quad (6.2.10)$$

In strictly neutral conditions C_g is a function of R_o only.

6.3 The Unstable Surface-flux Layer

Although observational determinations of the analytical forms of ϕ_n , ϕ_H and ϕ_w continue to be published there is now some agreement on their general shape.

(i) $0 \geq z/L \geq -1$

At the present time I recommend the Businger/Dyer and Hicks forms for not too unstable conditions.

Businger, J.A. 1966 Proc. Symp. "Arctic Heat Budget & Atmos. Circulation" (The Rand Corpn), 305-332

Dyer, A.J. & Hicks, B.B. 1970 Quart. J.R. Met.Soc., 26, 715-721.

$$\phi_n(z/L) = \left(1 - 16 \frac{z}{L} \right)^{-1/4} \quad (6.3.1)$$

$$\phi_w(z/L) = \phi_n(z/L) = \left(1 - 16 \frac{z}{L} \right)^{-1/2} \quad (6.3.2)$$

The observations then imply equality of ϕ_n and ϕ_H and also indicate a close approach to

$$\phi_n = \phi_m^2 \quad (6.3.3)$$

Therefore
$$R_i \approx \frac{z}{L} \quad (6.3.4)$$

and
$$R_f = \frac{z}{L} \left(1 - 16 \frac{z}{L} \right)^{1/4} \quad (6.3.5)$$

i.e. In the slightly unstable surface-flux layer R_i is found empirically to vary linearly with z for a given L .

Also
$$K_n = K_w = \frac{k \mu_n z}{\phi_n} = k \mu_n z \left(1 - 16 \frac{z}{L} \right)^{1/2} \quad (6.3.6)$$

$$K_m = \frac{k \mu_n z}{\phi_m} = k \mu_n z \left(1 - 16 \frac{z}{L} \right)^{1/4} \quad (6.3.7)$$

$$K_n = K_w = \frac{K_m}{\phi_m} \quad (6.3.8)$$

The Wind Profile

$$\frac{\partial \bar{u}}{\partial z} = \frac{\mu_n}{kz} \left(1 - 16 \frac{z}{L} \right)^{-1/4} \quad (6.3.9)$$

$$\bar{u}(z) = \frac{\mu_n}{k} \int_{z_o}^z \frac{\left(1 - 16 \frac{\eta}{L} \right)^{-1/4} d\eta}{\eta} \quad \text{where } \eta = z/L, \quad z_o = z_o/L,$$

$$\left. \begin{aligned} \text{Put } v &= (1 - 16 \frac{\eta}{L})^{1/4} \\ 4v^3 d\eta &= -16 d\eta \\ \eta &= (1 - 16 \frac{\eta}{L})^{1/4} \\ \eta_o &= (1 - 16 \frac{z_o}{L})^{1/4} \end{aligned} \right\} \begin{aligned} &= \frac{4\mu_n}{k} \int_{\eta_o}^{\eta} \frac{v^2 dv}{v^4 - 1} \\ &= \frac{4\mu_n}{k} \int_{\eta_o}^{\eta} \left[\frac{1}{4(v-1)} - \frac{1}{4(v+1)} + \frac{1}{2(v^2+1)} \right] dv \\ &= \frac{\mu_n}{k} \left\{ \ln \left[\frac{v-1}{v+1} \right] + 2 \tan^{-1} v \right\} \Bigg|_{\eta_o}^{\eta} \end{aligned}$$

The Temperature Profile

$$\frac{\partial \bar{\theta}}{\partial z} = \frac{T_*}{kz} \left(1 - 16 \frac{z}{L}\right)^{-1/2}$$

$$\bar{\theta}(z) - \bar{\theta}(0) = \frac{T_*}{k} \int_0^z \frac{(1 - 16\eta)^{-1/2}}{\eta} d\eta$$

$$\left. \begin{aligned} y &= (1 - 16\eta)^{1/2} \\ y dy &= -16 d\eta \end{aligned} \right\}$$

$$= \frac{2T_*}{k} \int_{T_*^2}^{T_0^2} \frac{dy}{y^2 - 1}$$

$$= \frac{T_*}{k} \int_{T_*^2}^{T_0^2} \left[\frac{1}{y-1} - \frac{1}{y+1} \right] dy$$

$$\left. \begin{aligned} T_*^2 &= (1 - 16z/L)^{1/2} \\ T_0^2 &= (1 - 16z/L)^{1/2} \end{aligned} \right\} = \frac{T_*}{k} \left\{ \ln \left[\frac{y-1}{y+1} \right] \right\}_{y=T_*^2}^{T_0^2} \quad (6.3.11)$$

The Specific Humidity Profile

$$\bar{q}(z) - \bar{q}(0) = \frac{q_*}{k} \left\{ \ln \left[\frac{y-1}{y+1} \right] \right\}_{y=T_*^2}^{T_0^2} \quad (6.3.12)$$

(ii) $z/L < -1$ Extremely unstable.

The extension to the more unstable regime must be carried out with caution.

At $z/L = -1$ we note from (6.3.4) and (6.3.5) that

$$Ri = -1 \quad (6.3.13)$$

and

$$R_f = \frac{K_H}{K_M} Ri$$

$$= (1 - 16 \frac{z}{L})^{1/4} Ri$$

$$\approx -2 \quad (6.3.14)$$

Therefore at $z/L = -1$ the rate of production of turbulent kinetic energy due to buoyancy forces is twice that due to the Reynolds stresses (the two are equal for $z/L = -0.56$).

Mechanically generated turbulent motion is apparently a very inefficient transporting agent compared to heat convection. Mechanical eddies are smaller and more isotropic than eddies produced by heating.

Free convection is said to occur when the vertical transfer of heat and momentum by mechanical turbulence can be neglected compared to that by heat convection. Sometimes strictly defined for $H(0) > 0$, $u_* \rightarrow 0$. i.e. $L \rightarrow 0$.

Fully forced convection, on the other hand, is the state where buoyancy does not affect the motion or the heat transfer coefficient and the dynamically generated turbulence is the only agent in transferring fluxes down the gradients.

There is probably a gradual transition from forced to free convection and the general state will be a mixture of these two called mixed convection.

In free convection, the vertical transports are independent of u_* which loses its significance as a scaling parameter and so L is no longer relevant for the profiles.

The remaining parameters for determining the gradient of potential temperature are

$$\frac{g}{T} \quad \text{and} \quad \frac{H(0)}{\rho C_p} \quad (6.3.15)$$

$$\text{i.e.} \quad \frac{\partial \bar{\theta}}{\partial z} = f_n \left(\frac{g}{T}, \frac{H(0)}{\rho C_p}, z \right) \quad (6.3.16)$$

Dimensional analysis produces

$$\frac{\partial \bar{\theta}}{\partial z} = -C \left(\frac{H(0)}{\rho C_p} \right)^{2/3} \left(\frac{g}{T} \right)^{-1/3} z^{-4/3} \quad (6.3.17)$$

where C is a constant best estimated about 0.84. (Lumley and Panofsky (1964) p.10) imply $1.07 \leq C \leq 1.39$ but these values are probably too high.)

$$\text{Therefore} \quad K_H = \frac{-H(0)}{\rho C_p \frac{\partial \bar{\theta}}{\partial z}} = C^{-1} \left(\frac{g H(0)}{\rho C_p T} \right)^{1/3} z^{4/3} \quad (6.3.18)$$

Recall that $\frac{gH(0)}{\bar{\rho} \bar{c}_p \bar{T}}$ is the rate of convective energy production.

Note that we have gone from $K_H \propto Z$ in the near-neutral situation to $K_H \propto Z^{4/3}$ in free-convection.

Integration of (6.3.17) gives

$$\bar{\theta}(z) - \bar{\theta}(z_r) = 3C \left(\frac{H(0)}{\bar{\rho} \bar{c}_p} \right)^{2/3} \cdot \left(\frac{g}{\bar{T}} \right)^{-1/3} \cdot (z^{-1/3} - z_r^{-1/3}). \quad (6.3.19)$$

Note that we cannot extend this type of profile down close to Z_0 , unless $Z_0/L < -1$.

Provided K_H/K_M tends to a finite limit as $|z/L|$ increases, then similar relations should apply for the wind shear and the wind profile.

$$\tau(0) = \bar{\rho} k_M \frac{\partial \bar{u}}{\partial z} = \bar{\rho} \mu_*^2. \quad (6.3.20)$$

$$\begin{aligned} \therefore \frac{\partial \bar{u}}{\partial z} &= \frac{k_M}{k_M} \cdot \mu_*^2 \cdot \frac{1}{k_M} \\ &= C \frac{k_M}{k_M} \cdot \mu_*^2 \left(\frac{gH(0)}{\bar{\rho} \bar{c}_p \bar{T}} \right)^{-1/3} z^{-4/3} \end{aligned} \quad (6.3.21)$$

The behaviour of K_H/K_M is not settled for free convection conditions.

Certainly for slight to moderately unstable conditions $K_H/K_M = \left(1 + 16 \frac{z}{L}\right)^{1/4}$ which is height dependent for a given L.

If in free convection K_H/K_M is virtually independent of height then

$$\frac{\partial \bar{u}}{\partial z} \propto z^{-4/3}$$

and $\bar{u} \propto z^{-1/3}$

The structure of the profiles in such conditions has not yet been universally agreed upon.

6.4 The Stable Surface-flux Layer

The stably stratified surface-flux layer (most commonly the nocturnal boundary layer condition) has not yet been analysed sufficiently to determine the ϕ_s 's with any degree of confidence. It is even debatable whether it is meaningful to prescribe ϕ_s 's in such conditions.

The turbulence is not continuously maintained in stably stratified conditions, instead we have relatively long periods with little or no turbulent activity punctuated at intervals by relatively short bursts of turbulent activity.

It would appear that for most of the time the critical Richardson number for the suppression of turbulence is exceeded but that slowly radiative and other effects cause the profile gradients to steepen and hence Ri falls to less than its critical value of about $\frac{1}{4}$ for the onset of turbulence.

During a short burst of activity there is turbulent mixing and transfer within the boundary layer which leads to a slow but steady deepening of the stable layer. The layer then returns to its quiescent near-laminar state.

One slight consolation is that this regime is generally of smaller practical importance than the unstable regime about which much more is known with confidence.

Although ϕ_s functions are less well determined they do exist. The formulations given here are due to Webb, E.K. (1970) Quart. J.R. Met.Soc., 96, 67-90.

$$(i) \quad 0 \leq z/L \leq 1$$

$$\begin{aligned} \phi_m = \phi_u = \phi_w &= 1 + \alpha \frac{z}{L} \\ &\approx 1 + 5.2 \frac{z}{L} \end{aligned} \quad (6.4.1)$$

$$k_M = k_H = k_w = \frac{k \mu_* z}{1 + 5.2 \frac{z}{L}} \quad (6.4.2)$$

$$R_i = R_f = \frac{z/L}{1 + 5.2 \frac{z}{L}} \quad (6.4.3)$$

$$0 \leq R_i \leq 0.16$$

$$\frac{z}{L} = \frac{R_i}{1 - 5.2 R_i} = \frac{R_f}{1 - 5.2 R_f} \quad (6.4.4)$$

These expressions for ϕ_s produce log-linear profiles.

$$\frac{\bar{u}(z)}{u_*} = \frac{\bar{\theta}(z) - \bar{\theta}(0)}{T_*} = \frac{\bar{q}(z) - \bar{q}(0)}{q_*} = \frac{1}{k} \left[\ln \frac{z}{z_0} + \frac{5.2}{L} (z - z_0) \right] \quad (6.4.5)$$

(ii) $z/L > 1$

The above log-linear law implies that $Ri \rightarrow \frac{1}{\alpha} \approx 0.2$ as $\frac{z}{L} \rightarrow +\infty$.

Webb (1970) has extended his study of the stable surface-flux layer to cases of strong stability and has suggested a departure from the log-linear form for $z/L \gg 1$.

With very limited data Webb suggests that the profiles are only quasi-determinate, approximating, on the average, a simple logarithmic form. This regime covers the range approximately $1 < z/L < (\alpha+1)$

i.e. $1 < z/L < 6.2$

$$\phi_m = \phi_u = \phi_w = 1 + \alpha = 6.2 \quad (6.4.6)$$

$$k_m = k_u = k_w = \frac{k u_* z}{1 + \alpha} = 0.16 k u_* z. \quad (6.4.7)$$

$$R_i = R_f = \frac{z/L}{1 + \alpha} = 0.16 \frac{z}{L} \quad (6.4.8)$$

$$(1 + \alpha)^{-1} < R_i < 1$$

i.e. $0.16 < R_i < 1$

These expressions for ϕ_s produce log-profiles (subject to large variability)

$$\frac{\bar{u}(z) - \bar{u}(z_r)}{u_*} = \frac{\bar{\theta}(z) - \bar{\theta}(z_r)}{T_*} = \frac{\bar{q}(z) - \bar{q}(z_r)}{q_*} = \frac{H \alpha}{k} \ln \frac{z}{z_r} \quad (6.4.9)$$

for $z/L, z_r/L$ in this range.

According to Webb, for $z/L > 1 + \alpha$ i.e. $R_i > 1$ there is a regime of extreme stability but this is practically unrepresented in the data examined.

H.3. All formulae for stable conditions and particularly for $z/L > 1$ should be used with caution. A more recent observational study by Hicks (1976) Quart. J.R. Met.Soc., 102, 535-551 substantiates Webb's log-linear regime up to about $z/L \approx 0.5$ but differs beyond. For $z/L > 10$ Hicks finds evidence for a linear profile regime.

1.5 Some Profile Comparisons

See Figures G, H, I, J, K.

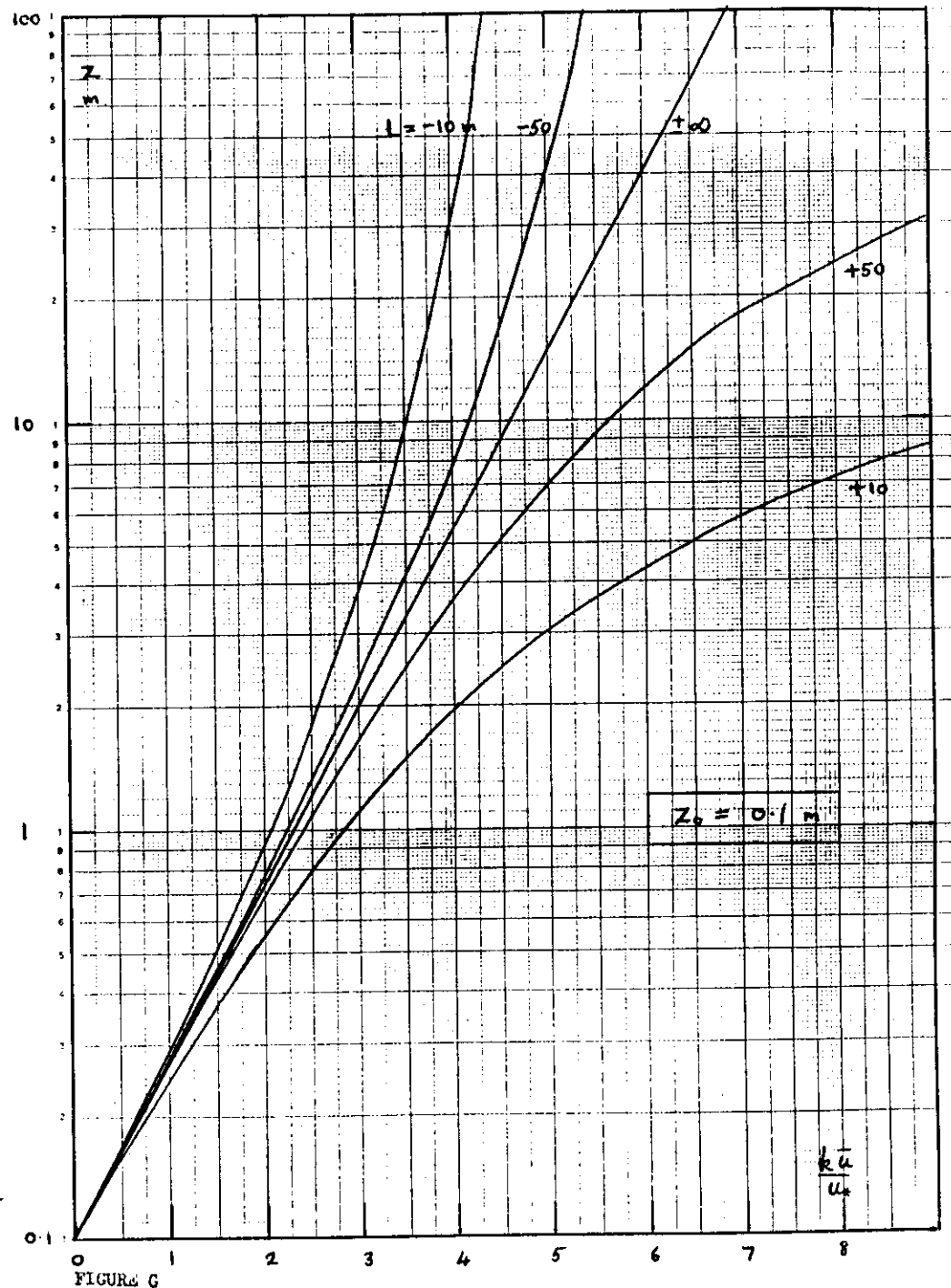


FIGURE G

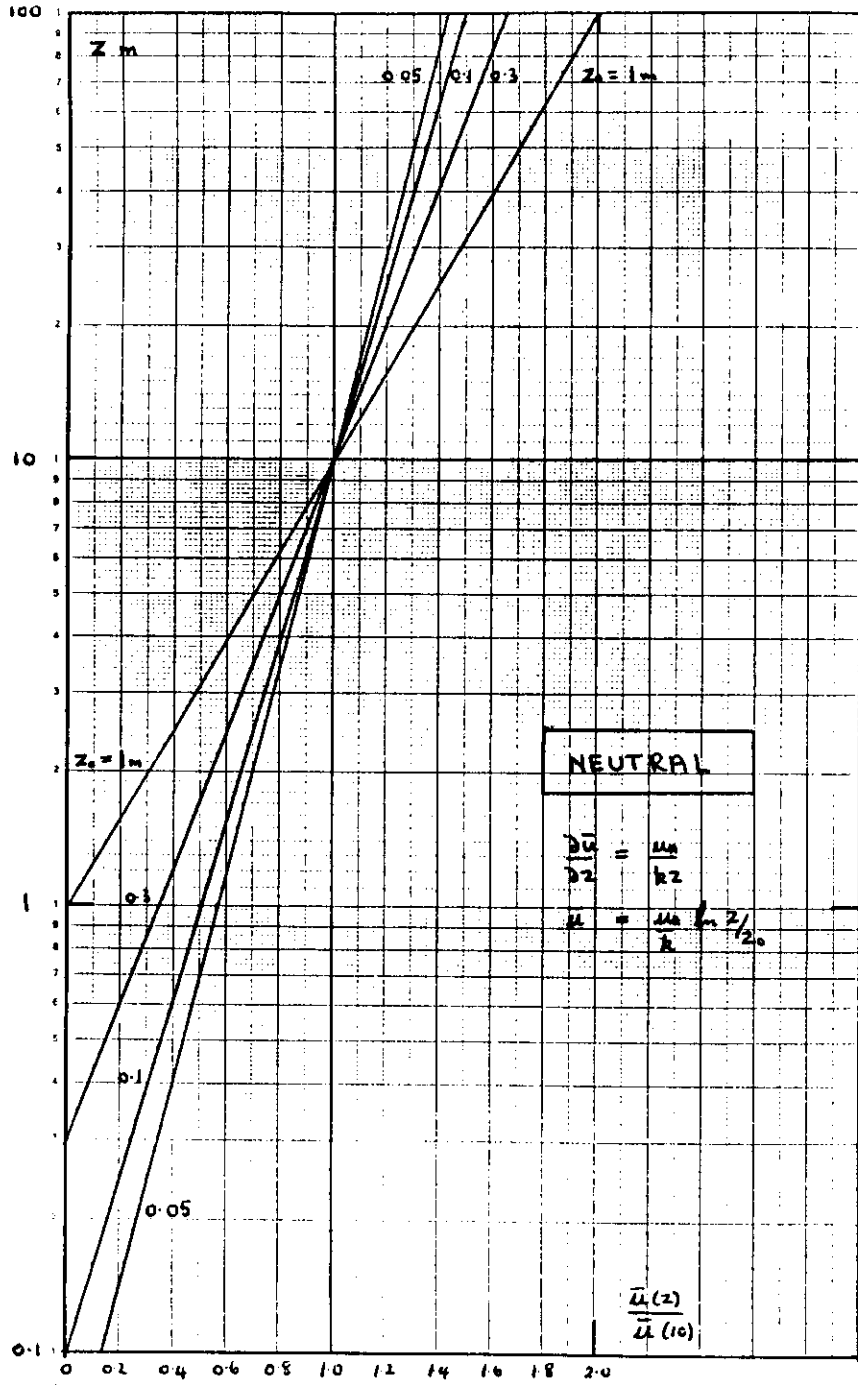


FIGURE H

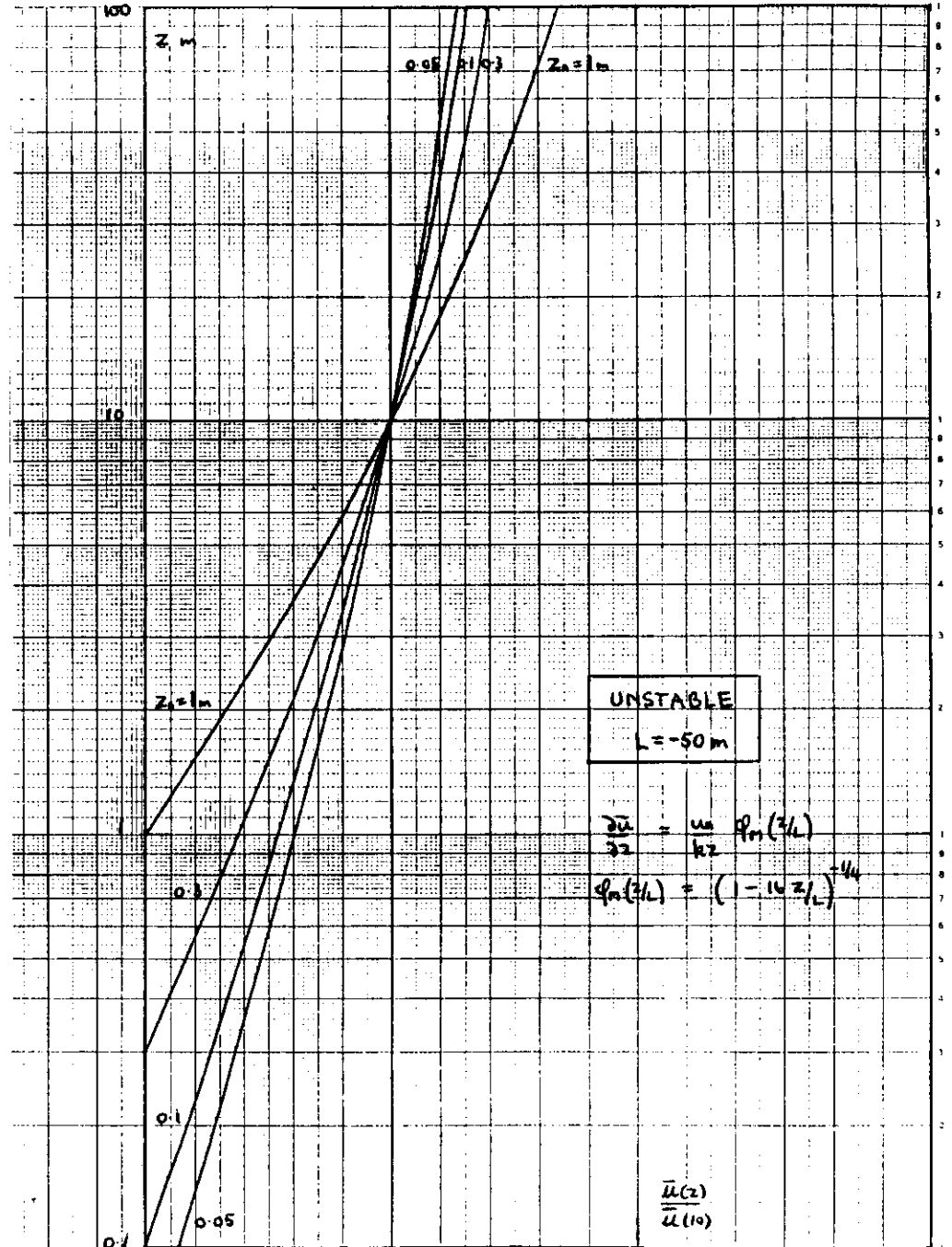


FIGURE I

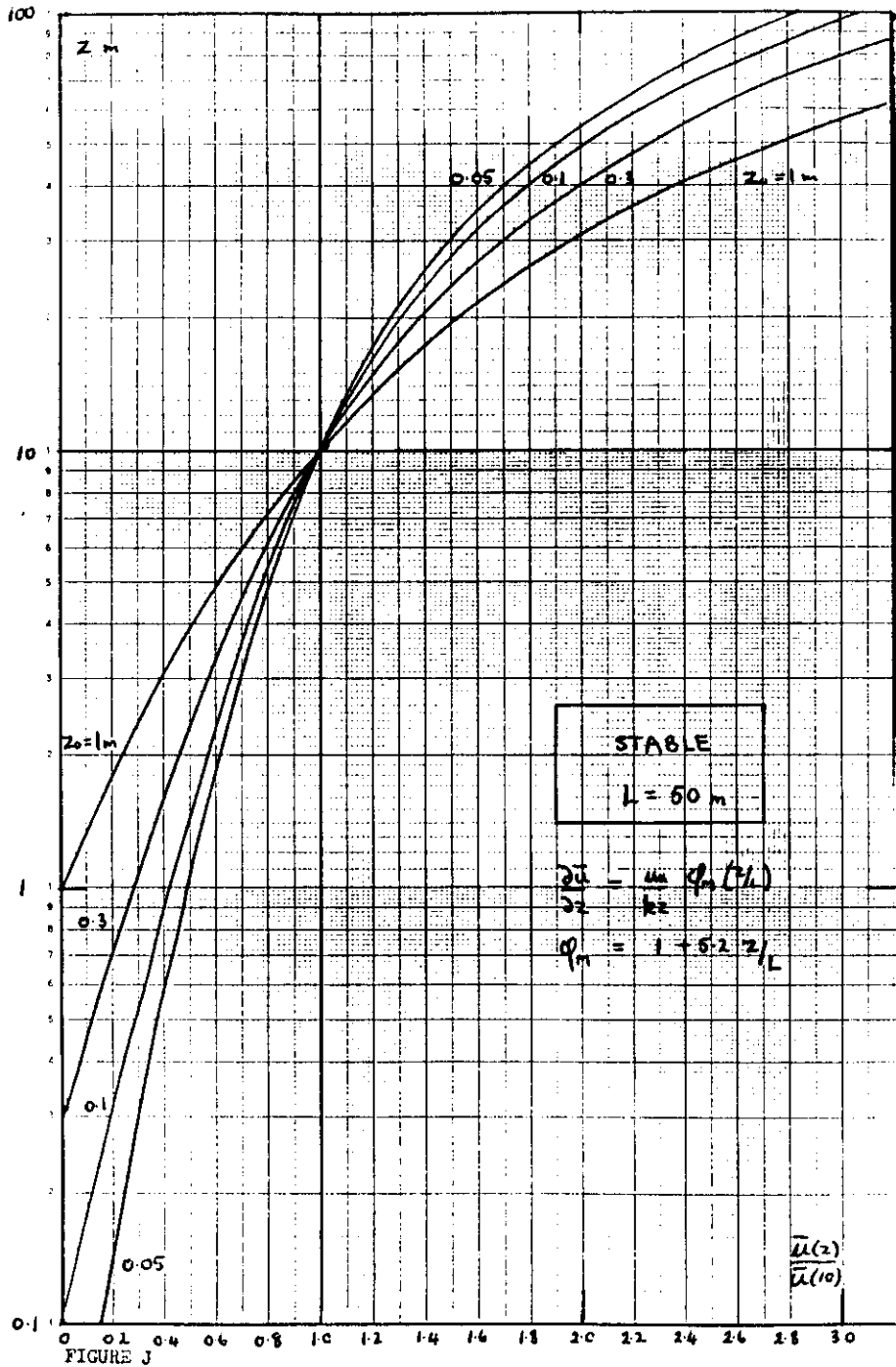


FIGURE J

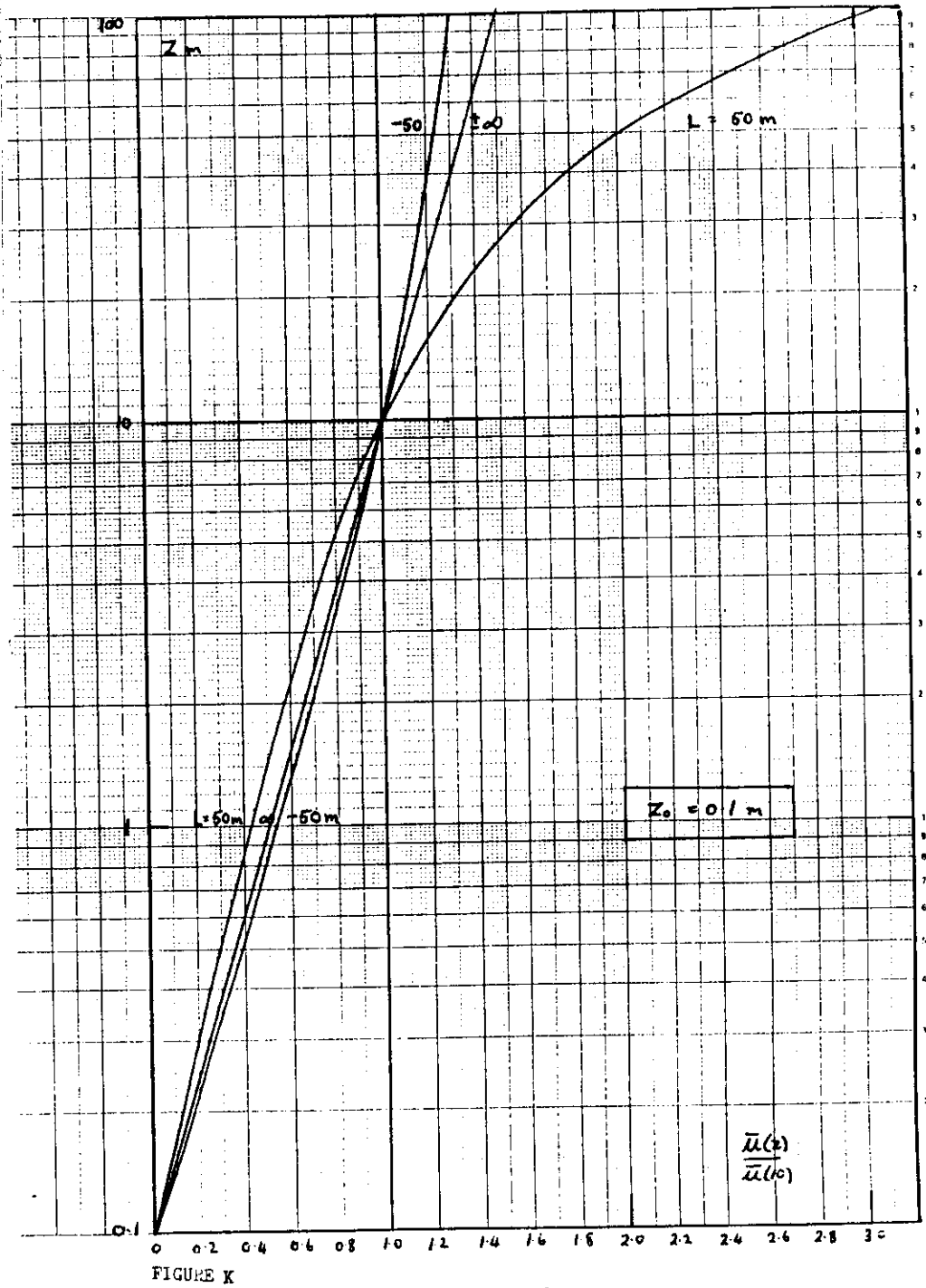


FIGURE K

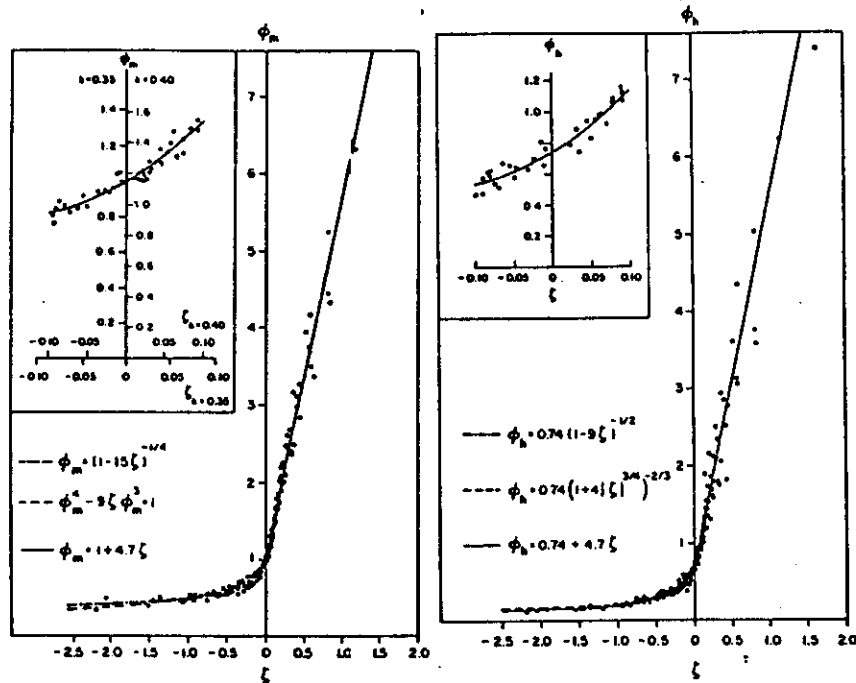


FIG. 1. Comparison of dimensionless wind shear observations with interpolation formulas.

FIG. 2. Comparison of dimensionless temperature gradient observations with interpolation formulas.

Figure 10.

(from Businger, et al., 1971)

	0.5	1	6	10	γ	k	α	Data Source
Webb (1970)	$\varphi_m = \varphi_w = \varphi_w = 1 + \alpha \gamma$		$1 + \alpha$	—	—	0.41	5.2	O'Neill 1953 Kerang 1962, 63, 64 Ray 1964, 65
Clarke (1970a)	$\varphi_m (= \varphi_w = \varphi_w) = \frac{1 + \alpha \gamma}{1 + 0.0079 \gamma (1 + \alpha \gamma)}$		$\frac{1 + \alpha}{1 + 0.0079 (1 + \alpha) \gamma}$			0.4	5	Kerang 1964 Ray 1965 (mostly)
Hicks (1976)	$\varphi_m = 1 + \alpha \gamma$	$(8 - \frac{4.25}{\gamma} + \frac{1}{\gamma^2})$			$c \gamma$ $c = 0.76$	0.41	5	Ray 1967
Businger et al (1971)		$\varphi_m = 1 + \alpha \gamma$ $\varphi_H = 0.74 + \alpha \gamma$				0.55	4.7	Kansas 1968

Table 1. A summary of the Monin-Obukhov similarity functions, $\varphi_s(\gamma)$, suggested by several recent observational studies of the stable atmospheric boundary layer.

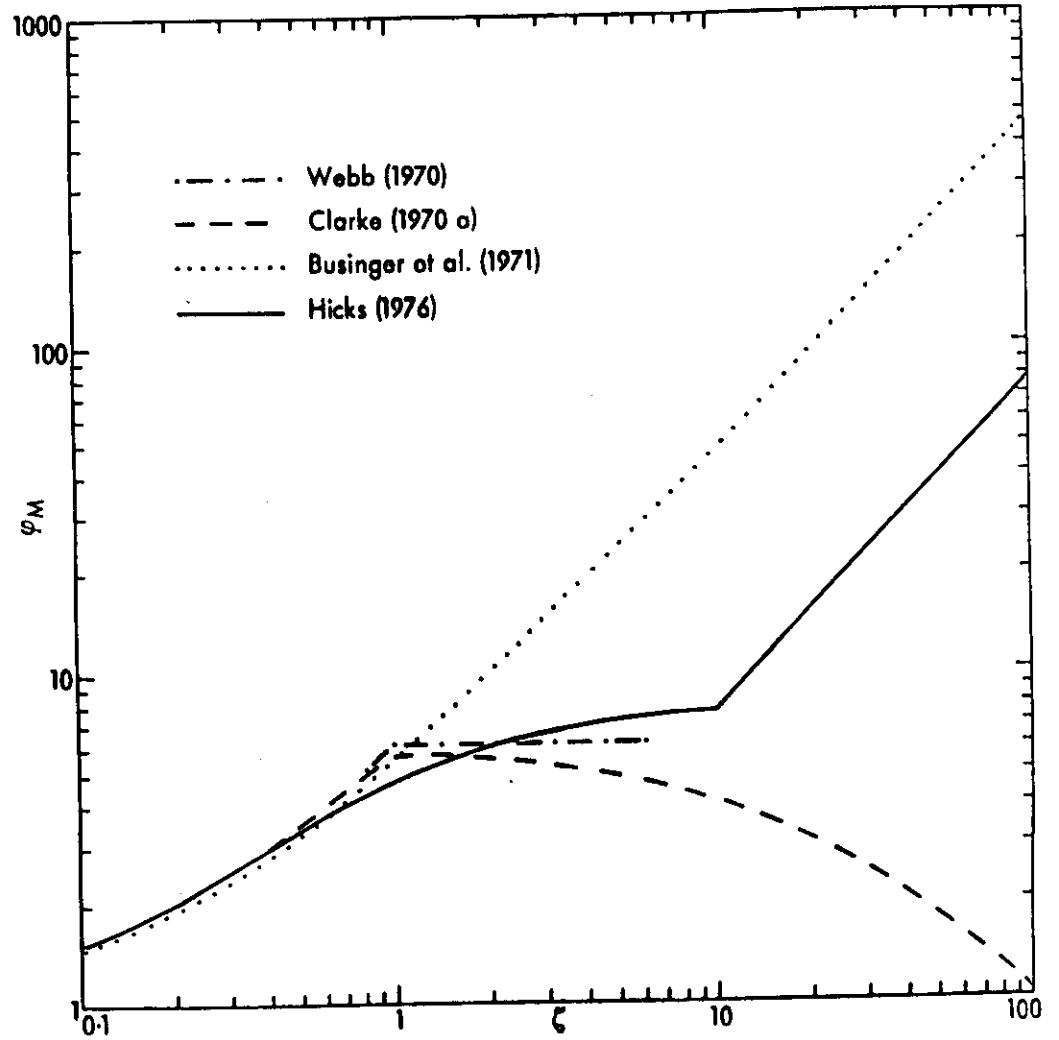


Figure 1 A comparison of the dependence of the similarity function φ_M on $\zeta = z/L$ suggested by several recent observational studies of the stable atmospheric boundary layer

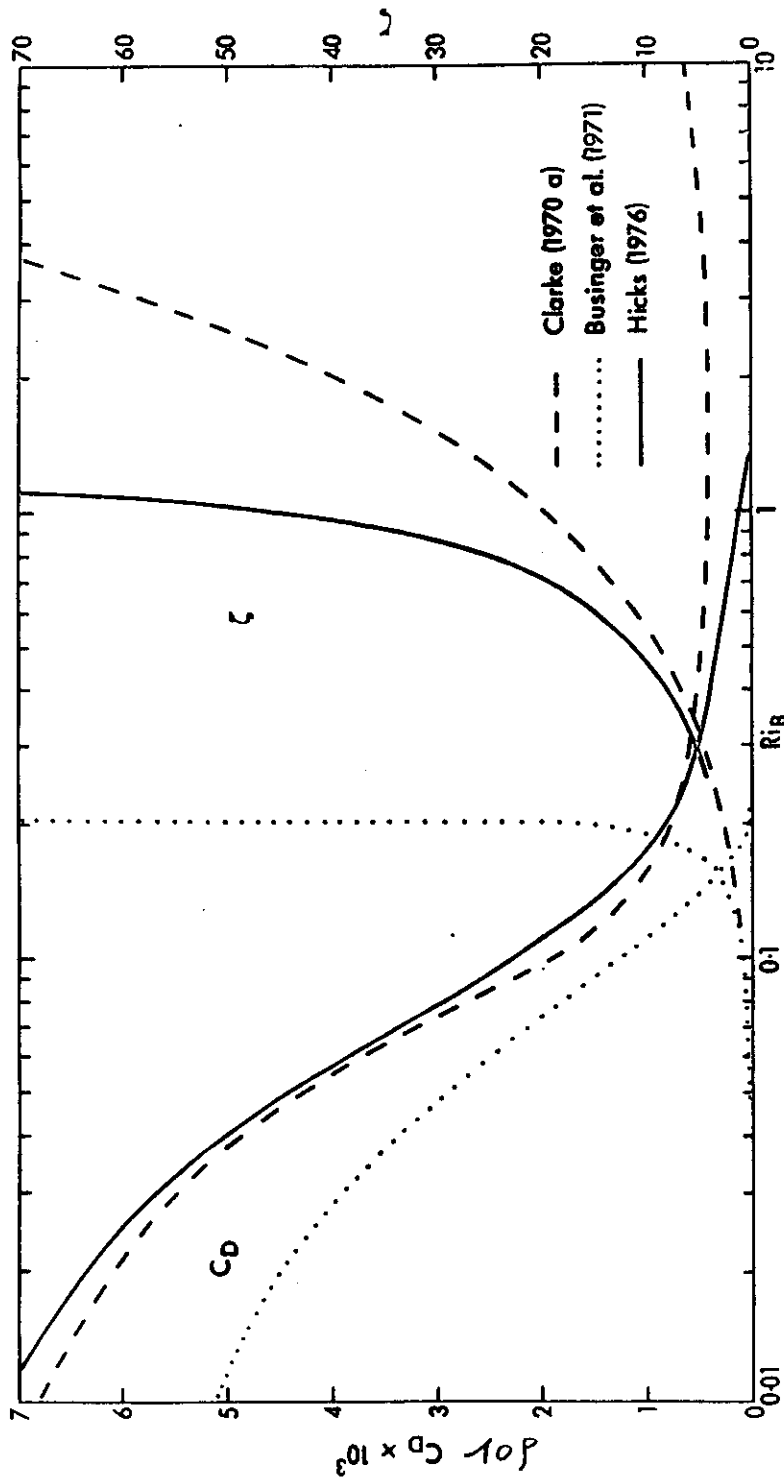


Figure 2 The drag coefficient, C_D , for $z = 10\text{m}$ and $z_0 = 0.1\text{m}$, and $\zeta = z/L$ as functions of the bulk Richardson number, Ri_B , for the layer surface to 10m . The curves have been derived from the indicated recent observational studies of the stable atmospheric boundary layer

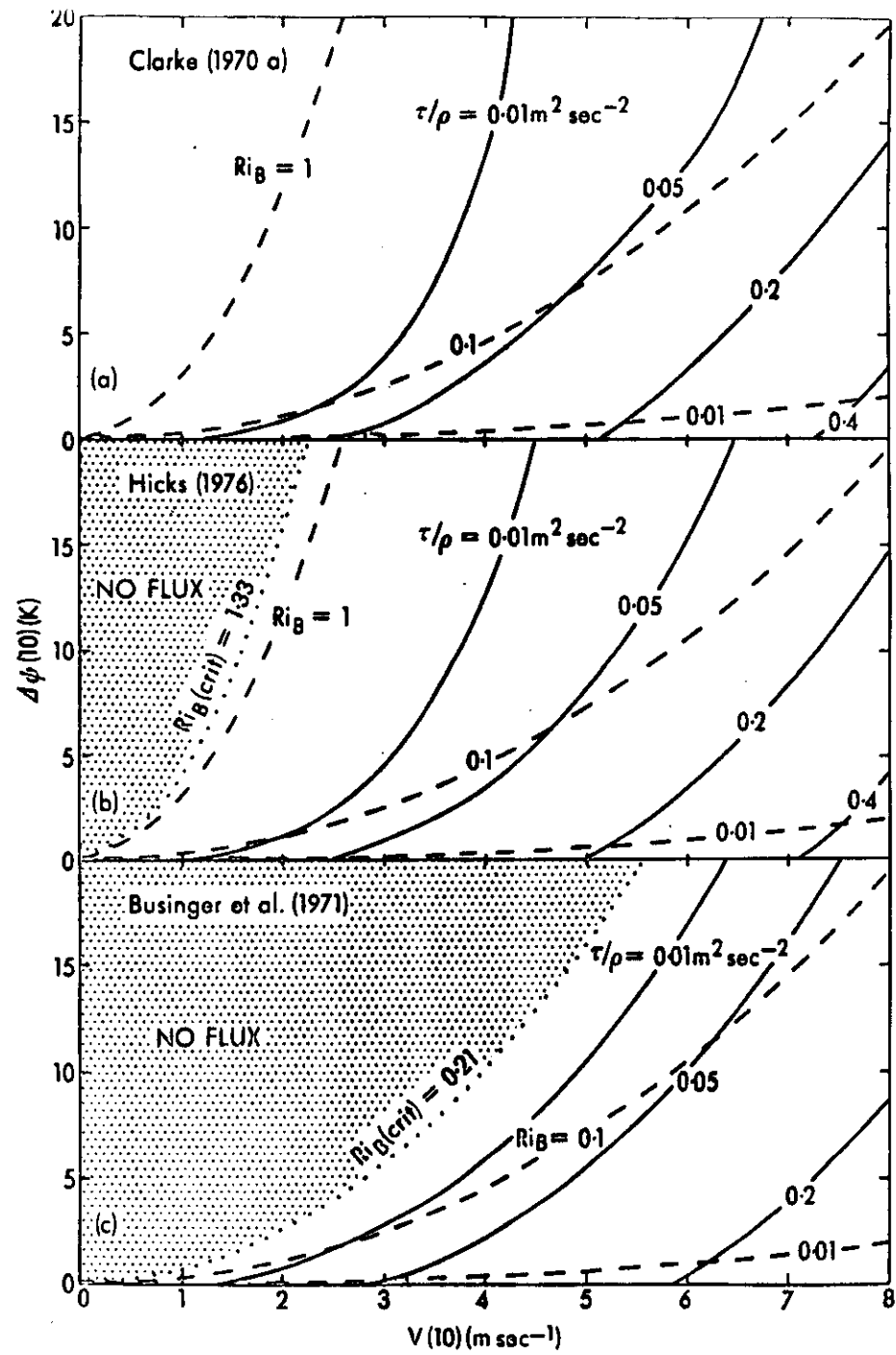


Figure 3 Isoplths of τ/ρ ($\text{m}^2 \text{sec}^{-2}$) — and Ri_B — — as functions of $V(z)$ (m sec^{-1}) and $\Delta\phi(z)$ (K) for $z = 10\text{m}$ and $z_0 = 0.1\text{m}$, using the values for C_D illustrated in Figure 2 110

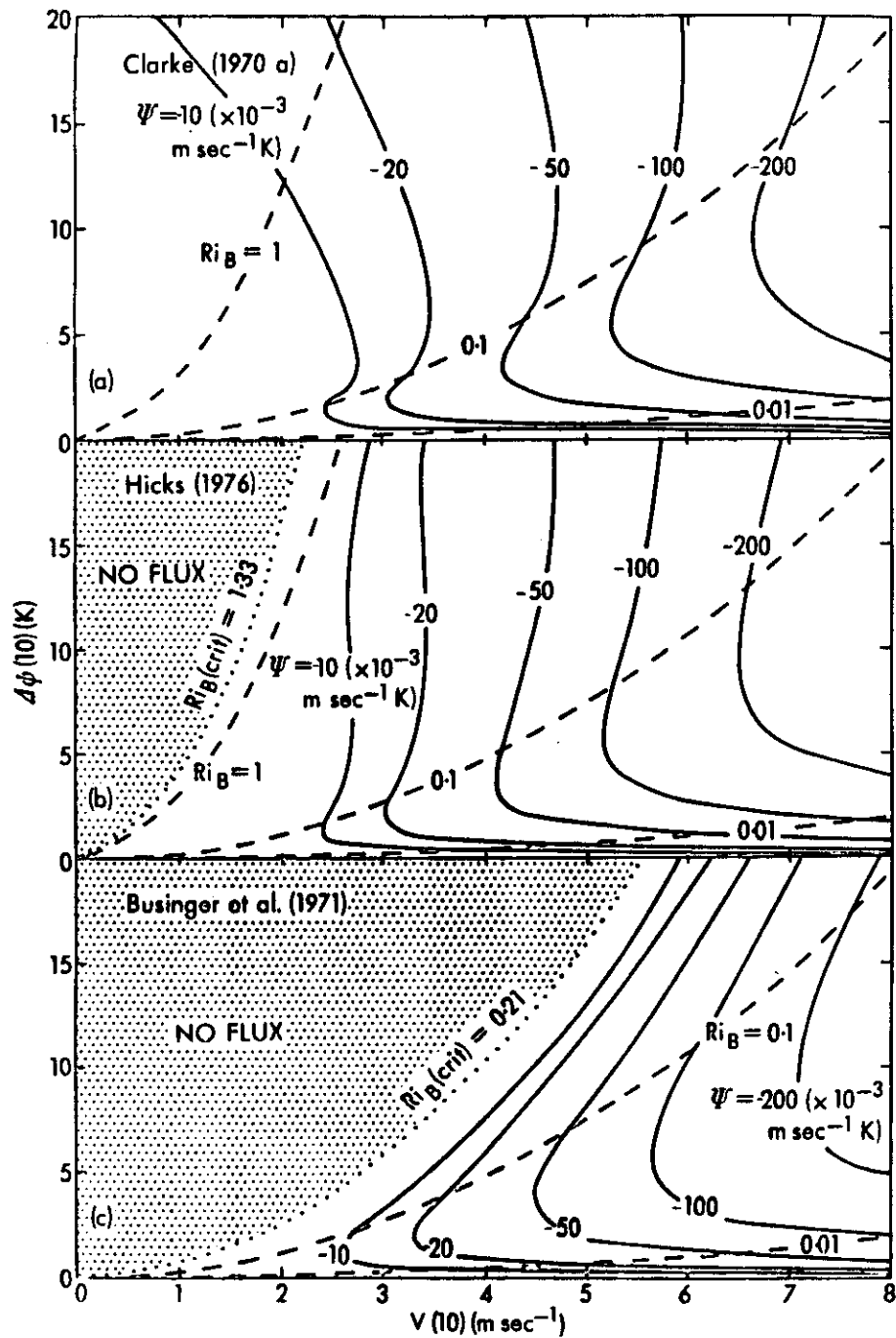


Figure 4 Isopleths of Ψ ($\times 10^{-3}$ m sec $^{-1}$ K) — and Ri_B -- as functions of $V(z)$ (m sec $^{-1}$) and $\Delta\phi(z)$ (K) for $z = 10$ m and $z_0 = 0.1$ m

111

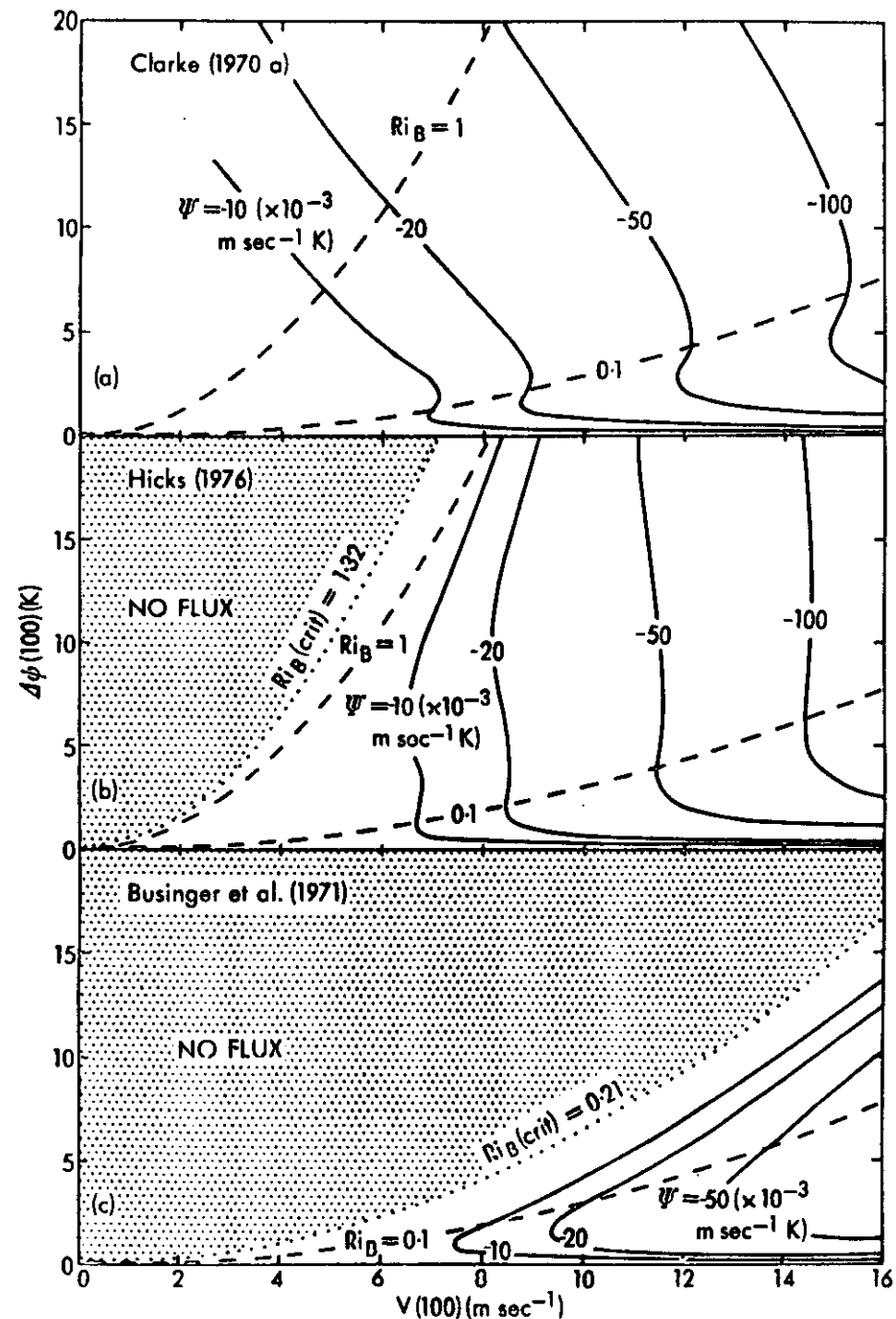
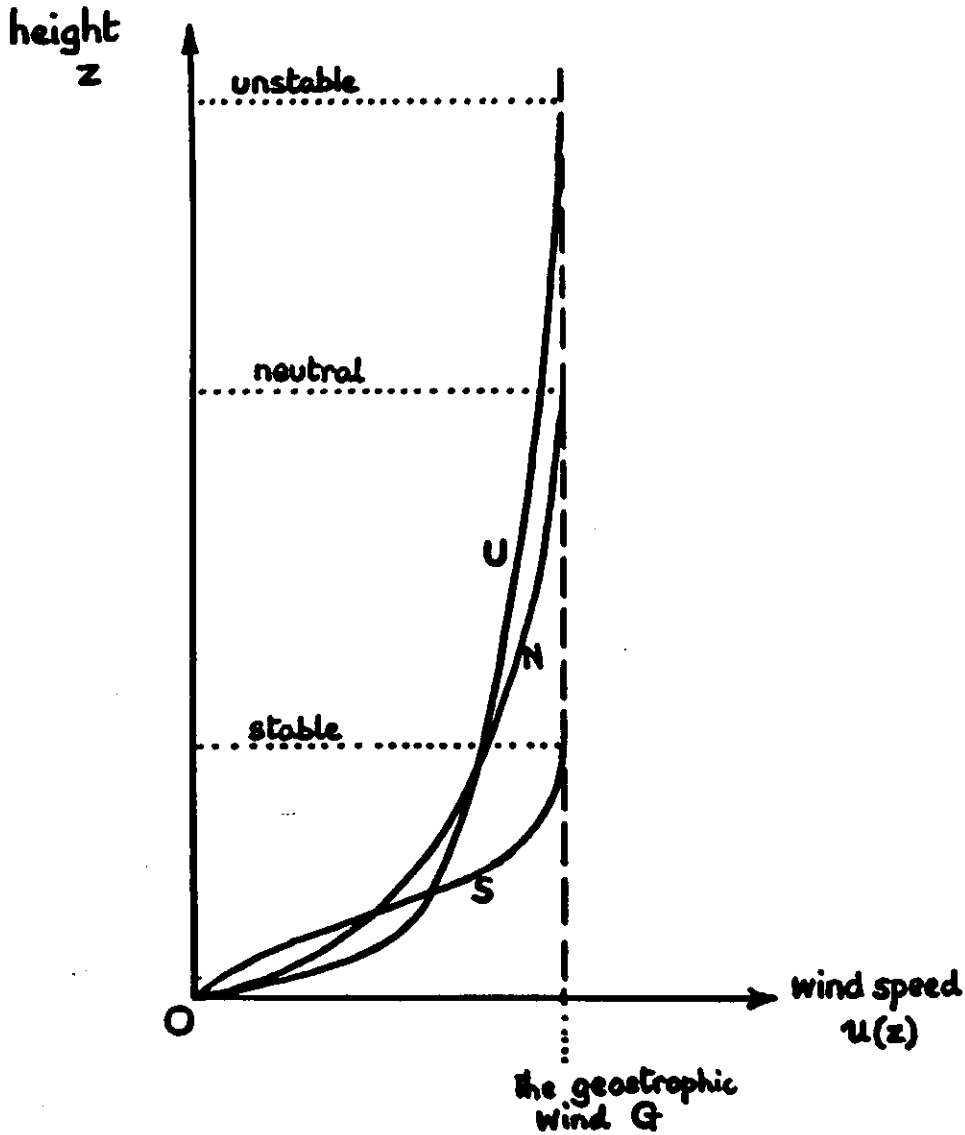


Figure 5 Isopleths of Ψ ($\times 10^{-3}$ m sec $^{-1}$ K) — and Ri_B -- as functions of $V(z)$ (m sec $^{-1}$) and $\Delta\phi(z)$ (K) for $z = 100$ m and $z_0 = 0.1$ m

112



Typical variations in the wind profile with stability.

6.6 Variances of Turbulent Characteristics

6.6.1 Basic definitions and approximations.

So far we have been concerned with profiles and fluxes. However, many applications depend on the characteristics of the turbulent fluctuations themselves. An important set of variables are the standard deviations of the three wind components. Take u parallel to the mean horizontal wind. By definition then $\bar{v} = 0$ and it is common to assume $\bar{w} = 0$.

The fluctuations θ' of the horizontal wind direction are given approximately (in radians) by

$$\theta' = \frac{v'}{\bar{V}}$$

where $\bar{V} = (\overline{u^2 + v^2})^{1/2}$ (often necessarily approximated by \bar{u})

and the fluctuations of the vertical angle, φ' , by

$$\varphi' = \frac{w'}{\bar{V}}$$

These approximations are strictly valid only for small angles, however in practice the errors are usually small.

The variances are defined by

$$\sigma_u^2 = \overline{u'^2}$$

$$\sigma_v^2 = \overline{v'^2} = (\bar{V} \sigma_\theta)^2$$

$$\sigma_w^2 = \overline{w'^2} = (\bar{V} \sigma_\varphi)^2$$

6.6.2 Variances of the wind components in the neutral surface layer.

Monin-Obukhov similarity theory requires that the standard deviations of the velocity components, normalised by the friction velocity, are functions only of z/L in the surface layer. In neutral conditions the normalised standard deviation should be constants, independent of height or roughness.

This hypothesis is borne out over homogeneous terrain for all the velocity components. Thus

$$\sigma_u = A u_*$$

$$\sigma_v = B u_*$$

$$\sigma_w = C u_*$$

Substitution of u_* from the logarithmic wind profile yields

$$\sigma_u / \bar{V} = \frac{kA}{\ln(z/z_0)}$$

$$\sigma_\theta = \sigma_v / \bar{V} = \frac{kB}{\ln(z/z_0)}$$

$$\sigma_\varphi = \sigma_w / \bar{V} = \frac{kC}{\ln(z/z_0)}$$

Note that in the neutral surface layer, σ_u / \bar{V} , σ_θ and σ_φ are independent of wind speed and u_* and depend only on z/z_0 (and the respective constants).

Table 2 (from Panofsky and Dutton (1984)) gives a list of estimates of A, B and C from observations over uniform terrain.

6.6.3 Variances of the wind components in the non-neutral surface layer.

It turns out that of the variances of the three velocity components only σ_w obeys Monin-Obukhov scaling, viz.

$$\sigma_w / u_* = \phi_3(z/L).$$

Fig 12 (from Panofsky and Dutton (1984)) illustrates one attempt to determine $\phi_3(z/L)$.

For fuller discussions see, for example, Pasquill and Smith (1983), Chap 2 or Panofsky and Dutton (1984), Chap 7.

TABLE 2 RATIOS OF STANDARD DEVIATIONS OF VELOCITY COMPONENTS TO FRICTION VELOCITY

Site	σ_u/u_*	σ_v/u_*	σ_w/u_*
<i>Flat Terrain</i>			
O'Neill, NE	2.42	1.73	—
Sublette, KS	2.45	1.90	1.25
Lander, B. C.	2.20	1.90	1.40
Beach Island, SC	2.30	1.90	1.35
Donaldson, MN	2.50	2.20	1.20
Guelph, Ontario*	2.50	1.85	1.22
St. Louis, MO*	2.39	1.79	1.26
Roskilde, Denmark [†]	2.30	2.10	1.10
Canterbury, NZ	2.43	1.93	1.20
Average	2.39 ± 0.03	1.92 ± 0.05	1.25 ± 0.03
<i>Rolling Terrain</i>			
Uppsala, Sweden	3.2	—	—
Erie, CO	2.65	2.00	1.20
Rock Springs, PA			
Nonmountain	3.20	2.90	1.24
Mountain	4.50	3.80	1.24

[†]12-17 min average, no trend removal

*Roughness lengths 0.7-1.7 m.

From Panofsky and Dutton (1984)

D. J. CARSON

Meteorological Office, Bracknell, UK

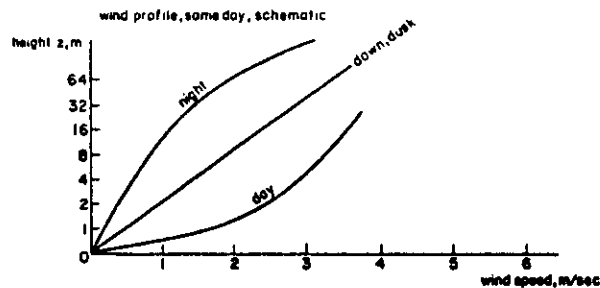


FIGURE 11 • Diurnal variation of wind profiles (schematic).
Panofsky and Dutton (1984)

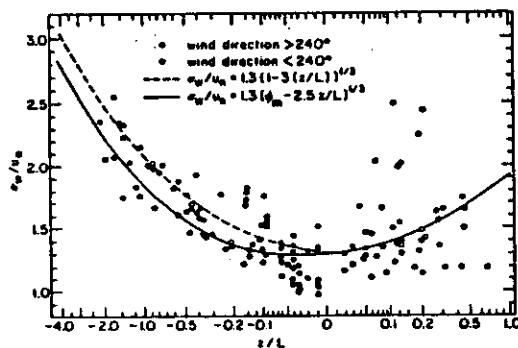


FIGURE 12 σ_w / u_* as a function of z/L at Rock Springs, Pa. below 8 m. Smooth lines represent mathematical fits recommended in the past. For wind direction less than 240° , the air had crossed a low mountain range.

From Panofsky and Dutton (1984)

ABSTRACT

This paper introduces the sub grid-scale, land-surface processes which, it is generally acknowledged, need to be included by parametrization in three-dimensional, numerical models for studying climate and climate change and for numerical weather prediction.

The discussion is restricted, in the main, to the relatively simple case of non-vegetated, land surfaces. The general boundary conditions for momentum transfer and the balance equations for energy and mass (moisture) transfer at a bare-soil surface are identified. The physical character and the parametrization of the varied flux-terms at the surface are considered systematically under the headings: Surface Radiative Properties and Fluxes; Surface Turbulent Exchanges; Soil Heat Conduction and the Land-surface Temperature; and Surface Hydrology and the Soil Water Budget.

Some of the particular problems associated with snow-covered, non-vegetated, land surfaces are described very briefly.

1. Introduction

The atmospheric boundary layer is the lowest layer of the atmosphere characterized by significant vertical flux divergences of momentum, heat and moisture which result directly or indirectly from interactions between the atmosphere and the underlying surface. The turbulent nature of boundary-layer flows is a vital factor in the efficient exchange of momentum, heat and moisture between the Earth's surface below and the 'free' atmosphere above. In general, up until fairly recently, designers and users of global atmospheric general circulation models (AGCMs) and operational numerical weather prediction models (NWPMS) have not been concerned with the details of boundary-layer and surface properties and processes in their own right but mainly for the influence they exert on weather systems and circulation characteristics on the much larger, synoptic or even global scales. However, the recent upsurge in the simultaneous developments of three-dimensional AGCMs for the study of climate and climate change and of increasingly sophisticated and more highly resolved operational NWPMS has resulted in more effort now being directed towards delineating details in boundary-layer structure and in the characteristics of surface climatologies. Studies with AGCMs have indicated considerable sensitivity of their simulations to changes in surface properties such as albedo, soil moisture and surface roughness. Also, some NWPMS now in operational service are expected to forecast the near-surface meteorological variables, and even changes in surface properties. The importance then of 'land-surface processes' and the need

to understand and represent them better in AGCMs and NWPMS are now well established. The respective rôles of these processes in the wider climatological context have been discussed elsewhere.

Following the Joint Scientific Committee Scientific Steering Group on Land-Surface Processes of the World Climate Research Programme (WCP, 1985), I shall adopt the pragmatical definition of land-surface processes as those phenomena which control the fluxes of heat, moisture and momentum between the surface and the atmosphere over the continents. These processes influence both the circulation of the atmosphere, often remotely, and the climate of the surface.

Many important dynamical and physical processes are governed by spatial (and temporal) scales very much smaller than the typical limits of resolution of either a numerical model or an observing system. Such sub grid-scale processes cannot be dealt with explicitly in the models; however, their statistical effects at the resolved scales must be included and are determined in terms of the explicitly resolved variables. This technique is called parametrization and usually introduces empirical terms (parameters) into a model's prescription of the processes. For a fuller discussion of parametrization in numerical models see, for example, Smagorinsky (1982).

My aim here is to introduce the range of sub grid-scale land-surface processes which it is generally recognised need to be represented by parametrizations in climate and numerical weather prediction models. Discussion is restricted in the main to non-vegetated land surfaces and focusses in particular on the surface energy and mass (moisture) fluxes. A more general and fairly comprehensive review of the then current practices in AGCMs was provided by Carson (1982), with an update for Meteorological Office models only in Carson (1986a). As implied above, the parametrization of land-surface processes is a very active field of research and model development and methods labelled 'current' may quickly become superseded. New approaches ('schemes') are being developed and tested continuously. A single paper cannot do justice to the range and complexity of tried schemes and unresolved problems even in the apparently restricted topic of land-surface processes. The special characteristics and problems of vegetated land surfaces, ice-covered surfaces and the ocean surface are being dealt with by other lecturers here at the Summer School. It should be assumed then throughout Sections 2-6 that discussions refer only to non-vegetated, snow-free, land surfaces, unless explicitly stated otherwise. Some of the particular problems associated with snow-covered, non-vegetated, land surfaces will be described briefly in Section 7.

It should also be stressed that there are many factors in a typical AGCM or NWPMS which will have a direct or indirect bearing on the character and performance of the land-surface processes but which are not themselves governed directly by, nor specified explicitly in terms of, surface properties. Obvious examples amongst the other physical parametrizations include: components of the radiation scheme; the cloud scheme; the representation of rainfall and snowfall; the delineation of the atmospheric boundary layer and the parametrization of turbulent mixing within it away from the surface; deep convection; etc. A numerical model's general structure with respect to, for example: horizontal domain; spatial and temporal resolutions; distribution and number of surface types; specification of orography; etc will also determine to some extent the quality of its simulations or predictions of the surface and near-surface

climatologies. Such considerations of the general problem of representing the effects of land-surface processes in AGCMs and NWPMS are beyond the scope of this introductory paper.

2. The Boundary Conditions for Momentum, Energy and Mass Transfer at a Bare-soil Surface

A natural and instructive way to delineate and introduce the various land-surface processes of interest is through the boundary conditions for momentum and the balance equations for the energy and mass (moisture) that apply at the surface. Most of the current generation of AGCMs and NWPMS involve such boundary conditions but with varying degrees of complexity and sophistication in their use and in the parametrizations chosen to represent individual components of the system. For the moment, let us consider in turn, the boundary constraints and relations between the momentum, energy and mass fluxes as depicted schematically in Figure 1 as a simplistic, air-soil interfacial problem.

Notation: The subscript o is used to denote surface values of variables and parameters, but only where necessary. In general, terms referred to only at the surface will not be given a subscript; soil fluxes and prognostic surface variables will be subscripted.

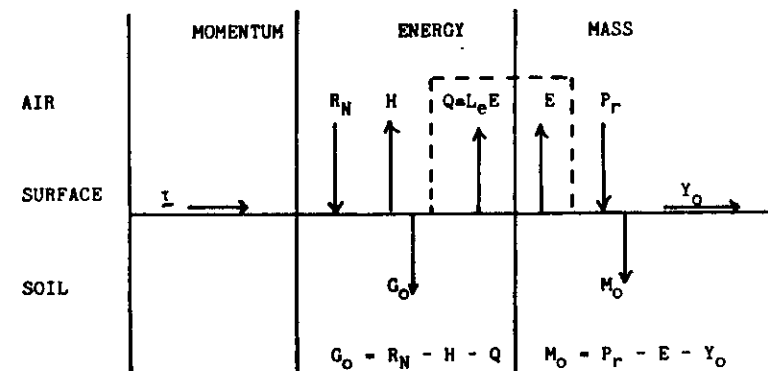


Figure 1. Schematic representation of the fluxes of momentum, energy and mass at a bare-soil surface.

2.1 Surface momentum flux (τ)

In an aerodynamic sense the atmospheric boundary layer is simply the lowest layer of the atmosphere under the direct influence of the underlying surface from which momentum is extracted and transferred downward to overcome surface friction. Thus the aerodynamically rough land surface provides a sink for atmospheric momentum, the removal of which at the surface is represented by the viscous drag, or horizontal shearing stress, τ , which, by convention, is a vectorial measure of the downward flux of horizontal momentum.

The surface boundary conditions for momentum transfer are:

a. NO-SLIP CONDITION: ie, the mean horizontal wind vector is zero at the surface.

b. \underline{u} (at the surface) is parallel to the limiting wind direction as the surface is approached.

$\underline{\tau}$, the horizontal shearing stress, has SI units of Nm^{-2} .

2.2 The surface energy flux balance

The energy flux balance at a bare-soil surface may be expressed as

$$G_o = R_N - H - Q \quad (1)$$

where R_N is the net radiative flux at the surface (defined positive towards the surface);

H is the turbulent sensible heat flux (defined positive when directed upward from the surface into the atmosphere);

$Q = L_e E$ represents the latent heat flux due to surface evaporation (defined positive when directed upward from the surface), where E is the turbulent water vapour flux (see Eqn (2)) and L_e is the latent heat of evaporation; and

G_o represents a flux of heat into the soil at the surface, and which, conventionally, is defined to be positive when directed into the soil.

The flux terms in Eqn (1) have SI units of Wm^{-2} .

2.3 The mass flux balance at the surface

For our purposes the mass flux balance at a bare-soil surface will be taken to be simply the moisture flux balance expressed as

$$M_o = P_r - E - Y_o \quad (2)$$

where P_r is the intensity of surface rainfall;

E is the surface evaporation rate (turbulent flux of water vapour);

Y_o denotes intensity of surface runoff; and

M_o represents the net mass flux of water into the soil layer.

As defined, the flux terms in Eqn (2) strictly have SI units of $\text{kg m}^{-2} \text{s}^{-1}$; however, it is fairly common practice to refer to the rates involved in terms of a representative depth (of water) per unit time.

Note:

1. The evaporative flux, E , appears explicitly in both Eqns (1) and (2) and thus provides a direct and important coupling between the surface heat and moisture budgets.
2. A knowledge of heat conduction and water transport in the soil is needed to parametrize the terms G_o and M_o , respectively. In AGCMs and WPMs this leads usually to the reformulation of Eqn (1) as a prognostic equation for the 'surface temperature', T_o , and of Eqn (2) as a prognostic equation for the mass of water stored in a specified depth of surface soil layer, ie the 'soil moisture content'. Further details of these soil processes and their representation in Eqns (1) and (2) are described more fully in Sections 5 and 6.

The boundary conditions and surface balance equations of Sections 2.1-2.3 involve a wide range of sub grid-scale physical and dynamical processes in both the atmosphere and the soil. It is convenient to consider the nature and parametrization of the various individual components under the following Section headings:

Section 3 Surface Radiative Properties and Fluxes (vid. R_N);

Section 4 Surface Turbulent Exchanges (vid. $\underline{\tau}$, H , Q and E);

Section 5 Soil Heat Conduction and the Land-Surface Temperature (vid. G_o); and

Section 6 Surface Hydrology and the Soil Water Budget (vid. P_r , Y_o and M_o).

3. Surface Radiative Properties and Fluxes

Since solar radiation provides most of the energy needed to maintain the general circulation of the atmosphere and since the major input of this energy to the Earth-atmosphere system occurs at the surface, it seems natural to start a discussion of land-surface processes by considering the surface radiative properties and fluxes. The term R_N in Eqn (1) acknowledges the importance of, and the need to determine, the net imbalance of radiative fluxes to and from the land surface expressed simply here as the sum of the net short-wave radiative flux, R_{SN} , and the net long-wave radiative flux, R_{LN} , ie

$$R_N = R_{SN} + R_{LN} \quad (3)$$

The components of R_{SN} and R_{LN} are shown schematically in Figure 2. Note the convention that the net radiative fluxes are positive when directed towards the surface.

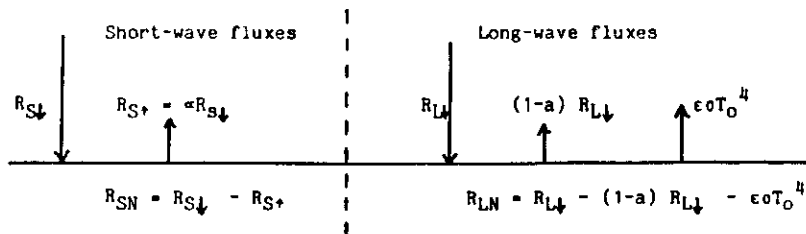


Figure 2. Schematic representation of the short- and long-wave radiative flux balances at a bare-soil surface.

3.1 Surface short-wave radiation balance

$$R_{SN} = (1-\alpha) R_{S\downarrow} \quad (4)$$

where $R_{S\downarrow}$ is the downward short-wave radiative flux, including both the direct solar flux and diffuse radiation from the sky, and

α is the surface short-wave reflectivity or albedo.

3.2 Surface long-wave radiation balance

$$R_{LN} = a R_{L\downarrow} - \epsilon \sigma T_o^4 \quad (5)$$

where $R_{L\downarrow}$ is the downward long-wave radiative flux,

a is the surface absorptivity to long-wave radiation,

$\epsilon \sigma T_o^4$ is the long-wave radiative flux emitted at the surface,

T_o is the surface temperature,

ϵ is the long-wave emissivity of the surface, and

σ is the Stefan-Boltzmann constant.

It is common practice to simplify Eqn (5) further by combining the definition of ϵ with Kirchoff's law to give $a=\epsilon$. Eqn (5) then reduces to

$$R_{LN} = \epsilon (R_{L\downarrow} - \sigma T_o^4) \quad (6)$$

and Eqn (3) becomes

$$R_N = (1-\alpha) R_{S\downarrow} + \epsilon (R_{L\downarrow} - \sigma T_o^4) \quad (7)$$

The parametrization of the radiative fluxes $R_{S\downarrow}$ and $R_{L\downarrow}$ is beyond the scope of this discussion. They are not normally classed as land-surface processes and may be regarded here as externally given forcing factors. It should be stressed though that a correct evaluation of $R_{S\downarrow}$ and $R_{L\downarrow}$ is a crucial element in establishing

sensible energy and moisture balances at the surface. The prediction of T_o is dealt with in Section 5. The remainder of this section concentrates on the surface radiative parameters, ϵ and α .

3.3 Surface long-wave emissivity (ϵ)

ϵ is known to have a wavelength dependence and to vary according to the character of the surface as discussed for example by Buechner and Kern (1965), Kondratyev (1972), Paltridge and Platt (1976) and Kondratyev et al (1982). Values quoted for the vertical emissivity range from 0.997 for wet snow to 0.71 for quartz. Kondratyev et al (1982) comment that, on average, the relative emissivities of natural underlying surfaces lie within the range 0.90-0.99 and they cite several authors who have inferred that 0.95 may be assumed as the mean relative emissivity of the Earth's surface. They do caution however that the problem of measuring the emissivity of natural surfaces is far from solved and that existing techniques will need to be improved to make such measurements on a large scale.

Although there are exceptions, the most common practice in AGCMs and NWPMS is still to assume explicitly or implicitly that all surfaces act like perfect black bodies for long-wave radiation with $\epsilon=1$. To a large extent this simply reflects the preoccupation of numerical modellers with other apparently more important and immediate problems with their physical parametrizations. I am sure that the increasing complexity and sophistication of land-surface descriptions in models will also generate more critical and discriminatory approaches to the specification of ϵ . This is most likely to be the case, for example, with the further development of models which attempt to include the explicit effects of vegetation in the climate system (see, for example, the models of Deardorff (1978) and Sellers et al (1986)).

3.4 Surface short-wave albedo (α)

α depends on the solar zenith angle, the spectral distribution of the solar radiation incident on the surface and whether that radiation is direct or diffuse, as well as on the character of the surface as determined by the vegetation (its type, density and state), the soil type, the soil moisture and whether the surface is snow- or ice-covered. Although generally a long way removed from representing the full complexity of its functional dependence on all such quantities, nevertheless α in AGCMs and NWPMS is usually accorded some variation with the broad character of the surface. In AGCMs it has a specified geographical dependence (see, for example, Carson (1982)) and in many models it is still the only land-surface or soil parameter which is given such a geographical variation (see, for example, Carson (1986a)).

A good illustration of the current status of the global specification of α suitable for use in large-scale atmospheric models is the recent work of Wilson and Henderson-Sellers (1985) on which is based the distribution of grid-box, snow-free, land-surface albedos used in the Meteorological Office operational weather forecasting and climate models (Carson, 1986a). Wilson and Henderson-Sellers (1985) have compiled detailed, global, $1^\circ \times 1^\circ$, latitude-longitude data sets of land cover and soils, respectively. These data can be manipulated to provide the corresponding characteristics for each model grid-box.

Table 1 gives their proposed albedo values, with a seasonal variation, for each of 23 selected land types; Table 2 gives typical bare-soil albedos as a simple function of soil colour and state of surface wetness.

Land Type Component	Annual	Summer	Winter
1 Water	0.07	0.07	0.07
2 Ice	0.75	0.60	0.80
3 Inland lake	0.06	0.06	0.06
4 Evergreen needleleaf tree	0.14	0.14	0.15
5 Evergreen broadleaf tree	0.14	0.14	0.14
6 Deciduous needleleaf tree	0.13	0.14	0.12
7 Deciduous broadleaf tree	0.13	0.14	0.12
8 Tropical broadleaf tree	0.13	0.13	0.13
9 Drought deciduous tree	0.13	0.13	0.12
10 Evergreen broadleaf shrub	0.17	0.17	0.17
11 Deciduous shrub	0.16	0.17	0.15
12 Thorn shrub	0.16	0.16	0.16
13 Short grass and forbs	0.19	0.20	0.18
14 Tall grass	0.20	0.17	0.22
15 Arable	0.20	0.25	0.16
16 Rice	0.12	0.12	0.12
17 Sugar	0.17	0.17	0.17
18 Maize	0.19	0.22	0.16
19 Cotton	0.19	0.22	0.17
20 Irrigated crop	0.25	0.25	0.25
21 Urban	0.18	0.18	0.18
22 Tundra	0.15	0.17	0.12
23 Swamp	0.12	0.12	0.12

Table 1. Short-wave albedos proposed by Wilson and Henderson-Sellers (1985) for 23 different types of surface cover.

Colour class	Light	Medium	Dark
Moisture state	wet dry	wet dry	wet dry
Albedos	0.18 0.35	0.10 0.20	0.07 0.15
Average	(0.26)	(0.15)	(0.11)

Table 2. Short-wave albedos proposed for bare soils by Wilson and Henderson-Sellers (1985).

Wilson and Henderson-Sellers propose that each grid-box effective α can be calculated from the algorithm



Figure 3. Snow-free land-surface albedos (%) used in the Meteorological Office's 15-level, global operational NWP.

$$\alpha = \sum_{i=1}^{23} (f_{vi} \alpha_{vi}) + f_s \alpha_s \quad (8)$$

where α_{vi} are the albedos of the 23 different land-cover types in Table 1 and f_{vi} are the corresponding fractions of grid-box covered; α_s is the albedo for the dominant soil type in the grid-box and f_s is the fraction of exposed bare soil. Figure 3 illustrates a section of the particular distribution of snow-free, land-surface albedos used currently in the Meteorological Office's 15-level, global, operational weather prediction model which has a regular, $1.5^\circ \times 1.875^\circ$, latitude-longitude horizontal grid, ie the typical mid-latitude grid-length is about 150 km.

4. Surface Turbulent Exchanges

4.1 Definition of the surface turbulent fluxes

The atmospheric boundary layer (planetary boundary layer; mixing layer) is the lowest layer of the atmosphere under the direct influence of the underlying surface. The flow in the atmospheric boundary layer is turbulent except possibly in very stable conditions, for example, such as those that prevail often at night in the presence of strong surface-based temperature inversions. The velocity, temperature, humidity and other properties in a turbulent flow can be considered as random functions in space and time and it is usually necessary to resort to a statistical approach to the calculation of many boundary-layer properties. In particular this introduces the concepts of mean values, fluctuations and variances into the description of the turbulent properties of the flow. For example, if ξ is some conservative quantity which fluctuates because of the turbulent motion, then it is usually written as

$$\xi = \bar{\xi} + \xi' \quad (9)$$

where $\bar{\xi}$ is some suitably defined mean value of ξ and ξ' is called the turbulent or eddy fluctuation (see schematic illustration in Figure 4).

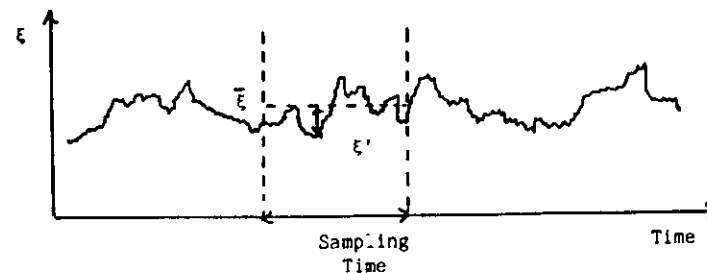


Figure 4. Schematic representation of the mean value, $\bar{\xi}$, and the eddy fluctuation, ξ' , determined for a particular sampling time from a time-trace of the fluctuating quantity ξ .

In the notation of Eqn (9), the term $\overline{w'\xi'}$, represents the eddy covariance of ξ and the vertical velocity component of the flow, w , and denotes the mean vertical turbulent flux of ξ at a given height in the atmospheric boundary layer. Let

$$F_{\xi} = (\overline{w'\xi'})_0 \quad (10)$$

denote the surface value of the mean vertical turbulent flux of ξ , then, in the context of our discussion of land-surface processes, the surface turbulent fluxes of particular interest are:

a. Momentum flux (τ)

$$\tau = \rho(-\overline{w'u'})_0 = -\overline{(w'v')}_0 \quad (11)$$

where u, v are the components of the horizontal wind vector, \underline{v} , and ρ is a representative mean air density near the surface (the bar notation to denote a mean value will be dispensed with except where essential to the interpretation of the terms involved). The conventional interpretation and vectorial character of the surface shearing stress, τ , were discussed in Section 2.1. The direction of τ is determined by the limiting wind direction as the surface is approached. An important parameter, the surface friction velocity u_* , is defined in terms of the magnitude of τ such that

$$|\tau| = \rho u_*^2 \quad (12)$$

b. Sensible heat flux (H)

$$H = \rho c_p (\overline{w'\theta'})_0 = -\rho c_p u_* \theta_* \quad (13)$$

where the potential temperature θ is used as the temperature which is conserved in the large-scale mixing and c_p is the specific heat of air at constant pressure. θ_* (like u_* in Eqn (12)) is introduced as a scaling parameter defined in terms of H and u_* , and is negative for a positive H (ie upward from the surface). The role of H in the surface energy balance is seen in Eqn (1).

c. Water vapour flux (E)

$$E = \rho (\overline{w'q'})_0 = -\rho u_* q_* \quad (14)$$

where q is the specific humidity and q_* is the corresponding surface scaling parameter (defined negative for positive evaporation from the surface). E , the surface evaporation rate, is not only an important direct component of the moisture flux balance at the surface (vid. Eqn (2)) but also appears in the latent heat flux term $Q = L_e E$ in the surface energy balance (vid. Eqn (1)).

From Eqns (11)-(14) our general expression Eqn (10) for the surface turbulent flux F_{ξ} can be extended to

$$F_{\xi} = (\overline{w'\xi'})_0 = -u_* \xi_* \quad (15)$$

which defines the surface scaling value ξ_* (for example as for u_* , θ_* and q_*) in terms of u_* and the mean vertical turbulent flux of ξ at the surface.

4.2 The surface-flux layer

Adjacent to the surface we can identify a shallow layer in which the turning of the wind with height may be ignored and the vertical fluxes of momentum, heat and water vapour may be approximated closely by their surface values (ie for many practical purposes the turbulent fluxes in this layer may be assumed to be virtually constant with height). The layer so-defined is often referred to as the constant-flux layer. However, this terminology can mislead the unwary (note, for example, that the turbulent fluxes generally have their largest vertical gradients at the surface) and it is better to use the more appropriate term of surface-flux layer.

4.3 Monin-Obukhov similarity theory

The Monin-Obukhov similarity hypothesis for the surface-flux layer is the most widely accepted approach for describing the properties of the surface layer. Brought down to the very simplest terms, similarity methods depend on the possibility of being able to express the unknown variables in non-dimensional form, there being suitable argument for saying there exist a length-scale, a velocity-scale (or time-scale) and a temperature- (and humidity-) scale relevant in doing this. The non-dimensional forms are then postulated to be universal in character and this will hold as long as the scales remain the relevant ones.

The Monin-Obukhov similarity hypothesis for the fully turbulent surface-flux layer (where the Coriolis force is neglected) states that for any transferrable property, the distribution of which is homogeneous in space and stationary in time, the vertical flux-profile relation is determined uniquely by the parameters

$$\frac{g}{T}, \frac{|\tau|}{\rho}, \frac{H}{\rho c_p}, \frac{E}{\rho} \quad (16)$$

where g/T is the Archimedeian buoyancy parameter, g is the acceleration due to gravity and T is a representative air temperature in the surface layer. From Eqns (12)-(14) these are equivalent to the set

$$\frac{g}{T}, u_*, \theta_*, q_* \quad (17)$$

where θ_* and q_* can be combined to give

$$\psi_* = \theta_* + 0.61 T q_* \quad (18)$$

which is very akin to a virtual potential temperature scaling value.

Instead of using the buoyancy parameter g/T it is convenient to use the length-scale, L , defined uniquely by g/T , u_* and ψ_* by the relation.

$$L = \frac{T u_*^2}{kg \psi_*} = \frac{\rho c_p T u_*^3}{kg (H + 0.61 c_p T E)} \quad (19)$$

and called the Monin-Obukhov length. k is the von Kármán constant (≈ 0.4) and is conventionally introduced solely as a matter of convenience. L is effectively constant in the surface-flux layer. The turbulent flow is classed as unstable when $L < 0$ (ie when the net surface buoyancy flux is positive); stable when $L > 0$ (ie when the surface buoyancy flux is negative); and neutral when $|L| \rightarrow \infty$ (ie when the surface buoyancy flux is zero).

Thus L , u_* , θ_* , q_* may be taken as the set of basic parameters which uniquely determine the relationships between the surface-layer vertical gradients of wind, potential temperature and specific humidity to the corresponding surface turbulent fluxes. Dimensional analysis leads to the vertical flux-gradient relationship expressed in the general form

$$\frac{\partial \xi}{\partial z} = \frac{z_*}{kz} \phi_\xi(z/L) \quad (20)$$

where z is height above the surface. $\phi_\xi(z/L)$ is hypothesized to be a universal function of z/L only which may be of different form for each mean transferrable property, ξ , and which has to be established empirically from analysis of surface-layer data. The overall observational evidence is that the ϕ_ξ decrease with unstable stratification (ie when $L < 0$) and increase with stable stratification ($L > 0$). For specified functions for ϕ_ξ , Eqn (20) can be integrated to provide flux-profile relationships for the surface layer, viz:

$$k \left[\xi(z) - \xi(z_r) \right] = \int_{z_r}^z \frac{\phi_\xi(\eta)}{\eta} d\eta \equiv \phi_\xi(\zeta, \zeta_r) \quad (21)$$

where $\zeta = z/L$ and $\zeta_r = z_r/L$, where z_r is some reference height at which ξ is known. In practice, Eqn (21) used in conjunction with Eqns (12)-(14) allows us to estimate the surface turbulent fluxes of momentum, heat and moisture from a knowledge of the corresponding surface-layer profiles of wind, potential temperature and humidity.

4.4 The Monin-Obukhov similarity functions (ϕ_ξ)

The general character of the similarity functions is fairly well established over a limited range of stability conditions, centred on neutral, but their specification for extreme stability conditions (both stable and unstable) is much more debatable and uncertain. The particular specifications of ϕ_ξ listed below are subjectively selected, albeit typical, examples of the type of formulae commonly adopted as the basis of parametrizations for the surface turbulent fluxes in numerical models. For fuller discussions of the variety of postulated, empirical forms of ϕ_ξ see, for example, Chap 6 of McBean et al (1979).

The general behaviour is that ϕ_ξ increases with increasing stability; ie decreasing turbulence decreases the mixing and hence increases the normalised gradient of ξ . Figure 5 illustrates schematically the changing character of the surface-layer wind profile throughout a clear day and a clear night. For details see, for example, Chap 6 of Panofsky and Dutton (1984).

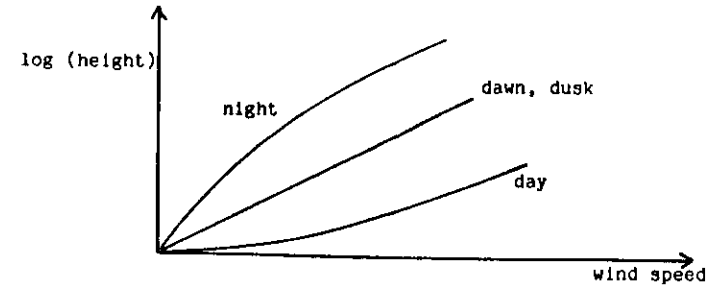


Figure 5. Schematic representation of diurnal variation of surface-layer wind profile.

4.4.1 Unstable and neutral conditions ($z/L \leq 0$)

Dyer and Hicks (1970):

$$\phi_H = \phi_E = \phi_M^2 = (1 - 16 z/L)^{-1/2} \quad 0 \leq z/L \leq 1 \quad (22)$$

where ϕ_M , ϕ_H and ϕ_E are the respective ϕ_ξ for the turbulent transfers of momentum, sensible heat and water vapour. Note that, strictly, the Dyer and Hicks (1970) formulae are limited to $|z/L| \leq 1$ and so other empirical approaches may need to be invoked for more unstable conditions. For a particular choice of extrapolation beyond the Dyer and Hicks limit towards the free-convection limit see Carson (1982, 1986a).

4.4.2 Stable conditions ($z/L > 0$)

Webb (1970):

$$\phi_H = \phi_E = \phi_M = \begin{cases} 1 + 5 z/L & 0 < z/L \leq 1 \\ 6 & 1 < z/L < 6 \end{cases} \quad (23)$$

The problem of extending the functional form of ϕ_ξ to highly stable conditions was discussed by Carson and Richards (1978).

4.5 The bulk transfer coefficient, C_ξ , and the aerodynamic resistance, r_ξ

It is standard practice, particularly in AGCMs and NWPMS, to represent the mean vertical surface turbulent flux, F_ξ , by

$$F_\xi = -C_\xi V(z_\xi) \Delta \xi(z_\xi) \quad (24)$$

where

$$\Delta \xi(z_\xi) = \xi(z_\xi) - \xi_0 \quad (25)$$

z_ξ is some specified height above the surface and within the boundary layer (and which may be regarded, without loss of generality, as the notional height of a particular numerical model's first level above the underlying surface); $V(z_\xi)$ is the mean horizontal wind speed (ie

$\bar{V}(z)$ at z_L ; $\xi(z_L)$ is the value of the property ξ at z_L and ξ_0 is its surface value. (Note again that the bar notation to denote mean values (see Eqn (9)) has been omitted to simplify the symbolism). C_E is the so-called bulk transfer coefficient, defined in a strictly mathematical sense by Eqn (24), and which, in general, is a complicated function of height, atmospheric stability, surface roughness and, for a vegetated surface, of other physical and physiological characteristics of the surface vegetation.

In bulk-aerodynamic form the surface turbulent fluxes of Eqns (11), (13) and (14) are:

$$a. \text{ Momentum flux } \tau = \rho C_D V(z_L) \bar{V}(z_L) \quad (26)$$

where C_D is the traditional 'drag coefficient'.

$$b. \text{ Sensible heat flux } H = -\rho c_p C_H V(z_L) (\theta(z_L) - \theta_0) \quad (27)$$

where C_H is the bulk transfer coefficient for heat transfer.

$$c. \text{ Water vapour flux } E = -\rho C_E V(z_L) (q(z_L) - q_0) \quad (28)$$

where C_E is the bulk transfer coefficient for water vapour transfer.

To determine the fluxes from Eqns (26)-(28) the C_E must be prescribed or expressed in terms of modelled variables and parameters and, in addition to the variables modelled explicitly at z_L , the surface temperature and humidity need to be known. The prediction of surface temperature, T_0 (simply related to θ_0), is discussed in Section 5. The surface specific humidity, q_0 , is not so easy to predict explicitly and its implied value is inextricably linked to the parametrization of the surface hydrology, which is discussed in Section 6. The Monin-Obukhov theory of Sections 4.3 and 4.4 provides a basis for a fairly sophisticated specification of the C_E which is described in the next section.

A related approach to Eqn (24) for the representation of the turbulent fluxes at natural surfaces is the so-called resistance approach. Turbulent transfer in the atmospheric boundary layer is seen as a process analogous to the flow of electric current and, in the spirit of Ohm's Law, F_E is written as

$$F_E = - \frac{\Delta \xi}{r_E} \quad (29)$$

where, in a similar manner to C_E in Eqn (22), Eqn (29) can be regarded as defining r_E , the aerodynamic resistance to the 'flow' of F_E .

The resistance approach has particular appeal when dealing with the complicated and multiple routes for sensible heat transfer and evaporation from vegetated surfaces (see, for example, Monteith (1965), Perrier (1982) or Rosenberg et al (1983)). It was, however, felt instructive to mention it here. Also, comparison of Eqns (24) and (29) yields

$$r_E = [C_E V(z_L)]^{-1} \quad (30)$$

4.6 C_E from Monin-Obukhov similarity theory

For a discussion of the large variety of specifications of C_E then in current use in AGCMs see, for example, Carson (1982). However, discussion here is limited to the approach most acceptable to boundary-layer experts and increasingly more prevalent in the current generation of AGCMs and NWPMs, viz, that based on the Monin-Obukhov similarity theory.

From Eqns (24) and (15) it is seen that

$$C_E = \left(\frac{u_*}{V(z_L)} \right) \left(\frac{-\xi(z_L)}{\Delta \xi(z_L)} \right) \quad (31)$$

For Monin-Obukhov theory to be appropriate then z_L must be fully within the surface layer so that Eqn (21) can be invoked in the particular form

$$k \frac{\Delta \xi(z_L)}{\xi_*} = \int_{\xi_0}^{\xi(z_L)} \frac{\phi_E(\eta)}{\eta} d\eta \equiv \Phi_E(\zeta_L, \zeta_E) \quad (32)$$

where $\zeta_L = z_L/L$ and $\zeta_E = z_E/L$ is defined such that

$$\xi(z_E) \equiv \xi_0 \quad (33)$$

The nature of the similarity formulation implies a logarithmic singularity in Φ_E as $z \rightarrow 0$. This is avoided by defining the level z_E as the virtual height at which the ξ -profile, defined by Eqn (21) and extrapolated towards the surface, attains the actual surface value ξ_0 . For momentum transfer, this level, denoted z_0 , is defined as the virtual height at which $V=0$ on the postulated wind profile. z_0 is called the surface roughness length and over a bare soil surface is a characteristic of the surface and is usually independent of the flow. There are also corresponding characteristic 'surface roughness lengths' for heat and water vapour transfer. The problems of evaluating effective areal roughness lengths and of discriminating between them for the different properties are complex and it remains common practice in large-scale numerical models to use the estimate for z_0 for all three profiles. This aspect of the overall problem is discussed below in Section 4.7.

From Eqns (31) and (32), C_E can be specified in terms of finite integrals of the Monin-Obukhov similarity functions, thus,

$$C_E = k^2 \Phi_M^{-1}(\zeta_L, \zeta_0) \Phi_E^{-1}(\zeta_L, \zeta_E) \quad (34)$$

$$\text{where } \Phi_M(\zeta, \zeta_0) = \int_{\zeta_0}^{\zeta} \frac{\phi_M(\eta)}{\eta} d\eta = \frac{kV(z)}{u_*} \quad (35)$$

and $\zeta_0 = z_0/L$. In general, with Φ_E specified as discussed, for example, in Section 4.4, then Eqn (34) gives C_E as a function of ζ_L , ζ_0 and ζ_E .

It is generally more convenient for modelling purposes to express C_E directly as a function of the explicitly modelled variables $V(z_L)$ and $\Delta \xi(z_L)$. This can be achieved by using a bulk Richardson number for the surface layer, R_{1B} , instead of ζ_L as the stability indicator, such that

$$Ri_B = \frac{gz_L}{T} \frac{[\Delta\theta(z_L) + 0.61T\Delta q(z_L)]}{V^2(z_L)} \quad (36)$$

This can be related implicitly to z_L through

$$Ri_B = \frac{k^2 C_D}{k C_H} z_L^3 \quad (37)$$

For a full description of the method and the assumptions made, see, for example, Carson and Richards (1978).

As an example, Figure 6 depicts the surface-layer bulk transfer coefficients used in the Meteorological Office 11-layer AGCM which are based on Monin-Obukhov similarity theory and in particular for part of the range of Ri_B (corresponding to a very small section of the abscissa in the Figure), on the specifications of ϕ_L given in Eqns (22) and (23). In that particular model $z_L = 100$ m, z_0 over land is 0.1 m and z_0 over sea is 10^{-2} m. The bulk transfer coefficients in Figure 6 are used in Eqns (26)-(28) to provide estimates of the surface turbulent fluxes τ , H and E , respectively.

4.7 Surface roughness length (z_0)

z_0 , like the surface albedo of Section 3, is a land-surface characteristic which has a marked geographical variation. In most of the current generation of AGCMs and NWPMS, z_0 has direct and indirect effects on the surface turbulent exchanges of sensible heat and moisture as well as on the surface shearing stress (see comments above in Section 4.6). However, the evaluation of an effective areal surface roughness length for heterogeneous terrain is an important practical issue that poses a variety of as yet unsatisfactorily resolved problems.

The effective areal z_0 for natural surfaces is rarely estimated from the wind profile and/or surface shear stress measurements. Instead, it is most likely to be determined indirectly from a knowledge of, for example: terrain relief (elevation, slope, etc); land use; type and distribution of the surface roughness elements. Algorithms, however qualitative, are needed to perform this function sensibly, at least in a fairly local ($1 \times 1 \text{ km}^2$) sense. The pros and cons of alternative approaches to the question of how to average over larger areas has been discussed by Carson (1986b).

Most standard boundary-layer text books provide a table of values of z_0 as a function of terrain type described qualitatively in terms of relief and vegetative characteristics (see, for example, Table 6.2 in Panofsky and Dutton (1984)). Such traditional relationships may well be adequate on the very local scale for the smoother, quasi-homogeneous types of terrain but can be expected to be less well founded for areal averages over rough, heterogeneous terrain, typical say of a European semi-rural landscape with small hills, woods, fields, crops, hedges, towns, lakes, etc. Wieringa (1986) has addressed this problem and produced a table giving effective areal z_0 in terms of a terrain classification when there are no significant orographic effects (see Table 3).

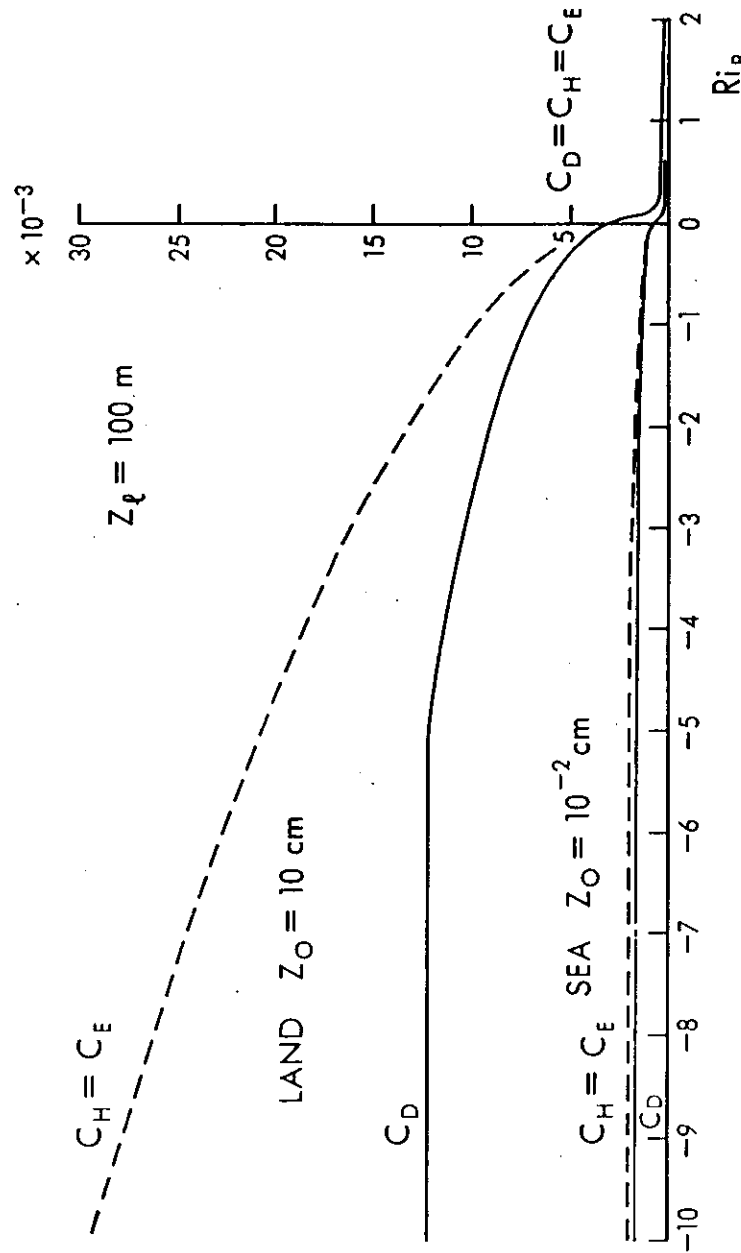


Figure 6. Surface layer bulk transfer coefficients derived from Monin-Obukhov similarity theory and used in the Meteorological Office's 11-layer AGCM.

For fuller discussions of issues concerning the evaluation of effective z_0 , the reader is referred to the recent papers by Smith and Carson (1977), Mason (1985), Carson (1986b), Wieringa (1986) and André and Blondin (1986).

Land use category	z_0 (m)
Sea (minimal fetch 5 km)	0.0002
Small lake, mud flats	0.006
Morass	0.03
Pasture	0.07
Dunes, heath	0.10
Agriculture	0.17
Road, canal (in Dutch landscape tree-lined)	0.24
Orchards, bushland	0.35
Forest	0.75
Residential built-up area ($H \leq 10$ m)	1.12
City centre (high-rise building)	1.6

Table 3. Effective mesoscale surface roughness length, z_0 (m), expressed as a function of land use and proposed by Wieringa (1986). H is the height of the major surface obstacles.

5. Soil Heat Conduction and the Land-surface Temperature

In our formulation of the energy flux balance at a bare-soil surface, Eqn (1), G_0 the sensible heat flux in the soil is equated to the net imbalance in the energy fluxes between the surface and the atmosphere. If the aim was solely to evaluate G_0 , then use of the surface energy balance, as depicted in Eqn (1), would be a legitimate method for obtaining such an estimate. Indeed, in principle, the energy balance method can be invoked to estimate any one of the terms in Eqn (1) if all the others are known by some other means.

The more direct, microphysical approach to understanding the soil heat flux term G_0 is through the study of heat transfer in the soil itself, a process which is predominantly that of heat conduction. In general, G_0 will depend in a complicated way on the soil's thermal properties which in turn depend on, for example, the type of surface, the type of soil and whether it is wet, dry, frozen or snow-covered, and whether it is bare soil or vegetation. In simple, general terms a thin surface layer of the soil stores heat during the day (strictly, from Eqn (1), when $R_N > H + Q$ ie G_0 is positive) and acts as a source of heat energy to the surface at night (strictly, when $R_N - H - Q < 0$ ie G_0 is negative). On longer, seasonal and annual time scales deeper soil layers act as a reservoir of heat which may be replenished during warm seasons and depleted during the cold seasons.

Good estimates of the detailed behaviour of G_0 throughout the day and throughout the year are now recognised as important to include in NWPMS, which attempt to forecast the characteristic diurnal cycle of land-surface temperatures, and also in climate models which need to simulate realistically and interactively the heat-storage properties of the soil over periods ranging from less than a day to at least several years.

Implicit in a knowledge of heat transfer through the soil is a knowledge of the soil temperature profile with depth. In particular, the land-surface temperature, T_0 , features in each of the terms in Eqn (1) and it is now the common practice in AGCMs and NWPMS to invoke the surface energy balance as a diagnostic relation or prognostic equation for evaluating T_0 . The variety of techniques commonly used in such models for representing G_0 in the surface energy balance has already been reviewed fairly comprehensively by, for example, Bhumralkar (1975), Deardorff (1978) and Carson (1982, 1986a). In order to illustrate the relationships between soil heat flux, soil temperature profile and the thermal properties of the soil, I shall restrict my discussion to those methods which rely on a knowledge of heat conduction in the soil and invoke either simple, one-dimensional, analytical models or attempt to model explicitly the soil heat transfer in a multi-layer soil model.

5.1 Heat transfer in a semi-infinite homogeneous soil

Most parametrizations of G_0 are now based on considerations of heat conduction and conservation in the soil. The problem is usually simplified by assuming a semi-infinite, spatially homogeneous soil layer with no horizontal heat transfer and no melting or freezing within it. This restricted and idealised one-dimensional problem is governed by:

- a. the soil heat conservation equation

$$\frac{\partial T_g}{\partial t} = -\frac{1}{C} \frac{\partial G}{\partial z_g} \quad (38)$$

where T_g is the soil (ground) temperature, G is the soil heat flux, C is the volumetric heat capacity of the soil (SI units: $J m^{-3} K^{-1}$), $z_g = -z$ is the vertical co-ordinate in the soil layer and t is time; and

- b. the flux-gradient relation for heat conduction

$$G = -\lambda \frac{\partial T_g}{\partial z_g} \quad (39)$$

where λ is the thermal conductivity of the soil (SI units: $W m^{-1} K^{-1}$).

Substitution of Eqn (39) into Eqn (38), with the assumption of homogeneity, yields the one-dimensional equation for conduction of heat in the soil, viz.

$$\frac{\partial T_g}{\partial t} = \kappa \frac{\partial^2 T_g}{\partial z_g^2} \quad (40)$$

where κ is the thermal diffusivity of the soil (SI units: $m^2 s^{-1}$) such that

$$\kappa = \lambda/C = \lambda/\rho_g c_g \quad (41)$$

where ρ_g is the uniform soil density and c_g is the specific heat capacity (SI units: $J kg^{-1} K^{-1}$).

The definitions and characteristics of the soil thermal properties C , λ , κ and c_g can be found in standard text books such as Geiger (1965), Sellers (1965), Oke (1978) and Rosenberg et al (1983). The values in Table 4 are given in Oke (1978) and illustrate the typical magnitudes of these terms for a few simple soil types (and for snow) and also indicate their sensitivity to how wet or dry the soil is.

Material	Remarks	ρ_g $kg m^{-3}$ $\times 10^3$	c_g $J kg^{-1} K^{-1}$ $\times 10^3$	C $J m^{-3} K^{-1}$ $\times 10^6$	λ $W m^{-1} K^{-1}$	κ $m^2 s^{-1}$ $\times 10^{-6}$	δ_d m	δ_a m
Sandy soil (40% pore space)	Dry	1.60	0.80	1.28	0.30	0.24	0.08	1.55
	Saturated	2.00	1.48	2.96	2.20	0.74	0.14	2.73
Clay soil (40% pore space)	Dry	1.60	0.89	1.42	0.25	0.18	0.07	1.34
	Saturated	2.00	1.55	3.10	1.58	0.51	0.12	2.26
Peat soil (80% pore space)	Dry	0.30	1.92	0.58	0.06	0.10	0.05	1.00
	Saturated	1.10	3.65	4.02	0.50	0.12	0.06	1.10
Snow	Fresh	0.10	2.09	0.21	0.08	0.10	0.05	1.00
	Old	0.48	2.09	0.84	0.42	0.40	0.10	2.00

Table 4. Thermal properties of natural materials (from Oke (1978)). ρ_g , c_g , C , λ and κ are defined in Section 5.1. δ_d and δ_a are the e-folding depths of the diurnal and annual soil temperature waves and are defined in Section 5.2.

A standard practice is to combine Eqns (38), (39) and the surface energy balance, Eqn (1), to produce a prognostic equation for T_0 (usually assumed equivalent to the soil surface temperature T_{g0}). The simplest approaches of this kind introduce the concept of an effective depth of soil D and an effective surface thermal capacity

$$C_{eff} = CD = \rho_g c_g D \quad (42)$$

defined such that

$$G_0 = C_{eff} \frac{\partial T_{g0}}{\partial t} \equiv CD \frac{\partial T_0}{\partial t} \quad (43)$$

Many AGCMs and NWPMS contain rather arbitrary and empirical selections of C_{eff} (see, for example, Carson (1982)) and with G_0 replaced by the RHS of the surface energy balance, Eqn (43) can be solved for T_0 .

Note however that C_{eff} (and D) can be defined more formally from consideration of the soil heat conservation equation (38). On the assumption that $G \neq 0$ as $z_g \rightarrow \infty$ then Eqn (38) can be integrated to give

$$G_0 = C \int_0^{\infty} \frac{\partial T_g}{\partial t} dz_g \quad (44)$$

which, when used to replace G_0 in Eqn (43), allows D to be defined in a strictly mathematical sense as

$$D = \left(\frac{\partial T_0}{\partial t} \right)^{-1} \int_0^{\infty} \frac{\partial T_g}{\partial t} dz_g \quad (45)$$

The following section describes a popular analytical approach in which Eqn (45) may be invoked to good advantage.

5.2 One-dimensional heat transfer in a semi-infinite, homogeneous soil whose surface is heated in a simple periodic manner

One simple, attractive and commonly adopted method of determining D in Eqn (43) is by appealing to the theory of heat transfer in a semi-infinite homogeneous medium when the surface is heated in a simple periodic manner (as discussed, for example, in Sellers (1965)).

If it is assumed that the surface temperature

$$T_0 \equiv T_g(0, t) = \hat{T}_g + a_0 \sin \omega t \quad (46)$$

where ω is the angular frequency of oscillation, \hat{T}_g is the mean soil temperature (over the period $P = 2\pi/\omega$), assumed to be the same at all depths, and a_0 is the amplitude of the surface temperature wave, then the solution of Eqn (40) is

$$T_g(z_g, t) = \hat{T}_g + a(z_g) \sin(\omega t - z_g/\delta) \\ = \hat{T}_g + a_0 \exp(-z_g/\delta) \sin(\omega t - z_g/\delta). \quad (47)$$

$$\delta = \left(\frac{\kappa P}{\pi} \right)^{1/2} = \left(\frac{2\lambda}{C_w} \right)^{1/2} \quad (48)$$

is the e-folding depth of the temperature wave of period P , i.e. it is the depth where the amplitude of the oscillation is reduced to $1/e$ (i.e. 0.37) times its surface value. Values of the e-folding depths corresponding to the diurnal and annual periods, respectively, are given for a range of soil types in Table 4.

The effective depth D corresponding to the soil temperature profile Eqn (47) is, from Eqn (45),

$$D = \frac{1}{a_0 \cos \omega t} \int_0^{\infty} a(z_g) \cos(\omega t - z_g/\delta) dz_g \\ = \frac{1}{\cos \omega t} \int_0^{\infty} \exp(-z_g/\delta) \cos(\omega t - z_g/\delta) dz_g$$

$$= \frac{\delta}{\sqrt{2}} \frac{\sin(\omega t + \pi/4)}{\cos \omega t} \quad (49)$$

Therefore D as defined in Eqn (43) is not only a function of the thermal diffusivity of the soil and the single frequency assumed for the simple periodic forcing at the surface but also varies with time according to Eqn (49). Substituting for D from Eqn (49) in Eqn (43) gives a prognostic equation for T_0 , viz.

$$\frac{\partial T_0}{\partial t} = \frac{\sqrt{2} G_0 \cos \omega t}{C \delta \sin(\omega t + \pi/4)} \quad (50)$$

which in turn can be expanded easily to give

$$\frac{\partial T_0}{\partial t} = \frac{2G_0}{C\delta} - \frac{2\pi}{P} (T_0 - \hat{T}_g) \quad (51)$$

This, I believe, is a relatively neat way of deriving Eqn (51) which was proposed by Bhumrakar (1975) and has come to be referred to as the 'force-restore method', a term introduced by Deardorff (1978).

The period of the diurnal temperature oscillation is normally used in Eqn (51) as that appropriate for determining the thermal capacity of the effective surface layer. Additional information about \hat{T}_g is required to solve Eqn (51). \hat{T}_g may be fixed or diagnosed over short periods of a few days but would need to be determined prognostically over the much longer periods of integration involved, for example, in climate modelling. Deardorff (1978) has suggested a second prognostic equation for \hat{T}_g analogous to Eqn (51) but with the appropriate effective depth determined by the e-folding depth of the annual temperature wave. Although there is some useful mileage in extending this simple, analytically-based method further (see, for example, Deardorff (1978) and Carson (1982)), such parametrizations soon become analogous to the more elaborate schemes which explicitly model the temperature profile through several soil layers.

5.3 Multi-layer soil models

The somewhat idealised analytical assumptions underlying the force-restore method and other simpler parametrizations can be avoided in principle by explicit modelling of the soil temperature profile and soil heat conduction with a multi-layer soil model of specified depth and with appropriate vertical resolution and boundary conditions. One approach, for example, would be to invoke Eqn (39) to evaluate G_0 explicitly from the modelled soil temperature profile such that

$$G_0 = \left[-\lambda \frac{\partial T_g}{\partial z_g} \right]_{z_g=0} \quad (52)$$

With this representation of G_0 , Eqn (1) could then be solved diagnostically for T_0 .

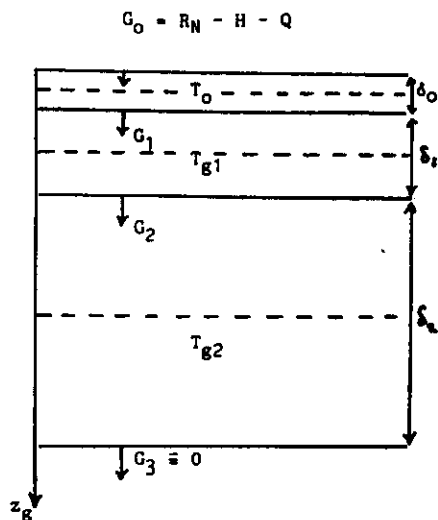


Figure 7. Schematic representation of a 3-layer, soil-temperature, finite-difference model. T_0 , T_{g1} and T_{g2} are the representative temperatures in the soil layers of depth δ_0 , δ_1 and δ_2 , respectively. G_0 , G_1 , G_2 and G_3 are the corresponding soil heat fluxes at the respective layer boundaries.

An alternative approach is represented schematically for a 3-layer soil-temperature model in Figure 7. Here the surface temperature T_0 is represented by the mean temperature of a very thin surface soil layer of depth δ_0 . The rate of change of T_0 with time is given by the soil heat flux divergence in the surface layer according to a simple finite difference form of Eqn (38), i.e.

$$\frac{\partial T_0}{\partial t} = \frac{G_0 - G_1}{C\delta_0} \quad (53)$$

G_0 is as usual the net imbalance of the terms on the RHS of Eqn (1) and G_1 , the soil heat flux into the next layer down, is determined from the explicitly modelled soil temperature profile from the heat conduction Eqn (39) written simply as

$$G_1 = \frac{2\lambda(T_0 - T_{g1})}{\delta_0 + \delta_1} \quad (54)$$

Therefore, from Eqns (53) and (54),

$$\frac{\partial T_0}{\partial t} = \frac{G_0}{C\delta_0} + \frac{2\lambda(T_{g1} - T_0)}{\delta_0(\delta_0 + \delta_1)} \quad (55)$$

and the same general technique is used to provide the corresponding predictive equations for the temperatures of the other soil layers.

In the 3-layer soil model of Figure 7, all three soil temperatures are treated as prognostic variables during integration of the model, with the boundary condition that the soil heat flux is zero at the lower soil boundary (ie $G_3 = 0$ in Figure 7). An alternative, popular lower boundary condition is to hold the bottom-layer soil temperature constant at its initialised value. This latter boundary condition is used, for example, in the 4-layer soil model in the current Meteorological Office fine-mesh operational forecasting model (Carson, 1986a) and also in the 3-layer soil model used at ECMWF (Blondin, 1986).

The selection of 'representative' soil thermal characteristics C and λ (and hence κ) and suitable soil-layer depths, $\delta_0 \dots \delta_1 \dots \delta_{n-1}$ where n is the number of explicitly resolved layers in the soil; remains a difficult, empirical and highly subjective business. On the basis of a comprehensive study of the amplitude and phase responses of multi-layer soil schemes to periodic surface temperature forcing, Warrilow et al (1986) have recommended a 4-layer soil-temperature scheme of the type depicted in Figure 7 for use in the Meteorological Office AGCM. Their paper gives full description of how the appropriate soil-model parameters were selected. For further discussion of values used in specific models see, for example, Blondin (1986) and Carson (1982, 1986a). Table 5 gives values of the main parameters likely to be incorporated into the most recent control version, the so-called 'Fourth Annual-Cycle Version', of the Meteorological Office 11-layer AGCM used for climate modelling research (Warrilow, private communication).

SOIL THERMAL PROPERTIES	Value
Volumetric heat capacity, C ($J m^{-3} K^{-1}$)	2.34×10^6
Thermal conductivity, λ ($W m^{-1} K^{-1}$)	0.56
Thermal diffusivity $\kappa = \lambda/C$ ($m^2 s^{-1}$)	2.39×10^{-7}
Thermal inertia $\gamma = (\lambda C)^{1/2}$ ($J m^{-2} K^{-1} s^{-1/2}$)	1145
Soil-layer depths: δ_0 (m) δ_1 [$r_1 = \delta_1 / \delta_0$] δ_2 [$r_2 = \delta_2 / \delta_0$] δ_3 [$r_3 = \delta_3 / \delta_0$] $1 \frac{3}{2} \delta_1$	0.037 0:143 [3.91] 0:516 [14:05] 1:639 [44:65] 2.335
Depth of the surface layer of soil determined by $\delta_0 = (\frac{2\lambda}{C\omega_0})^{1/2}$ ω_0 (s^{-1}) $P_0 = 2\pi/\omega_0$ (day)	where 3.5509×10^{-4} 0.2048 (ie 4.8 hr)
Thermal capacity of surface layer of soil: $C\delta_0$ ($J m^{-2} K^{-1}$)	8.59×10^4

Table 5. Physical properties selected by Warrilow (private communication) for use in the 4-layer soil-temperature model to be used in the Fourth Annual-Cycle version of the Meteorological Office 11-layer AGCM. The general approach is described fully in Warrilow et al (1986).

5.4 The land-surface temperature, T_0

Throughout this paper, following the general practice in AGCMs and NWPMS, it has been assumed that the land-surface temperature is a well-defined and unique property of any natural land surface and that the same ' T_0 ' is appropriate as: the radiative surface temperature of Eqn (7); the surface temperature as used in the extrapolated atmospheric boundary layer profiles and surface-flux formulae of Section 4; and the surface soil temperature related to the soil heat

flux as introduced above in Section 5. The 'surface temperatures' implied by these different physical processes at the surface must be closely related but they are not necessarily all the same. The ambiguity and difficulty in defining surface temperature become even greater when the surface has a vegetative canopy. Suffice it to state here that at present the problem is very poorly understood and that more observational and theoretical studies are needed before any significant differences between the ' T_0 ' can be clearly delineated and incorporated sensibly in AGCMs and NWPMS.

6. Surface Hydrology and the Soil Water Budget

Most of the current generation of AGCMs and NWPMS now include some form of 'interactive' surface hydrology, usually of a very rudimentary nature. Such parametrizations are termed 'interactive' in the sense that the soil has some recognised hydrological property that is allowed to vary in response to the model's continuously evolving atmospheric state and surface boundary conditions and which in turn exerts both direct and indirect influences on the surface fluxes themselves. The most common practice is to define a variable 'soil moisture content' for some notional depth of surface soil layer which is constrained at all times to satisfy the surface moisture flux balance as expressed in Eqn (2).

In direct analogy to the need to study heat conduction in the soil to provide a sound physical basis for evaluating the 'surface temperature', so also is there a corresponding need to understand more about the dynamics which govern the movement of water in the soil in order to model changes in the profile of 'soil moisture content'. Since the concepts of 'surface temperature' and 'soil moisture content' have been introduced here independently and in different sections, it is perhaps worth emphasizing again the strong, interactive coupling between the thermal and hydrological properties and processes in the soil. Not only does E (or Q) appear explicitly in both Eqns (1) and (2) but most of the other surface fluxes (including the momentum flux τ) depend to varying degrees on both the 'surface temperature' and the 'soil moisture content'. Indeed, in a model with both interactive surface hydrology and interactive land-surface temperature, the value of the 'soil moisture content' has an important bearing on the evaluation of T_0 , and vice-versa.

As in the case of the surface radiative fluxes R_{sd} and R_{ld} in the context of the surface energy balance (discussed in Section 3), the surface rainfall rate P_r is regarded here as an externally determined component of the surface moisture balance, Eqn (2). Accurate evaluation of P_r is of course of crucial importance in establishing a realistic surface moisture balance and also, through the coupling discussed above, a realistic surface energy balance. The other processes involved in the hydrology of a bare soil, including evaporation, surface runoff, and transport and storage of water in the soil are generally very complex and not so well understood nor as simple to parametrize sensibly as the individual terms in the surface energy balance. The very small-scale spatial inhomogeneities within a typical soil layer appear to be more important in the determination of soil moisture movement than for the heat flow and this presents formidable difficulties when trying to formulate a parametrization based soundly on underlying physical and dynamical hydrological principles. This is particularly so when one-dimensional hydrological models are applied to catchment-sized or typical AGCM/NWPM grid-box areas. Hence the importance of the HAPEX-MOBILHY project (André et al, 1986) aimed at studying the hydrological budget and evaporation flux at the scale of an AGCM grid

square, i.e. 10^4 km^2 . A two-and-a-half-month special observing period should provide detailed measurements of the relevant atmospheric fluxes and intensive remote sensing of surface properties. The main objective of the programme is to provide a data base against which parametrizations of the land-surface water budget can be developed and tested.

A proper discussion of the surface and sub-surface hydrology of natural soils is beyond the scope of this paper. For this the reader is referred to the recent fuller expositions by, for example, Brutsaert (1982a, b), Dooge (1982), Eagleson (1982) and Dickinson (1984) in which the problems of areal representation of hydrological processes are specifically discussed. The remainder of this section is restricted to an introduction to the most simple form of the basic equations which govern the movement of water in the soil and brief descriptions of some specific formulations for soil-water transport, evaporation and surface runoff. These examples although chosen quite subjectively should nevertheless give an indication of the general tenor and level of many of the current attempts to parametrize grid-scale hydrological processes.

6.1 Water transport in a homogeneous soil

There are various inter-related measures of soil moisture content, two of which are:

- χ , the soil moisture concentration, defined as the mass of water per unit volume of soil. (SI units: kg m^{-3}), and
- χ_v , the volumetric soil moisture concentration, defined as the volume of water per unit volume of soil and therefore dimensionless.

Therefore

$$\chi = \rho_w \chi_v \quad (56)$$

where ρ_w is the density of water. These are very appropriate measures in parametrizations based on simulating changes in the water mass of a specified layer of soil.

In general, several different forces are acting to bind the water to the soil and a less direct but nevertheless very useful measure of soil moisture content in the context of water movement is the soil moisture potential Ψ (also termed soil moisture tension, soil moisture suction, etc) which may be thought of as the energy needed to extract water from the soil matrix. It is common practice to express Ψ as a length, in a fashion analogous to the concept of a pressure head in hydraulics, such that at a level z_g in the soil

$$\Psi = \psi - z_g \quad (57)$$

where z_g represents the gravitational component of the moisture potential and ψ , the so-called matric potential, is the contribution to Ψ due mainly to capillarity and adsorption.

In an analogous fashion to the treatment of soil heat conduction in Section 5.1, consider the grossly simplified hydrology of a spatially homogeneous soil layer with no horizontal water movement and no melting or freezing within it. This restricted and idealised one-dimensional problem is governed by:

- the equation of continuity

$$\frac{\partial \chi}{\partial t} = \rho_w \frac{\partial \chi_v}{\partial t} = - \frac{\partial M}{\partial z_g} \quad (58)$$

where M is the vertical mass flux of water and χ , χ_v and M are functions of z_g and t ; and

- the flux-gradient relation (Darcy's Law)

$$M = -\rho_w K(\psi) \frac{\partial \Psi}{\partial z_g} \quad (59)$$

$$= -\rho_w K(\psi) \left(\frac{\partial \psi}{\partial z_g} - 1 \right)$$

where K , the hydraulic conductivity of the soil (SI units: ms^{-1}), is a function of ψ , which in turn is a function of z_g and t . Combining Eqns (58) and (59) yields the Richards' equation for the vertical movement of water in an unsaturated soil, viz.

$$\frac{\partial \chi_v}{\partial t} = \frac{\partial}{\partial z_g} \left[K(\psi) \left(\frac{\partial \psi}{\partial z_g} - 1 \right) \right] \quad (60)$$

Solving even the idealised Eqn (60) for reasonable boundary conditions is by no means a trivial matter. Proposals do exist which express ψ and $K(\psi)$ as functions of χ_v , although it should be stressed that these are highly empirical and difficult to justify in all but the most idealised circumstances. In such cases Eqn (60) takes the form of a diffusion equation for soil water

$$\frac{\partial \chi_v}{\partial t} = \frac{\partial}{\partial z_g} \left(\kappa_w(\chi_v) \frac{\partial \chi_v}{\partial z_g} \right) - \frac{\partial \kappa_w}{\partial z_g} (\chi_v) \quad (61)$$

where κ_w is a moisture diffusivity of the soil (SI units: $\text{m}^2 \text{s}^{-1}$) defined by

$$\kappa_w = K(\chi_v) \frac{\partial \psi}{\partial \chi_v} \quad (62)$$

Prognostic equations for soil moisture content based on the idealised hydrology of this section are beginning to appear in AGCMs and NWPMS; see, for example, the particular examples discussed in Dickinson (1984) and Warrilow et al (1986). One particular multi-layer soil hydrology scheme which has attracted considerable support from numerical modellers is the force-restore treatment of Deardorff (1978) in which he postulates equations for soil moisture transport of a form directly analogous to the corresponding force-restore equations for soil temperatures (vid. Eqn (51)). An effective 3-layer version of Deardorff's approach is used, for example, in ECMWF models (Blondin, 1986). However, the most common current

approach to modelling soil moisture content is probably still that based on a single surface soil layer and a more detailed discussion of only that example will suffice here.

6.2 Single-layer soil hydrology models

A common, rudimentary approach to the parametrization of the hydrological processes at a bare-soil surface is to monitor the change of soil moisture content in a single, shallow surface layer of notional depth δ_w , as depicted schematically in Figure 8.

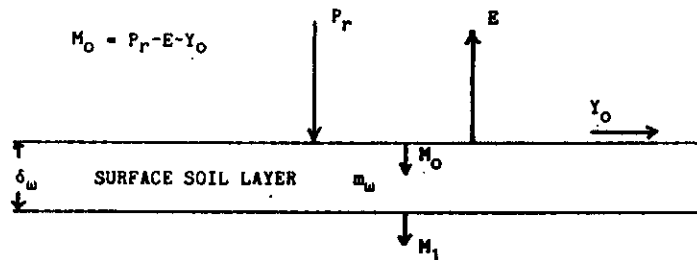


Figure 8. Schematic representation of the moisture balance of a surface layer of soil.

Let m_w denote the mass of liquid water per unit lateral area in the soil layer of depth δ_w , i.e.

$$m_w = \int_0^{\delta_w} \chi dz_g = \hat{\chi} \delta_w = \rho_w \hat{\chi}_v \delta_w = \rho_w d_w \quad (63)$$

where Eqn (63) also defines a layer-mean soil moisture concentration, $\hat{\chi}$, a corresponding layer-mean volumetric soil moisture concentration, $\hat{\chi}_v$, and d_w , a representative depth of water in the layer. Integration of Eqn (58) over the layer depth gives, from Eqn (63), the surface layer water mass balance equation in the form

$$\begin{aligned} \frac{\partial m_w}{\partial t} &= M_o - M_1 \\ &= P_r - E - Y_o - M_1 \end{aligned} \quad (64)$$

when M_o is substituted from Eqn (2).

M_1 is the vertical mass flux of water at the base of the surface layer. Apart from the surface runoff term Y_o , all other horizontal fluxes of soil water have been neglected. With P_r regarded in the present context as determined externally, then it remains here to illustrate with the aid of specific examples some of the problems of formulating parametrizations for E , Y_o and M_1 .

6.3 Evaporation at a bare-soil surface (E)

In principle, the surface evaporation rate E can be obtained as the residual flux from either the surface energy balance, Eqn (1), or the surface moisture balance, Eqn (2), and there are many empirical formulae for estimating E based on such approaches. A very useful introduction to the large variety of methods available can be found, for example, in Rosenberg et al (1983) and for more detailed discussions see, for example, Eagleson (1982) and Brutsaert (1982a, b). However, in this introduction to interactive soil temperature and soil moisture content parametrizations in AGCMs and NWPMS, I have selected the soil-flux terms G_o and M_o as the residual components in the surface balance equations (1) and (2), (see, for example, Eqns (51), (55) and (64)) and assumed implicitly that E can be evaluated in some independent manner.

Indeed, the method of estimating E has already been implied in principle in Section 4 where E as one of the main surface turbulent fluxes was ultimately parametrized in the bulk aerodynamic form of Eqn (28) as

$$E = -\rho C_E V(z_g)(q(z_g) - q_o) \quad (65)$$

with the recommendation that the bulk transfer coefficient C_E be evaluated from Monin-Obukhov similarity theory. It was however also noted that the surface value of the specific humidity q_o , required explicitly in Eqn (65) (and also, for example, in determining the bulk Richardson number defined by Eqn (36), and hence C_E) is not easy to determine. To overcome this problem it is standard practice to imply a value of q_o through relations with $q_{sat}(T_o)$, the saturation specific humidity at the surface which is readily determined as a function of surface temperature (and pressure) via the Clausius-Clapeyron relationship

$$\frac{dq_{sat}}{dT} \approx 0.622 \frac{L_1 q_{sat}}{R T^2} \quad (66)$$

where T is temperature, R is the specific gas constant for dry air and L_1 is the appropriate latent heat (i.e. L_e when the surface is not frozen).

Two common methods are:

- a. to specify a surface relative humidity, r_o , such that

$$q_o = r_o q_{sat}(T_o); \quad (67)$$

- b. to evaluate a potential evaporation rate

$$E_p = -\rho C_E V(z_g)(q(z_g) - q_{sat}(T_o)) \quad (68)$$

and to specify an empirical 'moisture availability function', β , (usually ranging from 0 for an arid surface to 1 for a saturated surface) such that the actual evaporation rate is given by

$$E = \beta E_p \quad (69)$$

The second method is by far the more commonly adopted. For a discussion and comparison of the two approaches see, for example, Nappo (1975) and for examples of their use in specific AGCMs see Carson (1982). It is worth noting in passing that an alternative relation in the spirit of Eqn (69) is used for computational convenience in some models and that is

$$\Delta q(z_g) = q(z_g) - q_0 = \beta(q(z_g) - q_{sat}(T_0)) \quad (70)$$

which implies that

$$q_0 = \beta q_{sat}(T_0) + (1-\beta)q(z_g) \quad (71)$$

The reasons for preferring Eqn (70) to Eqn (69) are discussed in Carson (1982) (and more fully in Carson and Roberts (1977)).

The most common method now employed is to express β as a simple linear function of the variable soil moisture content in the surface soil layer such that

$$\beta = \begin{cases} \hat{x}_v / \hat{x}_{v,c} & 0 \leq \hat{x}_v < \hat{x}_{v,c} \\ 1 & \hat{x}_v \geq \hat{x}_{v,c} \end{cases} \quad (72)$$

where $\hat{x}_{v,c}$ is a critical value of the mean volumetric soil moisture concentration below which $\beta < 1$, and is usually expressed as some fraction of a maximum allowable value of \hat{x}_v ie some nominal 'field capacity' $\hat{x}_{v,r}$. Eqn (72) for β can of course be simply reformulated in terms of any of the other standard measures of soil moisture content (see Eqn (63)) the most common of which is probably d_w .

A slight modification of Eqn (72), due to Warrilow et al (1986), is currently used in the Meteorological Office 11-layer AGCM, viz.

$$\beta = \begin{cases} 0 & 0 \leq \hat{x}_v < \hat{x}_{v,w} \\ \frac{\hat{x}_v - \hat{x}_{v,w}}{\hat{x}_{v,c} - \hat{x}_{v,w}} & \hat{x}_{v,w} \leq \hat{x}_v < \hat{x}_{v,c} \\ 1 & \hat{x}_v \geq \hat{x}_{v,c} \end{cases} \quad (73)$$

where $\hat{x}_{v,w}$ is called the 'wilting point'.

The critical value $\hat{x}_{v,c}$ used in Eqn (73) is not well defined but for simplicity, and in line with previous practice (see, for example, Carson (1982)) it is given by

$$\hat{x}_{v,c} = \hat{x}_{v,w} + \frac{1}{3}(\hat{x}_{v,r} - \hat{x}_{v,w}) \quad (74)$$

where $\hat{x}_{v,r}$ is a nominal 'field capacity' used only to define $\hat{x}_{v,c}$. The particular values of $\hat{x}_{v,w}$ and $\hat{x}_{v,r}$ being used globally in the Meteorological Office AGCM, which assumes for hydrological purposes only a single surface layer of soil of nominal depth $\delta_w = 1$ m, are listed in Table 6. With these values Eqn (73) reads

$$\beta = \begin{cases} 0 & 0 \leq \hat{x}_v < 0.08 \\ 20 \hat{x}_v - 1.6 & 0.08 \leq \hat{x}_v < 0.13 \\ 1 & \hat{x}_v \geq 0.13 \end{cases} \quad (75)$$

For a surface soil layer 1 m deep Manabe (1969), who first introduced interactive surface hydrology with Eqns (69) and (72) into an AGCM, originally selected 15 cm as his field capacity (ie for $d_{w,r}$ in terms of d_w used in Eqn (63)) and took $d_{w,c}/d_{w,r} (= \hat{x}_{v,c}/\hat{x}_{v,r}) = 3/4$. Carson's (1982) review of AGCMs indicates field capacities, $d_{w,r}$, in the range 10-30 cm and $1/3 - 3/4$ for the ratio $d_{w,c}/d_{w,r}$.

It should be borne in mind that the more complex and real practical issue to be addressed is that of determining the actual evapotranspiration from partially vegetated surfaces and not simply the evaporation from a bare-soil surface.

Depth of the surface layer of soil: δ_w (m)	1
Characteristics of the mean volumetric soil moisture concentration: \hat{x}_v	
Wilting point: $\hat{x}_{v,w}$	0.080
'Critical' point: $\hat{x}_{v,c}$	0.130
Nominal field capacity: $\hat{x}_{v,r}$	0.230
Saturation value: $\hat{x}_{v,s}$	0.445
Saturated hydraulic conductivity: K_s (mmh^{-1})	13.0
Surface infiltration rate: F (SI units: $\text{kg m}^{-2}\text{s}^{-1}$)	13.0 mmh^{-1} equivalent (= F/ρ_w)
Exponent in Eqn (82): c	6.6

Table 6. Soil hydrological characteristics used in the Warrilow et al (1986) hydrological scheme in the Meteorological Office 11-layer AGCM.

6.4 Surface runoff (Y_o)

Surface runoff is yet another of the complex surface hydrological processes which is treated very simplistically in current AGCMs and NWPMS. In models employing the single-layer water mass balance Eqn (64) the simplest approach is the so-called 'bucket model' for runoff

(usually implicitly combining both Y_0 and M_1 in Eqn (64) into a single 'total runoff' term). In this case, rainfall (modified by the evaporation loss) is allowed to increase the soil moisture content until the field capacity $d_{w,r}$ (or $\hat{x}_{v,r}$) is reached. Any further attempt to increase d_w (or \hat{x}_v) beyond the field capacity is implicitly assumed to be runoff water (including percolation to deeper layers) which plays no further part in the model's hydrological cycle. This identifies the original role played in these simple hydrological parametrizations by the field-capacity term, in addition to its use to define $d_{w,c}$ (or $\hat{x}_{v,c}$), as in Eqns (72)-(74). For a selection of the crude and highly empirical formulations used in specific AGCMs see, for example, Carson (1982).

A novel, but still relatively simple, parametrization has been developed by Warrilow et al (1986) for use in the Meteorological Office AGCM. It is based, with considerable simplification, on a scheme proposed by Milly and Eagleson (1982). An attempt has been made to allow for the spatial variability of rainfall since use of grid-box averages would give marked underestimation of the surface runoff. The rain is assumed to fall over a proportion μ of the grid-box where at present μ is chosen arbitrarily as 1 for the model's so-called 'large-scale dynamic rain' and as 0.3 for its 'convective rain'. These are thought to be conservatively high values. Eagleson and Qinliang (1985) have explored the likely coverage of a rainfall area for different catchment sizes and suggest that for an AGCM grid-square more appropriate values for μ are 0.6 and 0.05, respectively. The local rainfall rate, P_{rl} , throughout a grid-area is treated statistically as represented by the probability density function

$$f(P_{rl}) = \frac{\mu}{P_r} \exp\left(-\frac{\mu P_{rl}}{P_r}\right) \quad (76)$$

where P_r is the model's grid-point rainfall rate which is taken to represent the average grid-box rainfall.

The local surface runoff, Y_{0l} , is defined by

$$Y_{0l} = \begin{cases} P_{rl} - F & P_{rl} > F \\ 0 & P_{rl} \leq F \end{cases} \quad (77)$$

where F is a surface infiltration rate, deemed constant for a given soil, and at present given a fixed global value (equivalent to 13 mm h^{-1}). Integration of Y_{0l} over all values of P_{rl} yields an expression for the total surface runoff rate for a grid-area, viz,

$$Y_0 = P_r \exp(-\mu F/P_r) \quad (78)$$

6.5 The vertical mass flux of water at the base of the surface layer (M_1)

As indicated in the previous section, the simplest single-layer approaches typically assume explicitly that M_1 in Eqn (64) is negligible or implicitly that it combines with Y_0 to give a 'total runoff'. In the scheme of Warrilow et al (1986), adapted from Milly

and Eagleson (1982), M_1 , referred to as the gravitational drainage from the base of the surface layer, is acknowledged as a separate hydrological component of Eqn (64) that has to be parametrized.

Reference to Eqn (59) shows that

$$M_1 = -\rho_w [K(\psi) \left(\frac{\partial \psi}{\partial z_g} - 1 \right)]_{z_g = \delta_w} \quad (79)$$

Warrilow et al (1986) have argued, somewhat speculatively, that for horizontal averaging over a typical AGCM grid-area, the term $[K(\psi) \partial \psi / \partial z_g]_{z_g = \delta_w}$ is small and that M_1 in Eqn (79) can be represented simply by

$$M_1 = \rho_w [K(\hat{x}_v)]_{z_g = \delta_w} \quad (80)$$

with the further assumption that \hat{x}_v is effectively spatially homogeneous in the surface soil layer so that

$$M_1 = \rho_w K(\hat{x}_v) \quad (81)$$

Their particular prescription of the hydraulic conductivity as a function of \hat{x}_v , attributed to Eagleson (1978), is

$$K(\hat{x}_v) = K_s \left(\frac{\hat{x}_v - \hat{x}_{v,s}}{\hat{x}_{v,s} - \hat{x}_{v,w}} \right)^c \quad (82)$$

where $\hat{x}_{v,s}$ is termed the saturation value of \hat{x}_v , K_s the saturation conductivity (ie $K(\hat{x}_{v,s})$) and c is an empirically derived constant. For particular values of these quantities adopted globally by Warrilow et al (1986) see Table 6.

With the terms E , Y_0 and M_1 evaluated according to a particular model's approach selected from the wide range of methods implied and discussed in Sections 6.3-6.5, and with P_r determined by some other parametrization in the model, then Eqn (64) can be solved either in simple explicit fashion or by more subtle implicit methods to determine the change in m_w (and hence in \hat{x}_v , \hat{x} , d_w , etc). This concludes the introduction to parametrization of land-surface hydrological processes in AGCMs and NWPMS.

7. Snow-covered Surfaces

A particular class of non-vegetated land surfaces which have their own very special characteristics and exercise significant influence on the climate system over a wide range of time-scales is that comprised of snow- (and ice-) covered surfaces. As in the case of land-surface hydrology, it is generally true that little attention has yet been given to the representation in AGCMs and NWPMS of the special physical processes associated with such surfaces. However, I am confident that this particular area of the wider problem will receive increasing attention in the near future.

According to Kuhn (1982), in the course of the year about 50% of the Earth's land surface is covered by snow or ice. He also comments that, although the polar ice sheets contain about 99% of the Earth's fresh-water ice by mass, nevertheless the seasonal snow cover with its large areal extent and its high spatial and temporal variability may have an equal or

even greater impact on the atmospheric circulation. Undoubtedly then, a key issue will be how to deal sensibly with partial and rapidly changing snow cover, particularly in complex terrain, over the area of a typical grid-box in a large-scale numerical model. The proper treatment of the processes associated with snow-covered surfaces is a major topic in its own right. The brief comments here are no more than a postscript to the main discussion of bare-soil surfaces in Sections 2.6. For fuller expositions of the varied and complex characteristics and the effects of snow and its associated physical processes see, for example, Martinelli (1979), Male (1980), Gray and Male (1981) and IGS (1985). For discussions of snow covered surfaces aimed specifically at the AGCM parametrization problem see, in particular, Kuhn (1982) and Kotliakov and Krenke (1982).

7.1 Special conditions at snow- and ice-covered surfaces

Kuhn (1982) has listed the special conditions for snow and ice layers as:

- a. the surface temperature cannot exceed the melting temperature of ice;
- b. evaporation and sublimation take place at the potential rate;
- c. the short-wave albedo is generally high;
- d. the medium is permeable to air and water and transparent to visible radiation;
- e. the snow pack is a good thermal insulator;
- f. the layer has a high storage capacity for heat and water;
- g. the roughness of the surface is extremely low (but see comments below at Section 7.2c); and
- h. generally, the atmospheric surface layer over snow or ice is stably stratified.

Note that conditions a-h impinge on every aspect of the parametrization problem already discussed in Sections 2-6. The remainder of this section retraces our previous route and indicates briefly where modifications to the parametrizations are typically introduced into AGCMs and NWPMS in recognition of snow (or ice) covering the surface. In general the thermal and hydrological properties of the snow pack are represented very simply and crudely in such models.

7.2 The physical properties of snow- and ice-covered surfaces

- a. Short-wave albedo (α). It is firmly established that the physical coupling between snow and ice cover, albedo and the surface temperature is one of the most important feedback mechanisms to include in an AGCM. As indicated on the list above (7.1c), an important characteristic of snow- and ice-covered surfaces is their high reflectivity compared with other natural surfaces such that even a thin covering of fresh snow can alter significantly the albedo of a landscape. The local albedo of a

snow-covered surface is very variable and a complicated function of many factors including the age of the snow pack (α decrease markedly as the snow becomes compacted and soiled), the wavelength and angle of the incident radiation and even diurnal cycles in the state of the snow surface, particularly when conditions are right for surface melting. The albedo may lie anywhere in the range from 0.95 for freshly fallen snow to about 0.35 for old, slushy snow (see, for example, Kondratyev et al (1982)).

At present the coupling between snow and ice and the surface albedo is generally prescribed very simply. Three types of snow- or ice-covered surfaces are generally acknowledged, viz:

- (1) surfaces with instantaneously variable depth of snow either predicted or implied;
- (2) permanent or seasonally prescribed snow- and ice-covered land surfaces; and
- (3) permanent or seasonally prescribed areas of sea-ice.

The third category is not the concern of this paper. For models that 'carry' a snow depth a common approach still used is that of Holloway and Manabe (1971) who, following Kung et al (1964), introduced the following simple dependence of albedo on snow depth into an AGCM:

$$\alpha = \begin{cases} \alpha_l + (\alpha_s - \alpha_l) d_{sw}^{1/2} & d_{sw} < 1 \text{ cm} \\ \alpha_s & d_{sw} \geq 1 \text{ cm} \end{cases} \quad (83)$$

where α_l is the snow-free land surface albedo (see Section 3.4); α_s is the albedo of a deep-snow surface (assumed in this case to be 0.60); and d_{sw} is the water equivalent depth of snow (here expressed in cm). No allowance is usually made for the varying density of a snow pack and d_{sw} is assumed typically to be about $1/10$ of the actual snow depth (see further comments in Section 7.3). Therefore the assumption is that when the grid-point snow depth is greater than about 10 cm, then α is independent of snow depth and equal to 0.60. Eqn (83) is designed supposedly to take account of the fact that as the mean snow depth increases, not only does the snow cover surface irregularities more completely but also the area of the grid-box which is snow-free is likely to decrease.

In some models which predict and monitor snowfall, a single albedo value is used for any non-zero depth of snow (see Carson (1982, 1986a)). The first snowfall on a previously snow-free surface results in an immediate increase in surface albedo which will tend, at least initially, to accelerate the positive feedback of a further lowering of the surface temperature with an enhanced probability of further snow accumulation.

Typical model values for land- and sea-ice are in the range 0.5-0.8 (see Carson (1982, 1986a)).

b. Long-wave emissivity (ϵ). Kuhn (1982) states that this can be assumed to be unity for all practical purposes.

c. Surface roughness length (z_0). The effective z_0 for extensive, uniformly covered snow and ice fields and the 'local' value of z_0 for snow-covered, simple heterogeneous terrain may indeed be very small ($0(10^{-3}\text{m})$ or less). However, in general, the effective areal z_0 of natural, heterogeneous and complex terrain with varied relief and vegetation is very difficult to determine (see Section 4.7) and may be affected greatly or insignificantly by different degrees of snow cover. There is little scope for useful discussion of this problem in a global, large-scale modelling context except to note that, in principle, snow and ice cover can alter z_0 .

d. Thermal properties of snow. As noted above, a snow pack is generally a good thermal insulator for the soil below but to capture this effect in a climate model implies a delineation and explicit modelling of the heat conduction (and the hydrology) in and between the two media. In general the thermal and hydrological properties of snow and ice layers are treated very simply, if at all, in AGCMs and NWPMS (see below). The thermal properties of a snow pack will, like its density and albedo, depend in a complicated fashion on many factors. Values thought to be appropriate for snow are given in Table 4 for comparison with the range of soil values also included there.

7.3 Surface energy and mass flux balances at a snow-covered surface

The surface energy flux balance (Eqn (1)) is modified for complete snow cover such that

$$G_0 = R_N - H - Q_S - Q_F \quad (84)$$

where $Q_F = L_F S$ represents the latent heat flux required to affect phase changes associated with melting or freezing at the surface, where S is the rate of snowmelt (or ice melt) and L_F is the latent heat of fusion;

$Q_S = L_S E_S$ represents the latent heat flux due to surface sublimation by turbulent transfer, where E_S is the rate of sublimation and L_S is the latent heat of sublimation ($L_S = L_e + L_F$);

and G_0 is now strictly the flux of heat into the snow layer at its upper surface.

A simple budget equation, corresponding to that used for soil moisture content in a single soil layer (Eqn (64)), is also used for snow on the 'surface', viz.

$$\frac{\partial m_s}{\partial t} = P_s - E_s - S \quad (85)$$

where P_s , the only undefined term on the RHS, is the intensity of snowfall at the surface and m_s is the mass of snow lying per unit area of the surface. m_s is therefore treated like m_w as a surface

prognostic variable and is often represented as a snow depth, d_s , or more commonly as an equivalent depth of water, d_{sw} , (cf Eqn (63)) such that

$$m_s = \rho_s d_s = \rho_w d_{sw} \quad (86)$$

where ρ_s is the density of snow. Although it is recognised that the density of a snow pack varies, this again is a complicated issue in its own right and it is quite common practice in large-scale numerical models to assume simply that $\rho_s \approx 0.1 \rho_w$.

Eqn (85) is usually complemented by the surface-layer balance equation for the soil moisture content (Eqn (64)) modified to include the snowmelt term, ie

$$\frac{\partial m_w}{\partial t} = P_r - E + S - Y_0 - M_1 \quad (87)$$

Each model has its own system of checks and algorithms for deciding which of the terms in Eqns (85) and (87) are in force simultaneously. One popular approach is as follows. When snow is lying T_0 is not allowed to rise above 273 K and the snow depth accumulates without limit or decreases according to the net value of ($P_s - E_s$). If, however, snow is lying and the solution of the heat balance Eqn (84), excluding the terms Q_F , produces an interim surface temperature value $T_0' > 273$ K then sufficient snow (if available) is allowed to melt to maintain $T_0 = 273$ K. The heat required to melt the snow and reduce T_0 to 273 K can be evaluated by specifying an effective surface thermal capacity of the snow pack (cf Eqn (43)) such that

$$Q_F = L_F S = C_{eff,s} \frac{T_0' - 273}{\Delta t} \quad (88)$$

where Δt is the appropriate model time step. The change in the water equivalent snow depth, Δd_{sw} , resulting from the melting is determined from Eqn (85) and (88) such that

$$\begin{aligned} \Delta m_s &= \rho_w \Delta d_{sw} = -S \Delta t \\ &= -\frac{C_{eff,s}}{L_F} (T_0' - 273) \end{aligned} \quad (89)$$

It is usually assumed that the snow pack has no moisture holding capacity; all melted snow is added directly to the soil moisture content (through Eqn (87)) following the corresponding reduction (Δd_{sw}) in the snow depth. In all cases it is only when the snow disappears through melting or sublimation that evaporation of moisture is allowed to resume at the surface.

8. Concluding Remarks

It should be evident from Sections 2-7 that, in many respects, the representations of land-surface processes in AGCMs and NWPMS are still rather crude and simple. The demands for improvements will come from both climate modelling studies and numerical weather forecasting. Indeed, the steadily increasing number of studies with AGCM's has already amply demonstrated the sensitivity of such models to surface properties and

155

processes (see, for example, recent reviews by Mintz (1984), Rowntree (1983, 1984) and Rowntree et al (1985)). Parametrizations thought adequate at present will undoubtedly be seen to be deficient in models which couple interactively further components of the climate system. This is already apparent with respect to air-sea interactions in coupled ocean-atmosphere models. Although the major developments in the longer term are more likely to come from climate modelling studies, nevertheless valuable feedback is being obtained from the continuous close scrutiny of the various models' performances in the acutely critical arena of operational weather forecasting - especially of local, near-surface variables such as wind and temperatures.

A schematic resumé of the processes, variables and parameters introduced in this discussion of the specification of parametrizations for simple, non-vegetated land surfaces is given in Figure 9.

	Radiative	Thermal	Hydrological	Dynamical
'External forcing'	$R_{S\downarrow}, R_{L\downarrow}$		P_r, P_a	
Atmospheric variables		$\theta(T), q$		v
Surface variables	T_o		Q_e, d_s	
Surface parameters	α, ϵ			z_o
Surface fluxes	R_N	H $Q = L_e E$ $Q_r = L_r S$ $Q_s = L_s E_s$ G_o	E, E_s S M_o, X_o	τ
Sub-surface fluxes		G	M	
Sub-surface parameters		λ, C	δ K Significant values of X_v	
Sub-surface variables		T_g	X_v	

Figure 9. Schematic resumé of the processes, variables and parameters involved in the specification of parametrizations at simple, non-vegetated land surfaces.

REFERENCES

- André, J-C and Blondin, C 1986 'On the effective roughness length for use in numerical three-dimensional models', *Boundary-Layer Meteorol.*, **35**, 231-245.
- André, J-C, Goutorbe, J-P and Perrier, A 1986 'HAPEX-MOBILHY: A hydrologic and atmospheric experiment for the study of water budget and evaporation flux at the climatic scale', *Bull. Amer. Met. Soc.*, **67**, 138-144.
- Beuttner, K J K and Kern, C D 1965 'The determination of infrared emissivities of terrestrial surfaces', *J. Geophys. Res.*, **70**, 1329-1337.
- Bhumralkar, C M 1975 'Numerical experiments on the computation of ground surface temperature in an atmospheric general circulation model', *J. Appl. Met.*, **14**, 1246-1256.
- Blondin, C A 1986 'Treatment of land-surface properties in the ECMWF model'. Proceedings of the ISLSCP Conference on Parametrization of Land-surface Characteristics, Use of Satellite Data in Climate Studies, and First Results of ISLSCP, Rome 2-6 Dec 1985, 53-60, ESA SP-248.
- Brutsaert, W H 1982a 'Vertical flux of moisture and heat at a bare soil surface', *Land Surface Processes in Atmospheric General Circulation Models*, Ed. P S Eagleson, 115-168, CUP, Cambridge.
- Brutsaert, W H 1982b 'Evaporation into the atmosphere. Theory, history and applications'. D Reidel Publ. Co., Dordrecht.
- Carson, D J 1982 'Current parametrizations of land-surface processes in atmospheric general circulation models', *Land Surface Processes in Atmospheric General Circulation Models*, Ed P S Eagleson, 67-108, CUP, Cambridge.
- Carson, D J 1986a 'Parametrizations of land-surface processes in Meteorological Office numerical weather prediction and climate models', Unpublished Met Office Report, DCTN 37, Met O 20.

- Carson, D J 1986b 'Issues concerning the evaluation of effective surface roughness of heterogeneous terrain' Proceedings of the ISLSCP Conference on Parametrization of Land-Surface Characteristics, Use of Satellite Data in Climate Studies, and First Results of ISLSCP, Rome, 2-6 Dec 1985, 77-82, ESA SP-248.
- Carson, D J and Richards, P J R 1978 'Modelling surface turbulent fluxes in stable conditions', Boundary-layer Meteorol., 14, 67-81.
- Carson, D J and Roberts, S M 1977 'Concerning the evaluation of the turbulent fluxes at unsaturated surfaces'. Unpublished Met Office Report, Met O 20 Tech. Note No. II/103.
- Deardorff, J W 1978 'Efficient prediction of ground surface temperature and moisture, with inclusion of a layer of vegetation', J. Geophys. Res., 83, 1889-1903.
- Dickinson, R E 1984 'Modelling evapotranspiration for three-dimensional global climate models', Climate Processes and Climate Sensitivity, Geophys. Monograph 29, Maurice Ewing Vol. 5; 58-72, AGU.
- Dooge, J C I 1982 'Parametrization of hydrologic processes', Land Surface Processes in Atmospheric Circulation Models, Ed. P S Eagleson, 243-288, CUP, Cambridge.
- Dyer, A J and Hicks, B B 1970 'Flux-gradient relationships in the constant flux layer', Quart. J. R. Met. Soc., 96, 715-721.
- Eagleson, P S 1978 'Climate, soil and vegetation', Water Resources Research, 14, 705-776.
- Eagleson, P S 1982 'Dynamic hydro-thermal balances at mesoscale', Land Surface Processes in Atmospheric Circulation Models, Ed. P S Eagleson, 289-357, CUP, Cambridge.
- Eagleson, P S and Qinliang, W 1985 'Moments of catchment storm area', Water Resources Research, 21, 1185-1194.
- Geiger, R 1965 'The climate near the ground', Harvard Univ. Press, Cambridge, Mass.
- Gray, D M and Male, D H 1981 'Handbook of snow. Principles, processes, management and use', Eds. D M Gray and D H Male, Pergamon Press, Toronto.
- Holloway, J L, Jr and Manabe, S 1971 'Simulation of climate by a global general circulation model. I Hydrological cycle and heat balance', Mon. Weath. Rev., 99, 335-370.
- IGS 1985 Proc. Symp. Snow and Ice Processes at the Earth's Surface, Sapporo, Japan, 2-7 Sept. 1984, Annals of Glaciology, Vol. 6, Published by IGS, Cambridge.
- Kondratyev, K Ya 1972 'Radiation processes in the atmosphere', Second IMO Lecture, WMO - No. 309, WMO, Geneva.
- Kondratyev, K Ya, Korzov, V I 1982 'The shortwave albedo and the surface emissivity', Land Surface Processes in Atmospheric Circulation Models, Ed. P S Eagleson, 463-514, CUP, Cambridge.
- Mukhenberg, V V and Dyachenko, L N
- Kotliakov, V M and Krenke, A N 1982 'Data on snow cover and glaciers for the global climatic models', Ibid., 449-461.
- Kuhn, M 1982 'Vertical flux of heat and moisture in snow and ice', Ibid., 227-240.
- Kung, E C, Bryson, R A and Lenschow, D H 1964 'Study of a continental surface albedo on the basis of flight measurements and structure of the Earth's surface cover over North America', Mon. Weath. Rev., 92, 543-564.
- Male, D H 1980 'The seasonal snow cover', Chap 6 Dynamics of Snow and Ice Masses, Ed. S C Colbeck, Academic Press, New York.
- Manabe, S 1969 'Climate and the ocean circulation. I The atmospheric circulation and the hydrology of the Earth's surface', Mon. Weath. Rev., 97, 739-774.
- Martinelli, M, Jr 1979 'Snow', Research on Snow and Ice, Martinelli et al, Rev. Geophys. and Space Phys., 17, 1253-1256. (Refs 1266-1271):
- Mason, P J 1985 'On the parametrization of orographic drag', To appear in Proc. Seminar on Physical Parametrization for Numerical Models, Reading, 9-13 September 1985, ECMWF.

- McBean, G A, Bernhardt, K, Bodin, S, Litynska, Z, Van Ulden, A P and Wyngaard, J C 1979 The Planetary Boundary Layer, Ed. G A McBean, Chairman CAS Working Group on Atmospheric Boundary-Layer Problems, WMO-No. 530, Tech. Note No. 165, WMO, Geneva.
- Milly, P C D and Eagleson, P S 1982 'Parametrization of moisture and heat fluxes across the land surface for use in atmospheric general circulation models', MIT Report No. 279, Cambridge, Mass.
- Mintz, Y 1984 'The sensitivity of numerically simulated climates to land-surface boundary conditions', The Global Climate, Editor J T Houghton, 79-105, CUP, Cambridge.
- Monteith, J L 1965 'Evaporation and environment', Symp. Soc. Exptl. Biol., 19, Swansea, 8-12 September 1964, 205-234.
- Nappo, C J, Jr 1975 'Parametrization of surface moisture and evaporation rate in a planetary boundary layer model', J. Appl. Met., 14, 289-296.
- Oke, T R 1978 'Boundary Layer Climates', Methuen, London.
- Paltridge, G W and Platt, C M R 1976 'Radiative Processes in Meteorology and Climatology', Developments in Atmospheric Science, 5, Elsevier Sci. Pub. Co., Amsterdam.
- Panofsky, H A and Dutton, J A 1984 'Atmospheric Turbulence. Models and methods for engineering applications', John Wiley and Sons, New York.
- Perrier, A 1982 'Land surface processes: vegetation', Land Surface Processes in Atmospheric Circulation Models, Ed. P S Eagleson, 395-448, CUP, Cambridge.
- Rosenberg, N J, Blad, B L, and Verma, S B 1983 'Microclimate. The Biological Environment', Second Edition, John Wiley and Sons, New York.
- Rowntree, P R 1983 'Land surface processes in climate models - parametrization and model sensitivity', Report of the Fourth Session of the JSC, Venice, 1-8 March 1983, Appendix B, 57-75, WCRP, ICSU/WMO.
- Rowntree, P R 1984 'Review of general circulation models as a basis for predicting the effects of vegetation change on climate', To appear in Proc. United Nations Univ. Workshop on Forests, Climate and Hydrology - Regional Impacts, Oxford, 26-30 March 1984. Available as Unpublished Met Office Report, Met O 20 Tech. Note No. II/225.
- Rowntree, P R, Wilson, M R and Sangster, A B 1985 'Impact of land surface variations on African rainfall in general circulation models', Unpublished Met Office Report, DCTN 30, Met O 20.
- Sellers, P J, Mintz, Y, Sud, Y C and Dalcher, A 1986 'A simple biosphere model (SiB) for use within general circulation models', J. Atmos. Sci., 43, 505-531.
- Sellers, W D 1965 'Physical Climatology', The Univ. of Chicago Press, Chicago and London.
- Smagorinsky, J 1982 'Large-scale climate modelling and small-scale physical processes', Land Surface Processes in Atmospheric Circulation Models, Ed. P S Eagleson, 3-17, CUP, Cambridge.
- Smith, F B and Carson, D J 1977 'Some thoughts on the specification of the boundary layer relevant to numerical modelling', Boundary-layer Meteorol., 12, 307-330.
- Warrilow, D A, Sangster, A B and Slingo, A 1986 'Modelling of land surface processes and their influence on European climate', Unpublished Met Office Report, DCTN 38, Met O 20.
- WCP 1985 Report of the First Session of the JSC Scientific Steering Group on Land Surface Processes and Climate, Geneva, 21-25 Jan 1985, WCP-96, WMO/TD-No 43, WCRP, ICSU/WMO.
- Webb, E K 1970 'Profile relationships: the log-linear range and extension to strong stability', Quart. J. R. Met. Soc., 96, 67-90.
- Wieringa, J 1986 'Roughness-dependent geographical interpolation of surface wind speed averages', To appear in Quart. J. R. Met. Soc.

8. SURFACE ROUGHNESS OVER THE SEA

The physical appearance of the sea surface, and hence its characteristic z_0 , depend in general on many factors including fetch, wind speed and stability of the overlying boundary layer.

In very light winds ($< 2 \text{ ms}^{-1}$), the sea surface is aerodynamically smooth and z_0 is given by

$$z_0 = 0.1 \frac{\nu}{u_*}, \quad 0 \leq \frac{u_*^2}{g\nu} \leq 50$$

where u_* is the surface friction velocity, ν is the kinematic viscosity of the air and g is the acceleration due to gravity. Note that z_0 is supposed to decrease with increasing u_* .

Above 2 ms^{-1} , the air flow becomes turbulent and sea waves are an important feature. At short fetches, the waves are still developing and the drag is greater than at larger fetch when some sort of aerodynamic equilibrium is reached. The major part of the drag comes from the smaller ripples and motions which appear to be relatively independent of wind speed in moderate winds; the effective z_0 is then scattered about 0.1 mm.

The complex behaviour of z_0 with highly developed waves has been reduced to the Charnock (1955) formula :

$$z_0 = \frac{M u_*^2}{g} \quad (8.1)$$

where the 'constant' M was estimated as about 0.012 by Charnock but later by other authors to be in the higher range 0.035-0.05. In view of the observational scatter and dependence of such non-local factors as fetch, M should not be considered anything more than an order-of-magnitude constant to be applied cautiously in typical offshore conditions.

Equation (8.1) can be written

$$z_0 = \frac{M u_*^2}{g} = \frac{M}{g} C_D V^2$$

where C_D is the drag coefficient appropriate to the height, z , at which the wind speed V is measured.

In strictly neutral conditions in the surface layer,

$$C_D = \frac{k^2}{(\ln z/z_0)^2}$$

and so

$$\begin{aligned} V^2 &= \frac{gz_0}{\rho k^2} (\ln z/z_0)^2 \\ &= \frac{gz}{\rho C_D} \exp(-k C_D^{-1/2}) \end{aligned}$$

For given z , therefore, z_0 and C_D can be expressed as functions of $V(z)$ only.

Data for lower wind speeds almost always show a great deal of scatter, with a mean for C_D about 1.2×10^{-3} .

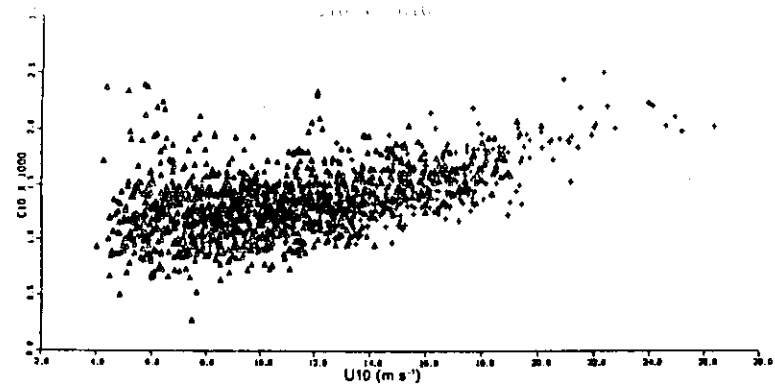


Figure 12 (a) — The drag coefficient of wind over open water, as measured by S. Pond and W. G. Large. Note the scatter in the data

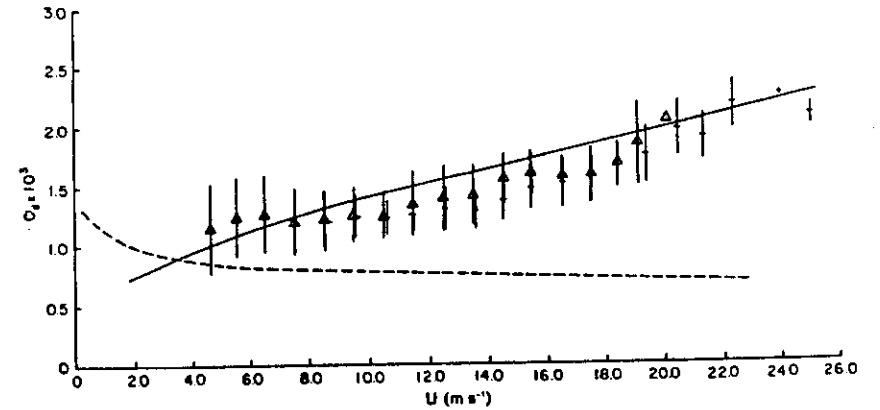


Figure 12 (b) — Same data as Figure 12 (a) displayed as means with standard deviations. The triangles refer to data obtained from the fixed mast operated in the north-west Atlantic by the Bedford Institute of Oceanography, while the crosses refer to data collected at Ocean Weather Station PAPA in the north-west Pacific. The dashed line indicates the drag of a very smooth surface such as glass, while the solid line corresponds to the Ellison-Charnock suggestion $\tau_0 = E u_*^2/g$, with E put at 0.015

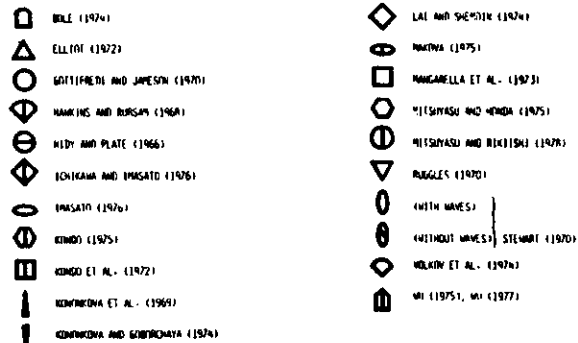
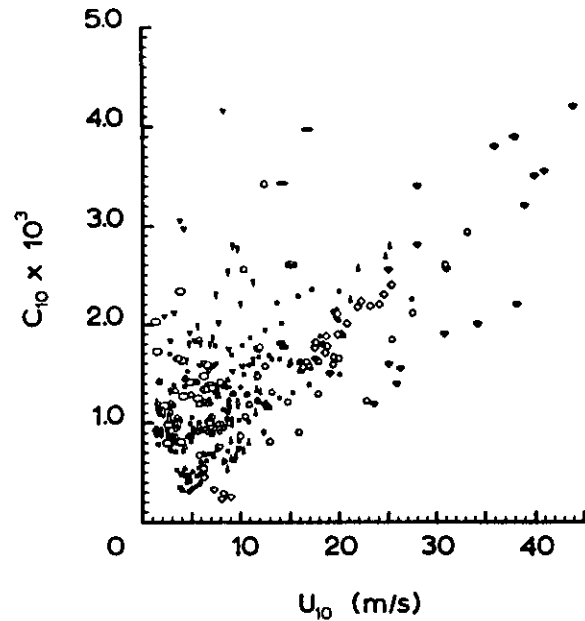


Fig. 1. Drag coefficient versus mean wind speed at 10-m height of some available data.

9. THE ATMOSPHERIC BOUNDARY LAYER AS A WHOLE

9.1 Rossby Number Similarity Theory for the Whole Atmospheric Boundary Layer

9.1.1 Introduction

The part of the boundary layer which has received most attention to date is the surface layer in which, by definition, the turning of the wind with height (and hence the Coriolis force) may be ignored, and the vertical fluxes of momentum, heat and water vapour are assumed to be virtually constant with height. The Monin-Obukhov similarity theory has, within a certain stability range, provided fairly satisfactory flux-profile relationships for the surface layer.

However, once above the surface layer and into the Ekman layer, where the wind gradually turns from its surface direction to the direction of the frictionless wind (sometimes the geostrophic wind) which exists outside the boundary layer, we run into difficulties. It is in this region that most of today's boundary-layer research is focused.

Not only is there the experimental problem of obtaining data outside the surface layer, but there is also the theoretical problem that insufficient soundly-based equations exist to complete the set required for solution.

Even in stationary, horizontally-homogeneous, neutral conditions there are essentially 5 independent unknowns - $\mu, \sigma, \tau_x, \tau_y$ and some parameter describing the turbulence e.g. K, L .

Five independent equations are needed. The set available is two momentum equations and 2 flux-gradient relationships. There are several methods available for obtaining the fifth equation, required to close the system, but they all rely on empirical or semi-empirical forms for quantities such as the eddy diffusivity, K , or some scale-length for the turbulence, L .

Even with a great many simplifications, solutions in some cases are difficult to obtain and although the methods have not been without their rewards, for most purposes they are at present not suitable for general use.

One approach with large-scale numerical models in mind is to attempt to relate the stress, heat flux and vapour flux at the Earth's surface and within the boundary layer to certain gross parameters readily available in the numerical model. Solutions must of course be consistent with relations already established within the surface layer.

In this approach, one decides, on more or less intuitive grounds, what are the controlling external parameters of boundary-layer structure and sets up a similarity theory in terms of appropriate combinations of the parameters, within the framework of the basic equations.

Brought down to the very simplest terms, these methods depend on the possibility of being able to express the unknown variables in non-dimensional form, there being suitable argument for saying there is a length-scale, a time-scale (or velocity-scale) and temperature and humidity scales relevant in doing this. The non-dimensional forms are then postulated to be universal in character and this will hold as long as the scales remain the relevant ones.

We cannot proceed very far without recognising that different length-scales are relevant in different parts of the boundary layer e.g. for small z the surface roughness z_0 is an important scale, whereas for large z the boundary layer depth h becomes the important scale. Large-scale features of the flow may be lost if z_0 is used everywhere as the length-scale while small-scale features of the flow that may occur close to the surface cannot be adequately described with h used as the length-scale.

We are therefore led to consider separately the flow in the surface layer and the flow in the outer portion of the boundary layer and to link the two regions in some way. The technique used to achieve this is based on the branch of analysis which deals with singular perturbation methods.

9.1.2 General theory

The first step is to decide which "external parameters" can be expected to determine the structure of the boundary layer.

For horizontally-homogeneous, stationary conditions these are assumed to be

$$z_0, v_g, \Delta T_0, (\Delta T_e), f, g/\theta \quad (1)$$

where ΔT_e denotes the difference in a property of its value at the top of the a.b.l. from its surface value. There may be some inadequacy in this list say for very low latitudes, while for the boundary layer over the sea z_0 becomes a function of other parameters. Stationarity is only upheld if conditions have remained effectively steady over a period of a few hours. The diurnal variations over land are generally too rapid to allow equilibrium conditions to be well set up and we shall return to this point later.

From the above five external parameters which contain three dimensional units, two non-dimensional combinations to be constructed

$$R_0 = v_g / fz_0 \quad \text{the surface Rossby Number} \quad (2)$$

$$\text{and } S = \frac{g \Delta T_0}{\theta + v_g} \quad \text{an external stability parameter.} \quad (3)$$

The similarity hypothesis then states that any non-dimensionally expressed characteristic property of the boundary layer

$$\text{e.g. } u_* / v_g, T_* / \Delta T_0 \quad \text{must be a function of } R_0 \text{ and } S, \text{ and any}$$

internally varying property

$$\text{e.g. } u / v_g, \tau_w / \rho_* (\theta - \theta_0) / \Delta T_0 \quad \text{must be a function of } R_0, S \text{ and of}$$

the non-dimensional height z/z_0 or $z f / v_g$ where $z_0, v_g / f$ are scaling-lengths provided by the five external parameters.

Because of the first set of relationships, the internally varying properties may also be expressed in terms of functions of the internal characteristics of the boundary layer which are

$$\mu_*, T_* (\sim H / c_p), (q_*) , \alpha \quad \text{with again } f, g/\theta \quad (4)$$

from which we may form one non-dimensional stability parameter

$$\begin{aligned} \mu &= -k^2 g \frac{(H / c_p)}{\theta} \frac{1}{f u_*^2} \left[= \frac{k^2 S T_* / \Delta T_0}{u_* / v_g} = f_n(R_0, S) \right] \\ &= \frac{k u_*}{f L} \quad \text{(Planetary Richardson Number)} \quad (5) \end{aligned}$$

and the length and velocity scales are u_* / f and u_* respectively.

Since μ can be expressed as a function of R_0, S only then μ can be used in place of S in the similarity formulation.

The similarity hypothesis states in particular that we may write

$$\frac{u_*}{v_g}, \frac{v_*}{v_g}, \alpha, \frac{T_*}{\Delta T_0}, \frac{q_*}{\Delta T_e} \quad (6)$$

as functions of R_0, μ only.

There is experimental evidence which generally gives some support to these relationships and also using the techniques of singular perturbation problems we can carry the theoretical formulation of the similarity hypothesis much further.

9.1.3 The Neutral Barotropic Boundary Layer

Horizontally-homogeneous, stationary, neutral, barotropic boundary layer.

In the neutral situation the stability parameter is not relevant and need not be considered in the similarity treatment.

In the inner layer we know that very near the boundary the flow should become independent of the Coriolis force, adjusting itself to zero at z_0 , and so z_0 is the relevant scaling-length in the inner layer.

To find a suitable scaling-length away from the surface layer we consider the momentum equations for the situation

$$\frac{\partial \mathbf{F}}{\partial z} = -f \rho (\mathbf{v} - \mathbf{v}_g) \times \mathbf{k} \quad (7)$$

where
$$\mathbf{v}_g = \frac{1}{\rho f} (\mathbf{k} \times \nabla p) \quad (8)$$

In component form these are

$$\frac{\partial \tau_x}{\partial z} = -f \rho (v - v_g) \quad (9)$$

and
$$\frac{\partial \tau_y}{\partial z} = f \rho (u - u_g) \quad (10)$$

Choose x-axis parallel to the direction of the surface stress and integrate (9), (10) from z_0 to ∞ .

$$\int_{z_0}^{\infty} f(v - v_g) dz = \tau_x / \rho = u_*^2 \quad (11)$$

$$\int_{z_0}^{\infty} f(u - u_g) dz = 0 \quad (12)$$

From (11) we see that u_* defines an integral scale-height of the boundary layer, since

$$\frac{u_*}{f} = \int_{z_0}^{\infty} \frac{v - v_g}{u_*} dz \quad (13)$$

The atmospheric boundary layer is thus characterized by the existence of two important length-scales z_0 and u_*/f , where

$$u_*/f \text{ is } O(10^4)$$

and the ratio $\frac{f z_0}{u_*}$ is typically of $O(10^{-4})$

(ex. $z_0 = 0.1 \text{ m}$, $f = 10^{-4} \text{ s}^{-1}$, $u_* = 0.5 \text{ m s}^{-1}$)

i.e. the problem is characterized by two length-scales whose ratio $\epsilon = \frac{f z_0}{u_*}$ tends to zero in real situations.

Further, ϵ is related to the Rossby Number,

$$\begin{aligned} \epsilon = \frac{f z_0}{u_*} &= \frac{f z_0}{V_g} \cdot \frac{V_g}{u_*} \\ &= \frac{1}{R_o} f(L_o), \text{ from similarity hypothesis} \\ &= \epsilon(L_o) \end{aligned} \quad (14)$$

171

$$\text{Therefore } \frac{v_g}{u_*} = f(\epsilon). \quad (15)$$

The similarity hypothesis and singular perturbation theory allow us to propose:

Inner layer:
$$\frac{u}{u_*} = F\left(\frac{z}{z_0}, \epsilon\right) \quad (16)$$

Since $\epsilon = \frac{f z_0}{u_*}$ is so small we can approximate $F(\frac{z}{z_0}, \epsilon)$ by an asymptotic expansion in terms of ϵ , which is valid provided z/z_0 does not become comparable with ϵ^{-1} , i.e. the expansion is valid for $z \ll u_*/f$

$$\frac{u}{u_*} \sim F_0\left(\frac{z}{z_0}\right) + F_1\left(\frac{z}{z_0}\right)\epsilon + F_2\left(\frac{z}{z_0}\right)\epsilon^2 + \dots \quad (17)$$

For large z this particular form of the expansion is not very suitable because we have noted $z/z_0 = O(\epsilon^{-1})$.

Outer layer:

At these heights the relevant scaling-length becomes u_*/f . Also we know that the upper boundary condition is $u \rightarrow u_g$ and from similar argument to that which led to (17) we know that u_g/u_* is a function of ϵ only. Therefore we can write,

$$\frac{u - u_g}{u_*} = f\left(\frac{fz}{u_*}, \epsilon\right) \quad (18)$$

which again we may represent by an outer asymptotic expansion

$$\frac{u - u_g}{u_*} \sim f_0\left(\frac{fz}{u_*}\right) + f_1\left(\frac{fz}{u_*}\right)\epsilon + f_2\left(\frac{fz}{u_*}\right)\epsilon^2 + \dots \quad (19)$$

We appeal now to the method of matched asymptotic expansions and the existence of an overlap domain where both expansions are valid.

Consider only the zeroth-order expansions:

$$\left. \begin{aligned} \frac{u}{u_*} &\sim F_0\left(\frac{z}{z_0}\right) \\ \frac{u - u_g}{u_*} &\sim f_0\left(\frac{fz}{u_*}\right) \end{aligned} \right\} \quad (20)$$

Write $\gamma = z/z_0$, $fz/u_* = \gamma \epsilon$

Matching principle implies

$$F_0(\gamma) = \frac{u_g}{u_*} + f_0(\gamma \epsilon) \quad (21)$$

172

Differentiate first with respect to γ , and secondly with respect to R_0 , recalling that $\epsilon = \epsilon(R_0)$, $u_g/u_* = f_0(R_0)$

$$F_0'(\gamma) = \epsilon f_0'(\gamma\epsilon) \quad (21)$$

$$0 = \frac{d}{dR_0} \left(\frac{u_g}{u_*} \right) + \gamma \frac{d\epsilon}{dR_0} f_0'(\gamma\epsilon) \quad (22)$$

Eliminating f_0' : $\gamma \frac{d\epsilon}{dR_0} F_0'(\gamma) + \epsilon \frac{d}{dR_0} \left(\frac{u_g}{u_*} \right) = 0$

i.e. $\gamma F_0'(\gamma) = - \left(\frac{d \ln \epsilon}{dR_0} \right)^{-1} \frac{d}{dR_0} \left(\frac{u_g}{u_*} \right) = \text{constant}, \quad (24)$

Since LHS is a function of γ only, whilst the RHS is a function of R_0 only,

$\therefore \gamma F_0'(\gamma) = 1/k$, say

$\therefore F_0(\gamma) = \frac{\ln \gamma}{k}$ so that lower b.c. is satisfied

i.e. $\frac{u}{u_*} = \frac{1}{k} \ln z/z_0 \quad (25)$

Also

$$\frac{d}{dR_0} \left(\frac{u_g}{u_*} \right) = -\frac{1}{k} \frac{d}{dR_0} \ln \epsilon$$

$\therefore \frac{u_g/u_*}{\epsilon} = \frac{1}{k} \left(\ln \frac{u_g}{f_2} - A \right) \quad (26)$

where A is a constant of integration.

Similarly for the v-component

Inner layer

$$\frac{v}{u_*} = G \left(\frac{z}{z_0}, \epsilon \right)$$

$$\sim G_0(z/z_0) + G_1(z/z_0)\epsilon + G_2(z/z_0)\epsilon^2 + \dots$$

$$\approx G_0(z/z_0) \quad (27)$$

Outer layer

$$\frac{v-v_g}{u_*} = g \left(\frac{fz}{u_*}, \epsilon \right)$$

$$\sim g_0 \left(\frac{fz}{u_*} \right) + g_1 \left(\frac{fz}{u_*} \right) \epsilon + g_2 \left(\frac{fz}{u_*} \right) \epsilon^2 + \dots$$

$$\approx g_0 \left(\frac{fz}{u_*} \right) \quad (28)$$

In the overlap domain

$$G_0(\gamma) = \frac{v_g}{u_*} + g_0(\gamma\epsilon) \quad (29)$$

The axes were chosen such that the x-axis is directed along the surface stress and hence $G_0(\gamma)$ is zero

i.e. $\frac{v}{u_*} = 0 \quad (30)$

Also

$$\frac{d}{dR_0} \left(\frac{v_g}{u_*} \right) = 0 \quad \text{since } g_0'(\gamma\epsilon) = 0$$

and so

$$\frac{v_g}{u_*} = \text{constant} = \frac{-\beta}{k}, \text{ say.} \quad (31)$$

One interesting thing to note about this analysis is that the logarithmic profile for u is strictly valid in the overlap region where $z \gg z_0$ and in so far as it is valid for smaller z, in practice, this appears to be fortuitous.

The result of the two equations (24), (31) is to provide relations between u_g/v_g , α and the surface Rossby Number.

The most useful forms are

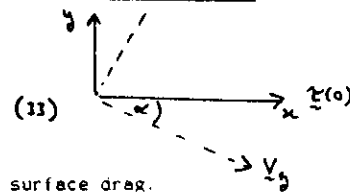
$$\frac{v_g^2}{u_*^2} = \frac{u_*^2 + v_g^2}{u_*^2} = \frac{\beta^2}{k^2} + \frac{1}{k^2} \left[\ln \left(R_0 \frac{u_*}{v_g} \right) - A \right]^2$$

$$\therefore \ln R_0 = A - \ln \left(\frac{u_*}{v_g} \right) + \left(\frac{k^2 v_g^2}{u_*^2} - \beta^2 \right)^{1/2} \quad (32)$$

and

$$v_g = -V_g \sin |\alpha|$$

$$\sin |\alpha| = \frac{\beta}{k} \left(\frac{u_*}{V_g} \right) \quad (33)$$



u_g/v_g is an important parameter related to the surface drag.

On dimensional grounds $\tau(\sigma)$ can be expressed

$$\tau(\sigma) = \rho u_*^2 = \rho C_G(z) V^2(z) = \rho C_G V_g^2 \quad (34)$$

and $C_G = \left(\frac{u_*}{V_g} \right)^2$ is known as the geostrophic drag coefficient.

$$\tan |\alpha| = -\frac{v_g}{u_g} = \frac{\beta}{\ln \left[\frac{u_*}{fz_0} \right] - A} \quad (35)$$

The constants of integration A, B have to be determined from observation.

k is of course the von Karman constant ≈ 0.4 .

9.1.4 The Non-neutral Barotropic Boundary Layer

Generalizations of the above techniques have been applied in the horizontally-homogeneous, steady-state, non-neutral, barotropic boundary layer. In this case the need to include the stability parameter μ into the similarity and perturbation analyses adds a further complication.

Suffice it to say that the forms of the equations already obtained for the neutral case remain valid, only now A and B must be considered universal functions of μ .

i.e. we now have the general expressions

$$\ln h_0 = A(\mu) - \ln\left(\frac{u_*^2}{v_*^2}\right) + \left(\frac{k^2 v_*^2}{u_*^2} - B^2(\mu)\right)^{1/2} \quad (36)$$

$$\tan |\alpha| = \frac{B(\mu)}{\ln\left(\frac{u_*}{f z_0}\right) - A(\mu)} \quad (37)$$

$$\frac{u_g}{u_*} = \frac{1}{k} \left(\ln\left[\frac{u_g}{f z_0}\right] - A(\mu) \right) \quad (38)$$

$$\frac{v_g}{u_*} = -\frac{B(\mu)}{k} \quad (39)$$

In addition we have the relation

$$\frac{T_*}{k \Delta_r \theta} = \frac{\alpha_0}{\ln\left[\frac{u_*}{f z_0}\right] - C(\mu)} \quad (40)$$

where α_0 is the ratio k_n/k_m for near-neutral conditions (take ≈ 1) and C is a further function of μ which must be determined from observation.

If we include the effects of water vapour in the stability parameter we could obtain a similar expression to (40) for $q_0/k \Delta_r \theta$ and introduce a further universal function of μ , $D(\mu)$.

9.1.5 Evaluation of the functions A, B, C

The values of A, B and C have to be found from more sophisticated numerical models or from field experiments.

Currently accepted values for neutral conditions are $A = 1.7$, $B = 4.3$ (with at least $\pm 10\%$ uncertainty in each).

Currently accepted variations of A, B and C with μ are shown in the following "Figure 10" (after Arya (1975), Quart J R Met Soc, 101, 147-161). Note that A, B and C all change rapidly with μ near $\mu = 0$ (neutral

stability) suggesting that "neutral" results are likely to be very unrepresentative. Also note the rapid approach to constant values of A, B and C for large negative μ (unstable conditions).

9.1.6 Evaluation of $u_g/v_g, \alpha$ as functions of μ, S, R_0

The following figures give a selection of evaluations of u_g/v_g and α as functions of R_0 , μ or S, based on the Rossby Number similarity theory.

The figures from Smith et al (1972) for a forest canopy illustrate an alternative representation for a given z_0 where the stability parameter has been expressed in terms of incoming solar radiation.

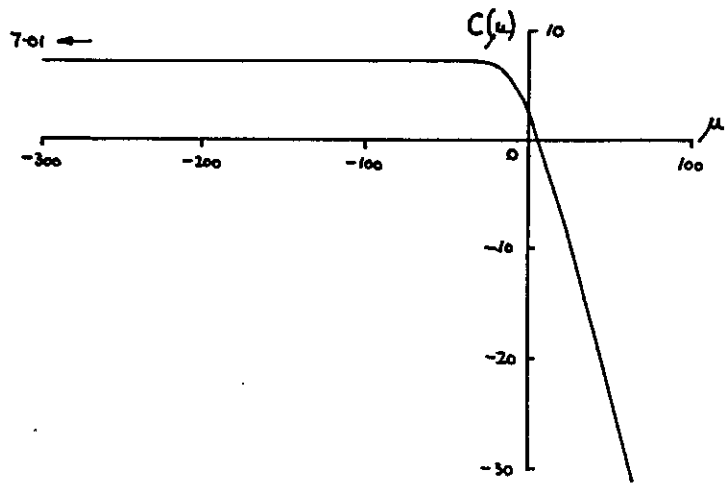
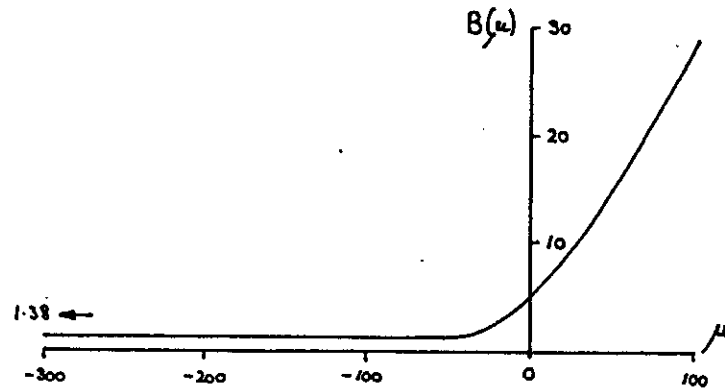
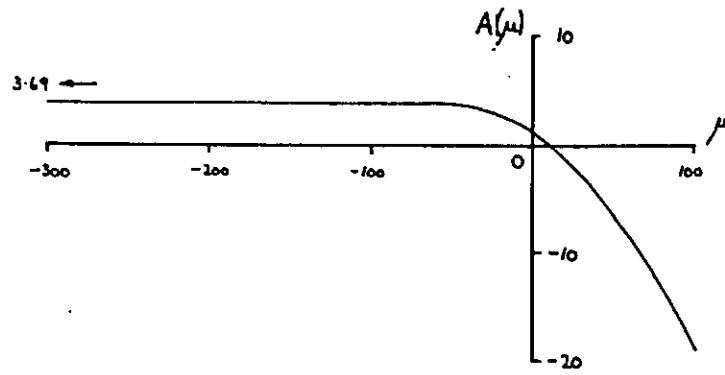
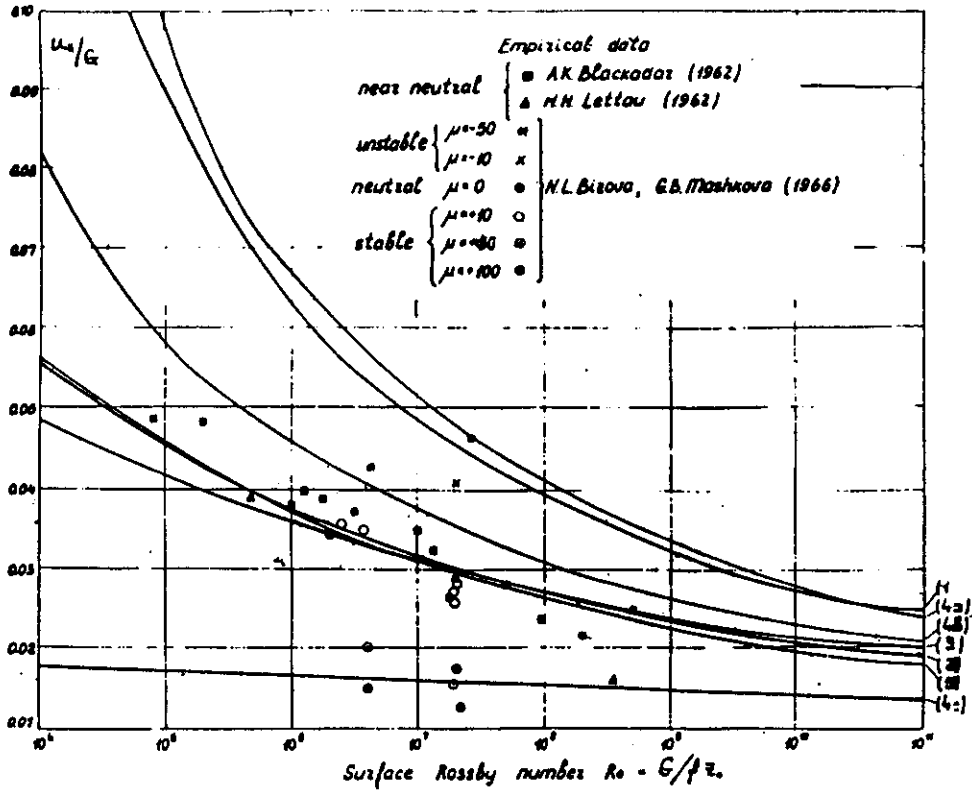


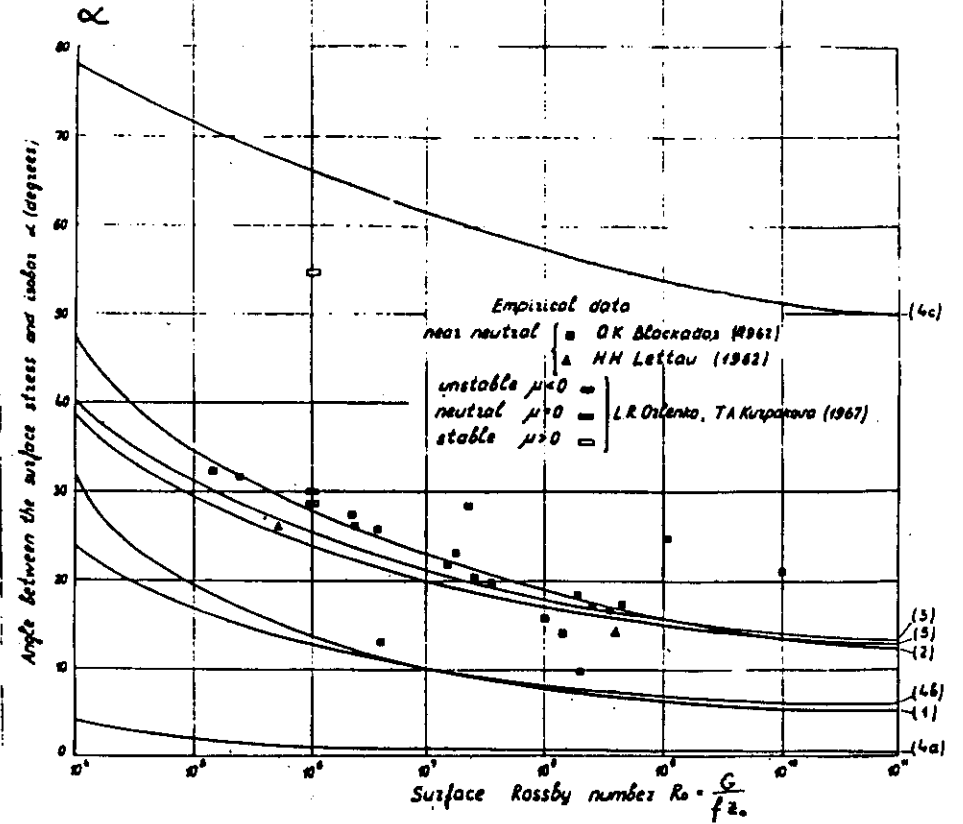
FIGURE 10 : VARIATION OF A, B, AND C WITH STABILITY PARAMETER μ .
 (AFTER ARYA, 1975). $\mu = \frac{h}{L} = \frac{u_s}{FL}$.



Theoretical curves:

- (1) A.S. Monin (1950)
- (2) A.K. Blackadar (1962) } neutral $\mu=0$
- (3) H.H. Lettau (1962)
- (4) I.M. Bobileva, S.S. Zilitinkevich, D.L. Laichtman (1965)
 - a - unstable $\mu=100$
 - b - neutral $\mu=0$
 - c - stable $\mu=100$
- (5) J.F. Appleby, W.D. Ohmsted (1966) - $\mu=0$

Figure 8



Theoretical curves:

- (1) A.S. Monin (1950)
- (2) A.K. Blackadar (1962) } neutral $\mu=0$
- (3) H.H. Lettau (1962)
- (4) I.M. Bobileva, S.S. Zilitinkevich, D.L. Laichtman (1965)
 - a - unstable $\mu=100$
 - b - neutral $\mu=0$
 - c - stable $\mu=100$
- (5) J.F. Appleby, W.D. Ohmsted (1966) - $\mu=0$ neutral

Figure 9

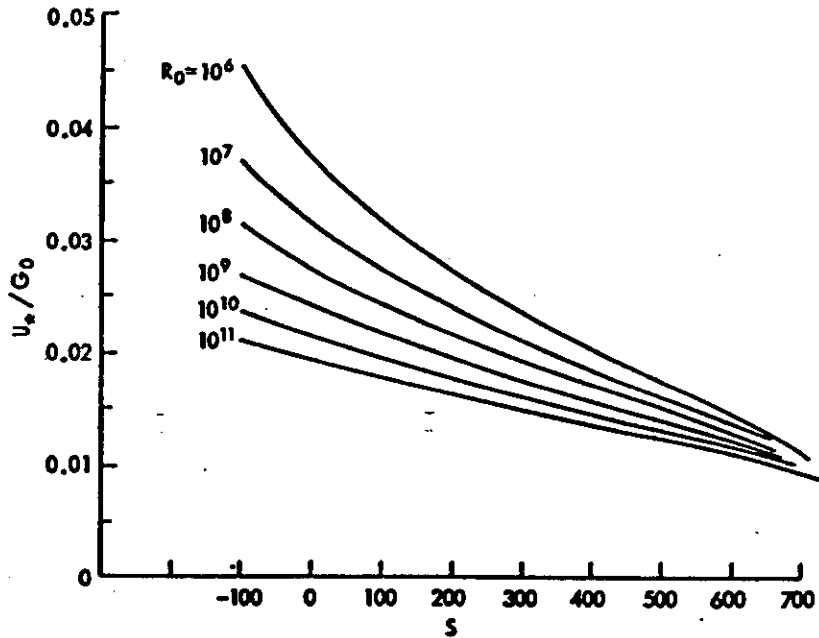
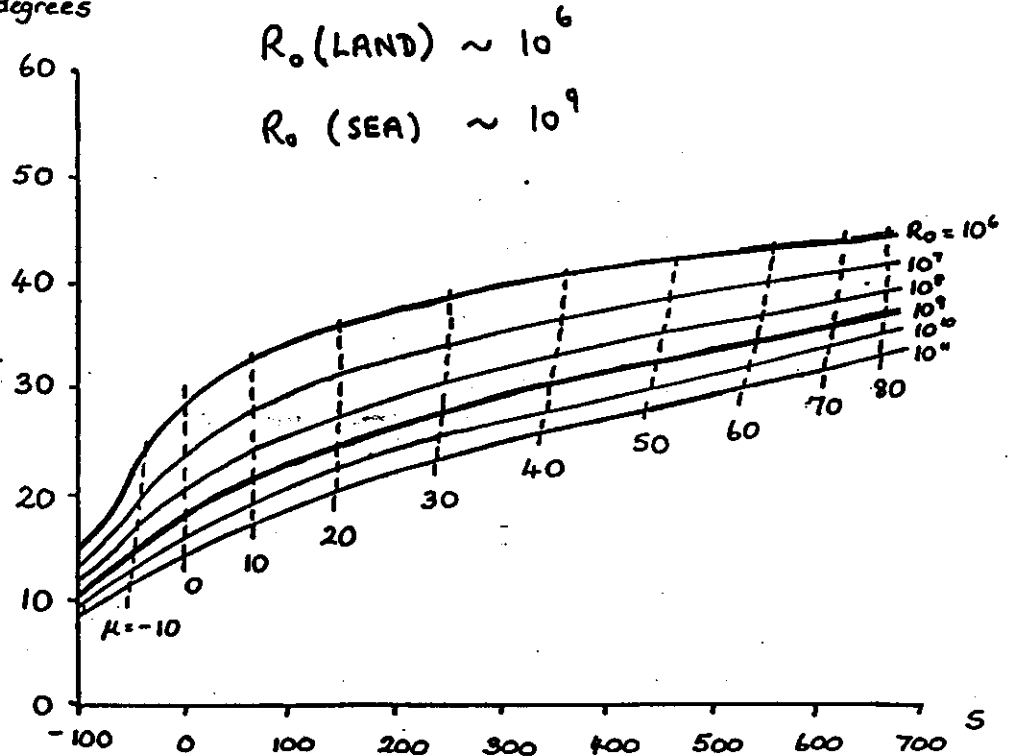


Fig.10 — Nomogram of $\frac{u_s}{G_0}$ as a function of R_0 and S for near-neutral and stable conditions based on Wangara data (Arya, 1974)

α_0 , degrees



Nomograms of α_0 as a function of R_0 and S for near-neutral and stable conditions (based on Wangara data).

ARYA (1975)

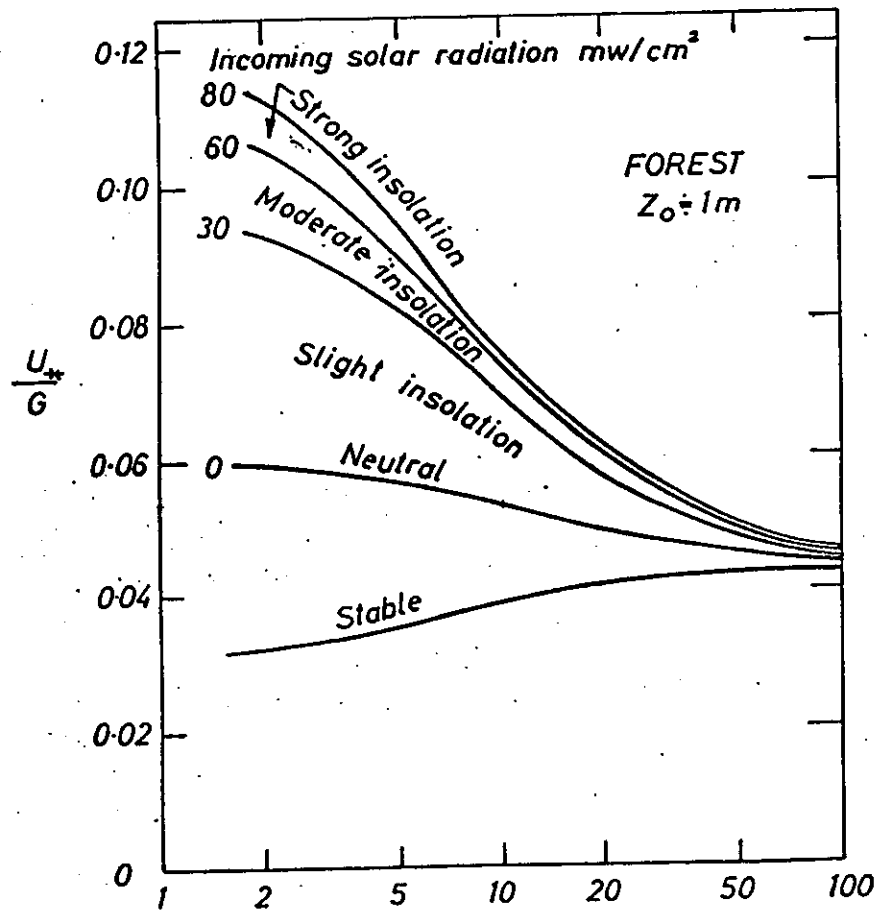


Figure 3. The friction velocity at the top of the trees expressed as a function of geostrophic wind speed and incoming solar radiation.

[SMITH, F.B., CARSON, D.J. and OLIVER, H.R. 1972 B.L.M. 3, 176-190]

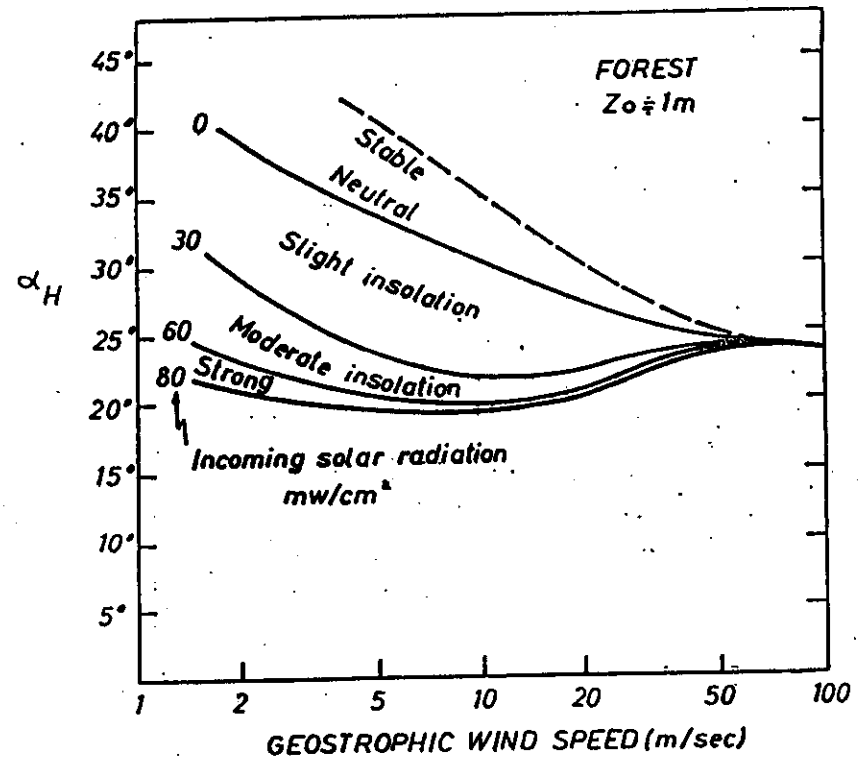


Figure 4. The turning of the wind at the top of the trees from the geostrophic wind direction as a function of geostrophic wind speed and incoming solar radiation.

[SMITH, F.B., CARSON, D.J. and OLIVER, H.R. 1972 B.L.M. 3, 178-190]

SIMPLE THERMAL MODELS

The history of simple thermal models for parameterizing the development of the convectively unstable boundary layer capped by a stable layer can be traced through the papers of Ball (1960), Lilly (1968), Deardorff et al (1969), Tennekes (1972) and Carson (1973). We summarize here the method and results of the model discussed in depth by Carson (1973) and independently proposed by Betts (1973).

The potential temperature profile, as illustrated in Fig. , is defined by

$$\theta(z,t) = \begin{cases} \theta_c(t) & z < h \\ \theta_s(z,t) = \theta_0 + \gamma(t)z & z > h \end{cases} \quad (1)$$

where h is nominally the depth of the convectively unstable boundary layer, θ_0 is the effective surface temperature obtained by extrapolating the stable lapse rate down to $z = 0$, and $\gamma(t)$ is the vertical gradient of θ in the capping stable layer.

Advection, radiation and evaporation are not considered here although in certain circumstances each or all of these processes can be important. In this case the simple heat balance equation is

$$\frac{\partial H}{\partial z} = -\rho c_p \frac{d\theta}{dt} = -\rho c_p \left[\frac{\partial \theta}{\partial t} + w(z) \frac{\partial \theta}{\partial z} \right], \quad (2)$$

$$\text{such that } H(z,t) = 0 \quad z > h, \quad (3)$$

where $H(z,t)$ is the sensible eddy heat flux, $w(z)$ is the mean, synoptically-induced vertical velocity, ρ is the mean air density and c_p is the specific heat of air at constant pressure.

Certain features of the simple model, such as the linearity of $w(z)$

and $H(z,t)$ with height and the exponential increase of $\gamma(t)$ with time are derived from Eqs. (1)-(3), as indeed is the expression for the entrained sensible eddy heat flux

$$H(h,t) = -\rho c_p w_e(t) \Delta\theta(t), \quad (4)$$

$$\text{where } w_e(t) = \frac{dh}{dt} - w(h) \quad (5)$$

is the entrainment rate and

$$\Delta\theta(t) = \theta_s(h,t) - \theta_c(t) \quad (6)$$

is the step discontinuity in θ across the interface at $z = h$.

The system of equations is closed by parameterizing the entrainment process at $z = h$. In this simple model it is postulated that the degree of entrainment is controlled, to a first approximation, by the intensity of the thermal bombardment of the interface which, in turn, is directly proportional to the magnitude of the surface sensible heat flux. Hence the closure equation is

$$H(h,t) = -A H(0,t) \quad 0 \leq A \leq 1. \quad (7)$$

Straightforward analysis produces an ordinary differential equation for the development of the convectively unstable layer,

$$h \frac{d(\gamma h)}{dt} = \frac{H(0,t) - 2H(h,t)}{\rho c_p} \quad (8)$$

which although not explicitly dependent on A , does depend on A being constant. Strictly, in keeping with the assumptions, Eq. (8) should be written

$$\frac{dh^2}{dt} + 2\bar{\rho} h^2 = \frac{2(1+2A)H(0,t)}{\rho c_p \gamma(t)}, \quad (9)$$

where $\tilde{\beta} = -\frac{\omega(z)}{z} = \text{constant},$ (10)

and $\gamma(t) = \gamma(0) \exp(\tilde{\beta}t).$ (11)

Integration of Eq. (9), with $h(0) = 0$, gives

$$h^2(t) = \frac{2(1+2A) \exp(-2\tilde{\beta}t)}{\rho c_p \gamma(0)} \int_0^t \exp(\tilde{\beta}\tau) H(0,\tau) d\tau, \quad (12)$$

and the corresponding evolutionary expressions for $w_e^2(t)$, $\Delta\theta(t)$ and $\theta_c(t)$ are,

$$w_e^2(t) = \frac{(1+2A) H(0,t)}{\rho c_p \gamma(t) h(t)}, \quad (13)$$

$$\Delta\theta(t) = \frac{A \gamma(t) h(t)}{1+2A}, \quad (14)$$

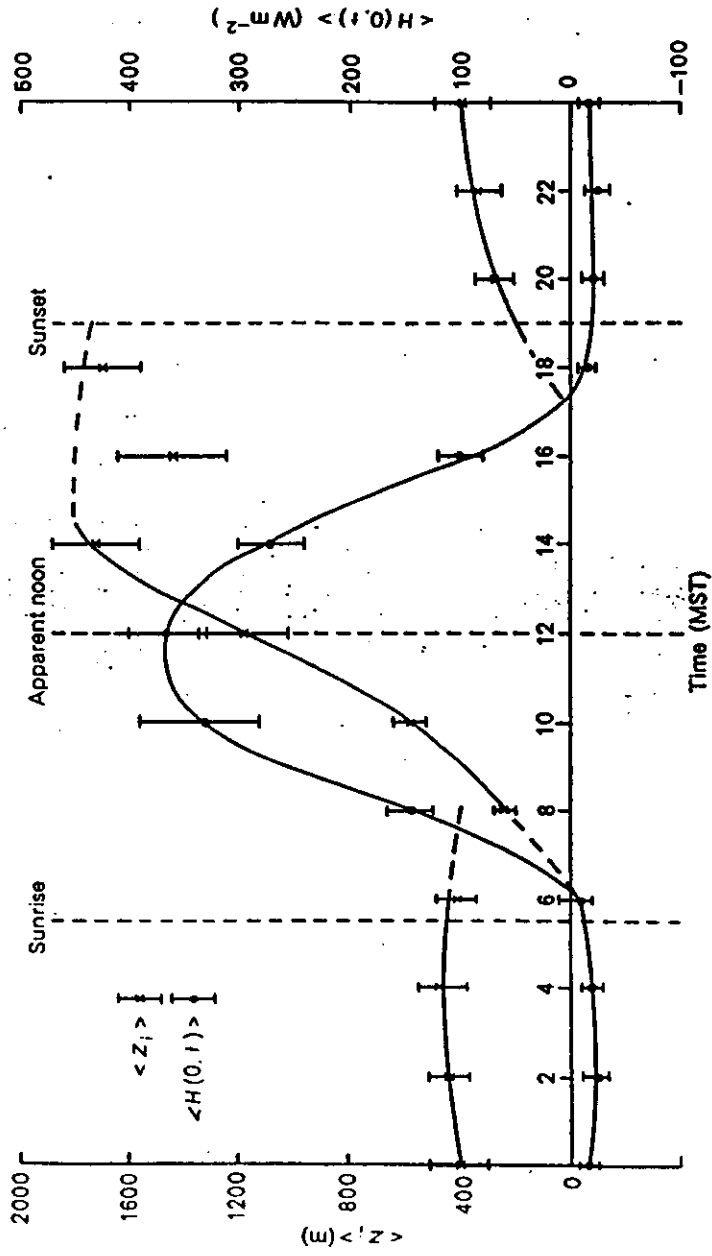
and $\theta_c(t) = \theta_0 + \left(\frac{1+A}{1+2A}\right) \gamma(t) h(t).$ (15)

The value of A which characterises the degree of interfacial mixing realised in the atmosphere during the typical development of a convectively unstable boundary layer remains to be chosen.

The extreme value $A = 1$ derives from Ball (1960) who, in his consideration of the integrated local turbulent kinetic energy balance equation, assumed that the contribution from molecular dissipation could be neglected. The other extreme, $A = 0$, describes the situation where the boundary layer is growing without entraining heat across the interface, i.e. $\Delta\theta$ in Eq. (4) is zero whereas $w_e^2(t)$ remains finite. In such circumstances the interface is a passive one with no mixing across it and we shall use the term encroachment of the stable layer by the unstable layer to

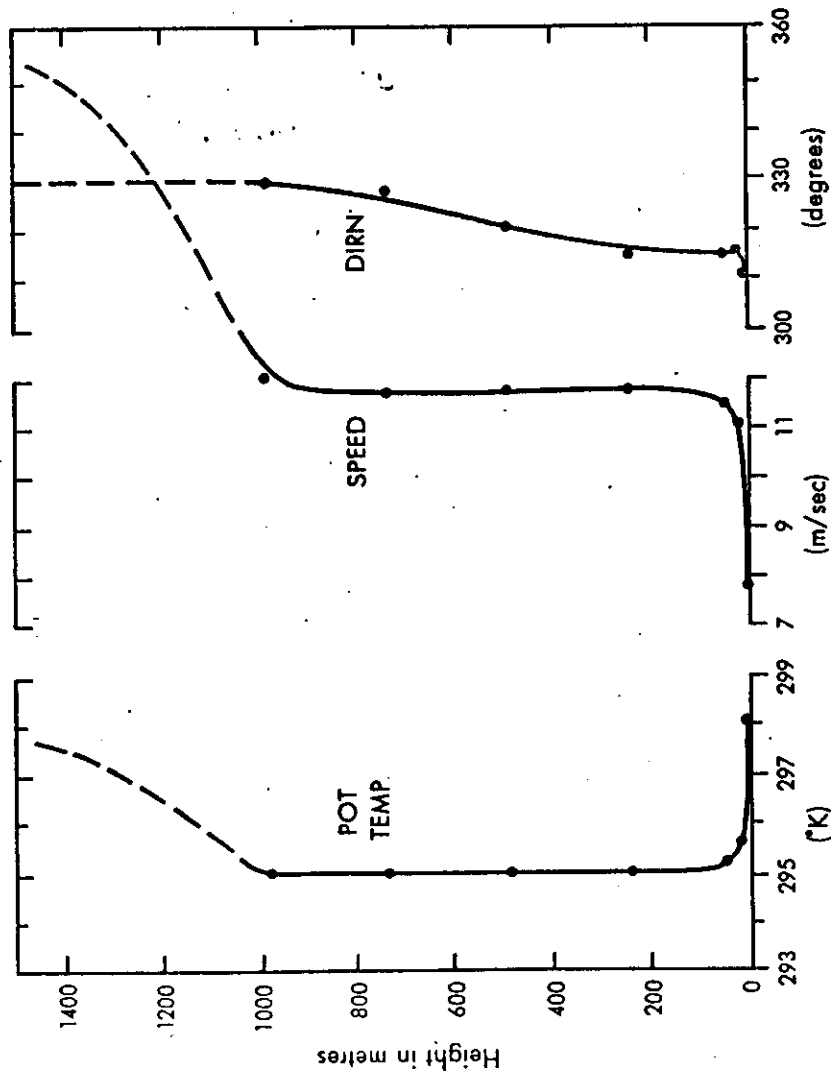
describe this process. Such a state is strictly never realised in the atmosphere but is closely approached in the laboratory studies of penetrative convection by Deardorff *et al.* (1969) and when weak thermal activity is eroding a strong inversion, such as a nocturnally established inversion (Carson, 1973).

Available evidence favours small values of A ; 0.2 is suggested by Deardorff (private communication) and Tennekes (1972), and Betts (1973) quotes evidence for 0.25. It seems unlikely that A remains constant throughout the various phases of the boundary layer's evolution and Carson (1973) from his analysis of the O'Neill 1953-data has suggested that A varies quite significantly during the day, being very small soon after dawn and reaching a maximum value, as high as 0.5, during a period of a few hours following the time of maximum surface heating.



188

Figure 3. The mean boundary layer thickness, $\langle z_i \rangle$, and sensible heat flux at the surface, $\langle H(0, t) \rangle$, deduced for the O'Neill data, plotted with standard errors as functions of time of day (Mean Solar Time). Carson (1973).



189

Figure 1. Mean profiles associated with a convective boundary layer

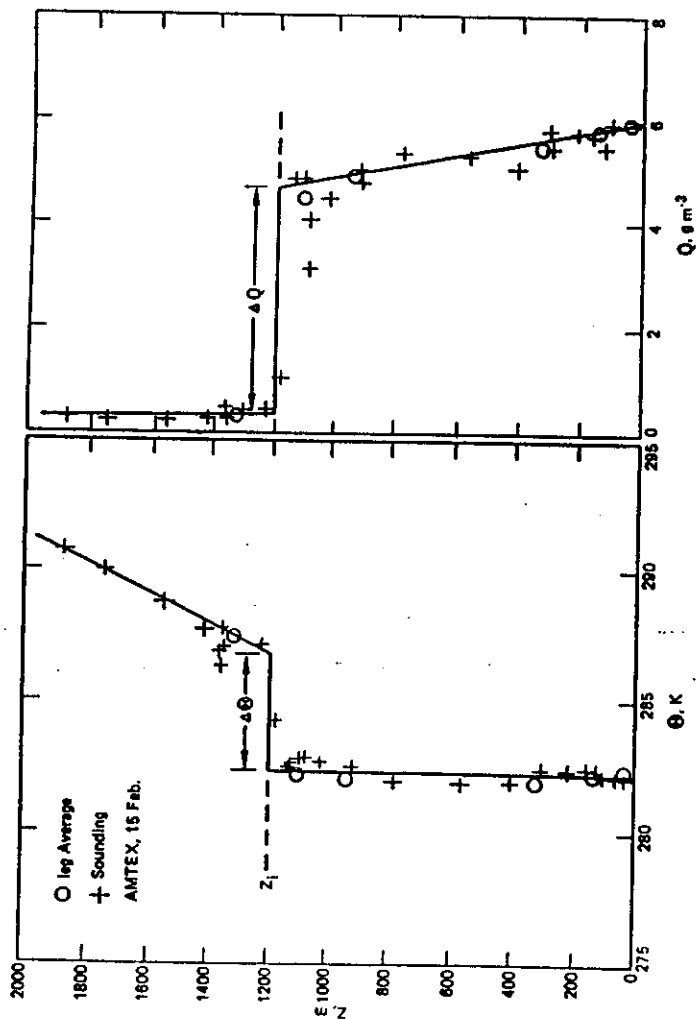


Figure 2 Vertical profiles of mean potential temperature and mean absolute humidity as measured over the sea in the AMTEX experiments. Note the strong jumps in both properties at z_1 . (Figure reproduced from Musseau et al (1979))

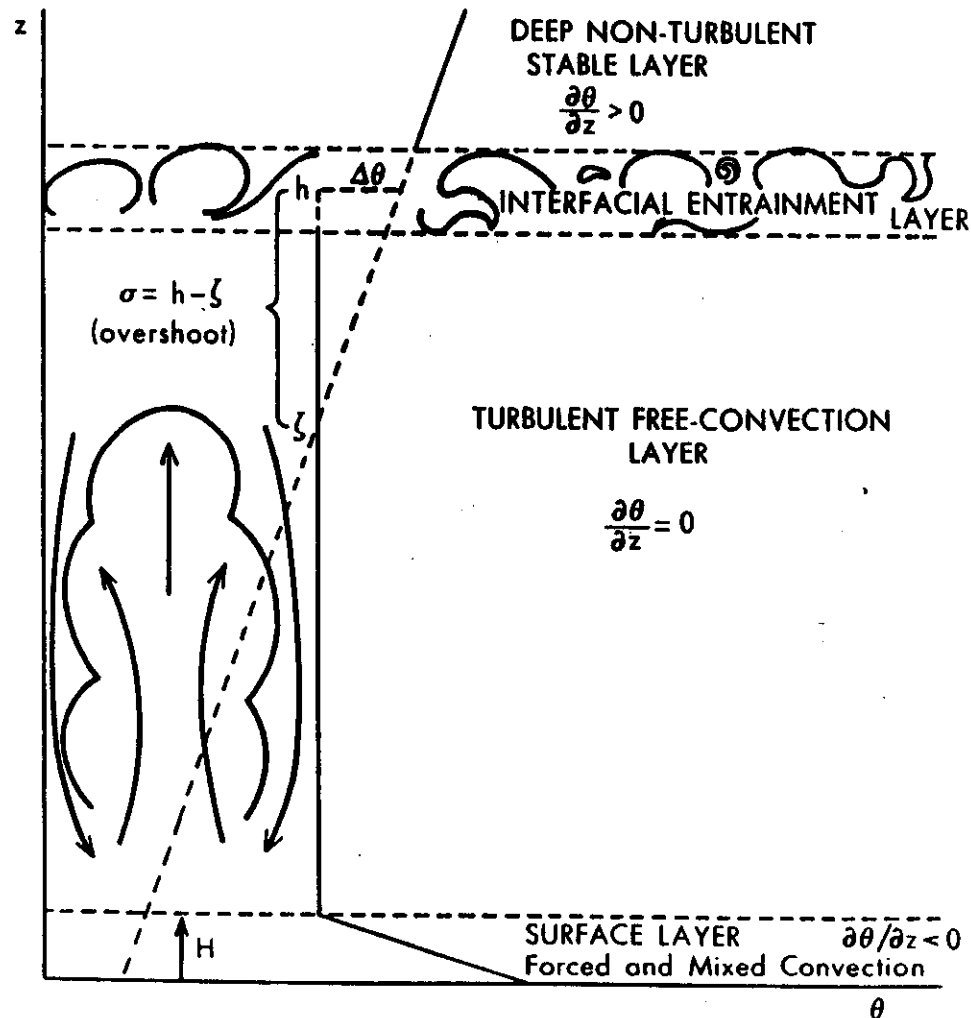
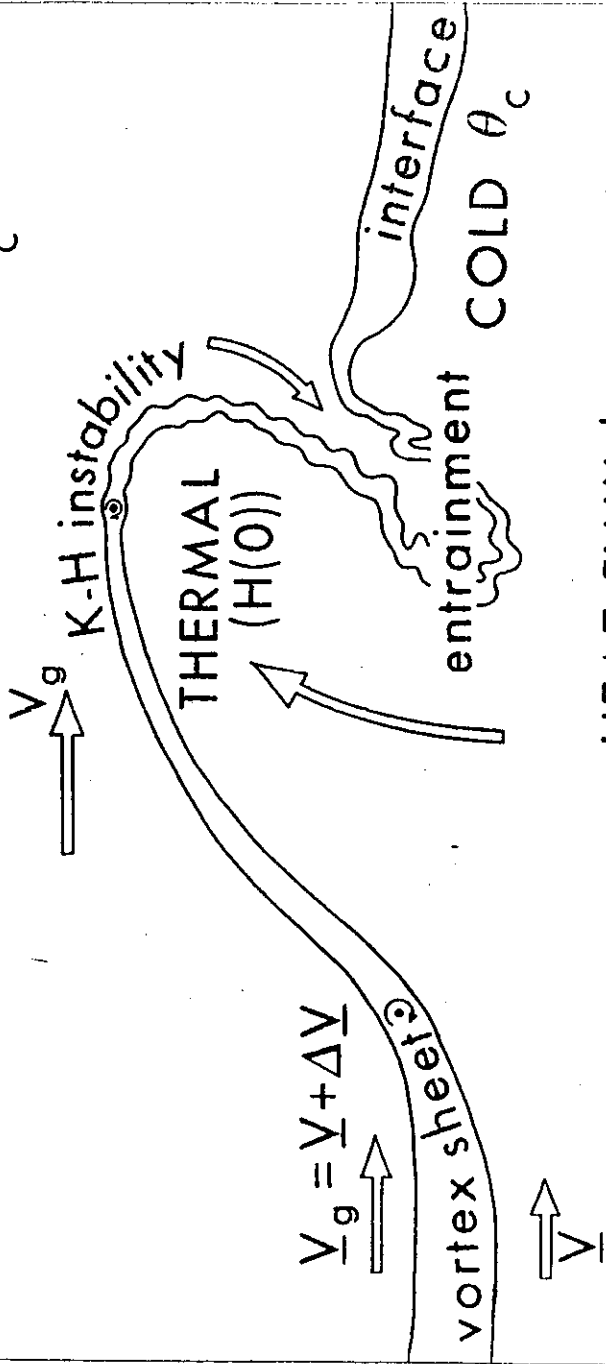


Figure 4. Schematic representation of the developing convectively unstable boundary layer and the adopted potential temperature profile, $\theta(z)$.

Carson (1973)

SCHEMATIC PICTURE OF ENTRAINMENT

WARM
 $\theta = \theta_c + \Delta\theta$



HEAT FLUX by entrainment
 $= fn(H(0); \Delta V; \Delta\theta)$

Fig.1

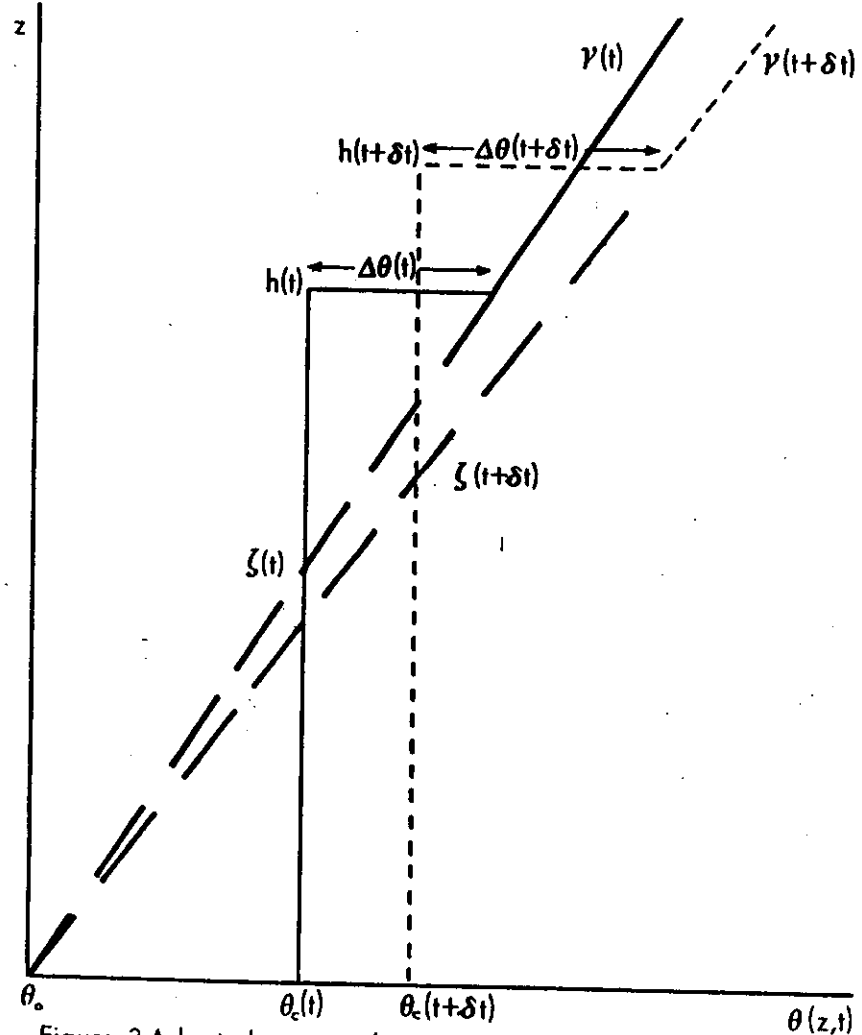


Figure 3. Adopted potential temperature profiles as a function of z and t and a representation of the parameters h , ζ , $\Delta\theta$, γ , θ_0 and θ_c .

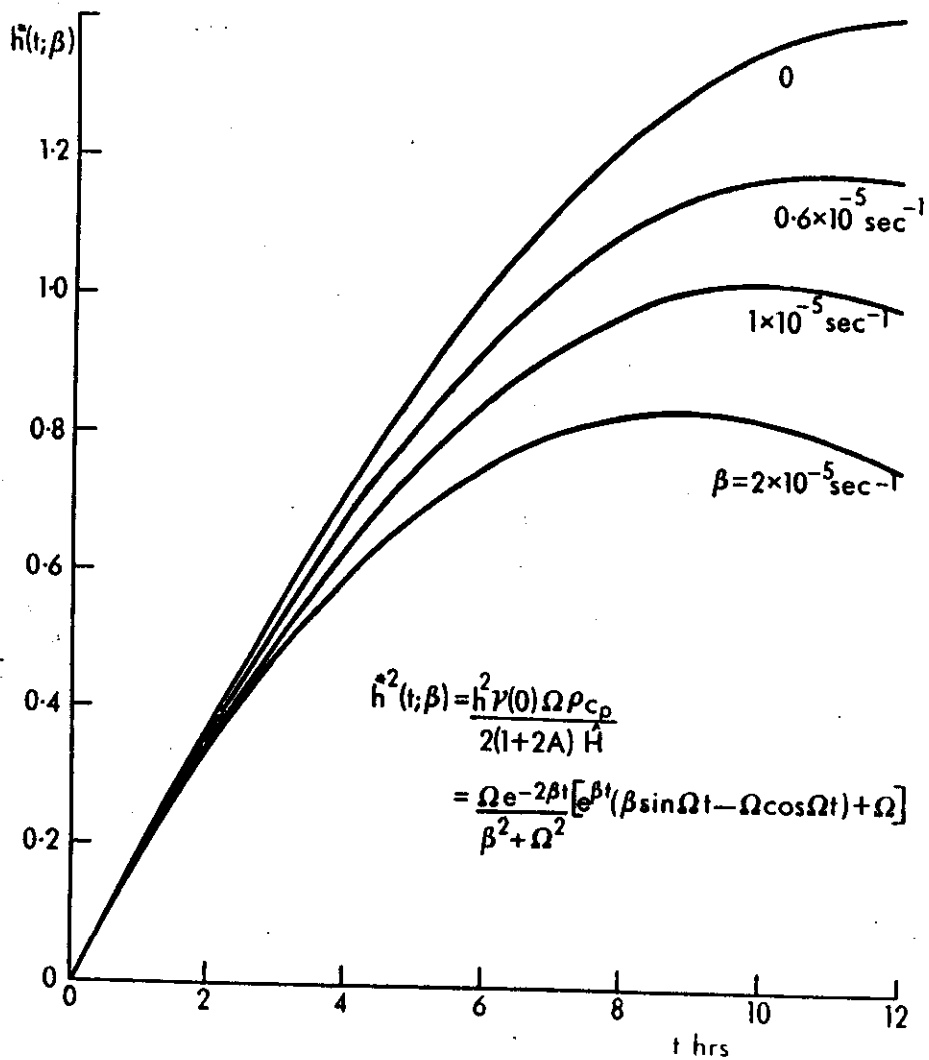


Figure 4. The non-dimensional depth \hat{h}^* as a function of time and various values of the subsidence parameter β . Sinusoidal heat flux model.

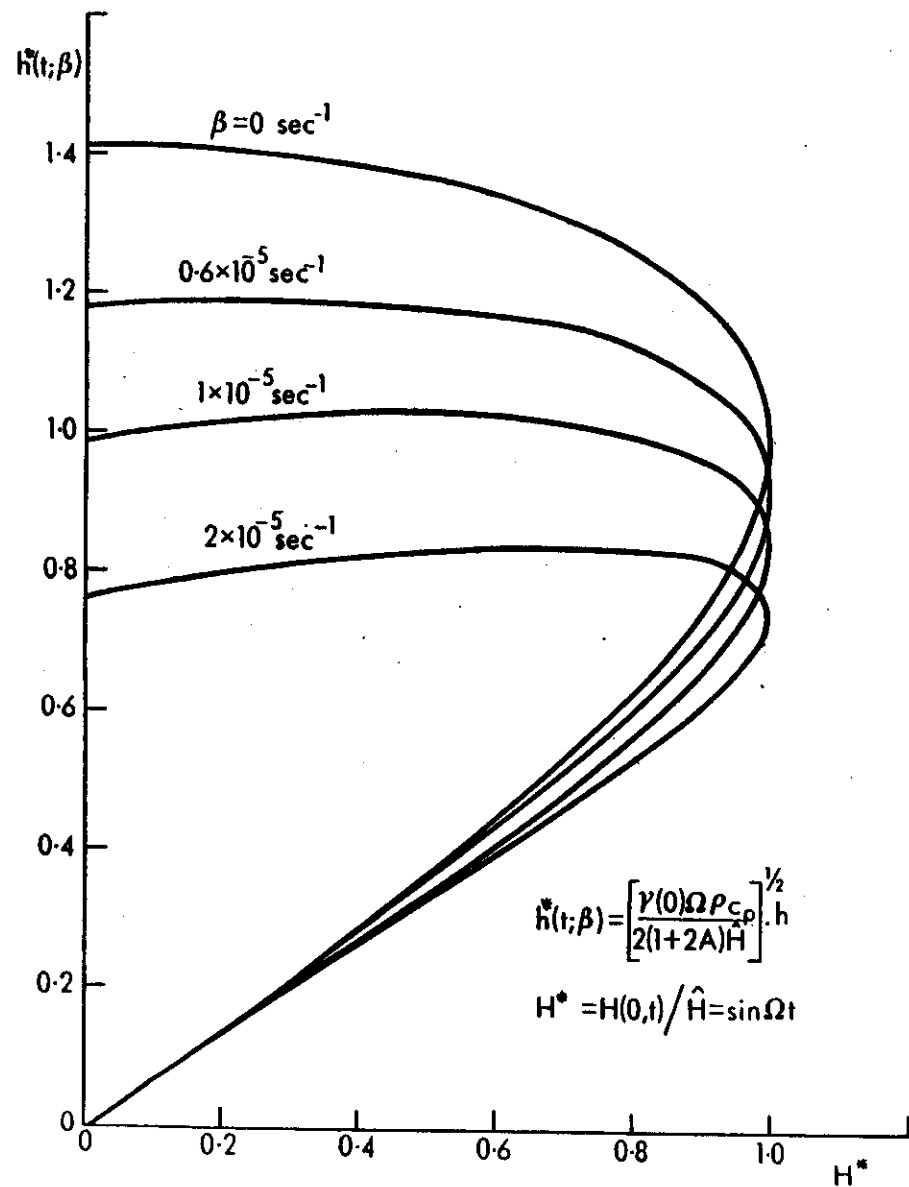


Figure 5. The non-dimensional depth \hat{h}^* as a function of the subsidence parameter β and the non-dimensional sinusoidal heat flux H^*

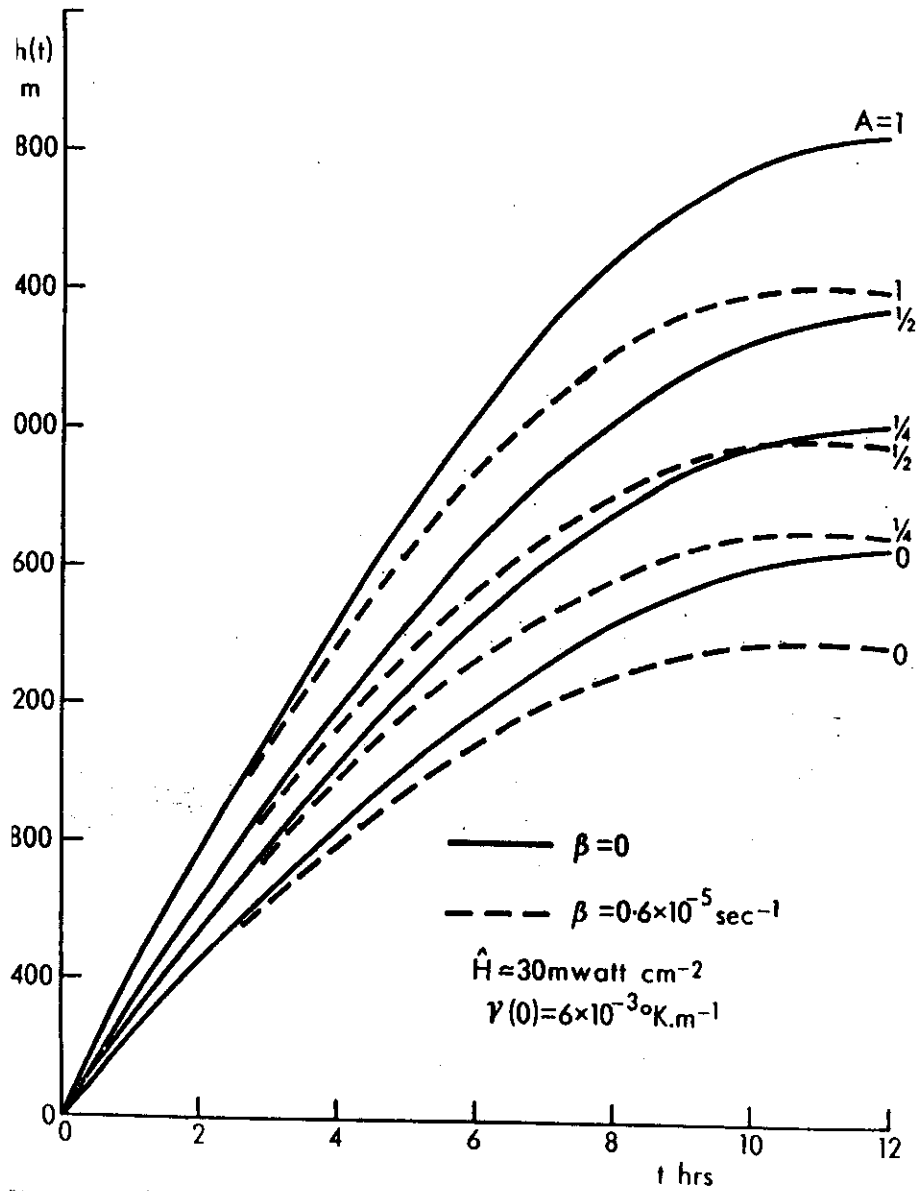


Figure 6. The development of the depth of the convectively unstable boundary layer, $h(t)$, for various degrees of interfacial mixing, for typical values of $\gamma(0)$ and \hat{H} in the cases of no subsidence and typical subsidence. Sinusoidal heat flux model.

196

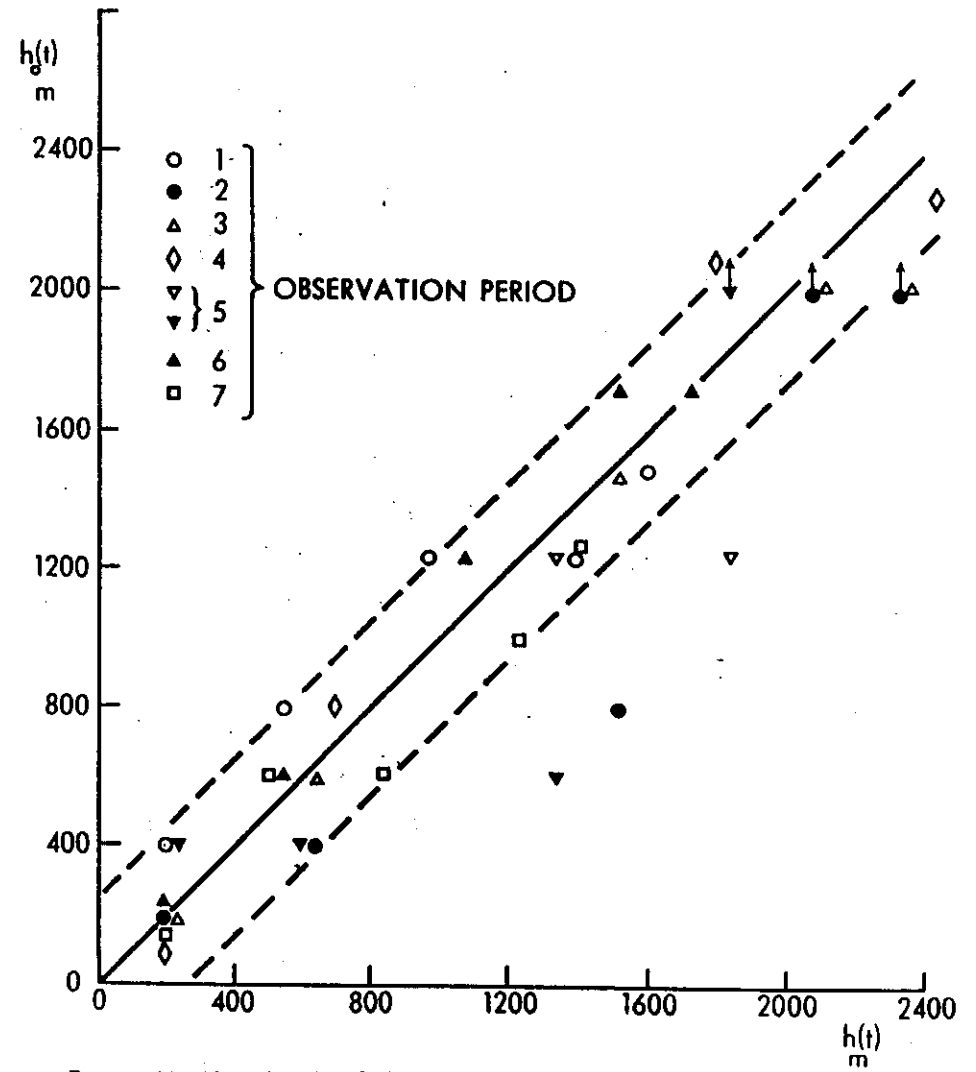


Figure 13. The depth of the O'Neill boundary layer, $h_o(t)$, estimated from profiles, against the depth, $h(t)$, predicted using a three-phase model. The broken lines are $h_o(t) = h(t) \pm 255$ m, where 255 m is the standard error about the line $h_o(t) = h(t)$, the correlation coefficient being 0.93.

197

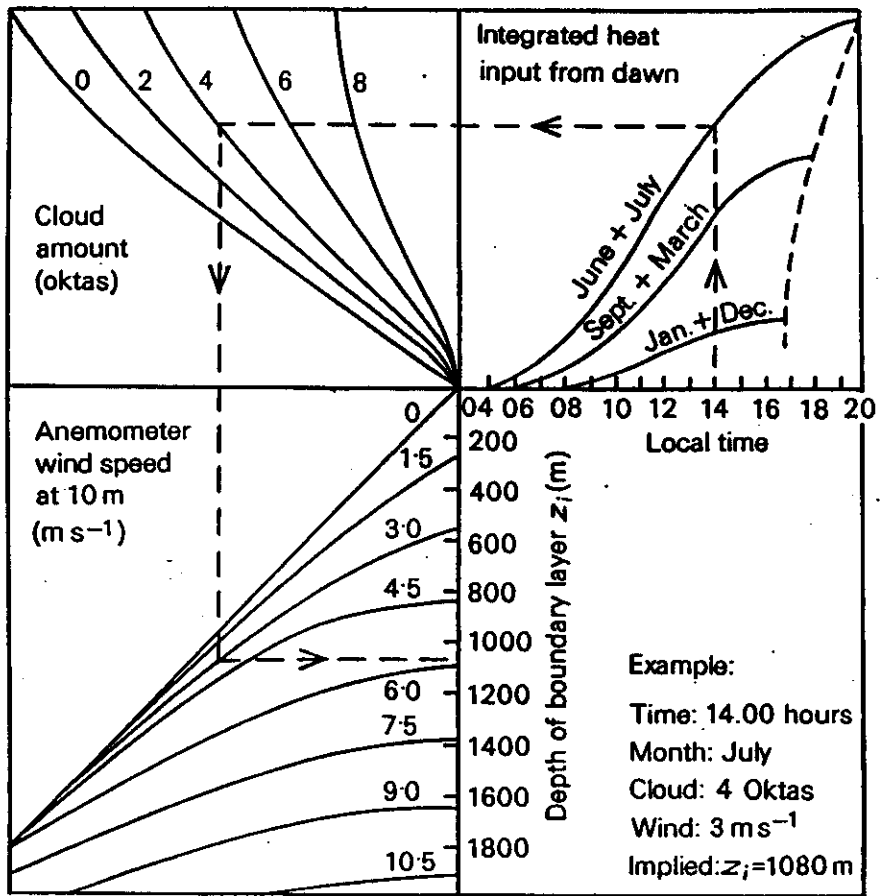


FIGURE 7 A nomogram for estimating the depth of the boundary layer in the absence of marked advective effects or basic changes in weather conditions. The example shows how the diagram is to be used. Smith and Carson (1974)

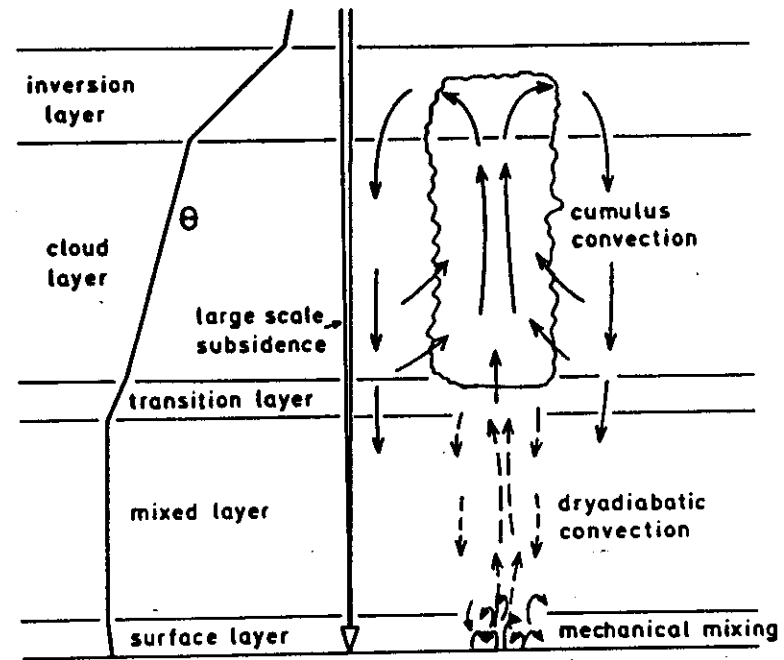


Figure 8. Scheme of dominant processes in a multilayered atmospheric boundary layer. θ = potential temperature.